UNIVERSIDAD AUTÓNOMA DE MADRID

FACULTAD DE CIENCIAS

DEPARTAMENTO DE BIOLOGÍA MOLECULAR

REGULACIÓN Y FUNCIÓN DE LA INTERACCIÓN DE LA INTEGRINA α4β1 CON LOS DOMINIOS HEP II Y HEP III DE FIBRONECTINA. PAPEL EN LA REORGANIZACIÓN DEL CITOESQUELETO Y LA FORMACIÓN DE MATRICES DE FIBRONECTINA

TESIS DOCTORAL

ALFREDO MAQUEDA FERNÁNDEZ

2007

UNIVERSIDAD AUTÓNOMA DE MADRID

FACULTAD DE CIENCIAS

DEPARTAMENTO DE BIOLOGÍA MOLECULAR

REGULACIÓN Y FUNCIÓN DE LA INTERACCIÓN DE LA INTEGRINA α4β1 CON LOS DOMINIOS HEP II Y HEP III DE FIBRONECTINA. PAPEL EN LA REORGANIZACIÓN DEL CITOESQUELETO Y LA FORMACIÓN DE MATRICES DE FIBRONECTINA

Este trabajo ha sido realizado por **Alfredo Maqueda Fernández** para optar al grado de Doctor, en el Centro de Investigaciones Biológicas de Madrid (CSIC), bajo la dirección de la Dra. Ángeles García Pardo.

Fdo: Dra. Ángeles García Pardo.

A mi familia y a Marta

Dar las gracias en primer lugar a la Dra. Ángeles García-Pardo por brindarme la oportunidad de realizar la tesis doctoral en su laboratorio, y dedicar parte de su tiempo a mi formación.

Gracias a mis compañeros de laboratorio, que también por ellos se saca adelante la tesis, a mi "madre adoptiva" muchas gracias Rubia, a Chevi por enseñarme lo bueno y lo malo de esta etapa, a Javi (nuestro dj), a Elizabeth (con "z" de zuperman), a Mª Jesús (la última adquisición) por ayudarme a dar el último empujón, y a Eva, Espe y Beni que también son parte de ella.

A la gente de los laboratorios del ala de Inmunología, que están actualmente o han pasado por aquí, tanto a los becarios como a los investigadores, gracias por crear ese buen ambiente y ofrecerme vuestra ayuda siempre (Tito, Leyre, Alex, Paloma, Carmen, Iciar, "Barbas", Ely, Santiago, Jorge, Esther, Elenita, Goiko, Belén, Olga, Iría, Oihane, Sara, Rubén, Víctor, Joaquín, Rubén, Marisa, Soti, Maru, Kiko, Isa, "Perry Mason", Rosa, Pablo).

A los futboleros, a los de las cañas (rubenes, floras, etc..) y a los que ya están fuera del CIB pero siguen siendo mis amigos Pepe, Gema, Miriam, Isra y Esther.

A la gente del laboratorio del Dr. Carlos Cabañas (Carlos, Lola, Susi, Noelia, Lorena), muchas gracias por hacerme un hueco en vuestro laboratorio y hacerme sentir parte de el.

A la gente del laboratorio de la Dra. Mª José Calzada por permitirme colaborar con ellos en algo tan interesante.

A todos aquellos del CIB, que me han prestado su apoyo científico y logístico, personal administrativo, servicio técnico, citometría de flujo (Pedro), microscopia (Marigel, Maite, Silvia) y a los que me dejo en el tintero.

A los Drs. Francisco Sánchez-Madrid, Carmelo Bernabeu, Ángel Corbí, José Luis Rodríguez-Fernández y Germán Rivas, así como al resto de Drs. mencionados a lo largo de esta tesis, por habernos facilitado reactivos y prestarme su ayuda.

A mis amigos de siempre (madrileños y villacañeros), por intentar comprender esto de la ciencia y ayudarme a desconectar, Jaimito al final lo conseguí.

A mis padres, a mi hermana, a Javi, a la pequeña Fátima, a María, a Santiago y a Marga, así como al resto de mi familia por todo el apoyo que me han dado en este tiempo.

Y en especial a Marta por estar siempre a mi lado.

Índice

Moyano, J.V., **Maqueda, A**., Albar, J.P., and García-Pardo, A. "*A synthetic peptide from the heparin-binding domain III (repeats III4-5) of fibronectin promotes stress fiber and focal adhesión formation in melanoma cells".* Biochemical Journal 2003 (371) 565-571……..***ANEXO IV***.

Moyano, J.V., **Maqueda, A.**, Casanova, B., and García-Pardo, A. "*α4β1 integrin/ligand interaction inhibits α5β1–induced stress fiber and focal adhesions via downregulation of RhoA and induces melanoma cell migration".* Molecular Biology of the Cell 2003 (14) 3699-3715……..…….....***ANEXO V***.

CD de material adicional.……...…***ANEXO VI.***

Abreviaturas

Acm	Anticuerpo/s monoclonal/es.
ADN	Ácido Desoxirribonucleíco.
ADNc	Ácido Desoxirribonucleíco complementario.
ARNm	Ácido Ribonucleíco mensajero.
BSA	*Bovine Serum Albumine*, albúmina de suero bovino.
CMD	*Carboxy-Methyl Dextran*, carboxi-metil-dextrano.
CHX	*Cyclohexamide*, cicloheximida.
Cyt-D	*Cytochalasin-D*, citocalasina D.
DAPI	4´-6 diamidino-2-fenilindol.
DTT	1, 4 dithiothreitol.
EDC	1-Etil-3-(3-Dimetilaminopropil) Carbodimida.
EGF	*Epidermal Growth Factor*, factor de crecimiento epidérmico.
EDTA	*Ethylen-Diamine-Tetra-acetic Acid*, ácido etilen-diamino-tetra-acético.
FAK	*Focal Adhesion Kinase*, quinasa de adhesión focal.
FBS	*Fetal Bovine Serum*, suero fetal bovino.
FITC	*Fluorescein IsoThioCyanate*, iso-tiocianato de fluoresceína.
FN	Fibronectina.
GAG	Glucosaminoglicanos.
GAP	*GTPase-activating factor*, factor activador de GTPasa.
GDI	*GDP-Dissociation Inhibitor*, inhibidor de disociación de GDP.
GDP	*Guanosine Di-Phosphate*, guanosín difosfato.
GEF	*Guanosine nucleotide Exchange Factor*, factor de intercambio de nucleótidos de guanosina.
GFP	*Green Fluorescent Protein*, proteína verde fluorescente.
GST	*Glutathion-Sulphur-Transferase*, transferasa de azufre a glutatión.
GTP	*Guanosin-Tri-Phosphate*, guanosín trifosfato.
HBP/III5	*Heparin-Binding Peptide in repeat III5*, peptido que une heparina en la repetición III5.
Hep	Dominio de unión a heparina de la fibronectina.
HEPES	*4-(2-hidroxethyl) piperazine 1-ethanesulfonic acid*, ácido 4-(2-hidroxietil) piperacina 1-etanosulfonico.
HLA	*Human Leucocitary Antigen*, antigeno leucocitario humano.
HRP	*horseradish peroxidase*, peroxidasa de rábano.

IPTG Isopropyl β-D-1-thiogalactopyranoside.

IL Interleuquina

IIICS Segmento de conexión de tipo III.

LFA *Lymphocyte Function associated Antigen*, antigeno de función leucocitaria.

LPA *LysoPhosphatidic Acid*, ácido lisofosfatídico.

MEC *Extracelular Matrix*, matriz extracelular.

MMP *Matrix MetalloProteinase*, Metaloproteasa de matriz.

MTOC *Microtubule Organizing Center*, centro organizador de microtúbulos.

NHS N-hidroxisuccinamida.

PAGE *Poly-Acrylamide Gel Electroforesis*, electroforésis en geles de poliacrilamida.

PDGF *Platelet Derived Growth Factor*, factor de crecimiento derivado de plaquetas.

PBS *Phosphate Buffered Saline*, solución salina tamponada.

PCR *Polymerase Chain Reaction*, reacción en cadena de la polimerasa.

PG Proteoglicanos.

PGCS Proteoglicanos tipo Condroitín-Sulfato.

PGHS Proteoglicanos tipo Heparán-Sulfato.

PI3K *Phosphatidyl Inositol-3-Kinase*, fosfatidil-inositol-3-quinasa**.**

PI(4)5K *Phosphatidyl Inositol-4-Phosphate 5-Kinase*, fosfatidilinositol-4-fosfato 5-quinasa.

PKC *Protein Kinase C*, proteína quinasa C.

p-Lys *Poly-D-Lysine*, poli-D-lisina.

PMA *Phorbol 12-Miristate 13-Acetate*, forbol 12-miristato 13-acetato.

PMSF *Phenyl Methyl Sulfonyl Fluoride*.

PT *Pertussis Toxin*, toxina pertúsica.

RCC *Renal Cancer Cells*, células de cancer renal.

RIPA *Rapid InmunoPrecipitatión Assay*, ensayos de inmunoprecipitación rápida.

ROCK *Rho Coiled-Coil Kinase*.

SDF-1 *Stromal-cell Derived Factor-1*, factor derivado de células estromales-1.

SDS S*odium Dodecyl Sulfate*, dodecil sulfato de sodio.

PAGE *Poli-Acrylamide Gel Electrophoresis*, electroforesis en geles de poliacrilamida.

PYK *Proline- rich Tyrosine Kinase*, tirosín quinasa rica en prolina.

TBS *Tris Buffered Saline*, solución salina tamponada con Tris.

TCR *T-Cell Receptor*, receptor de células T.

TGF-β1 *Transforming Growth Factor-β1*, factor de crecimiento transformante β1.

TNF *Tumor Necrosis Factor*, factor de necrosis tumoral.

TRITC *Tetra-methyl-Rhodamine Iso-ThioCyanate*, iso-tiocianato de tetra-metil rodamina.

VCAM *Vascular Cell Adhesión Molecule*, molécula de adhesión celular vascular.

VHL *von Hippel Lindau tumor suppresor gene*, gen supresor de tumores de von Hippel Lindau.

VLA *Very Late activation Antigen*, antigeno de activación tardia.

Abstract

Regulation of the activity of α4β1 is essential in hematopoiesis, lymphocyte extravasation and in the inflammatory response. α4β1 may be activated by intracellular (chemokines, phorbol esters, CD3-crosslinking) or extracellular (Mn^{2+}, anti-β1 mAb TS2/16) stimuli, and activation results in increased adhesion and/or affinity for its ligands. To determine if these stimuli produce the same or different post-adhesion events, we have studied the cytoskeleton organization and intracellular signaling following activation of α4β1 in T cells. Treatment with Mn^{2+}, α-CD3 mAb or SDF-1α, followed by attachment to the fibronectin (FN) fragments FN-H89 (Hep II + IIICS), FNIII4-5 (Hep III) or to VCAM-1, resulted in cell polarization and migration. In contrast, activation with PMA or TS2/16 induced cell spreading and strong adherence. Video microscopy and Transwell analyses confirmed these results, which also correlated with different resistance to detachment under flow. Activation of RhoA or transfection with V14RhoA or V12Rac1, abolished the α4β1-induced cell polarization but did not affect cell spreading. Moreover, Rac1 activity was distinctly modulated by agents that induce a polarized or spread phenotype. The tyrosine kinase Pyk2 was highly phosphorylated upon induction of cell polarity but not during cell spreading. These results reveal novel properties of α4β1 integrin, namely the ability to trigger two types of T-cell cytoskeletal response with different signaling requirements.

Since the Hep II and Hep III domains have structural and functional homologies, we have also studied if the Hep III domain (like Hep II) plays a role in FN fibrillogenesis. We show that the III4-5 repeats constitute a novel region in FN involved in self-association and fibrillogenesis. Mutational analyses in the proteoglycan-binding sequence HBP/III5 of the FNIII4-5 fragment, revealed that the first two arginines of HBP/III5 were involved in FN-binding, while the last two arginines of this sequence regulated matrix assembly. Both properties appear to function independently and at different times during fibrillogenesis. As an example of the physiological relevance of the FN matrix, we have studied renal cancer cells (RCC) lacking the VHL tumor-suppressor protein, which are unable to assemble FN. We have found that these cells have a defective activation of the RhoA GTPase, possibly due to an increased p190RhoGAP phosphorylation. Moreover, expression of a dominant negative RhoA mutant in VHL(+) RCC decreased FN fibrillogenesis, while expression of constitutively active RhoA in VHL(-) cells induced formation of a FN matrix. These results strongly suggest an important role for RhoA in some of the defects observed in RCC VHL(-).

Introducción

I. La matriz extracelular y sus receptores celulares

1. La matriz extracelular.

La matriz extracelular (MEC) es una estructura tridimensional, compuesta por una compleja red de macromoléculas que son secretadas fuera de la célula. Esta malla de macromoléculas es esencial para mantener la correcta organización y propiedades físicas de las células, los tejidos y los órganos, además de ser un terreno propicio para que determinadas células puedan establecerse o migrar sobre ella. Aunque la MEC ha sido vista clásicamente como una estructura cuya función era dar un soporte estructural a células y tejidos, se ha ido descubriendo que dependiendo de la composición particular que presente, también puede ejercer un papel más dinámico, siendo importante en la señalización y comunicación celular, modificando su composición y función en procesos como desarrollo, morfogénesis, migración, proliferación o respuestas inflamatorias (Martin *et al.*, 2002; Yamada *et al.*, 2003; Midwood *et al.*, 2004)

Las interacciones entre la MEC y las células se producen a través de receptores situados en la superficie de la célula, fundamentalmente integrinas y proteoglicanos (PG). Ambos receptores sirven de enlace entre la MEC y el citoesqueleto, principalmente de actina (Calderwood *et al.*, 2000; Hynes, 2002), de forma que la adhesión entre célula y MEC sea consistente y tenga un efecto en la célula, bien sea estabilizando las interacciones, o bien ejerciendo una fuerza mecánica (tensión) para migrar o cambiar de forma.

1.1 Composición de la matriz extracelular.

La MEC está compuesta de una variedad de proteínas versátiles y polisacáridos secretados localmente por las células adyacentes que son ensamblados de manera muy organizada, aunque esto no le priva de ser una estructura muy dinámica. La variación en su composición determinará, en última instancia, las propiedades de cada tejido.

Hay dos clases principales de macromoléculas que componen la MEC:

1) Los glucosaminoglicanos (GAG), los cuales se pueden encontrar unidos covalentemente a proteínas, llamándose entonces proteoglicanos.
2) Proteínas fibrosas, que a su vez son de dos tipos:
   - Estructurales, como el colágeno o la elastina.
   - Adhesivas, como la fibronectina (FN), la laminina o la tenascina.

Los GAG y PG forman un entramado altamente hidratado a modo de gel en el que las proteínas fibrosas están embebidas. Estos "geles" proporcionan resistencia a fuerzas compresivas, y sirven además como un reservorio de factores de crecimiento (Dallas *et al.*, 1995) y de proteínas morfogenéticas del hueso (Gregory *et al.*, 2005). En cambio, las proteínas fibrosas como el colágeno proporcionan a los tejidos resistencia a fuerzas de tensión, o adhesividad a células y a otras macromoléculas, como en el caso de la FN.

1.2 La molécula de Fibronectina.

La FN es una glicoproteína heterodimérica de unos 450 kDa cuyas cadenas (A y B) están unidas por dos puentes disulfuro en su extremo C-terminal (figura 1). La FN puede presentarse en forma soluble (plasma y otros fluidos) o insoluble (MEC, superficie celular) (Hynes, 1986). La FN está compuesta por repeticiones de tres tipos diferentes de homología estructural denominadas I, II y III, que se distribuyen en regiones o dominios funcionales (figura 1). Estos dominios contienen sitios de unión a otras macromoléculas (como fibrina, heparina/proteoglicanos o colágeno), así como a células.

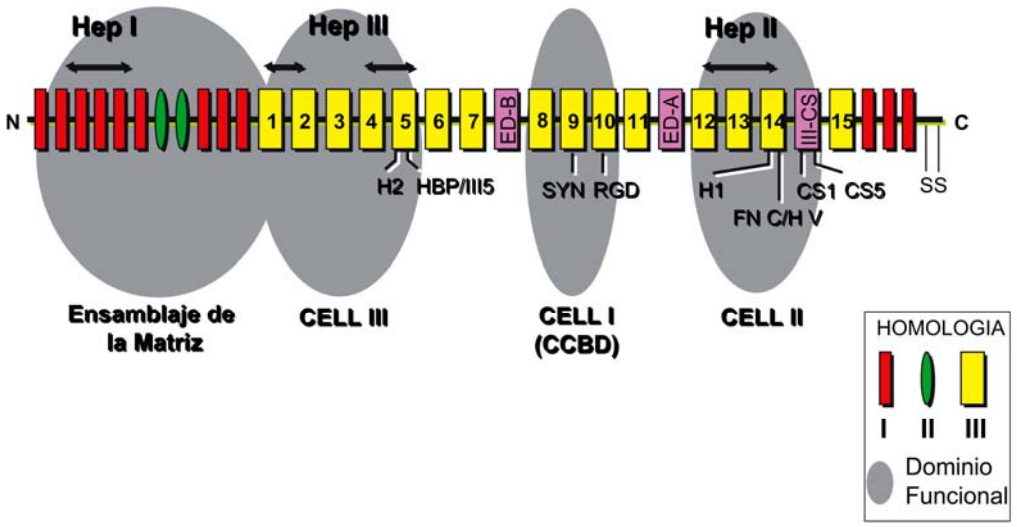

Figura 1. Diagrama de la estructura completa de la molécula de Fibronectina. Los tres tipos de repeticiones estructurales están esquematizadas por pequeños óvalos y rectángulos (ver recuadro), mientras que los dominios funcionales están delimitados por grandes óvalos (ver recuadro). En negrita aparece marcada su funcionalidad y también los sitios funcionales más relevantes de la molécula.

Además, la FN está sujeta a procesos de procesamiento alternativo de ARNm en tres regiones: el extra dominio A (ED-A), el extra dominio (ED-B) y el segmento de conexión tipo III (IIICS) o región V en FN de rata (Schwarzbauer *et al.*, 1983;

Kornblihtt *et al.*, 1985; Schwarzbauer *et al.*, 1987). Las regiones ED-A y ED-B sólo están presentes en FN celular. La región IIICS está presente en ambas cadenas de la FN celular, mientras que sólo está en la cadena A de la FN plasmática. Es más, la región IIICS contiene múltiples sitios de procesamiento alternativo, que dan lugar a varias isoformas que contienen 120, 95, 84, 64 ó 0 aminoácidos, respectivamente en esta región (figura 2). La isoforma de 120 representa la región IIICS completa. La presencia de una u otra isoforma depende de la localización, desarrollo, o de situaciones patológicas. Así, la forma mayoritaria en plasma es la que contiene 89 residuos en la región IIICS (García-Pardo et al., 1987).

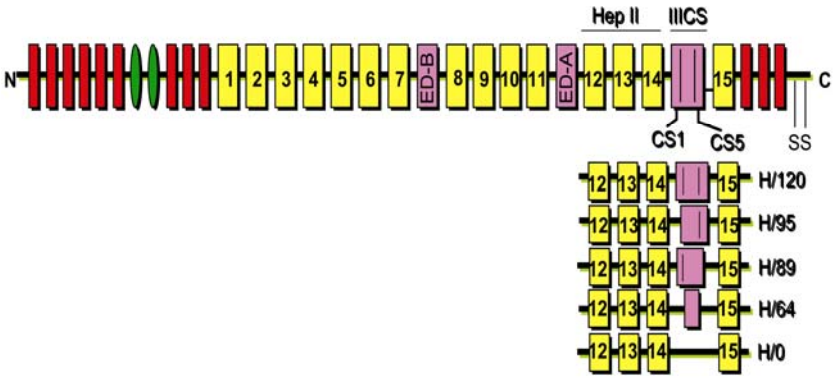

Figura 2. Esquema de los fragmentos recombinantes que contienen las 5 diferentes variantes de *splicing* alternativo de la región HepII/IIICS ("H"). El número asignado a cada variante se refiere al número de aminoácidos que posee la región IIICS. CS1 y CS5 son secuencias reconocidas por la integrina α4β1.

La función principal de la FN es la de mediar adhesión celular. Destaca en este aspecto la región central de la molécula (CCBD, *Central Cell-Binding Domain*), porque contiene el motivo típico de adhesión RGD en la repetición III10 (figura 1), capaz de unir las integrinas α5β1 y αvβ3, entre otras. Si bien dicha secuencia por sí sola es capaz de inhibir adhesión, no lo es tanto de mediarla eficazmente. Para tal fin, requiere el denominado "sitio sinergístico (SYN)", localizado en la repetición III9 (figura 1) y cuya secuencia es PHSRN. Estudios llevados a cabo en nuestro laboratorio demostraron que la integrina α4β1 en estado activado también es capaz de unirse a la secuencia RGD (Sánchez-Aparicio *et al.*, 1994).

Existen otras regiones de interacción con células que se localizan en los dominios de unión a heparina Hep I, Hep II y Hep III. El dominio Hep I interacciona con células a través de receptores no identificados. Además de la capacidad de unirse a heparina, Hep I está implicado fundamentalmente en formación de matrices de FN (Aguirre *et al.*, 1994; Hocking *et al.*, 1994; Christopher *et al.*, 1997).

El dominio Hep II es el que muestra mayor avidez por heparina y también está implicado en fibrilogénesis (Bultmann *et al.*, 1998; Santas *et al.*, 2002). Además Hep II media adhesión celular a través de sitios específicos que unen la integrina α4β1 y/o PG de superficie celular. Estos sitios están localizados en la repetición III14 (figura 1) y corresponden a las secuencias IDAPS (sitio H1) y WQPPRARITGY (Sitio FN-C/H V). IDAPS es un ligando de α4β1 en células de melanoma (Mould and Humphries, 1991) y linfocitos (Domínguez-Jiménez *et al.*, 1996), aunque algunas células hematopoyéticas requieren activación previa de α4β1 para su reconocimiento (Sánchez-Aparicio *et al.*, 1993). La secuencia WQPPRARITGY es capaz de unir proteoglicanos tipo heparán-sulfato (PGHS) e inducir adhesiones focales en fibroblastos adheridos a CCBD a través de α5β1 (Mooradian *et al.*, 1993; Woods *et al.*, 1993). La estructura cristalográfica del dominio Hep II (repeticiones III12-14) muestra sin embargo, que la secuencia IDAPS se halla en la conexión entre las repeticiones III13 y III14, siendo inaccesible a la integrina. Su papel, por tanto, podría ser estabilizar la secuencia WQPPRARITGY, que sí interaccionaría con α4β1, representando un novedoso sitio de interacción con integrinas (Sharma *et al.*, 1999).

Existen otros dos sitios activos de la FN, que se localizan dentro del segmento IIICS adyacente al dominio Hep II (figura 1). Son las secuencias DELPQLVTLPHPNLHGPEILDVPST (sitio CS1) y GEEIQIGHIPREDVDYHLYP (sitio CS5). Ambas secuencias median adhesión celular a través de la integrina α4β1 (y α4β7 para CS1), aunque CS1 se une con mucha mayor afinidad, siendo de hecho el principal ligando de α4β1 (Wayner *et al*., 1989; Guan *et al*., 1990). Más recientemente se ha identificado un nuevo sitio de unión a heparina en la región IIICS, capaz de mediar adhesión de células de melanoma a través de proteoglicanos tipo condroitín-sulfato (PGCS) en cooperación con la integrina α4β1 (Mostafavi-Pour *et al.*, 2001). La relevancia biológica de este sitio es aún desconocida.

El dominio central Hep III, que une heparina sólo a baja concentración de sal, se caracterizó en nuestro laboratorio como una nueva región de adhesión celular (Moyano *et al*., 1997). Dentro de esta región, se identificaron dos secuencias activas KLDAPT (sitio H2) y WTTPRAQITGYRLTVGLTRR (sitio HBP/III5), ambas situadas en la repetición III5 (figura 1). Estas secuencias son estructural y biológicamente homólogas a las secuencias H1 y FN-C/H-V de la repetición III14 antes mencionadas. Al igual que ellas, H2 y HBP/III5 median adhesión de linfocitos y células de melanoma a través de

su interacción con las integrinas α4β1 y α4β7 (H2) y PGCS (HBP/III5) (Moyano et al., 1997, 1999, 2003a, 2003b).

1.3 Formación de la matriz de Fibronectina (fibrilogénesis).

El ensamblaje de la matriz de FN es un proceso activo, que consta de múltiples interacciones con receptores celulares, con componentes de la MEC y con otras moléculas de FN, lo que contribuye a la elongación y estabilización de las fibrillas. Como se muestra en la figura 3, este proceso se compone de varios pasos que conllevan la ruptura de las interacciones intramoleculares FN-FN y el consiguiente estiramiento de la FN, dejando expuestos sitios crípticos de unión a FN que participan en fibrilogénesis (Hynes, 1990; Mosher, 1993; Mao and Schwarzbauer, 2005).

La matriz de FN se encuentra implicada en diferentes procesos biológicos, como adhesión celular, diferenciación y crecimiento. Además establece y mantiene la morfología celular, interviene en procesos de homeostasis y trombosis, reparación de tejidos, transformación oncogénica, cierre de heridas y migración celular (Hynes, 1990; Adams and Watt, 1993; Boudreau and Jones, 1999). Un ejemplo de una de estas implicaciones, es cómo la pérdida de la matriz de FN es una característica de los procesos de transformación y tumorogénesis in vivo. Así el gen supresor de tumores VHL (von Hippel-Lindau) parece que regula la deposición de la matriz extracelular (Ohh *et al.*, 1998) y está implicado en dichos procesos. Está descrito que las células de cáncer renal VHL(-) promueven y mantienen la angiogénesis tumoral permitiendo la infiltración de los tumores a los vasos (Kurban *et al.*, 2006). Uno de los aspectos de esta tesis doctoral ha sido el estudio de las posibles causas que impiden la formación de matrices de FN por células de cáncer renal.

El estiramiento de la FN necesario para su polimerización (ver figura 3), se inicia por la interacción de ésta con receptores de superficie celular, como integrinas y moléculas de masa molecular aparentemente larga (*Large Apparent Molecular Mass molecules*, LAMMs) (McDonald *et al.*, 1987; Zhang and Mosher, 1996) que no han sido identificadas. La principal integrina que media el proceso es α5β1, que reconoce la secuencia RGD, localizada en la repetición III10 de la FN (Fogerty *et al.*, 1990). Otras integrinas que pueden realizar esta función son αvβ3 y αIIβ3, pero sólo bajo determinadas circunstancias. La integrina α4β1 activada también está implicada en este proceso, uniéndose a la región IIICS, siendo esta vía independiente de la de α5β1. La unión FN-receptor provoca la exposición de sitios crípticos que participan en el

autoensamblaje de FN, siendo la interacción receptor-citoesqueleto importantísima para este proceso.

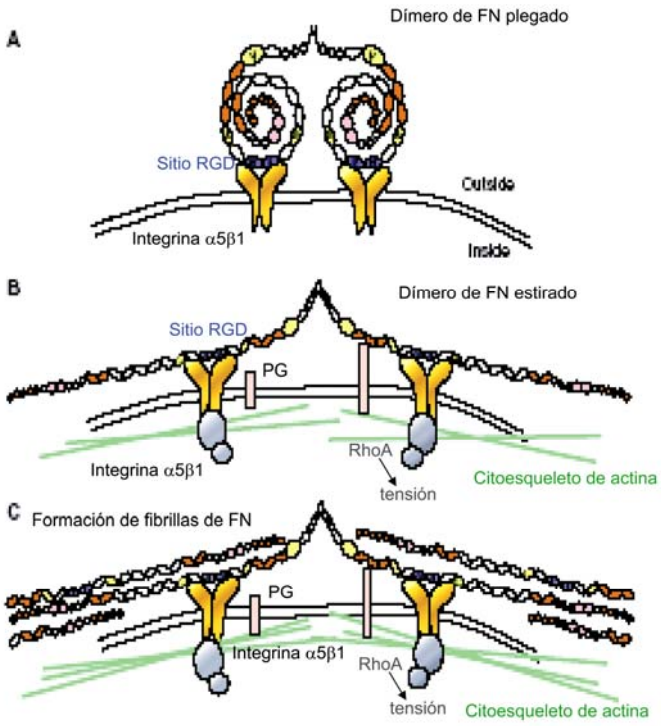

Figura 3. Esquema de la fibrilogénesis de FN. (A): **Paso 1.** Unión de la FN a receptores celulares. (Inicialmente la integrina α5β1). **(B)**: **Paso 2.** Intervienen otros receptores celulares (PG) y se induce una reorganización del citoesqueleto de actina, activándose complejos de señalización intracelular (Ej: RhoA). **(C)**: **Paso 3.** La capacidad de contracción celular, permite un cambio conformacional en la FN, que provoca la exposición de los sitios crípticos de unión a FN, y el autoensamblaje de las moléculas de FN entre sí y con otras proteínas de la MEC (Mao and Schwarzbauer, 2005).

Se han identificado varios dominios de la FN implicados en fibrilogénesis. El más crítico es el dominio de autoensamblaje I1-5, localizado en la región amino terminal de la molécula. Esta región es esencial ya que su pérdida inhibe por completo la fibrilogénesis de FN (Schwarzbauer, 1991). Además, los fragmentos proteolíticos de 29 kDa y 70 kDa, que contienen esta región (ver figura 11, pag 28) bloquean la fibrilogénesis (McKeown-Longo and Mosher, 1985; McDonald *et al.*, 1987). Otras regiones implicadas en el ensamblaje de matriz de FN son las repeticiones III1, III2, III9-10 y III12-14 (McKeown-Longo and Mosher, 1985; Aguirre *et al.*, 1994; Hocking *et al.*, 1994; Bultmann *et al.*, 1998; Sechler *et al.*, 2001; Mao and Schwarzbauer, 2005). Las regiones III1, III2 y III12-14 interaccionan con la región amino terminal (repetición I1-5) y la adición de fragmentos que contiene estas regiones inhiben la formación de las fibrillas de FN (McKeown-Longo and Mosher, 1985; Aguirre *et al.*, 1994; Hocking *et al.*, 1994; Bultmann *et al.*, 1998). Los sitios de unión a FN de la repetición III1 son crípticos (Aguirre *et al.*, 1994), mientras que la actividad del dominio III12-14 parece venir determinada por la región IIICS (Santas *et al.*, 2002). A pesar de que muchas de las regiones de FN que participan en su ensamblaje para formar la matriz, están

identificadas desde hace tiempo, se desconocen por completo los mecanismos que regulan este ensamblaje.

La mayoría de las regiones de FN que participan en fibrilogénesis unen heparina y/o PG (Hynes, 1990). La región III12-14 constituye el dominio de unión a heparina II (Hep II) y la región I1-5 el dominio Hep I (figura 11). La región III1 también une PG (Mercurios and Morla, 2001; Gui *et al.*, 2006) y forma parte del dominio de unión a heparina III (Hep III), que también comprende las repeticiones III4-5 ya mencionadas. Dada la similitud funcional a nivel de adhesión celular entre los dominios Hep III y Hep II, en esta tesis se ha estudiado la posible función de la región III4-5 en fibrilogénesis.

2 Receptores celulares para la matriz extracelular.

2.1 Las integrinas.

El término integrina fue propuesto para describir una familia de receptores integrales de membrana que unían o integraban el citoesqueleto con la matriz extracelular (Hynes, 1987). La expresión de las integrinas se restringe a los metazoos, no encontrándose homólogos en procariotas, plantas u hongos (Hynes and Zhao, 2000; Whittaker and Hynes, 2002). Las integrinas están implicadas en gran diversidad de procesos, y se expresan prácticamente en todos los tejidos y tipos celulares. Estas moléculas, a parte de ser de crucial importancia durante el desarrollo y la homeostasis, tienen un papel esencial en determinados procesos del sistema inmune, tales como la adhesión leucocitaria al endotelio y su posterior extravasación hacia tejidos u órganos linfoides secundarios, recirculación leucocitaria, adhesión a células presentadoras de antígenos, procesos inflamatorios, control del ciclo y de la diferenciación celular entre otros (Hynes, 2002; Kinashi, 2005).

2.1.1 Estructura de las integrinas.

Estructuralmente las integrinas son glicoproteínas transmembrana heterodiméricas de tipo I cuyas subunidades se denominan α (120-180 kDa) y β (90-110 kDa). Ambas subunidades están unidas por enlaces no covalentes y poseen un pequeño dominio citoplásmico, una región transmembrana y un dominio extracelular (Pribila *et al.*, 2004) (figura 4 A).

La subunidad α está compuesta por siete dominios homólogos alrededor de un eje de pseudosimetría (modelo del β-propeller) (Springer, 1997) (figura 4 A y B). De los siete dominios homólogos, los últimos cuatro (o tres en algunas integrinas) del extremo

amino terminal están implicados en coordinar la unión de cationes, mediante motivos similares al *EF-hand*. Al menos 8 subunidades α contienen en su tercio amino terminal una inserción de unos 200 residuos entre las repeticiones 2 y 3, conocida como dominio I (insertado). El dominio I es homólogo al dominio A del factor de Von Willebrand, por lo que también se le llama dominio de tipo A de la subunidad α (dominio αA) (figura 4 A).

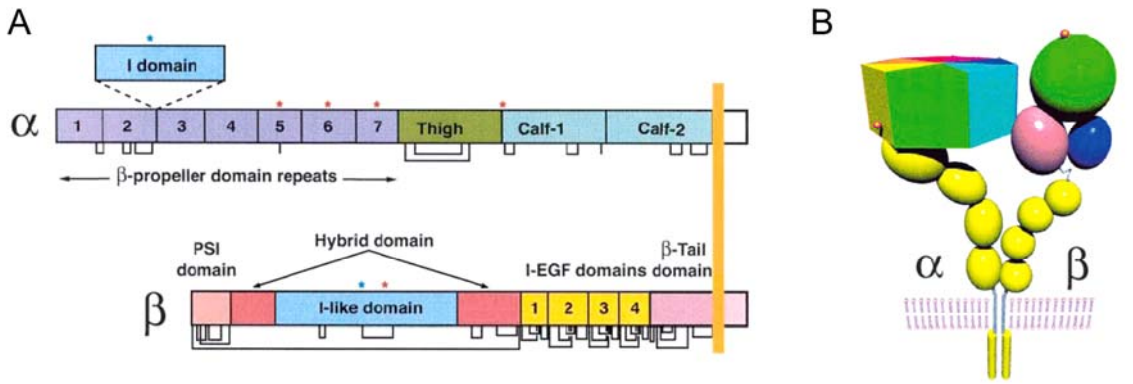

Figura 4. **Estructura de las integrinas. A)** Organización por dominios de la estructura primaria de una integrina. Los asteriscos en azul indican sitios de unión de Mg^{2+} y los rosas de unión de Ca^{2+}. Las líneas muestran puentes disulfuro. **B**) Estructura tridimensional de una integrina. La subunidad α muestra en diferentes colores los 7 dominios del β-propeller, empezando por el verde y terminando en el amarillo, bajo éste emergen 4 módulos de láminas-β (ovoides amarillos). En la subunidad β, el dominio A está representado en verde, seguido de una zona poco conocida (rosa) junto al dominio PSI (plexinas, semaforinas e integrinas) en azul, emergiendo debajo los 4 módulos similares a EGF (bolas amarillas). Los sitios de unión a cationes se representan con bolitas naranjas (Takagi *et al.,* 2002; Humphries, 2000).

La subunidad β contiene cuatro repeticiones ricas en cisteínas con homología a los módulos de EGF (factor de crecimiento epidérmico) en su parte carboxilo terminal y una serie de plegamientos en el extremo amino terminal, producidos por puentes disulfuro, con estructura similar al dominio A (dominio hibrido). La región que interactúa con el ligando es altamente conservada y susceptible de unir cationes. De esta forma, parte del dominio A de la subunidad α, que contiene repeticiones que unen cationes, podría interactuar con el dominio A de la subunidad β formando un complejo entramado de sitios de coordinación de cationes, bautizado como el sitio de adhesión dependiente de iones metálicos (*metal ion-dependent adhesion site*, MIDAS) (Lee *et al.*, 1995).

Las colas citoplasmáticas de ambas subunidades son bastante cortas, de unos 40 aminoácidos, a excepción de la subunidad β4 que se extiende unos 1000 residuos hacia el interior de la célula. A pesar de ello, están directamente implicadas en la modulación de la afinidad de las integrinas, así como en señalización intracelular.

Por tanto, en la interacción de las integrinas con el ligando, intervienen tres regiones, dos en la subunidad α: 1) el motivo similar a *EF-hand* en la mitad N-terminal de la subunidad α y 2) el dominio en el extremo N-terminal de la subunidad α (*β-propeller*) y una tercera localizada en la subunidad β, en el dominio-A (dominio híbrido).

2.1.2 Clasificación de las integrinas.

Actualmente se conocen 18 subunidades α y 8 subunidades β, cuya combinación da lugar al menos a 24 integrinas diferentes (Hynes, 2002; Kinashi, 2005; Kinashi and Katagiri, 2005). La subunidad α es la que confiere a la integrina la especificidad de unión al ligando, agrupando a las integrinas en cuatro grupos: aquellas que reconocen la secuencia RGD en moléculas como la FN, las que median adhesión por el reconocimiento de las lamininas en la membrana basal, las que reconocen el colágeno y por último las que su expresión está restringida a leucocitos (Plow *et al.*, 2000). En función de la subunidad β, las integrinas se pueden clasificar en cuatro subfamilias: 1) La subfamilia β1 o VLA (*Very Late activation Antigens*) que comprende 12 heterodímeros que comparten la subunidad β1 (CD29) (α1-α11β1 y αvβ1) y reconocen principalmente proteínas de la MEC. 2) La subfamilia β2 (CD18) o integrinas específicas de leucocitos, se compone de 4 miembros. 3) La subfamilia β3 o citoadhesinas, y 4) la subfamilia β7 (α4β7 y αEβ7), que se expresa fundamentalmente en linfocitos y está implicada en el alojamiento (*homing*) de estas células. Todas estas combinaciones de subunidades de las integrinas se muestran en la figura 5.

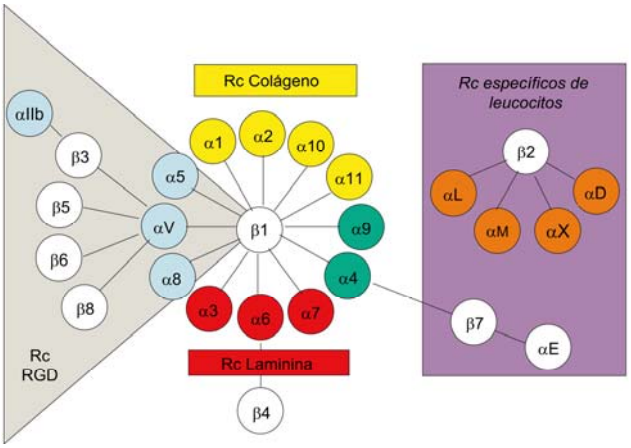

Figura 5. Esquema de la familia de las integrinas en mamiferos. Se muestran las posibles combinaciones entre las subunidades α y β (Hynes, 2002). Cada subunidad β se puede unir a varias subunidades α. Las integrinas marcadas en amarillo se unen a colágeno; las marcadas en rojo son receptores de la laminina; las marcadas en azul reconocen la secuencia RGD presente en la fibronectina y en la vitronectina, y las integrinas de expresión restringida a leucocitos están marcadas en naranja. Abrev. Rc: receptores.

2.1.3 Regulación de las integrinas.

La actividad biológica de las integrinas está altamente regulada y se han descrito numerosos procesos tanto de activación como de desactivación de las mismas. La actividad de las integrinas, ésto es su capacidad para unirse al ligando, puede inducirse por estímulos intracelulares recibidos a través de otros receptores de la superficie celular, lo que se conoce como señalización *inside-out* (desde dentro hacia fuera) o por estímulos procedentes del medio extracelular o señalización *outside-in* (desde fuera hacia dentro) (Carman and Springer, 2003).

La activación desde el interior al exterior (*inside-out)* puede venir producida por quimioquinas (Ej: SDF-1α), por la unión de otros ligandos a sus correspondientes receptores (como factores de crecimiento, interleuquinas o incluso ligandos de otras integrinas), o por tratamientos con ésteres de forbol (Ej: PMA o PdBU) que activan la PKC, la cual modula la activación de las integrinas (Hynes, 1992; Dedhar, 1999; Schwartz and Ginsberg, 2002).

En el laboratorio, se puede inducir la activación de las integrinas desde fuera a dentro (*outside-in*) por varios métodos, entre los que destacan la utilización de Acms (como TS2/16, dirigido frente a la subunidad β1) (Arroyo *et al.*, 1992; Arroyo *et al.*, 1993) o de algunos cationes, como Mn^{2+} o Mg^{2+} (mientras que el Ca^{2+} suele inhibir la activación). Desde hace tiempo se ha utilizado el Mn^{2+} como activador de integrinas. Mould et al., (2002) demostraron que la activación inducida por Mn^{2+} conduce a un cambio conformacional en la hélice α1 del dominio-A de la subunidad β, equiparable al de una activación fisiológica producida por señalización del tipo *inside-out*. Estas activaciones por modulación del entorno catiónico son dependientes del tipo celular, estado y naturaleza del ligando. Los cambios conformacionales son necesarios para la interacción con el ligando, tras la cual se inician una serie de cascadas de señalización de fuera hacia el interior (*outside-in*) implicadas en numerosos procesos como *anoikis*, o migración celular (Dedhar, 1999).

La actividad adhesiva de las integrinas se regula mediante cambios en la afinidad y/o avidez de la integrina (Hughes and Pfaff, 1998; Liddington and Ginsberg, 2002; Carman and Springer, 2003). Las variaciones en la afinidad pueden ser el resultado de cambios conformacionales de la integrina que poseen su origen en la porción citoplásmica de la misma, y que resultan en alteraciones del sitio de unión del ligando (Chan *et al.*, 2003; Kinashi, 2005). Así, cuando las integrinas están en una

conformación inactiva, de baja afinidad por sus ligandos, las colas citoplásmicas de las cadenas α y β están interaccionando entre sí. Esto hace que los dominios extracelulares se encuentren "doblados", con una topología en forma de V invertida, que impide la interacción con el ligando (figura 6). Ciertas proteínas citoplásmicas, especialmente la talina, son capaces de romper la interacción entre las dos colas citoplásmicas de las integrinas, separándolas y produciendo un despliegue de las regiones extracelulares que conduce a una conformación activa de la integrina con alta afinidad por sus ligandos (Emsley *et al.*, 2000; Xiong *et al.*, 2001; Liddington and Ginsberg, 2002; Takagi *et al.*, 2002; Vinogradova *et al.*, 2002; Carman and Springer, 2003; Kim *et al.*, 2003). El estado de alta afinidad de las integrinas también puede inducirse *in vitro* mediante la exposición a cationes divalentes como Mn^{2+} o Mg^{2+} (Jakubowski *et al.*, 1995; Stewart and Hogg, 1996).

La activación de las integrinas también se produce por cambios en la avidez, que implican la agrupación o *clustering* de integrinas sin que se produzcan cambios en la afinidad (Hynes, 1992; Hughes and Pfaff, 1998). Estos cambios ocurren gracias a la fluidez de la membrana plasmática que incrementa la densidad de receptores en una determinada zona, permitiendo así la formación de interacciones adhesivas multivalentes entre las integrinas y sus ligandos, y dando como consecuencia una mayor fuerza adhesiva conjunta. El aumento de la avidez de las integrinas puede inducirse también *in vitro* mediante la presencia de ésteres de forbol (Chan and Cybulsky, 2004). En este aumento de la avidez pueden estar implicadas ciertas proteínas de la familia de las RasGTPasas, en concreto Rap1 y Rap2 (Katagiri *et al.*, 2003; Katagiri *et al.*, 2004), aunque éstas también regulan la afinidad de las integrinas.

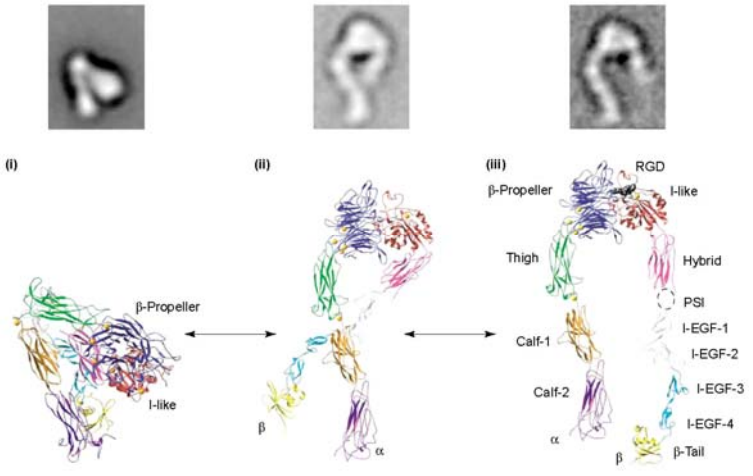

Figura 6. Cambios conformacionales de las integrinas asociados con la regulación de la afinidad. Modelo de regulación del estado de afinidad de las integrinas en el que se observa la transición desde un estado de baja afinidad o conformación "doblada" **(I)** a un estado de alta afinidad o conformación "extendida" **(III)** (Carman and Springer, 2003).

2.1.4 La integrina α4β1 (VLA-4, CD49d/CD29).

La integrina α4β1 es el principal receptor de adhesión en células del sistema inmune, principalmente en leucocitos, junto a α4β7 (Hynes, 1992; Shimizu *et al.*, 1999). Es la integrina que más se expresa en linfocitos (T y B), aunque también se expresa en monocitos, basófilos, eosinófilos, mastocitos, timocitos y progenitores hematopoyéticos (Lobb and Hemler, 1994; Rose *et al.*, 2002), así como en otros tipos celulares, como células derivadas de la cresta neural (Bednarczyk and McIntyre, 1992; Issekutz *et al.*, 1996). Se expresa notablemente en algunas células tumorales no-hematopoyéticas, como células de melanomas o de rhabdomiosarcoma, mientras que en otros tipos celulares, sobre todo adherentes, está ausente o se expresa minoritaria y/o temporalmente.

La subunidad α4 (CD49d) es una glicoproteína transmembrana de 999 aminoácidos y carece de dominio I (Takada *et al.*, 1989; Hemler *et al.*, 1990). La región extracelular (N-terminal) contiene tres sitios de unión a cationes divalentes, 12 sitios de N-glicosilación y 24 residuos de cisteína con capacidad de formar puentes disulfuro intracatenarios. El gen de α4 codifica para una proteína de 150 kDa (Takada *et al.*, 1989), la cual puede degradarse en dos fragmentos de 80 kDa (amino terminal) y 70 kDa (carboxilo terminal) por proteolisis en la zona central de la molécula, en vez de en el extremo carboxilo terminal, como en otras subunidades α (Teixidó *et al.*, 1992). Esta degradación no afecta a la totalidad de las moléculas de α4. Además de estas dos formas, se ha identificado otra de 180 kDa, aunque su presencia no es constante (Hemler *et al.*, 1990; Teixidó *et al.*, 1992; Teixidó and Sánchez-Madrid, 1993). El dominio citoplasmático de α4 es crucial en la regulación de su actividad y en la especificidad en la adhesión celular, requiriéndose la presencia de una secuencia mínima, aunque no específica, de aminoácidos tras el motivo GFFKR del dominio citoplasmático (Kassner and Hemler, 1993; Kassner *et al.*, 1994).

La subunidad β1 (CD29) es también una glicoproteína transmembrana de 778 aminoácidos (Takada *et al.*, 1989) y se caracteriza por tener una región rica en cisteínas en el extremo C-terminal de la parte extracelular (probablemente formando puentes disulfuro) formada por cuatro dominios homólogos al EGF. En el extremo N-terminal (extracelular) se encuentra una región altamente conservada, implicada en el reconocimiento del ligando, así como un dominio de unión a cationes divalentes (Hemler *et al.*, 1990), formando junto a la subunidad α el sitio MIDAS ya mencionado.

Papel de α4β1 en procesos biológicos.

Además de ser un receptor para los varios sitios de FN ya mencionados (CS1, CS5, H1 y H2) (Wayner *et al.*, 1989; García-Pardo and Ferreira, 1990; Guan and Hynes, 1990; Mould *et al.*, 1991; Moyano *et al.*, 1999), la integrina α4β1 interacciona también con la proteína del endotelio VCAM-1 (*Vascular Cell Adhesión Molecule)* (Elices *et al.*, 1990) (figura 7). VCAM-1 es una glicoproteína de membrana perteneciente a la superfamilia de las inmunoglobulinas, y su expresión puede inducirse por factores como TNF-α, IL-1, IL-4 e IL-13 (Osborn *et al.*, 1989; Neish *et al.*, 1992; Swerlick *et al.*, 1992; Sironi *et al.*, 1994). Estructuralmente VCAM-1 está compuesta por 7 repeticiones de dominios de inmunoglobulinas, aunque como consecuencia del *splicing* alternativo es expresada en formas de 6 y 8 dominios. Los dominios 1 y 4 son los responsables del reconocimiento de la integrina α4β1. También se ha descrito que VCAM-1 puede interaccionar con las integrinas αDβ2 y α9β1 (Grayson *et al.*, 1998; Taooka *et al.*, 1999).

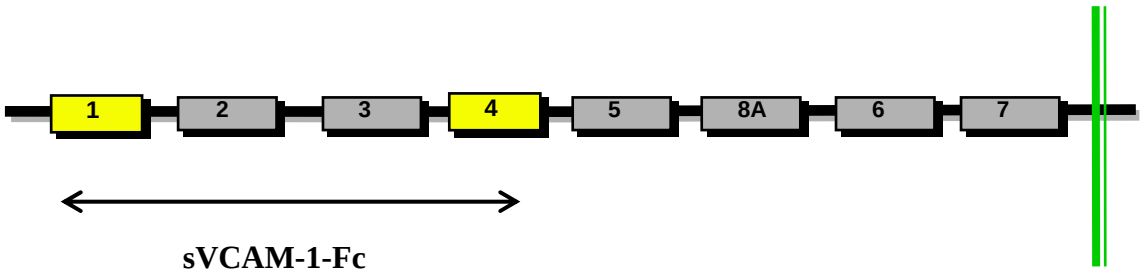

Figura 7. **Estructura de la proteína endotelial VCAM-1.** Posee 8 dominios de tipo inmunoglobulina, de los cuales los dominios 1 y 4 (en amarillo) son los responsables del reconocimiento de la integrina α4β1. En este trabajo se ha utilizado una forma recombinante soluble de VCAM-1 humano (sVCAM-1-Fc), que contiene los dominios del 1 al 4 fusionados con la región Fc de la IgG1 humana.

También se han identificado otros ligandos de α4β1 como el propolipéptido del factor de von Willebrand (Isobe *et al.*, 1997), la proteína bacteriana invasina (Isberg and Leong, 1990), trombospondina (Yabkowitz *et al.*, 1993) y osteopontina (Bayless *et al.*, 1998). También se ha descrito la posibilidad de que α4β1 medie adhesión célula-célula (Campanero *et al.*, 1990; Altevogt *et al.*, 1995; Humphries et al., 2007).

Las integrinas α4 están implicadas en numerosas funciones del sistema inmunitario, tales como el rodamiento y adhesión fuerte de leucocitos sobre el endotelio (Alon *et al.*, 1995; Johnston *et al.*, 1996), el reclutamiento de leucocitos a sitios de

inflamación, y el control de la migración linfocitaria (Butcher and Picker, 1996). Por tanto, juega un papel importante en patologías inflamatorias o autoinmunes (Lobb and Hemler, 1994; Rose *et al.*, 2002). Por su capacidad de mediar adhesión, migración y de regular la apoptosis celular, α4β1 juega también un papel importante en la migración e invasión de órganos de ciertos tumores hematopoyéticos, como la leucemia mieloide crónica (Verfaillie *et al.*, 1992), el mieloma múltiple (Uchiyama *et al.*, 1992; Uchiyama *et al.*, 1993) o la leucemia linfocítica crónica (García-Gila et al., 2002; de la Fuente *et al.*, 1999, 2002). Asimismo, la ligación de la integrina α4β1 regula la proliferación de células progenitoras hematopoyéticas (Hurley *et al.*, 1995), la eritropoyesis (Sadahira *et al.*, 1995) y el desarrollo embrionario (Yang *et al.*, 1995). Por último la integrina α4β1 provee de señales coestimuladoras para la activación y diferenciación de las células T y participa en la interacción de las células T con las células presentadoras de antígeno (Mittelbrunn *et al.*, 2004; Pribila *et al.*, 2004). La regulación de la actividad de α4β1 es por lo tanto crucial para el desarrollo y función del sistema inmune y su estudio ha sido uno de los objetivos de esta tesis doctoral.

2.2 Los proteoglicanos.

Existen 2 tipos de proteoglicanos: los asociados a la MEC y los presentes en superficie celular. Los PG de superficie celular son principalmente de dos tipos, heparán-sulfato (PGHS) y condroitín-sulfato (PGCS) y su distribución es variada, encontrándose en numerosas células, incluyendo linfocitos, células epiteliales o fibroblastos.

Una de las principales funciones de los PG de superficie celular es la de cooperar con otros receptores, fundamentalmente con integrinas. La función de las integrinas generalmente está complementada y modulada por otros receptores que actúan en *cis*, formando complejos receptores (Porter and Hogg, 1998). Durante los últimos años se ha estudiado extensamente el papel que ejercen los PG como co-receptores de integrinas y las rutas señalizadoras que llevan asociadas. Existen dos tipos de colaboración integrina-PG bien estudiados: la cooperación de α5 con PGHS y la cooperación de α4 con PGCS. Respecto a la primera, se ha visto que los PGHS, fundamentalmente el sindecano 4, se localizan en adhesiones focales formadas por fibroblastos junto a las integrinas, y se requieren para la formación de estas estructuras (Woods and Couchman, 1998; Mostafavi-Pour *et al.*, 2003; Midwood *et al.*, 2006). Los sindecanos señalizan a través de la PKC y son capaces de activar la pequeña GTPasa Rho (Woods and

Couchman, 1992; Saoncella *et al.*, 1999). Con respecto a la colaboración α4-PGCS, la adhesión a través de α4β1 a fragmentos recombinantes de la FN que contienen el dominio Hep II y las diferentes formas de procesamiento alternativo de IIICS (incluido el sitio CS1) está modulada por PGCS (Iida *et al.*, 1992; Beauvais-Jouneau *et al.*, 1997). Esta regulación se produce a través de una secuencia de aminoácidos existente en la integrina α4β1, denominada SG1 (KKEKDIMKKTI) que une directamente PGCS, afectando a las propiedades de unión a ligando de dicha integrina (Iida *et al.*, 1998). Además se ha visto que es necesaria la cooperación entre la integrina α4β1 activada por Mn^{2+} y el PGCS para que se produzca la adhesión al fragmento recombinante FNIII4-5 de la FN (Moyano *et al.*, 1999). Otro ejemplo de esa colaboración es entre α4β1 y el PG NG2 (Iida et al., 1995). El complejo α4β1/NG2 activa a la RhoGTPasa Cdc42, que a su vez activa a la tirosín quinasa Ack-1, fosforilando a p130Cas, la cual esta implicada en motilidad e invasividad tumoral (Eisenmann *et al.*, 1999).

3. Relación matriz extracelular- citoesqueleto.

En general, las integrinas deben estar unidas al citoesqueleto para ejercer sus funciones en el interior de la célula (Ej: señalización intracelular), pero esta unión no es directa: el puente de unión entre el exterior (integrinas) y el interior (citoesqueleto, citoplasma) consiste en el reclutamiento de numerosas proteínas que interaccionan entre sí. Entre las proteínas que unen la integrina α4β1 al citoesqueleto, están talina, α-actinina, vinculina y paxilina. El reclutamiento de estas proteínas da lugar a una cadena de transducción de señales de manera bidireccional y a unas estructuras macromoleculares que se localizan en regiones de adhesión al substrato y que están perfectamente orquestadas con funciones tanto de soporte como señalizadoras. Estas estructuras suelen asociarse con filamentos de actina y otras proteínas asociadas como miosina, proporcionando una gran capacidad plástica a la célula. Se pueden englobar en cuatro grandes clases: adhesiones (o contactos) focales, adhesiones fibrilares (o contactos MEC), complejos focales y podosomas (Chen *et al.*, 1985; Singer *et al.*, 1988; Zamir *et al.*, 1999; Geiger *et al.*, 2001).

La interacción integrina-MEC también genera señales intracelulares además de mecanismos sensoriales capaces de detectar las fuerzas de tensión mecánica en el entorno celular, determinando cambios fisiológicos en última instancia también mediante señalización (Ingber, 1999). Entre estos procesos destacan algunos tan

importantes como supervivencia, crecimiento, diferenciación y motilidad celular (Dedhar, 1999; Giancotti and Ruoslahti, 1999; Schwartz and Ginsberg, 2002).

Por otro lado, la adhesión celular mediada por la integrina α4 suele asociarse en algunos casos con una función opuesta al resto de las integrinas, aumentando la migración celular e inhibiendo la extensión celular y la formación de adhesiones focales, regulando por tanto el citoesqueleto (Chan *et al.*, 1992; Hemler *et al.*, 1992).

II. Mecanismos moleculares que regulan la reorganización del citoesqueleto

4. Las GTPasas.

Las GTPasas son proteínas monoméricas con un tamaño comprendido entre 20 y 40 KDa y que han sido identificadas en organismos eucariotas desde levaduras a humanos. Existen más de 100 miembros de GTPasas formando la denominada superfamilia Ras. Esta superfamilia se divide a su vez en 5 familias: Ras, Rho, Rab, Sar1/Arf y Ran (Bar-Sagi and Hall, 2000). Estas proteínas presentan dos conformaciones: la inactiva, en la que se encuentran unidas a nucleótidos de guanosina difosfato (GDP) y la activa, en cuyo caso tienen unidos nucleótidos de guanosina trifosfato (GTP). El ciclo de activación e inactivación de las GTPasas está regulado por los siguientes 3 tipos de moléculas (figura 8):

1) Los factores de intercambio de nucleotidos de guanina (GEF, *guanosine nucleotide exchange factor*), los cuales catalizan el intercambio de GDP por GTP, facilitando la salida del GDP por desestabilización tanto del nucleótido unido como del Mg^{2+} (Zhang *et al.*, 2000), lo que conduce a la activación de la GTPasa.

2) Proteínas denominadas GAP (*GTPase-activating protein*), que activan la hidrólisis del GTP mediante la actividad GTPasa (Schmidt and Hall, 2002; Schmidt *et al.*, 2002; Bernards and Settleman, 2004), lo que se traduce en su inactivación, ya que el GDP bloquea el centro catalítico.

3) Proteínas reguladoras denominadas GDI (*GDP-dissociation inhibitor*), que inhiben el intercambio de GDP por GTP, manteniendo a la GTPasa en su estado inactivo, e inhibiendo por tanto la disociación del GDP (Schwartz and Shattil, 2000; Takai *et al.*, 2001).

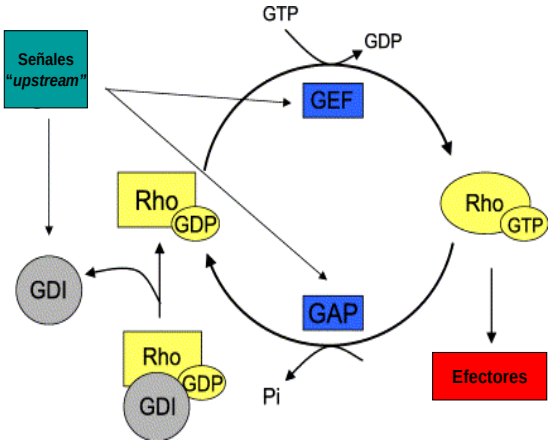

Figura 8. Ciclo de activación y desactivación de las GTPasas de la familia Rho. Las proteínas GEF favorecen el intercambio de GDP por GTP, llevando a la activación de la GTPasa, la cual actuará sobre efectores *downstream*. Las proteínas con actividad GAP hidrolizan el GTP conduciendo a la inactivación de la GTPasa. Las proteínas GDI inhiben el intercambio de GDP por GTP. Las proteínas que regulan la actividad de las GTPasas Rho pueden a su vez ser activadas por moléculas *upstream* (Raftopoulou and Hall, 2004).

4.1. Las RhoGTPasas y su relación con el citoesqueleto.

Las GTPasas de la familia Rho fueron descubiertas por su homología con Ras (*Ras HOmology*) (Madaule and Axel, 1985). La familia Rho está formada por 20 miembros distintos, 10 de los cuales se encuentran en mamíferos, siendo los más estudiados tres, Rho, Rac y Cdc42 (Wherlock and Mellor, 2002). En base a sus funciones y secuencia, los miembros de la familia Rho se han clasificado en 5 subfamilias y 3 miembros independientes (figura 9) (Burridge and Wennerberg, 2004).

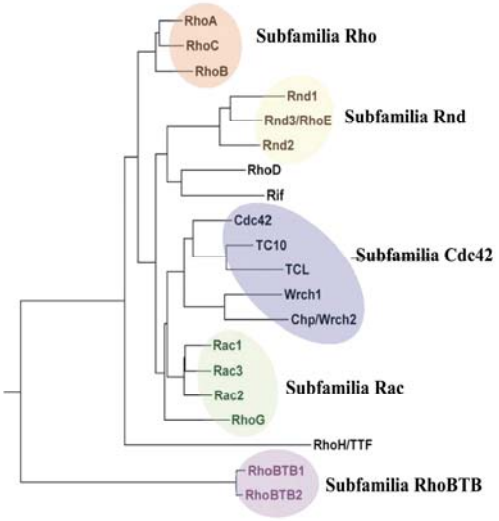

Figura 9. Clasificación de los miembros de las GTPasas de la familia Rho (Burridge and Wennerberg, 2004)

Las proteínas de la subfamilia Rho contribuyen a la contractilidad, y en concreto, RhoA es esencial para la formación de fibras de estrés y adhesiones focales. Las proteínas de la subfamilia Rac, en concreto Rac1, están asociadas a la formación de ondulaciones en la membrana o lamelipodios. Cdc42 un miembro de la subfamilia del mismo nombre promueve la formación de filopodios, que son como espículas que sobresalen del cuerpo celular (Nobes and Hall, 1995). Las proteínas de la subfamilia Rnd tienen dominios GTPasa constitutivamente activos y aparentemente antagonizan la

señalización de las proteínas de la subfamilia Rho. La función de las proteínas pertenecientes a la subfamilia RhoBTB es aún desconocida. Gran parte de los estudios realizados sobre la función de las GTPasas se centran en células adherentes, que presentan características citoesqueléticas completamente distintas a los linfocitos T utilizados en esta tesis, donde destaca la ausencia de fibras de estrés.

Existen diversos estímulos capaces de desencadenar la activación de las GTPasas Rho, entre ellos varias quimioquinas y diversos factores de crecimiento, como PDGF, EGF y TGF-β1 (Laudanna *et al.*, 1996; Soede *et al.*, 2001; Edlund *et al.*, 2002; Bartolome *et al.*, 2003). También se ha descrito que la unión de diversos receptores de adhesión (cadherinas, integrinas y miembros de la superfamilia de las inmunoglobulinas) con sus ligandos pueden regular el estado de activación de estas GTPasas (Braga, 2002; DeMali *et al.*, 2003).

Las GTPasas Rho activas interaccionan con diversas moléculas efectoras, a través de las cuales ejercen sus acciones (Burridge and Wennerberg, 2004). Entre éstas se incluyen la regulación de la migración y adhesión celular tras la reorganización del citoesqueleto de actina, la regulación de la transcripción génica, del ciclo celular y del tráfico membranal (Laudanna *et al.*, 1997; D'Souza-Schorey *et al.*, 1998; del Pozo *et al.*, 1999; Burridge and Wennerberg, 2004). Por tanto, las GTPasas de la subfamilia Rho tienen una gran importancia en muchos procesos fisiológicos como la reparación de heridas, contracción muscular, o mantenimiento de la morfología celular. También intervienen en algunas situaciones patológicas como la invasión tumoral o la artritis reumatoide (Etienne-Manneville and Hall, 2002).

Se ha sugerido que las proteínas Rac juegan un papel clave en la extensión del frente de avance de la célula, mientras que las proteínas Rho participarían en la retracción del urópodo (Worthylake and Burridge, 2001; Xu *et al.*, 2003; Vicente-Manzanares and Sánchez-Madrid, 2004). Todos los miembros de la subfamilia Rac, estimulan la formación de lamelipodios u ondulaciones de membrana, controlando por tanto procesos de adhesión y migración celular a través del remodelado del citoesqueleto de actina (Ridley *et al.*, 1992), aunque no puede descartarse que regulen la adhesión celular independientemente de este proceso. RhoA controla el citoesqueleto de actina fundamentalmente a través de la serín-treonín quinasa ROCK (Amano *et al.*, 2000), mientras que Rac estabiliza los filamentos de actina a través de las serín-treonín quinasas PAK, PI(4)5K y WAVE (Burridge and Wennerberg, 2004).

4.2 La proteína p190RhoGAP.

En la presente tesis doctoral se ha estudiado uno de los GAP de las RhoGTPasas, la proteína p190RhoGAP. P190RhoGAP es una proteína de 190 KDa que se fosforila en tirosinas. Se la asocia con la F-actina tras la ligación o activación de integrinas β1 (Nakahara *et al.*, 1998; Arthur and Burridge, 2001). En humanos existen dos formas homólogas, p190-A y p190-B, que contienen un dominio N-terminal GTPasa y un dominio C-terminal RhoGAP. Hemos estudiado la forma p190-A porque *in vivo* demostraba preferencia sólo por RhoA (Ridley *et al.*, 1993). La actividad RhoGAP está regulada por fosforilación, por estimulación a través de factores de crecimiento o por adhesión celular. Los residuos de tirosinas de la porción central de p190 son fosforilados por quinasas (como c-Src) (Haskell *et al.*, 2001), dando lugar a un cambio conformacional en p190 que promueve su actividad GAP, disminuyendo por tanto los niveles de RhoA e inhibiéndose la señalización a proteínas efectoras. Esto sucede por ejemplo en células de melanoma, donde tras la señalización mediada por la integrina α4β1, la fosforilación de p190 inactiva RhoA y ésto se traduce en la inducción de protusiones citoplasmáticas y migración celular (Moyano *et al.*, 2003b).

5. La proteína Pyk-2 (Proline-rich tyrosine kinase 2).

Pyk-2 es una tirosín quinasa citoplásmica perteneciente a la familia de la *Focal Adhesión Kinase* (FAK), cuya expresión está restringida a las células hematopoyéticas, neuronales y de origen epitelial (Avraham *et al.*, 1995; Lev *et al.*, 1995; Yu *et al.*, 1996). Pyk-2 también se conoce como *RAFTK, CAKβ, CADTK o FAK2.*

La organización estructural que presenta Pyk-2 es similar a la de FAK (figura 10), la cual da nombre a la familia. Pyk-2 posee un extremo amino terminal donde se encuentra el dominio de tipo Banda 4.1, un dominio central donde reside la capacidad tirosín quinasa, y un extremo carboxilo terminal rico en prolinas y con una región FAT *(Focal Adhesión Targeting sequence)* (Avraham *et al.*, 2000). Pyk-2 carece de dominios SH2 y SH3 y de los sitios de miristoilación característicos de otras tirosín quinasas, pero contiene sitios de unión a los dominios SH2 y SH3 de otras proteínas, como al sitio SH2 de la subunidad reguladora p85 de la PI3K (fosfatidilinositol-3-quinasa) (Toker and Cantley, 1997). Además posee cuatro tirosinas situadas en las posiciones 402, 579, 580 y 881, y se autofosforila en la tirosina en la posición 402.

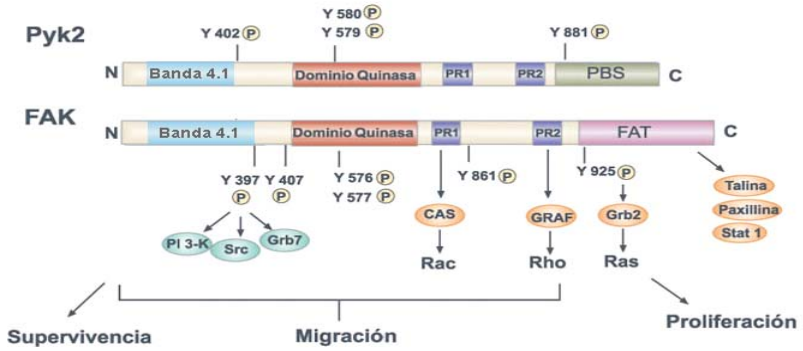

Figure 10. Estructura y función de los miembros de la familia FAK. La familia de las tirosín quinasas FAK está compuesta por 2 miembros FAK (panel inferior) y Pyk-2 (panel superior).

Pyk-2 es estimulada por varios tipos de receptores entre los que se encuentran los receptores de quimioquinas, el TCR y las integrinas (Dikic *et al.*, 1996; Ganju *et al.*, 1998; Katagiri *et al.*, 2000). Cuando Pyk-2 está activado, se autofosforila en la tirosina 402, la cual se une a c-Src a través del dominio SH2 de ésta, lo que conlleva la activación de Src. Cuando Src está activo fosforila a Pyk-2 en las Tirosinas 579 y 580, lo que aumenta la actividad de Pyk-2 (Sanjay *et al.*, 2001) y le permite regular numerosas funciones. Una de las características más importantes de Pyk-2 es que tras su activación, Pyk-2 puede interaccionar con múltiples moléculas, entre las que se encuentran proteínas de anclaje como p130Cas, otras tirosín quinasas como miembros de la familia Src y proteínas citoesqueléticas, como paxilina (Ostergaard *et al.*, 1998; Rodríguez-Fernández *et al.*, 1999) y talina. El hecho de que Pyk-2 se una a proteínas citoesqueléticas o se re-distribuya durante el spreading celular inducido por las integrinas (Vicente-Manzanares and Sánchez-Madrid, 2004), sugiere la implicación de Pyk-2 en motilidad celular. Se ha relacionado a Pyk-2 con la inducción de polarización celular en células T (Rodriguez-Fernández *et al.*, 2001), y se ha comprobado que en células NK está asociada a la proteína Vav, que es un GEF de la RhoGTPasa Rac, (Gismondi *et al.*, 2003). También se conoce que Pyk-2 es el enlace entre la adhesión mediada por integrinas y las RhoGTPasas (Wittchen *et al.*, 2005) y que se fosforila tras la interacción α4β1-VCAM-1 o α4β1–Acs anti-α4 (van Seventer *et al.*, 1998; Gismondi *et al.*, 2003). Otras de las funciones reguladas por Pyk-2 son: modulación de canales iónicos (Lev *et al.*, 1995), activación de la cascada MAP kinase (Dikic *et al.*, 1996), regulación de la apoptosis (Xiong and Parsons, 1997; Zhao *et al.*, 2000), y regulación del citoesqueleto celular (Okigaki *et al.*, 2003). Pyk-2 juega por tanto un papel central en la ruta de señalización de las integrinas. Debido a estas características y a su relación con la activación de la integrina α4β1, Pyk-2 ha sido objeto de estudio en la presente tesis doctoral.

Objetivos

1. ***Estudiar el efecto de los varios estímulos que activan la integrina $\alpha 4\beta 1$ en la reorganización del citoesqueleto de actina, inducida tras la adhesión celular a sus diferentes ligandos.***

2. ***Determinar si existe una señalización intracelular dependiente del estímulo que activa la integrina $\alpha 4\beta 1$ y de la respuesta celular que origine.***

3. ***Determinar el posible papel del dominio de unión a heparina III (Hep III) de fibronectina (ligando de $\alpha 4\beta 1$) en la formación de matrices de fibronectina. Estudiar la relevancia fisiológica de estas matrices.***

Materiales y Métodos

Células y cultivos celulares.

Los linfoblastos T humanos fueron aislados a partir de células mononucleares de sangre periférica de donantes sanos mediante gradientes de Ficoll-Hypaque (Amersham Pharmacia Biotech, Uppsala, Suecia) y tratados con 10 μg/ml de fitohemaglutinina (Amersham Pharmacia Biotech) durante 48 h. A continuación las células se lavaron y crecieron en RPMI 1640 (Gibco-Invitrogen, Paisley, Reino Unido), suplementado con 10% de suero fetal bovino (FBS) (Gibco-Invitrogen), 40 μg/ml de gentamicina (Gibco-Invitrogen) e interleuquina-2 (20 U/ml) (Eurocetus BV, Ámsterdam, Holanda). Los linfoblastos se utilizaron transcurridos 10-12 días desde su obtención.

La línea celular T de leucemia humana Jurkat se obtuvo de la Dra. Margarita López-Trascasa (Hospital la Paz, Madrid). Las células fueron cultivadas en medio RPMI 1640 suplementado con un 10% de FBS y 40 μg/ml de gentamicina. Previamente a todos los experimentos (excepto donde se indique lo contrario), estas células fueron privadas de suero durante 3 h.

La línea celular B Ramos (linfoma de Burkitt) se obtuvo de la American Type Culture Collection (Rockville, MD, EEUU). La línea K562 (eritrocítica) transfectada con la subunidad de la integrina α4 se obtuvo del Dr. Joaquín Teixidó (Centro de Investigaciones Biológicas, Madrid).

Los fibroblastos primarios humanos se obtuvieron del Dr. Juan Miguel Redondo (Centro Nacional de Investigaciones Cardiovasculares, Madrid), y se cultivaron en medio DMEM (Gibco-Invitrogen), suplementado con 10% FBS y 40 μg/ml gentamicina.

La línea celular 786-0 y las líneas parentales de cáncer renal URCC, RCC4 y RCC10, fueron obtenidas de la Dra. Mª José Calzada (Hospital de la Princesa, Madrid), mantenidas en RPMI 1640 con GLUTAMAX-1 (Gibco-Invitrogen) suplementado con 10% FBS y crecidas a 37ºC y 5% CO_2.

Anticuerpos, reactivos y enzimas.

El acido lisofosfatídico (LPA), la citocalasina-D (Cyt-D), el forbol 12-miristato 13-acetato (PMA), la condroitinasa ABC, la trombina, el 4´-6 diamidino-2-fenilindol (DAPI), la cicloheximida (CHX) y la faloidina marcada con TRITC se compraron a Sigma-Aldrich (St. Louis, MO, EEUU). El SDF-1α (CXCL12) se compró a R&D

Systems (Minneapolis, MN, EEUU). La toxina pertúsica (PT) y el inhibidor de ROCK (Y-27632) se compraron a Calbiochem-Novabiochem Co (San Diego, CA, EEUU).

Los anticuerpos utilizados en este trabajo se muestran en la siguiente tabla:

ANTICUERPO	ESPECIFICIDAD	PROCEDENCIA
TS2/16	Subunidad β1 (activador de la integrina)	Dr. F. Sánchez-Madrid (Hospital de la Princesa, Madrid)
HP 2/1	Subunidad α4 (función bloqueante)	Dr. F. Sánchez-Madrid
Alex 1/4	Subunidad β1 (no activador de la integrina)	Dr. F. Sánchez-Madrid
W6/32	HLA	Dr. F. Sánchez-Madrid
Anti-CD3	CD3	Serotec (Oxford, UK)
Anti-Tubulin	Tubulina	Santa Cruz Biotechnology (Santa Cruz, CA, EEUU)
Anti-RhoA	GTPasa Rho	Santa Cruz Biotechnology
Anti-PY20	Tirosinas fosforiladas	Biomol Research Laboratories Inc. (Plymouth Meeting, PA)
Anti-Rac	GTPasa Rac	BD Biosciences Pharmingen (San Diego, CA, EEUU)
Anti-Pyk2	Src-quinasa Pyk-2	Santa Cruz Biotechnology
Anti-p190RhoGAP	p190RhoGAP	Upstate Biotechnology (New York, NY, EEUU).
Anti-Fibronectina	Fibronectina	Dra. A. García-Pardo (Centro de Investigaciones Biológicas, CSIC)

Tabla 1. Anticuerpos utilizados en este trabajo

Fragmentos de FN.

La figura 11 representa esquemáticamente los fragmentos utilizados en esta tesis y su localización en la molécula de FN. Los fragmentos recombinantes FN-H89 y FN-H0 cuyo ADNc fue obtenido del Dr. Martin Humphries (University of Manchester, UK), se produjeron y purificaron como está descrito (Mould *et al.,* 1994). El fragmento FN-H89 contiene las repeticiones III12-14 (dominio Hep II), 89 aminoácidos de la región IIICS incluyendo la secuencia CS1, pero no CS5 y la repetición III15. El fragmento FN-H0 se diferencia del FN-H89 en que no contiene la región IIICS.

Los ADNcs correspondientes a los fragmentos FNIII4, FNIII5, FNIII4-5, y FNIII4-6, que abarcan el dominio Hep III de la FN, clonados en el vector pQE-3/5 (obtenidos del Dr. Luciano Zardi, Istituto Nazionale per la Ricerca sul Cancro, Genova, Italia) se expresaron en la cepa bacteriana *E. coli DH5α* y se indujo la proteína con 1 mM IPTG (Calbiochem-Novabiochem Co). Al cabo de 16 h las bacterias se lisaron por sonicación en 10 mM Tris pH 7.4, 50 mM NaCl, 10 μg/ml aprotinina, 2.5 μg/ml leupeptina, 1 mM PMSF. Las proteínas se purificaron mediante cromatografía de afinidad en columnas de heparina-sefarosa (Amersham Pharmacia Biotech), equilibradas en 10 mM Tris pH 7.4, 50 mM NaCl, eluyendo con concentraciones crecientes de NaCl (150 mM, 300 mM y 500 mM). Finalmente, las proteínas se dializaron frente a 10 mM Tris/50 mM NaCl o PBS.

La generación de los mutantes de FNIII4-5 se llevó a cabo por PCR usando como molde el ADNc clonado en el vector pQE3/5. Los cebadores (*primers*) utilizados para cada mutación fueron los siguientes:

MUTACIÓN	Cebador sentido	Cebador complementarío
HBP/III5R1	5'TACTGTCCTGGTGAGATGGACTCCA CCTGCGGCCCAGATA-3'	5'- TCTGGGCCGCAGGTGGAGT-3'
HBP/III5R2	5'-ACAGGATACGCACTGACCGTG-3'	5'- GCCTCTTCGGGTAAGGCCCACGGT CAGGCGTATCCTGT-3'
HBP/III5 R3R4	5'-ACCGCAGCAGGCCAGCCCAG-3'	5'-GCCTGCTGCGGTAAGGCCCAC-3'

Tabla 2. ADNs iniciadores utilizados en el presente trabajo

Para la doble mutación HBP/III5R1R2 se usó el ADNc mutado HBP/III5R2 como molde y los *primers* usados para generar la mutación HBP/III5R1. Las secuencias de ADN de todos los mutantes clonados en el vector pGEM-T Easy (Promega Corp., Madison, WI, EEUU) se verificaron en un secuenciador automático ABI-Prism 377 (Applied Biosystems-Prism-Perkin Elmer, Foster City, CA, EEUU). Posteriormente se subclonaron en los sitios *Mfe* I y *Hin*d III en el vector pQE-3/5 y transfectaron en *E. coli DH5α*. Los ADNcs mutados se expresaron y purificaron como el fragmento parental FNIII4-5.

El ADNc correspondiente a las repeticiones III7-10 clonado en el vector pET (donado por el Dr. Harold Erickson, Duke University Medical Center, Durham, NC,

EEUU) se expresó en *E. coli* con 0.1 mM IPTG y se purificó como está descrito (Auckill *et al.,* 1993), excepto que para la elución de la columna mono-Q (Amersham-Pharmacia Biotech) se usó un gradiente de 0 a 350 mM NaCl en 20 mM Tris pH 7.5, 1 M urea.

El fragmento recombinante FNIII12-14 (dominio Hep II) fue donado por la Dra. Donna M. Peters (University of Wisconsin Medical School, Madison, WI, EEUU).

Los fragmentos proteolíticos de 29 kDa (repeticiones I1-5) y de 80 kDa (repeticiones III4-11) se obtuvieron tras la digestión tríptica de la FN plasmática humana, siguiendo la metodología ya descrita (García-Pardo *et al.*, 1983; García-Pardo *et al.*, 1989).

El fragmento proteolítico de 70 kDa (repeticiones I1-9 y las 2 repeticiones de tipo II) se preparó por digestión de la FN con catepsina D y tripsina, siguiendo el método ya descrito (Peters and Mosher, 1987).

La proteína recombinante VCAM-1 se obtuvo del Dr. Roy Lobb (Albor Biologics Inc.,Westwood, MA, EEUU), o se preparó a partir de células COS-7 mediante electroporación con 5 μg de plásmido por cada millón de células, a 200 V y 960 μF con el sistema GenePulser II de Bio-Rad Laboratories (Hercules, CA, EEUU). Las células electroporadas se crecieron durante 7 días recogiendo después los sobrenadantes. Estos sobrenadantes se clarificaron por centrifugación y se aplicaron a una columna de Proteína A-sefarosa, eluyéndose la proteína VCAM-1 con Glicina-HCl 0.1 M pH 3.0.

La pureza de todos los fragmentos se comprobó en geles de poliacrilamida (SDS-PAGE).

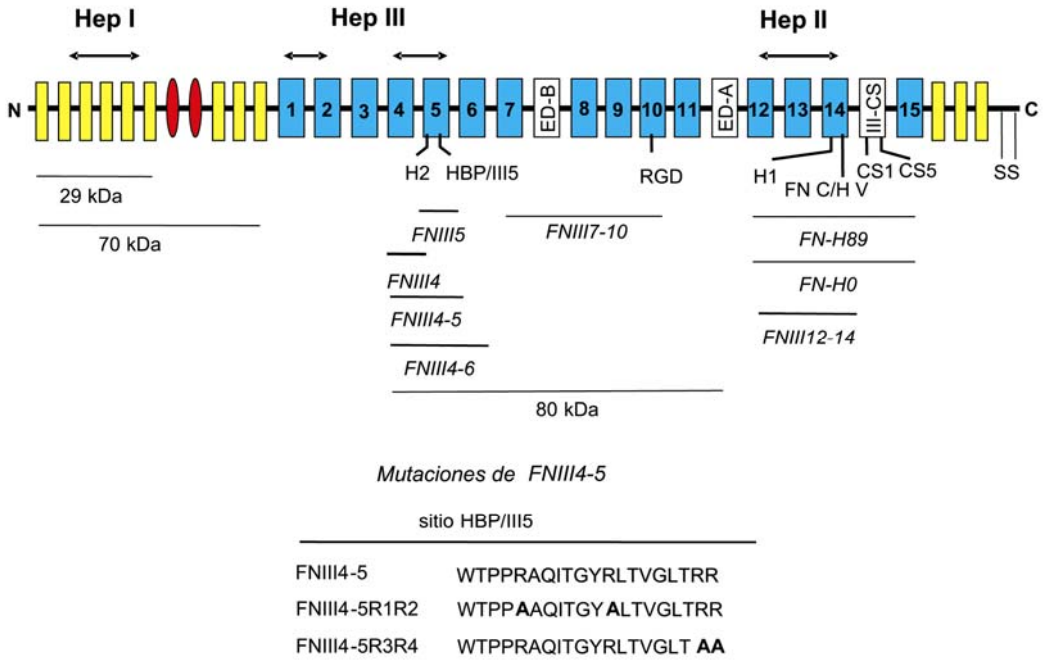

Figura 11: Fragmentos recombinantes y proteolíticos de la molécula de FN utilizados en esta tesis doctoral. Los fragmentos proteolíticos son indicados por sus correspondientes pesos moleculares, mientras que los fragmentos recombinantes FN-H89 y FN-H0 son indicados por el número de aminoácidos que contienen de la región de *splicing* alternativo IIICS. Los fragmentos recombinantes correspondientes al dominio Hep III están marcados como FNIII, especificando después las repeticiones que contienen. Dentro de los fragmentos recombinantes derivados del FNIII4-5 se especifican en negrita los residuos mutados en estos fragmentos.

Otras proteínas recombinantes y construcciones.

El ADNc de la enzima recombinante C3 transferasa (C3T) clonado en el vector pGEX-2T (regalo del Dr. Alan Hall, University College, London, UK) fue expresado y purificado como está descrito (Dillon *et al.*, 1995) con las siguientes modificaciones: las bacterias se lisaron en 50 mM Tris pH 7.5, 100 mM NaCl, 5 mM $MgCl_2$, 1 mM DTT, 1 mM PMSF, 2.5 µg/ml de leupeptina y 10 µg/ml de aprotinina (C3T buffer). Los sobrenadantes que contienen la proteína fusionada a la glutation-S-transferasa (GST), se incubaron durante toda la noche a 4ºC con bolitas de glutation-agarosa, se centrifugaron y la proteína de fusión se cortó con 5 U/ml de trombina (Sigma-Aldrich). La trombina fue retirada incubando con 10 µl de bolitas de una suspensión de p-aminobenzamidina-agarosa durante 30 min a 4ºC. Las bolitas se centrifugaron y la C3T se dializó frente a C3T buffer sin inhibidores. Se comprobó la pureza por SDS-PAGE.

La proteína verde fluorescente (*green fluorescent protein*, GFP) fusionada a los ADNc de las pequeñas Rho GTPasas codificantes para V14RhoA (mutante activo), N12RhoA (dominante negativo), V12Rac1 (mutante activo), N17Rac1 (dominante

negativo), clonados en el vector pEGFP-C1 (Clontech, Palo Alto, CA, EEUU) en *E.Coli DH5α* fueron obtenidos del Dr. Francisco Sánchez-Madrid. El ADNc plasmídico se aisló mediante *minipreps* (Gibco-Invitrogen).

Las construcciones Q63LRhoA (constitutivamente activo) y N19RhoA (dominante negativo) fueron donadas por el Dr. Silvio Gutkind (Bethesda, MD, EEUU). Estas construcciones fueron subclonadas en el sitio BamH1/EcoR1 del vector retroviral pLZR IRES-GFP.

Activación de las integrinas.

La activación de la integrina α4β1 se llevó a cabo incubando las células (en un volumen final de 300 µl) en el "medio de adhesión/TBS" compuesto por 10 mM Tris pH 7,5, 150 mM NaCl, 1% BSA, 10 mM HEPES (para el tratamiento con Mn^{2+}), o en el "medio de adhesión/RPMI" compuesto por RPMI-1640, 1% BSA, 10 mM HEPES (para el resto de tratamientos). Las células se incubaron con alguno de los siguientes activadores: Mn^{2+} (0.2-2 mM), TS2/16 (0.1-5 µg/ml) o PMA (5-50 ng/ml) durante 20 min a 37ºC. Para el tratamiento con SDF-1α las células se activaron con SDF-1α (150 ng/ml) durante 1 min a 37ºC. Para la activación vía CD3 se incubaron las células con 20 µg/ml del Acm anti-CD3 en "medio de adhesión/RPMI", durante 30 min a 4ºC, seguido de la incubación durante 5 min a 4ºC con un anticuerpo anti-IgG de ratón generado en cabra (DAKO A/S, Copenhague, Dinamarca). Alternativamente, se activó la integrina con el Acm anti-CD3 (0.1-2 µg/ml) coinmovilizado con ligandos de la integrina α4β1 (FN-H89 o VCAM-1).

Ensayos de adhesión celular estáticos.

Se tapizaron tiras de 8 pocillos de fondo plano con superficies de unión a aminas de N-hidroxisuccinamida (Costar Co, Cambridge, MA, EEUU) durante toda la noche a 4ºC con las proteínas o fragmentos recombinantes correspondientes, diluidos en 0.1 M borato sódico, pH 8.5. La adhesión de las células no tratadas o tratadas con los diferentes agentes activadores de la integrina α4β1 (Mn^{2+} 1 mM, PMA 50 ng/ml, o TS2/16 5 µg/ml) se llevó a cabo durante 45 min a 37ºC, excepto para el tratamiento con SDF-1α (150 ng/ml), en el que el tiempo de adhesión fue de 2 min. Las células adheridas se fijaron con 1.25% glutaraldehído en PBS, se tiñeron con 0.1 % azul de

toluidina en PBS, y se cuantificaron leyendo la absorbancia a 620 nm en un lector de placas Multiskan Bichromatic (Labsystems, Helsinki, Finlandia), usando curvas de calibración. La densidad óptica a 620 nm fue prácticamente una función lineal del número de células adherido. Además, la adhesión se cuantificó también visualmente en un microscopio invertido (Nikon Diaphot, Kawasaki, Japón).

Ensayos de adhesión celular en cámara de flujo.

Los ensayos de adhesión celular en cámara de flujo con células T humanas se realizaron siguiendo un método ya descrito (Stein *et al.*, 2003). Se tapizaron placas petri con 15 µl del fragmento FN-H89 (5 µg/ml o 1.2 µg/ml, en PBS), bloqueando a continuación con 0.5% BSA en PBS. Las placas fueron incorporadas como la pared inferior de una cámara de flujo paralelo (IQUUM, Boston, MA, EEUU), acoplada a una cámara CCD (LEICA DMIL) según la figura que se muestra a continuación.

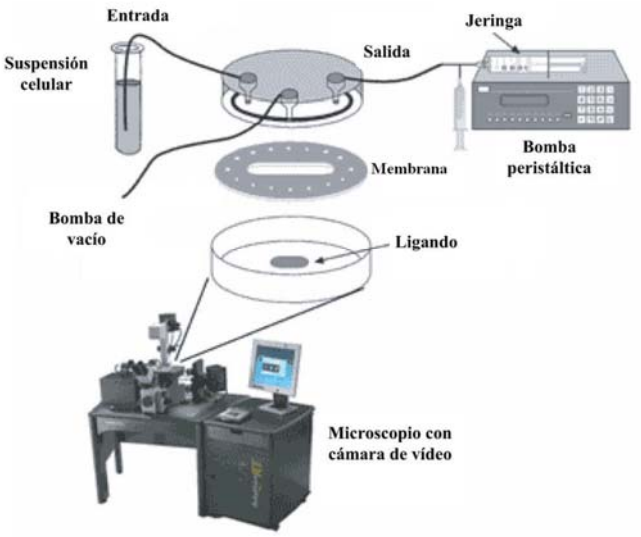

Figura 12. Sistema *in vitro* de adhesión en cámara de flujo y dispositivo de videomicroscopía utilizado para la grabación a tiempo real de la adhesión de células T bajo condiciones que simulan el flujo sanguíneo fisiológico.

Las diferentes suspensiones celulares ($1x10^6$ células/ml), no tratadas o tratadas con los diferentes agentes activadores de la integrina $\alpha4\beta1$ (Mn^{2+} 0.2 mM, PMA 50 ng/ml o TS2/16 5 µg/ml), fueron perfundidas a 1 ml/min antes de ajustar el flujo a 1 dina/cm^2 (0.204 ml/min). Para evaluar la resistencia al flujo, las células se pasaron por la cámara sometidas a un flujo de 1 dina/cm^2, primero durante 2 min y después sin flujo

durante 10 min, para permitir así su adhesión firme. Tras ello se aplicó un flujo que se fue aumentando de forma creciente cada 30 seg desde 0.5 dinas/cm^2 hasta alcanzar 6 dinas/cm^2. El número de células que permanecieron adheridas con cada flujo se determinó como el porcentaje del número total de células adheridas tras el periodo inicial de adhesión de 10 min.

Ensayos de inmunofluorescencia.

Inmunofluorescencia para linfocitos T

Los cubreobjetos de cristal se tapizaron con alguno de los siguientes sustratos: poli-D-lisina (p-Lys, 10 μg/ml), FN-H89 (8 μg/ml), VCAM-1 (5 μg/ml) o Acm anti-CD3 (0.1 μg/ml) junto a FN-H89 o VCAM-1, diluidos en 40 μl de PBS durante 2 h a 37ºC, y se colocaron posteriormente en placas de 24 pocillos (Beckton-Dickinson, Franklin Lakes, EEUU). En algunos ensayos antes de la activación de la integrina se trataron previamente las células Jurkat privadas de suero con 4 μg/ml de citocalasina D, o con 1 U/ml de condroitinasa ABC durante 30 min. 80x10^3 células se añadieron a cada pocillo y se incubaron durante 1 h a 37ºC. Las células adheridas se fijaron con 3.5% formaldehído en PBS durante 10 min a temperatura ambiente; después se permeabilizaron con 0.5% Tritón X-100 en PBS frío durante 3 min y se bloquearon durante 30 min con 1% BSA en PBS. La F-actina se tiñó con 25 μg/ml de faloidina-TRITC en PBS, 1% BSA, 10 mM NaN_3 durante 15 min y la tubulina con un Acm específico (1 h a 37ºC); posteriormente las células se incubaron con un anticuerpo anti-IgG de ratón marcado con FITC. Los cristales fueron fijados a portas con Mowiol-DAPI. Las muestras se observaron en un microscopio de epifluorescencia Axioplan (Zeiss, Göttingen, Alemania) y se fotografiaron con una cámara CCD (Photometrics Inc, Tucson, AZ, EEUU). Al menos se contaron 10 campos para cada condición. La tinción con DAPI se utilizó para ver la integridad del núcleo y la ausencia de apoptosis.

Inmunofluorescencia para fibroblastos humanos

Los fibroblastos humanos (140 x 10^3) en DMEM y 7.5% FBS se añadieron a cubreobjetos de cristal previamente cubiertos con 10 μg/ml de FN. Después de 1 h de adhesión, se sustituyó el medio por otro con DMEM, 0.2% BSA, y cicloheximida (CHX, 25 μg/ml) y las células se mantuvieron durante 3h a 37ºC. Tras este tiempo, se reemplazó el medio por otro similar que contenía 4 μg/ml de FN completa sóla o en

combinación con 200 μg/ml de los varios fragmentos de FN, incubando las células durante toda la noche a 37ºC. Se lavó la monocapa celular con PBS, se fijó con 4% paraformaldehído y se bloqueó con TNB (0.1 M Tris-HCl, 0.15 M NaCl, 0.5% de agente bloqueante). A continuación se incubaron las células con un Ac policlonal anti-FN, seguido de una tinción con un anticuerpo anti-IgG de conejo marcado con Alexa488. Los cristales fueron fijados a portas con Mowioll. Las fibrillas de FN se observaron en un microscopio de epifluorescencia Axioplan, y se fotografiaron con una cámara CCD.

Inmunofluorescencia para células de cáncer renal (RCC)

Las células se crecieron durante 3 días en RPMI/10% FBS libre de FN sobre cubreobjetos de cristal, previamente cubiertos o no con 10 μg/ml de FN. Las células se levantaron con 0.5% Tritón-X100 y 20 mM NH_4OH/PBS. Los cubreobjetos se fijaron con 3% paraformaldehído y se lavaron con TBS/0.5% Tween-20. Los sitios de unión no específicos se bloquearon con TNB. Se incubaron los cubreobjetos con un Ac policlonal anti-FN, seguido de una tinción con un anticuerpo anti-IgG de conejo marcado con rodamina Red™-X (Molecular Probes, Inc, Eugene, OR, EEUU), y se fijaron los cristales a portas con Mowioll. Las fibrillas de FN se observaron en un microscopio Leica DMR (Leica Microsystems, Mannheim, Alemania) equipado con el software QFISH. En algunos ensayos se trataron previamente las células con LPA (6 μM), o con Y-27632 (5 μM) durante 60 min.

Citometría de flujo.

Para llevar a cabo el análisis de marcadores celulares mediante citometría de flujo, las células ($1x10^5$) se incubaron durante 30 min a 4ºC con 100 μl de sobrenadante de cultivos (dilución 1:2) o fluido ascítico (dilución 1:100) conteniendo los Acms apropiados, o con 25 μg/ml de Acm purificado. Las células se lavaron 2 veces con PBS, 1% BSA, 10 mM NaN_3 frío, y se resuspendieron en 100 μl de una dilución 1:30 de fragmentos $F(ab')_2$ de IgG de conejo conjugadas a la FITC (Dako A/S), analizándose finalmente en un citómetro de flujo (Coulter Epics XL, Miami, FL, EEUU).

En el caso del análisis de células transfectadas con vectores de expresión con GFP, las células fueron lavadas con PBS, 1% BSA, 10 mM NaN_3 frío y resuspendidas en PBS, siendo posteriormente analizadas en un citómetro de flujo (Coulter Epics XL).

Transfección celular.

La línea celular Jurkat ($30x10^6$ células/punto) se transfectó de forma transitoria con diferentes vectores de expresión mediante electroporación utilizando el sistema de Electro Square Porator ECM 830 (BTX, San Diego, CA, EEUU). Dichos vectores de expresión (1 μg/10^6 células) se incubaron en 400 μl de RPMI 1640 frío, 2.5% FBS, y se añadieron posteriormente al interior de cubetas de electroporación de 0.4 cm. Para las construcciones de RhoA se utilizaron dos pulsos de 5 mseg y 310 V mientras que para las construcciones de Rac las condiciones fueron dos pulsos de 10 mseg y 230 V. Las cubetas se mantuvieron en hielo y a continuación las células se cultivaron en medio de crecimiento durante 24 horas a 37ºC. La eficiencia de transfección fue determinada mediante citometría de flujo resultando ser entre el 40 y el 60%.

Infección retroviral.

Estas infecciones fueron realizadas en el Hospital de la Princesa, por el grupo de la Dra. Mª José Calzada. Se utilizaron las construcciones constitutivamente activa (Q63LRhoA) y dominante negativa (N19RhoA) de RhoA, y la línea celular 786-0. Se subclonaron las construcciones en el sitio BamH1/EcoR1 del vector retroviral PLZR IRES-GFP y la posterior infección se realizó como está descrito (Calzada *et al.*, 2006).

Ensayos de migración celular.

Para los ensayos de migración celular, las células Jurkat ($2x10^5$ células/punto) se plaquearon en la parte superior del filtro de cámaras *Transwell* (Costar) de 5 μm de tamaño de poro que previamente habían sido tapizados con 8 μg/ml de FN-H89 o VCAM-1 sólos o coinmovilizados con el Acm anti-CD3 (0.1 μg/ml). Los compartimentos inferiores contenían 600 μl de medio de adhesión y 100 ng/ml de SDF-1α. Las células no tratadas o tratadas con Mn^{2+} (0.2 mM), PMA (10 ng/ml) o TS2/16 (5 μg/ml), fueron resuspendidas en el medio de adhesión, añadidas a la parte superior de los *Transwells*, e incubadas durante 7 horas a 37ºC. El nivel de migración de las células fue analizado por citometría de flujo, para lo cual se pasó cada muestra en las mismas condiciones.

Ensayos de videomicroscopia.

Las células Jurkat (0.5 x10^6) privadas de suero, se trataron con diferentes estímulos (0.2 mM Mn^{2+}, 150 ng/ml SDF-1α , 5 µg/ml TS2/16, 50 ng/ml PMA) y se añadieron a placas Petri de 35 mm de diámetro, que habían sido previamente tapizadas con el fragmento recombinante FN-H89 (1.2 µg/ml), con el Acm anti-CD3 (0.1 µg/ml) sólo o con la mezcla de ambos. Las imágenes fueron adquiridas cada 30 seg durante un periodo de una hora usando el microscopio Leica DM-IRE2 (Leica Microsystems) equipado con una cámara digital. Los fotogramas fueron compilados con el programa VideoMach (www.gromada.com) y las células que migraban fueron cuantificadas a partir de los videos por 5 investigadores independientemente.

Inmunoprecipitación y western blotting.

Las células (10x10^6/punto) pretratadas o no con los diferentes agentes activadores de la integrina α4β1, se añadieron a placas de 6 pocillos (Beckton-Dickinson), que habían sido previamente cubiertos con 8 µg/ml de FN-H89, 0.1 µg/ml del Acm anti-CD3, o ambos ligandos coinmovilizados. A diferentes tiempos de adhesión se lisaron las células con 500 µl de la solución de lisis RIPA (50 mM Tris pH 7.5, 150 mM NaCl, 1% NP-40, 0.5% desoxicolato, 0.1% SDS, 1 mM $NaVO_4$, 1 mM NaF, 1 mM PMSF, 10 µg/ml aprotinina y 2.5 µg/ml leupeptina). Se usaron 15 µl del sobrenadante para análisis de la proteína total y el volumen restante se incubó toda la noche a 4ºC con una solución que previamente había estado acoplándose durante 2 h a 4ºC. Esta solución se componía de 50 µl de bolitas de proteína A-agarosa (Amersham Pharmacia Biotech) recubiertas con 1 µg de Acm anti-Pyk2, o de bolitas sin Acm (*mock*). Las bolitas se lavaron con tampón RIPA y las proteínas unidas fueron eluídas en solución de Laemmli hirviendo 5 min a 100ºC.

Las proteínas fueron separadas en geles de poliacrilamida al 7.5% en presencia de SDS y electrotransferidas a membranas de nitrocelulosa (Bio-Rad Laboratories). Las membranas fueron bloqueadas con 5% de leche desnatada en PBS durante 2 horas, excepto para ver fosforilación, en cuyo caso el bloqueo se realizó con 3% BSA en PBS. Las membranas se incubaron 2 h a temperatura ambiente con los anticuerpos correspondientes disueltos en solución de bloqueo. Las proteínas fosforiladas presentes en el inmunoprecipitado se detectaron usando el Acm PY20 (Biomol Research Laboratories Inc.), mientras que la proteína total se detectó usando un Acm específico.

Después de lavar las membranas con 0.1% de Tween-20 en PBS, fueron finalmente incubadas 1 h con anticuerpos secundarios conjugados con HRP. Las proteínas se visualizaron usando el substrato quimioluminiscente ECL Supersignal West Femto (Pierce, Rockford, IL, EEUU). Para la cuantificación de las bandas, las autorradiografías fueron densitometradas en un densitómetro GS800 (Bio-Rad Laboratories), usando el programa Quantity-One™ (Bio-Rad Laboratories).

En determinados ensayos las membranas fueron sometidas a un proceso de *stripping* (30 min a 50ºC en una solución que contenía 100 mM 2-β-mercaptoetanol, 2% SDS y 62.5 mM Tris-HCl pH 6.7) para liberar los anticuerpos unidos y poder reutilizar las membranas para nuevas determinaciones.

Ensayos de regulación de la actividad GTPasa.

Para el análisis de la inactivación de RhoA por C3T, las células Jurkat se incubaron toda la noche en presencia de 50 μg/ml C3T en RPMI, 2% FBS en placas de 6 pocillos. Para la activación de RhoA por LPA, las células previamente tratadas o no con C3T se incubaron con 1 μM LPA en RPMI, 10 mM HEPES, 1% BSA durante 60 min a temperatura ambiente en una noria. C3T fresca fue añadida de nuevo durante esta incubación para aquellas células previamente tratadas con este inhibidor.

El dominio de unión a Rho activo C21 de Rhotekina y el dominio PAK que une Rac y Cdc42 activas, fusionados a la GST y clonados en el vector pGEX-3T (Amersham Pharmacia Biotech), fueron regalo del Dr. John Collard (The Netherlands Cancer Institute, Ámsterdam, Holanda). Las proteínas se expresaron en *E. coli DH5α* y se purificaron como está descrito (Sander *et al.,* 1999). Para los ensayos de arrastre (*pull-down*), se distribuyeron $3x10^7$ células privadas de suero en una placa de 6 pocillos previamente tapizados con el fragmento recombinante FN-H89 durante toda la noche y bloqueados con 1% BSA durante 1 h a 37ºC. A diferentes tiempos, las células adheridas se lisaron con 500 μl de tampón RIPA enfriado en hielo y estos lisados se clarificaron por centrifugación. Se utilizaron 15 μl del sobrenadante para determinar la cantidad total de las GTPasas y el volumen restante se incubó con 300 μl de C21-GST (o PAK-GST) y 50 μl de bolitas de glutation-agarosa (dilución 1:2) durante toda la noche a 4º C. Las bolitas se lavaron y las proteínas unidas se eluyeron hirviendo en tampón de carga de Laemmli. Las muestras se separaron por SDS-PAGE conteniendo el 15% de acrilamida y se transfirieron a membranas de nitrocelulosa (Bio-Rad Laboratories).

RhoA y Rac1 se detectaron mediante Acms específicos y posterior incubación con anticuerpos anti-IgG de ratón conjugados con HRP (Dako). Las bandas de proteína se visualizaron y cuantificaron, como se ha explicado.

Análisis de la fosforilación de p190RhoGAP.

Las células RCC VHL(+) y VHL(-), se lisaron en 500 µl de solución de lisis RIPA. Se usaron 15 µl del sobrenadante para análisis de la proteína total y el volumen restante se incubó toda la noche a 4ºC con 4 µg del Acm anti-p190RhoGAP, o con un Acm anti-CD45 T200 (*mock*) previamente unidas a bolitas de proteína G-agarosa como se ha explicado. Las bolitas se lavaron con tampón RIPA y las proteínas unidas fueron eluidas en solución de Laemmli. Las proteínas fueron separadas en geles de poliacrilamida al 7.5% en presencia de SDS y electrotransferidas a membranas de nitrocelulosa. Las proteínas fosforiladas presentes en el inmunoprecipitado fueron detectadas usando un Acm PY20 (Biomol Research Laboratories Inc) y con un anticuerpo secundario conjugado con HRP.

Ensayos de unión entre diferentes regiones de FN.

Para medir las interacciones entre los diferentes fragmentos de FN o entre fragmentos y FN, se utilizó un Biosensor óptico IAsysPlus (Labsystems Affinity Sensors, Cambridge, UK). Los fragmentos FNIII4-5, FNIII7-10, 70 kDa y la molécula de FN completa resuspendidos en 10 mM Tris, 50 mM NaCl, pH 7.5, se inmovilizaron en cubetas de doble-cavidad acopladas a un hidrogel de carboxi-metil-dextrano (CMD), siguiendo las instrucciones técnicas de la casa comercial. Este proceso de inmovilización consistió en el lavado de la cubeta con PBS/Tween-20 0.5% y la posterior activación de los grupos carboxilos del hidrogel tras la incorporación de 2 compuestos N-hidroxisuccinamida (NHS) y 1-etil-3-(3-dimetilaminopropil) carbodimida (EDC) y terminó con la adición del ligando a inmovilizar. Tras la inmovilización del ligando se añadió etanolamina 1 M pH 8.5 (para bloquear los sitios no acoplados) y finalmente se estableció una línea base al añadir el buffer en el que va equilibrada la muestra. Una vez inmovilizado el ligando y establecida la línea base, los fragmentos solubles (equilibrados en el mismo buffer que el ligando) fueron añadidos de forma paulatina hasta alcanzar la saturación. El cambio en el índice de refracción y en el grosor de la superficie es detectado por el Biosensor dando lugar a una respuesta

que fue monitorizada y cuantificada (arc/seg). A lo largo de todo el proceso (tanto inmovilización como interacción) tanto las cubetas como los fragmentos solubles se mantuvieron a una temperatura de 22ºC.

Ensayos de ensamblaje de matriz de FN.

Para medir la capacidad de ensamblaje de la matriz de FN, se siguió un método ya descrito (Bultmann *et al.*, 1998; Santas *et al.*, 2002). Se cultivaron fibroblastos humanos (3×10^4 células/punto) durante 24 o 48 h en placas de 96 pocillos. La monocapa celular, ya en confluencia, fue lavada e incubada posteriormente durante 3 horas a 37ºC en un medio libre de suero con ^{125}I-FN o ^{125}I-29 kDa, en presencia o ausencia de los competidores fríos (fragmentos de FN sin marcar). Tras este tiempo la monocapa celular fue lavada y los niveles de incorporación de ^{125}I fueron analizados en un contador γ.

Análisis estadístico.

Para analizar estadísticamente las diferencias entre medias de pares de datos se utilizó la prueba t de student y el programa GraphPad Instat (GraphPad Software, San Diego, CA). Se consideraron significativos los valores de $p < 0.05$. Las diferencias significativas fueron representadas como *** $p < 0.001$; ** $p < 0.01$ y * $p < 0.05$.

Resultados

1. Efecto de las diferentes activaciones de la integrina α4β1 a nivel reorganización del citoesqueleto de actina

En trabajos anteriores del laboratorio se había demostrado que el dominio de unión a heparina III (Hep III) de la FN (figura 13), objeto de estudio en la presente tesis, constituía un ligando de la integrina α4β1, pero sólo tras la activación de esta integrina con Mn^{2+} o con el Acm anti-β1 TS2/16 (Moyano *et al*., 1999).

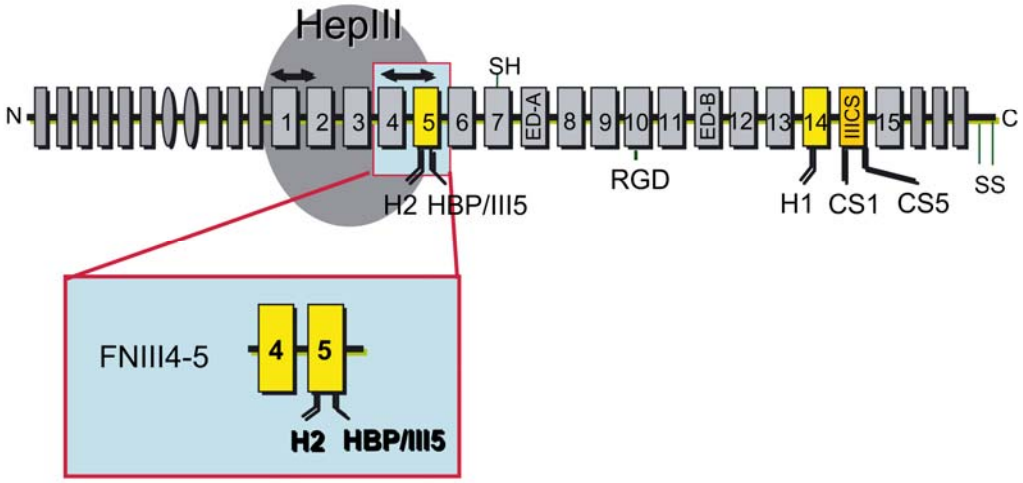

Figura 13. Esquema de un monómero de FN y localización del fragmento recombinante FNIII4-5. Dentro del dominio Hep III de la FN, se han identificado 2 secuencias mediadoras de adhesión, el sitio H2 que une las integrinas α4β1 y α4β7 activadas y el sitio HBP/III5 que une proteoglicanos de tipo condroitín-sulfato (PGCS). Ambas secuencias se encuentran localizadas en la repetición III5 englobada dentro del fragmento recombinante FNIII4-5.

Como se muestra en la figura 14 A, las células Jurkat tratadas con uno de estos dos estímulos se unían de forma eficiente al fragmento recombinante FNIII4-5 que contiene el dominio Hep III de FN. Estos estudios demostraron también que la adhesión celular a FNIII4-5 involucraba además de a la integrina α4β1, a proteoglicanos de tipo condroitín-sulfato (PGCS). De forma importante la contribución de ambos receptores a la adhesión a FNIII4-5 era diferente dependiendo del estímulo utilizado para la activación de α4β1. En la figura 14 B, se observa como el PGCS es importante en la activación de α4β1 con Mn^{2+}, donde parece ser necesaria la cooperación entre ambos receptores, algo que no ocurre cuando α4β1 era activada por el Acm TS2/16.

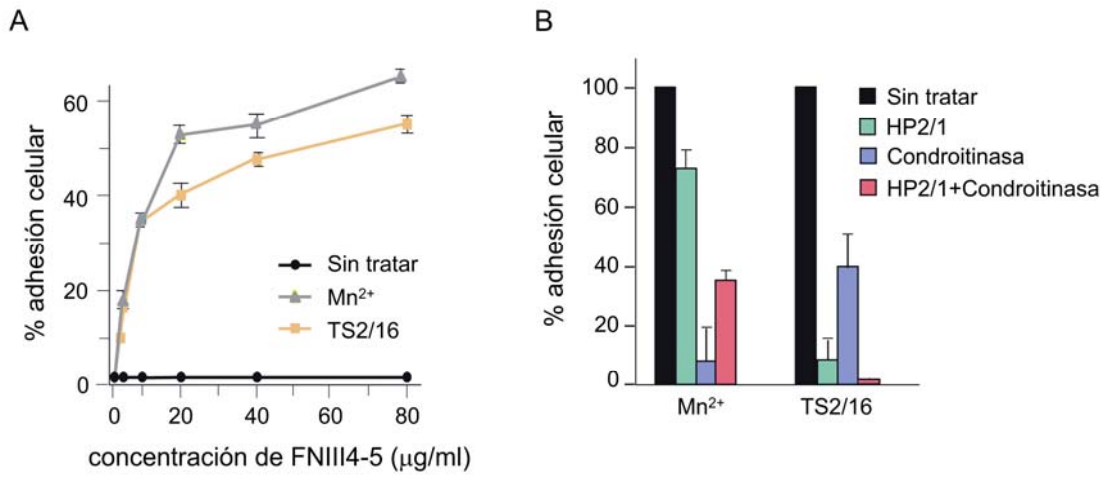

Figura 14. Caracterización de la adhesión de las células Jurkat al fragmento recombinante FNIII4-5. **A**: Adhesión a concentraciones crecientes del fragmento FNIII4-5 de células Jurkat sin tratar (control) o tratadas con Mn^{2+} o el Acm TS2/16, representándose la media de al menos 3 ensayos. **B**: Efecto del Acm anti-α4 (HP2/1, 5 µg/ml) y de la enzima degradante de proteoglicanos tipo condroitín-sulfato (condroitinasa ABC, 1 U/ml), en la adhesión de las células Jurkat tratadas con Mn^{2+} o con el Acm TS2/16. Las células fueron preincubadas durante 30 min con HP2/1 o con condroitinasa ABC y añadidas a pocillos tapizados con FNIII4-5 (40 µg/ml), representándose la media del porcentaje de células adheridas de 4 experimentos diferentes.

Diferentes activaciones "outside-in" de α4β1 inducen diferente reorganización del citoesqueleto de actina tras la adhesión de células Jurkat a FNIII4-5.

Los resultados anteriores sugerían que el Mn^{2+} y el TS2/16 inducían diferentes estados de activación de la integrina α4β1. Para determinar si estas diferencias se traducían en distintas respuestas celulares en eventos posteriores a la adhesión, se estudio en primer lugar el efecto de ambos estímulos de α4β1 sobre la reorganización del citoesqueleto de actina inducida tras la adhesión de células Jurkat al fragmento recombinante FNIII4-5. Como se puede observar en la figura 15 tras la adhesión al fragmento FNIII4-5 (rango 12-50 µg/ml), las células Jurkat sin tratar permanecen con una morfología redondeada, mientras que las tratadas con el agente estimulador Mn^{2+} (1 mM), presentan una morfología elongada en un 68% de las células. El tratamiento con el Acm TS2/16 (5 µg/ml) sin embargo, induce una morfología celular redondeada pero extendida (morfología de "*spreading*"), donde el 79% de las células presentan un tamaño mucho mayor que las no tratadas o las tratadas con Mn^{2+}, es una morfología celular aplastada.

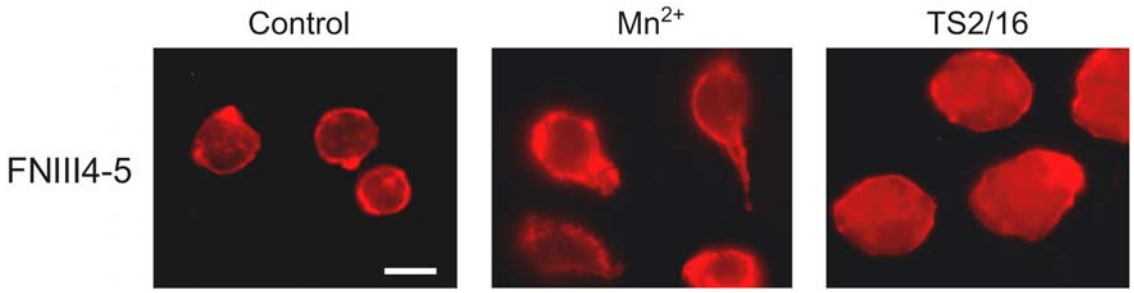

Figura 15. Efecto de las activaciones "*outside-in*" de la integrina α4β1 en la reorganización del citoesqueleto de células T tras su adhesión al ligando FNIII4-5. Las células Jurkat (80 x10^3 células/punto) no tratadas (control) o tratadas con Mn^{2+} (1 mM) o TS2/16 (5 μg/ml) se adhirieron a FNIII4-5 (50 μg/ml) durante 60 min, se fijaron y se tiñó la F-actina con faloidina-TRITC. El experimento se repitió 3 veces con resultados equiparables, mostrándose uno representativo. Barra, 5 μm.

La condroitinasa inhibe la reorganización del citoesqueleto de actina inducida tras la activación de α4β1 con Mn^{2+} pero no la inducida tras la activación con TS2/16.

Estudiamos a continuación si la contribución de PGCS y α4β1 era también diferente a nivel de reorganización del citoesqueleto, dependiendo del estímulo utilizado para activar la integrina α4β1. Para ello se analizó, mediante ensayos de inmunofluorescencia, el efecto de inhibidores tanto de PGCS (condroitinasa ABC, 1 U/ml) como de la subunidas α4 de la integrina (Acm HP2/1, 25 μg/ml). Como se observa en la figura 16, la preincubación de las células con condroitinasa ABC reduce la adhesión celular y suprime la morfología elongada en un 76% de las células tratadas con Mn^{2+}; sin embargo el tratamiento con condroitinasa ABC no tiene ningún efecto tras la activación de α4β1 con el Acm TS2/16. La preincubación con el Acm HP2/1 y posterior activación con Mn^{2+} reducía parcialmente la adhesión celular y el porcentaje de células que presentan una morfología elongada. El Acm HP2/1 inhibía totalmente la adhesión tras la activación con TS2/16.

En conjunto estos resultados confirman la existencia de diferencias funcionales a nivel de eventos post-adhesión, con respecto a la activación de α4β1 inducida por Mn^{2+} o por el Acm TS2/16, tras la adhesión de células Jurkat al fragmento FNIII4-5.

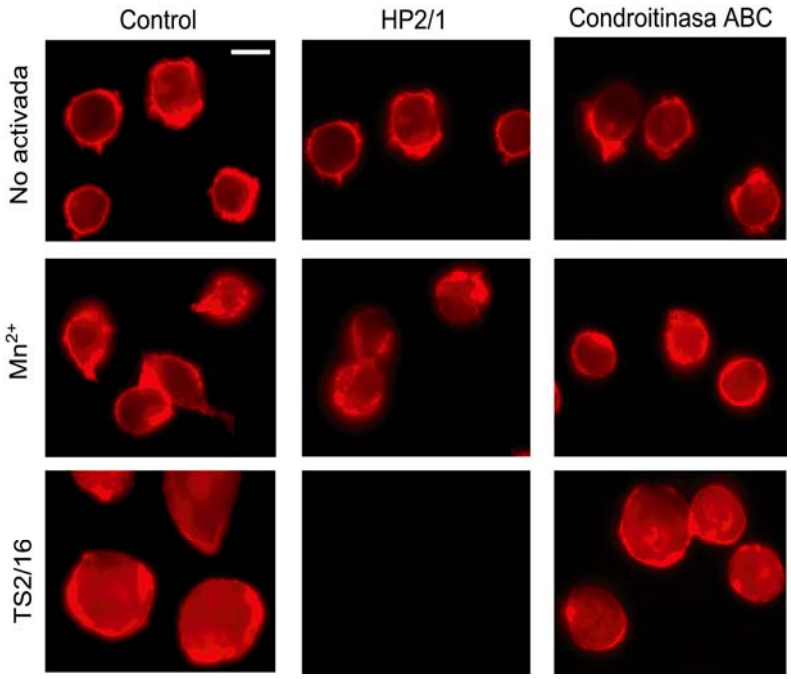

Figura 16. La condroitinasa inhibe la reorganización del citoesqueleto inducida por Mn^{2+} pero no la inducida por TS2/16 Células Jurkat con o sin una incubación previa con condroitinasa ABC (1 U/ml) o con el Acm HP2/1 (25 μg/ml), fueron tratadas con Mn^{2+} (1 mM) o con TS2/16 (5 μg/ml) y se añadieron a cubreobjetos tapizados previamente con FNIII4-5 (50 μg/ml) Las células se dejaron en adhesión durante 60 min a 37ºC, y posteriormente fueron fijadas y teñidas con faloidina-TRITC. Las células control en este caso fueron tratadas con Mn^{2+} o TS2/16 pero no recibieron más tratamiento. Barra, 10 μm.

El efecto diferencial de las activaciones "outside-in" sobre la reorganización del citoesqueleto, se observa también tras la adhesión de células Jurkat a otros ligandos de α4β1 en la molécula de fibronectina.

Se estudió a continuación si la diferente reorganización del citoesqueleto observada tras la adhesión al fragmento FNIII4-5 ocurría también tras la adhesión de células Jurkat a otros ligandos de α4β1 dentro de la molécula de FN. La figura 17 muestra los ligandos de α4β1 en la región IIICS (sitio CS1) y en el dominio Hep II (sitio H1) de la FN. Para estos ensayos se utilizaron los fragmentos recombinantes FN-H89 (sitios H1 y CS1) y FN-H0 (sitio H1) (Mould *et al*. 1994).

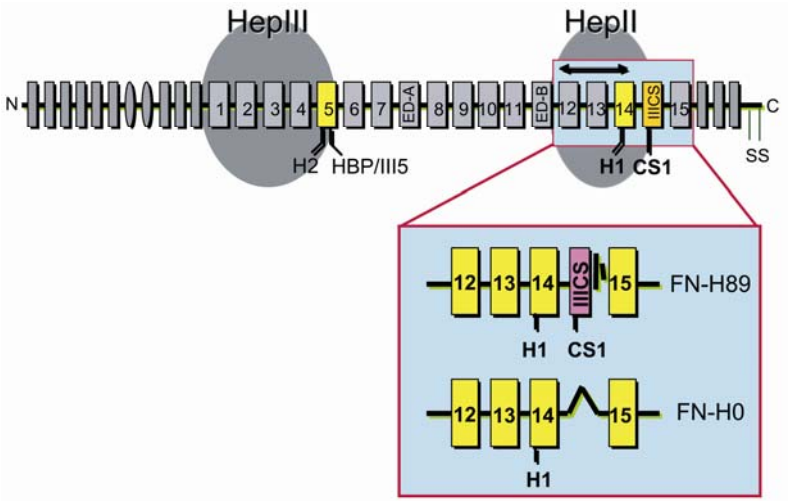

Figura 17. Esquema de los ligandos de α4β1 en las regiones Hep II y IIICS de la molécula de FN. Las proteínas recombinantes FN-H89 y FN-H0 contienen diferentes variantes de *splicing* de la región IIICS. El número asignado a cada una se refiere al número de residuos aminoacídicos que presenta la región IIICS. FN-H0 tiene una única secuencia de unión a la integrina α4β1 la región H1, localizada en la repetición III14. FN-H89 aparte de H1 posee otra secuencia de unión a α4β1, conocida como CS1, que es la región de mayor afinidad de esta integrina.

Como se muestra en la figura 18, el tratamiento de las células Jurkat con Mn^{2+}o con el Acm TS2/16 y su posterior adhesión a FN-H0 (rango 5-30 μg/ml), o FN-H89 (rango 0.6-15 μg/ml), da lugar al mismo patrón diferencial a nivel de análisis del citoesqueleto de actina, que el observado en células adheridas a FNIII4-5.

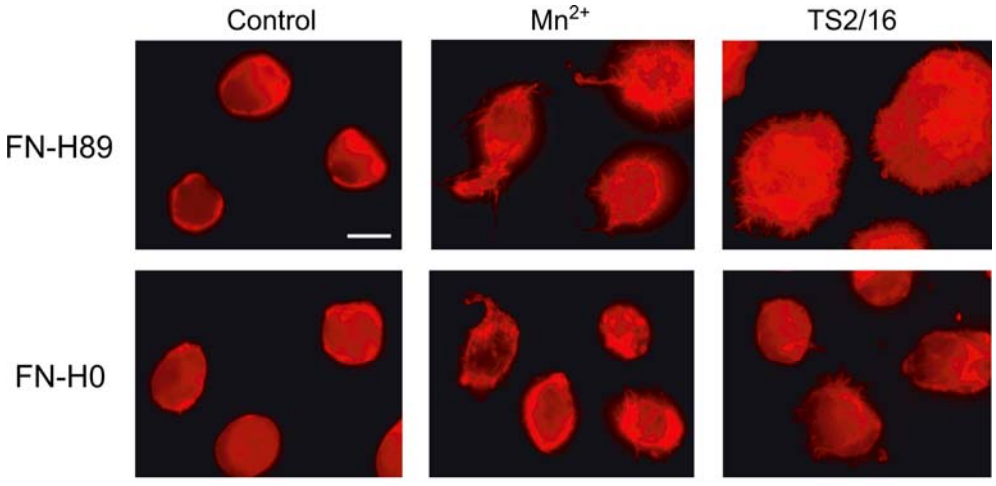

Figura 18. Efecto de las activaciones *"outside-in"* de la integrina α4β1 en la reorganización del citoesqueleto de células T tras su adhesión a otros ligandos de α4β1. Las células Jurkat (80 $x10^3$ células/punto) no tratadas (control) o tratadas con Mn^{2+} (1 mM) o TS2/16 (5 μg/ml) se adhirieron a FN-H0 (30 μg/ml) o FN-H89 (8 μg/ml), durante 60 min, se fijaron y se tiñó la F-actina con faloidina-TRITC. El experimento se repitió 3 veces con resultados equiparables, mostrando uno representativo. Barra, 5 μm.

Las células Jurkat no tratadas (control) permanecen con una morfología redondeada, mientras que tras el tratamiento con Mn^{2+} se induce una morfología celular elongada, y una extensión celular redondeada (*spreading*) tras el tratamiento con el Acm TS2/16. Además se puede observar como sobre FN-H89 la morfología elongada es más evidente, diferenciándose perfectamente el cuerpo celular y las proyecciones citoplásmicas (tipo filopodios) en un 75% de las células (figura 18). Mientras que en las células tratadas con el Acm TS2/16, se observaba la morfología extendida ("*spreading")* en un 85% de las células, y una formación de lamelipodios en torno a la célula en un 35% de las células. Dado que el efecto diferencial de la activación "*outside-in*" de la integrina α4β1, a nivel de reorganización del citoesqueleto, era más potente tras la adhesión al fragmento FN-H89, se eligió este ligando de α4β1 para posteriores estudios.

Para determinar si los PGCS jugaban el mismo papel diferencial en la respuesta inducida tras la adhesión a FN-H89 que tras la adhesión a FNIII4-5, se realizaron los mismos ensayos de inmunofluorescencia en presencia de condroitinasa ABC y el Acm HP2/1. En todos los casos se obtuvieron resultados similares a los obtenidos para FNIII4-5, siendo necesaria la contribución de los PGCS tras la activación de α4β1 con Mn^{2+} pero no tras la activación con el Acm TS2/16 (datos no mostrados).

La diferente reorganización del citoesqueleto no es exclusiva de la línea celular Jurkat.

Para comprobar si esta diferente reorganización del citoesqueleto de actina tras la activación "*outside-in"* de la integrina α4β1, se puede generalizar a células T primarias, se realizaron las inmunofluorescencias con linfoblastos T humanos. Como se muestra en la figura 19, tras la adhesión a FN-H89, las células no tratadas presentan una morfología redondeada, mientras que las tratadas con Mn^{2+} presentan una morfología elongada en un 65%. Como en el caso de células Jurkat el tratamiento con TS2/16 induce una morfología extendida (aplastada) en un 75% de las células.

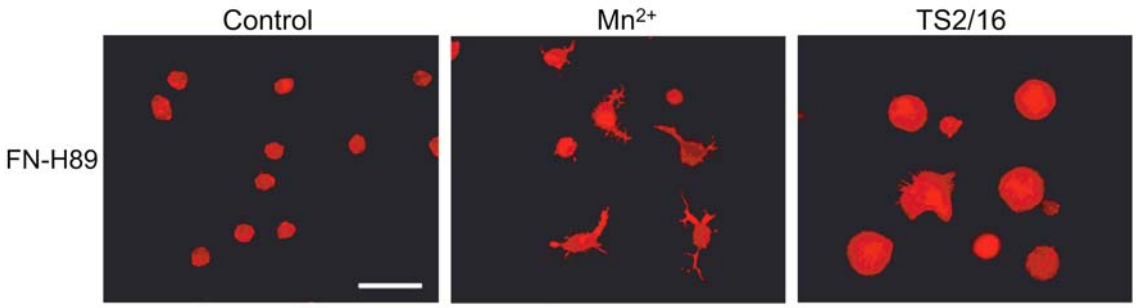

Figura 19. Efecto de las diferentes activaciones *"outside-in"* de la integrina α4β1 en la reorganización del citoesqueleto inducida tras la adhesión de linfoblastos-T humanos a FN-H89. Linfoblastos-T (80 x10^3 células/punto) no tratados (control) o tratados con Mn^{2+} (1 mM) o TS2/16 (5 µg/ml) se adhirieron a FN-H89 (8 µg/ml) durante 60 min, se fijaron y se tiñeron con faloidina-TRITC. El experimento se repitió 4 veces con resultados equiparables. Barra, 10 µm.

A continuación se estudió si el efecto observado a nivel de reorganización de citoesqueleto de actina, era o no específico de linfocitos T. Para ello se realizaron ensayos de inmunofluorescencia con la línea celular B Ramos (linfoma de Burkitt), y la línea eritrocítica K562 transfectada de forma estable con la integrina α4. Como se muestra en la figura 20, en ambos casos, tras la activación de la integrina α4β1 con Mn^{2+} se observa una morfología elongada, observándose perfectamente un cuerpo celular y las proyecciones citoplásmicas de las células, mientras que tras la activación con el Acm anti-β1 TS2/16 se observa una morfología extendida con lamelipodios en torno a la célula.

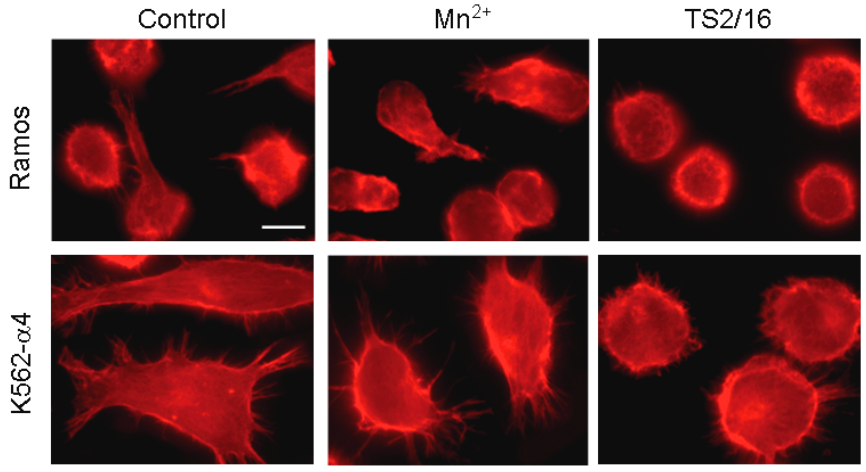

Figura 20. Efecto de las diferentes activaciones *"outside-in"* de la integrina α4β1, en diferentes líneas celulares. Diferentes líneas celulares (80 x10^3 células/punto) no tratadas (control) o tratadas con Mn^{2+} (1 mM) o TS2/16 (5 µg/ml) se adhirieron a FN-H89 (8 µg/ml) durante 60 min, se fijaron y se tiñó la F-actina con faloidina-TRITC. El experimento se repitió 3 veces con resultados equiparables. Barra, 5 µm

En conjunto los resultados anteriores nos muestran que la diferente reorganización del citoesqueleto de actina obtenida tras diferentes estímulos "*outside-in*" de α4β1, no está restringida a la línea celular Jurkat ni a células T, sino que también ocurre en otros tipos celulares. Por tanto, para posteriores estudios se siguió utilizando como modelo la línea celular Jurkat.

La diferente reorganización del citoesqueleto ocurre también tras adhesión al ligando endotelial de α4β1 VCAM-1, y es específica del citoesqueleto de actina.

Se quiso determinar si la adhesión al ligando endotelial de la integrina α4β1, VCAM-1, tras las diferentes activaciones "*outside-in*" de la integrina, tenía el mismo efecto a nivel de reorganización del citoesqueleto que el observado sobre los ligandos de FN.

Para esto se realizaron los ensayos de inmunofluorescencia sobre VCAM-1 (rango 0.3-10 μg/ml). Como se observa en la figura 21 existe un efecto similar al que se observa sobre el fragmento recombinante FN-H89: las células no tratadas mantienen una morfología redondeada, el tratamiento con Mn^{2+} induce una morfología elongada y el tratamiento con TS2/16, una morfología extendida. Para confirmar que esta respuesta era mediada por la interacción de la integrina α4β1 con su ligando, se añadieron las células Jurkat a poli-D-lisina (p-Lys, 10 μg/ml), no observándose ninguna diferencia a nivel de reorganización del citoesqueleto entre las células Jurkat no tratadas (control) y las tratadas con Mn^{2+} o con el Acm TS2/16 (figura 21).

Se comprobó también que la respuesta observada era debida al efecto activador del Acm TS2/16. Para ello se trataron las células Jurkat con el Acm anti-β1 (Alex1/4), que no activa la integrina. Como se observa en la figura 21, las células presentaban una morfología redondeada tras la adhesión celular a VCAM-1 (o a FN-H89, no mostrado), similar a las células control.

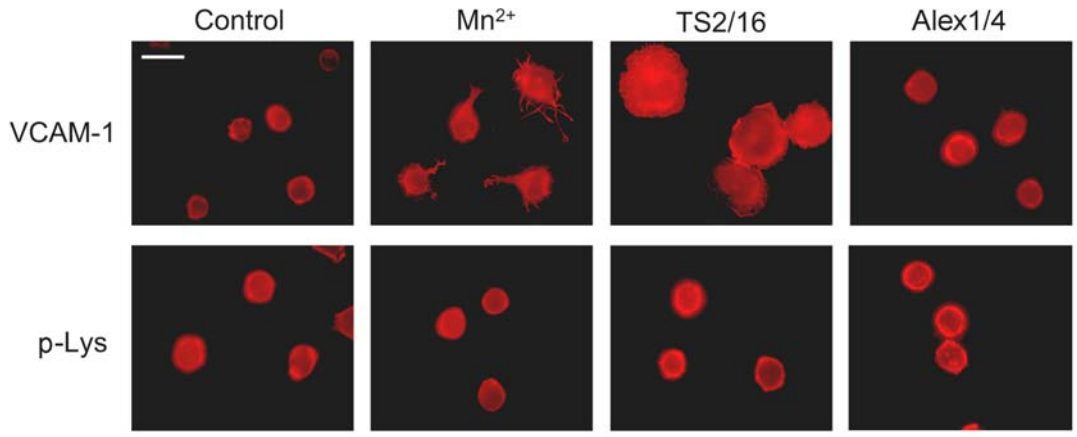

Figura 21. Efecto de las diferentes activaciones *"outside-in"* de la integrina α4β1 en la reorganización del citoesqueleto de células T sobre VCAM-1 o p-Lys. Las células Jurkat (80 x10^3 células/punto) no tratadas (control) o tratadas con Mn^{2+} (1 mM), TS2/16 (5 μg/ml) o Alex1/4 (5 μg/ml) se adhirieron a VCAM-1 (5 μg/ml) y p-Lys (10 μg/ml) durante 60 min, se fijaron y se tiñeron con faloidina-TRITC. El experimento se repitió como mínimo 3 veces con resultados equiparables. Barra, 10 μm.

Se hicieron además otros controles para confirmar que era la reorganización del citoesqueleto de actina lo que provocaba ese cambio en los patrones morfológicos. Se estudió en primer lugar la localización del centro organizador de microtúbulos (MTOC), tras las diferentes activaciones de la integrina α4β1. Los resultados mostraron que en células no activadas, el MTOC presenta una localización central en un 90% de las células (figura 22), mientras que tras la activación con Mn^{2+} el MTOC se desplaza a la parte trasera de la célula (en el 85% de las células), localizándose en la zona próxima a la proyección citoplásmica, algo característico de células polarizadas (Rodríguez-Fernández *et al.* 1999; Vicente-Manzanares and Sánchez-Madrid 2004). Sin embargo tras el tratamiento con el Acm TS2/16 en un 90% de las células la localización del MTOC es central (figura 22).

En segundo lugar se comprobó que el tratamiento con citocalasina-D (Cyt-D, 4 μg/ml) previo a la activación de la integrina, inhibe tanto la morfología elongada inducida por Mn^{2+} como la morfología extendida inducida por el Acm TS2/16, como se muestra en la figura 22. Estos resultados demuestran que las diferentes morfologías observadas implican la reorganización del citoesqueleto de actina.

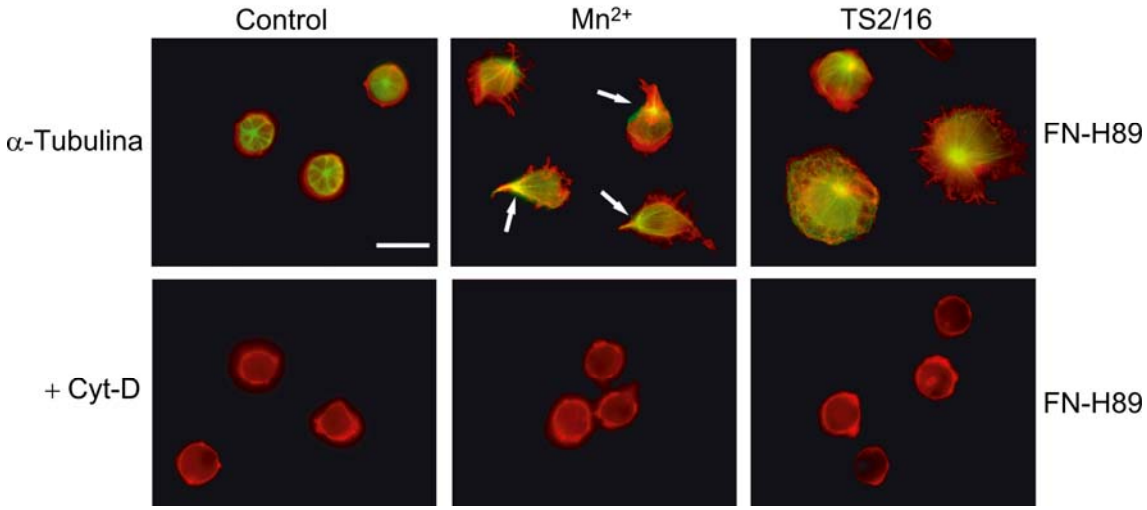

Figura 22. La reorganización del citoesqueleto de actina es la causante de los diferentes patrones morfológicos observados. Las células Jurkat (80 x10^3 células/punto) no tratadas (control) o tratadas con Mn^{2+} (1 mM) o TS2/16 (5 μg/ml) se adhirieron a FN-H89 (8 μg/ml) durante 60 min, se fijaron y se tiñó la F-actina con faloidina-TRITC (rojo). La organización de microtúbulos se visualizó con un Acm anti-tubulina y con un Ac secundario etiquetado con FITC (verde). Por otra parte, las células no tratadas o tratadas con Mn^{2+} o TS2/16 fueron preincubadas durante 30 min con Cyt-D (4 μg/ml). El experimento se repitió 3 veces con resultados equiparables. Barra, 10 μm.

Diferentes activaciones "inside-out" de la integrina α4β1, dan lugar a una diferente reorganización del citoesqueleto de actina, tras la adhesión celular a ligandos de esta integrina.

Las integrinas pueden activarse por mecanismos "*outside-in*" ya comentados (Mn^{2+} o el Acm TS2/16) o mecanismos "*inside-out*" (PMA, Acm anti-CD3 o SDF-1α). Como se explicó en la introducción, los primeros actúan directamente sobre la integrina, mientras que los segundos lo hacen a través de rutas de señalización internas, inducidas tras su unión a los correspondientes receptores celulares.

En primer lugar confirmamos que tanto los activadores "*outside-in*" como los "*inside-out*" aumentan la adhesión de α4β1 a sus ligandos FN-H89 y VCAM-1 (Pribila *et al*., 2004) de forma estadísticamente significativa ($p \leq 0.001$) en todos los casos (figura 23).

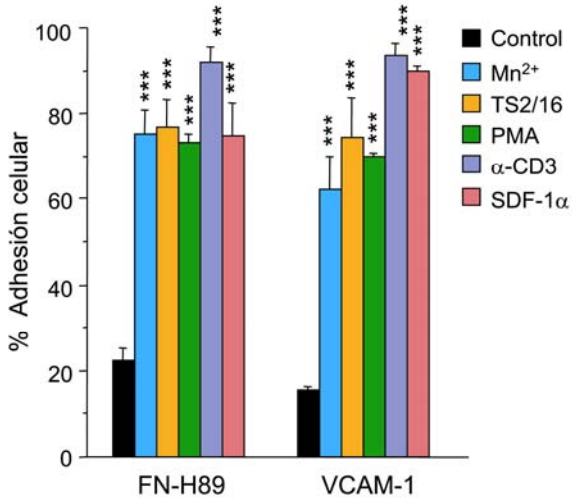

Figura 23. Incremento de la adhesión celular al fragmento recombinante FN-H89 y a VCAM-1 por diferentes activadores de la integrina α4β1. Las células Jurkat no se trataron (control) o se trataron durante 30 min a 37^0 C con 1 mM Mn^{2+}, 5 μg/ml TS2/16, 50 ng/ml PMA, 20 μg/ml Acm anti-CD3, o durante 1 min con 150 ng/ml de SDF-1α. Las células ($6x10^4$/pocillo) se añadieron a pocillos previamente cubiertos con FN-H89 (3 μg/ml) o VCAM-1 (2.3 μg/ml); después de 45 min (2 min para el tratamiento con SDF-1α), las células adheridas se tiñeron con 0.1% de azul de toluidina y se cuantificaron por la determinación de la absorbancia a 620 nm en un lector de placas. Los valores representan la media de 3 ensayos diferentes con sus respectivas desviaciones estándar. ***, indica diferencias estadísticamente significativas con respecto al control ($p \leq 0.001$).

Como se muestra en la figura 24, la activación "*inside-out*" de la integrina α4β1 también produce una diferente reorganización del citoesqueleto de actina dependiendo del estímulo utilizado. El tratamiento con PMA, seguido de la adhesión al fragmento FN-H89 o a VCAM-1, da lugar a una morfología de "*spreading*" celular en un 80% de las células, similar a la observada tras la activación con el Acm TS2/16. Sin embargo la activación de la integrina por CD3 (ya sea por la coinmovilización del Acm anti-CD3 junto con FN-H89 o VCAM-1 (figura 24), o por el entrecruzamiento de CD3 en suspensión y la posterior adhesión a FN-H89 (o VCAM-1, resultado no mostrado), da lugar a una morfología polarizada en un 68% de las células, similar a la que se observaba tras la activación con Mn^{2+}.

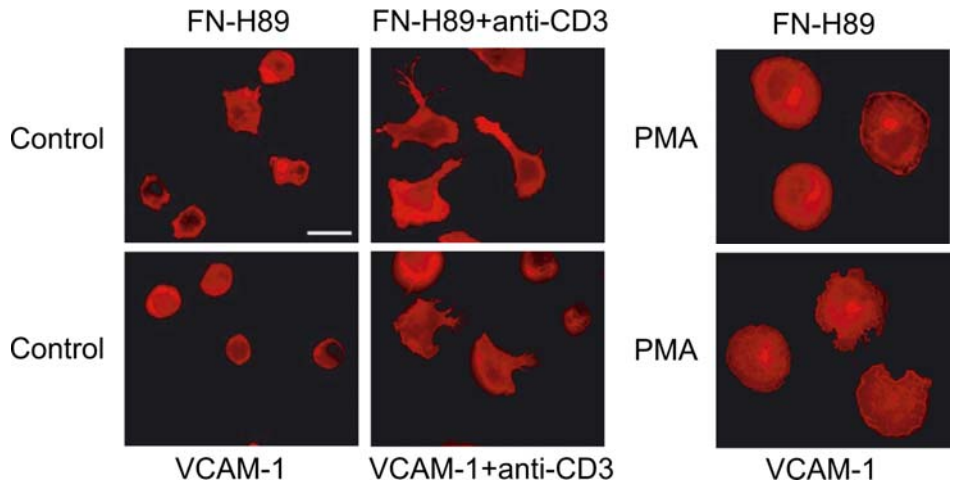

Figura 24. Efecto de diferentes activaciones "*inside-out*" de la integrina α4β1 en la reorganización del citoesqueleto de las células T. Las células Jurkat (80 x10^3 células/punto) no tratadas (control) o tratadas con PMA (50 ng/ml) se adhirieron a FN-H89 (8 μg/ml), a VCAM-1 (5 μg/ml), o al Acm anti-CD3 (0.1 μg/ml) coinmovilizado junto a FN-H89 o VCAM-1 durante 60 min, se fijaron y se tiñeron con faloidina-TRITC. El experimento se repitió 3 veces con resultados equiparables. Barra, 10 μm.

Para confirmar que el Acm anti-CD3 a la concentración 0.1 μg/ml activaba la integrina, se realizaron ensayos de adhesión celular, cuyos resultados fueron un aumento del 15% al 77% de adhesión tras la coinmovilización del Acm con FN-H89 (resultados no mostrados). Además, como se muestra en la figura 25, se observó en ensayos de inmunofluorescencia que utilizando como ligando sólo el Acm anti-CD3 a dicha concentración, las células presentan una adhesión pobre y una morfología redondeada. Como control a esta activación por el Acm anti-CD3, se utilizó el Acm anti-HLA W6/32, inmovilizado sólo o en combinación con FN-H89 o VCAM-1, observándose una morfología redondeada en todos los casos, similar a la observada con las células no tratadas (control) (figura 25).

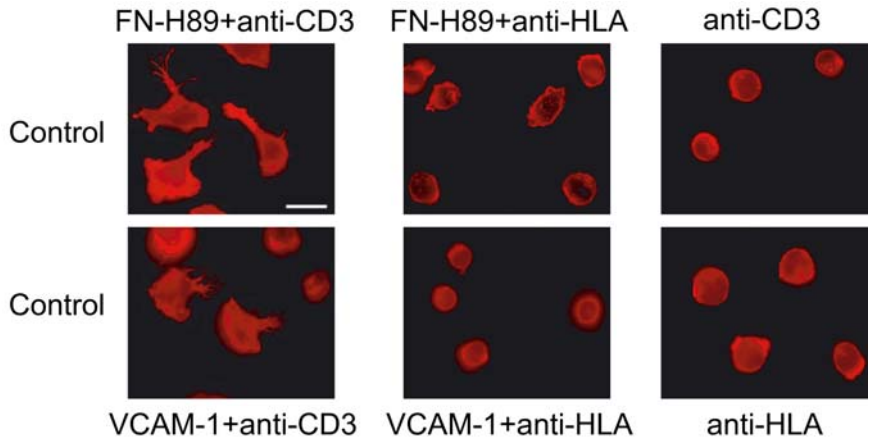

Figura 25. El Acm anti-CD3 (0.1 μg/ml) es el causante de la morfología elongada en células-T. Células Jurkat (80 x10^3 células/punto) no tratadas (control) se adhirieron a cubreobjetos, cubiertos de la mezcla FN-H89/anti-CD3 o VCAM-1/anti-CD3. Como control, los cubreobjetos se cubrieron con FN-H89 o VCAM-1 junto con un Acm anti-HLA. Asimismo, se inmovilizaron los Acm anti-HLA y anti-CD3 sólos. Al cabo de 60 min las células se fijaron y se tiñeron con faloidina-TRITC. El experimento se repitió 5 veces con resultados equiparables. Barra, 10 μm

Para determinar si esta diferente reorganización del citoesqueleto tras la activación "*inside-out*" de la integrina α4β1, se podía generalizar a células T primarias, como ocurría con las activaciones "*outside-in*", se realizaron las inmunofluorescencias con linfoblastos T humanos adheridos a FN-H89. Como se muestra en la figura 26, las células no tratadas (control) presentan una morfología redondeada, mientras que las tratadas con el Acm anti-CD3 presentan una morfología polarizada en un 70%. Los mismos resultados se obtuvieron para células adheridas a VCAM-1 (datos no mostrados). Además tras el tratamiento con PMA (50 ng/ml) se inducía una morfología extendida (aplastada) en un 75% de las células. Por lo tanto sí podemos generalizar esta respuesta a todos los linfocitos T.

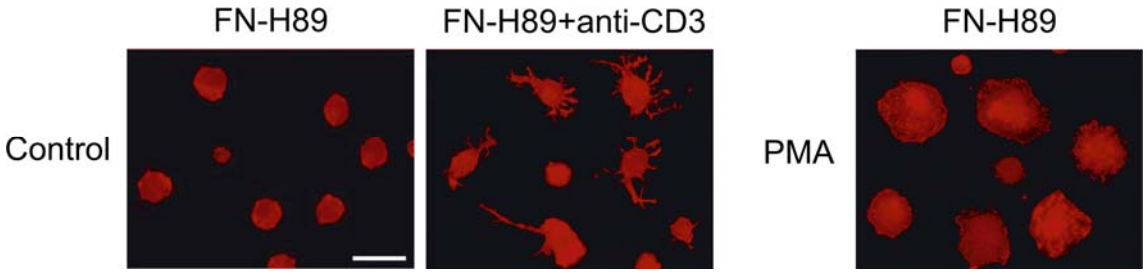

Figura 26. Efecto de las diferentes activaciones "*inside-out*" de la integrina α4β1, en linfoblastos-T. Linfoblastos-T (80 x10^3 células/punto) no activados (control) o activados con PMA (50 ng/ml) se adhirieron a FN-H89 (8 μg/ml) o al Acm anti-CD3 (0.1 μg/ml) junto a FN-H89 (8 μg/ml) durante 60 min, se fijaron y se tiñeron con faloidina-TRITC. El experimento se repitió 3 veces con resultados equiparables. Barra, 10 μm.

Para confirmar que los dos patrones morfológicos observados no representan diferentes estadios de un mismo proceso, primero se incrementó el tiempo de adhesión de las células tratadas con Mn^{2+} o con el Acm anti-CD3 hasta 3 h, observándose que el fenotipo elongado no evolucionaba hacia el fenotipo de morfología extendida (resultados no mostrados). En segundo lugar se analizó la morfología celular tras utilizar diferentes concentraciones de los diferentes agentes activadores. Como se muestra en la figura 27, la activación con Mn^{2+} o con el Acm anti-CD3, no induce el patrón de morfología extendida a ninguna de las concentraciones examinadas, resultando una morfología elongada en un 55%, 65%, y 80% de las células, durante la activación con 0.2, 0.5, y 2 mM de Mn^{2+}respectivamente. La misma morfología elongada se observaba en un 75% de las células en respuesta a 0.5, 1, y 2 µg/ml del Acm anti-CD3. Por otra parte, concentraciones bajas de TS2/16 (0.1-2 µg/ml) o PMA (5- 25 ng/ml) no daban lugar a una polarización celular, observándose en un 70-85% de las células un fenotipo de morfología extendida.

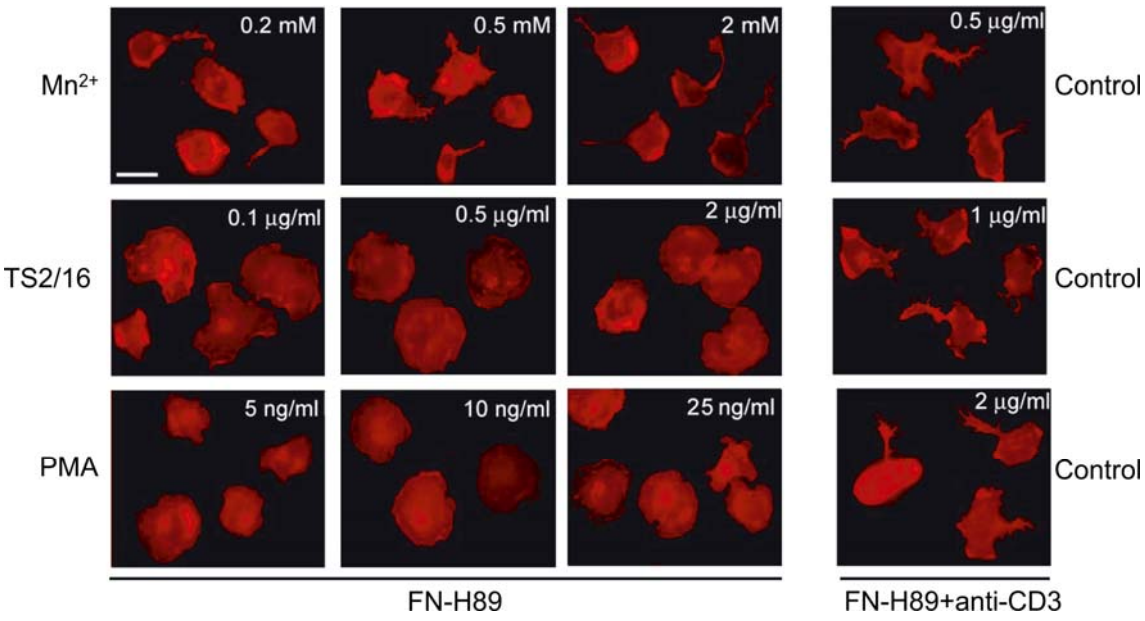

Figura 27. Efecto de la dosis de los diferentes agentes activadores de la integrina α4β1 en la reorganización del citoesqueleto de actina. Células Jurkat ($80x10^3$ células/punto) fueron tratadas con diferentes concentraciones de los diferentes agentes activadores de la integrina y fueron adheridas posteriormente a cubreobjetos tapizados con FN-H89 (8 µg/ml). Las células no tratadas (control) se añadieron sobre cubreobjetos tapizados con FN-H89 (8 µg/ml) más la concentración indicada del Acm anti-CD3. Se adhirieron durante 60 min, se fijaron y se tiñeron con faloidina-TRITC, para visualizar la F-actina. El experimento se repitió 4 veces con resultados equiparables. Barra, 10 µm

2. Efecto de las diferentes activaciones de la integrina α4β1 en migración celular y señalización intracelular

Tras comprobar que existen diferencias a nivel de adhesión y de reorganización del citoesqueleto de actina tras las diferentes activaciones de la integrina α4β1 y que estas diferencias no dependen de la fuerza del estímulo y son específicas para cada estímulo, se estudió lo que ocurría a otros niveles post-adhesión, como son migración celular y señalización intracelular.

Los agentes activadores de la integrina α4β1 que dan lugar a una polarización de la célula T inducen también migración celular y baja resistencia al despegue celular ("detachment") en condiciones de flujo.

La polarización es una característica de la migración linfocitaria, y es lo que se observaba tras el tratamiento de la célula T con Mn^{2+}. Esto nos llevó a analizar si las células Jurkat eran inducidas a migrar o a adherirse dependiendo del estímulo que activase a la integrina α4β1. La figura 28, muestra los resultados obtenidos tras el estudio de la migración celular a nivel de videomicroscopía de contraste de fases. Las células tratadas con los diferentes agentes activadores fueron añadidas a placas tapizadas con el fragmento recombinante FN-H89 a una concentración de 1.2 μg/ml (dicha concentración se eligió tras utilizar diferentes dosis y comprobar que una elevada concentración de sustrato prevenía la migración celular). Los resultados obtenidos confirmaron lo que ya se había visto a nivel de reorganización del citoesqueleto. Las células Jurkat no tratadas y adheridas a FN-H89 (control) presentaban una alta motilidad y el 23% de las células migraban al azar, siendo su morfología más o menos redondeada (vídeo 1). En las células activadas en condiciones de "*outside-in*", tras la activación de la integrina por Mn^{2+} (0.2 mM) se producía una clara migración en un 12% de las células y polarización en el 55% (vídeo 2). Este mismo patrón se observaba tras la activación con SDF-1α (150 ng/ml) (vídeo 3), donde existía migración en el 14% de las células. Sin embargo tras la activación por TS2/16 se abolía la migración celular y un 70% de células presentaban un patrón de morfología celular extendida, con proyecciones tipo lamelipodios en torno a la superficie celular (vídeo 4).

Algo similar se observó bajo condiciones de señalización "*inside-out*". Así, el tratamiento con PMA (50 ng/ml) inducía un patrón heterogéneo, donde el 6% de las

células migraban, y un 75% hacían "*spreading*" (vídeo 5). Sin embargo tras la adhesión de células Jurkat sin tratar a FN-H89 coinmovilizado con el Acm anti-CD3, se producía una clara migración en un 11% de las células y polarización en el 60% (vídeo 6). Como control a esta activación se utilizó la adhesión al Acm anti-CD3 sólo, observándose que este ligando no inducía migración celular (vídeo 7).

En la figura 28 A se muestran fotogramas representativos de cada uno de los tratamientos, a los tiempos de adhesión indicados, observándose en todos los casos una cinética similar. A partir de los 15-20 minutos las respuestas empiezan a ser evidentes, teniendo un efecto máximo a los 60 min, y permaneciendo durante al menos 180 min (resultados no mostrados). La figura 28B muestra la cuantificación del % de células que migran en cada caso. Los vídeos completos mostrando los resultados mencionados con cada una de las activaciones, se muestran en el CD adjuntado como material adicional.

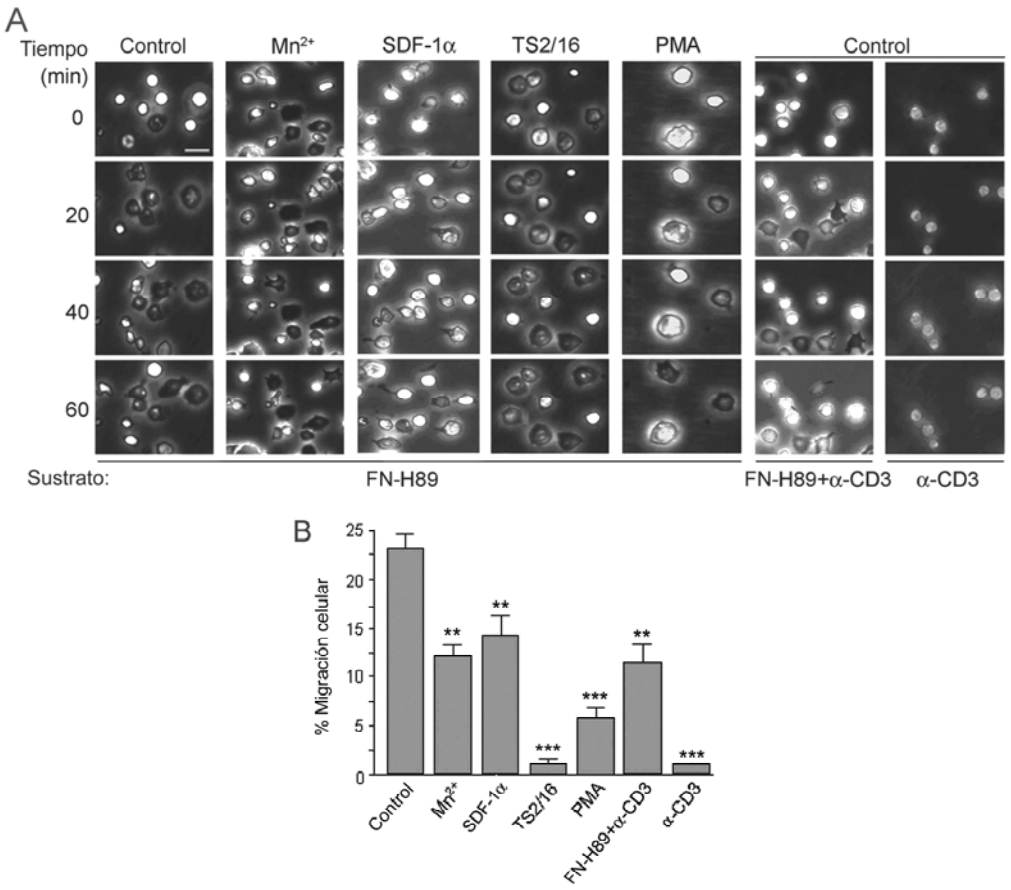

Figura 28. Análisis por videomicroscopía del efecto diferencial de las diferentes activaciones de la integrina α4β1 en la migración de las células T. A: Las células Jurkat ($5x10^5$ células/punto) no tratadas (control) o tratadas con Mn^{2+} (0.2 mM), SDF-1α (150 ng/ml), TS2/16 (5μg/ml) o PMA (50 ng/ml), se añadieron a cubreobjetos cubiertos con el sustrato adecuado (FN-H89, 1.2 μg/ml y el Acm anti-CD3 (α-CD3, 0.1 μg/ml) sólo o coinmovilizado con FN-H89. Los ensayos se realizaron a 37ºC y las células se fotografiaron cada 30 seg durante 1 h, mostrándose 4 tiempos representativos para cada condición. Barra, 10 μm. **B**: Cuantificación de los resultados obtenidos por videomicroscopía, con sus respectivas desviaciones estándar. El análisis estadístico se refiere a la migración de las células activadas con respecto a las células no tratadas (**, $p \leq 0.01$; ***, $p \leq 0.001$).

En un segundo abordaje experimental, se estudió la migración celular utilizando cámaras Transwell recubiertas con VCAM-1. Como se muestra en la figura 29, los resultados son similares a los obtenidos por videomicroscopía: tras la activación de la integrina α4β1 con bajas concentraciones de Mn^{2+} (0.2 mM) o Acm anti-CD3 (0.1 μg/ml), el porcentaje de migración celular que se observa es similar o un poco más elevado al de las células no tratadas (control). Sin embargo, tras el tratamiento con PMA (10 ng/ml) o TS2/16 (5 μg/ml), este porcentaje se inhibe significativamente. Los mismos resultados se obtuvieron con células adheridas a FN-H89 (no mostrados). En conclusión y a pesar de existir diferencias cuantitativas entre los 2 tipos de ensayos, lo que se observa claramente es que en ambos la activación de la integrina α4β1 por Mn^{2+} o el Acm anti-CD3, induce migración celular, mientras que la activación por TS2/16 o PMA, induce una adhesión firme.

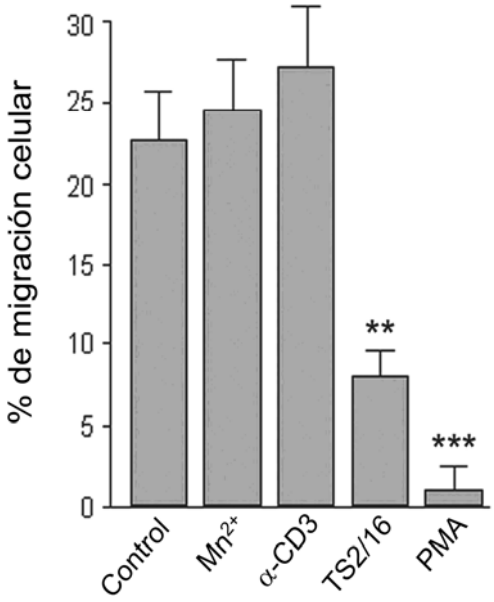

Figura 29. Efecto diferencial de las diferentes activaciones de la integrina α4β1 en la migración de células Jurkat en cámaras Transwell. Las células Jurkat ($2x10^5$) no tratadas (control) o tratadas con los diferentes agentes estimuladores, se añadieron a la cámara superior de filtros Transwell (tamaño de poro 5 μm), previamente tapizados con 8 μg/ml de VCAM-1. Las células no tratadas se añadieron también a Transwell tapizados con la mezcla VCAM-1/α-CD3 (8 μg/ml/0.1 μg/ml). Al medio que se dispensa en la cámara inferior del Transwell se le añadió SDF-1α (100 ng/ml). Las células que habían migrado se cuantificaron tras 7 h a 37ºC, mediante citometria de flujo, expresándose como el % de células totales. Los valores son la media de 3 experimentos independientes con sus desviaciones estándar. El análisis estadístico se refiere a la migración de las células activadas con respecto a las células no tratadas (**, $p \leq 0.01$; ***, $p \leq 0.001$).

Los anteriores abordajes para el estudio de la migración celular se realizaron bajo condiciones estáticas, por lo que se quiso comprobar si ocurría lo mismo en condiciones más fisiológicas, es decir dinámicas. Para ello se utilizó una cámara de flujo y células Jurkat adheridas a FN-H89. La figura 30, muestra que todas las activaciones de la integrina α4β1 provocan un aumento en la resistencia al flujo con respecto a las células no tratadas (control), pero la resistencia que provoca el tratamiento con Mn^{2+} (0.2 mM) es muy inferior a la mostrada tras el tratamiento con PMA, o con el Acm TS2/16.

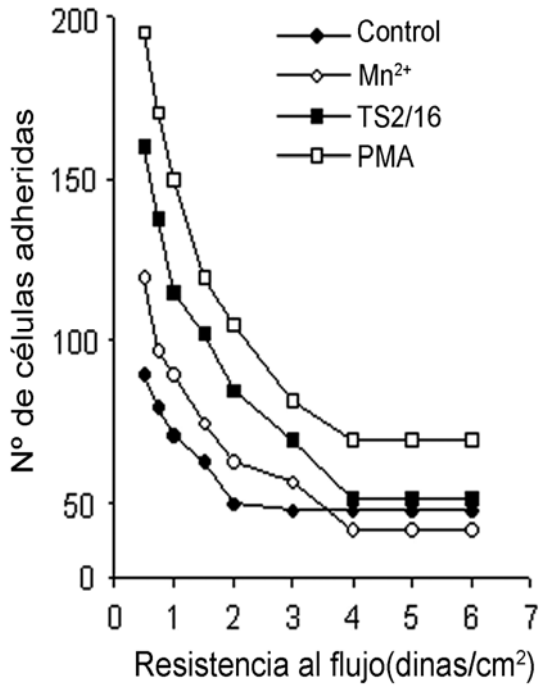

Figura 30: Efecto diferencial de las diferentes activaciones de la integrina α4β1 sobre la resistencia al despegue celular bajo condiciones de flujo. Se tapizaron placas petri con 15 µl de PBS conteniendo el fragmento recombinante FN-H89 (5 µg/ml). Bloqueandose a continuación con 0.5% BSA en PBS. Posteriormente esas placas fueron incorporadas como la pared inferior de una cámara de flujo paralelo. Las células Jurkat ($1x10^6$/ml) no tratadas (control) o tratadas con 0.2 mM Mn^{2+}, 5 µg/ml TS2/16 o 50 ng/ml PMA, se perfundieron a través de la cámara con un flujo de 1 dina/cm^2 en un medio libre de suero. Después de 2 min, el flujo se detuvo, dejando a las células adherirse durante 10 min, y se cuantificaron. Tras este tiempo se restauró el flujo que se fue incrementando cada minuto a razón de 0.5 dinas/cm^2. La resistencia al flujo se determino por el recuento del número de células que permanecen adheridas, después de cada intervalo.

Por lo tanto las diferentes activaciones de la integrina α4β1 dan lugar a diferentes respuestas, observándose un fenotipo migratorio o un fenotipo estacionario, dependiendo del estímulo utilizado, tanto en condiciones estáticas como de flujo.

La activación de las GTPasas RhoA y Rac1 afecta al fenotipo migratorio y polarizado inducido por la integrina α4β1, pero no afecta a la inducción de adhesión firme y morfología celular extendida ("spreading").

Una vez comprobado que existen diferencias a nivel de reorganización del citoesqueleto de actina y de migración celular tras los diferentes tratamientos de la integrina α4β1, se analizó lo que podría ocurrir a nivel de señalización intracelular. Puesto que tanto la migración como la reorganización del citoesqueleto de actina son procesos regulados por los miembros de la familia de las RhoGTPasas (Burridge and Wennerberg 2004), se investigó la posible implicación de RhoA en la ruta de señalización inducida por los diferentes estímulos de la integrina α4β1. En primer lugar se estudió el efecto de la activación exógena de RhoA con el activador específico LPA (Ridley and Hall 1992) y la posterior adhesión celular al fragmento FN-H89. Como se muestra en la figura 31, la activación con LPA tiene un efecto dramático en la activación de la integrina por Mn^{2+} ya que en el 88% de las células se observa una

desaparición significativa ($p \leq 0.001$) de la morfología polarizada. Además este efecto se revertía en un 65% de los casos, tras el tratamiento de las células con un inhibidor específico de RhoA como C3T. Sin embargo la activación con LPA no tenía ningún efecto sobre las células activadas con el Acm TS2/16 o sobre las células en que no se había activado la integrina α4β1 (control). Los mismos efectos se observaron tras la activación de la integrina con PMA (RhoA no tiene efecto alguno) o con el Acm anti-CD3 (RhoA induce pérdida de la polarización) (resultados no mostrados). Estos resultados indican que la activación exógena de RhoA inhibe casi totalmente la respuesta celular inducida por el tratamiento con Mn^{2+} pero no afecta la respuesta causada por el Acm TS2/16.

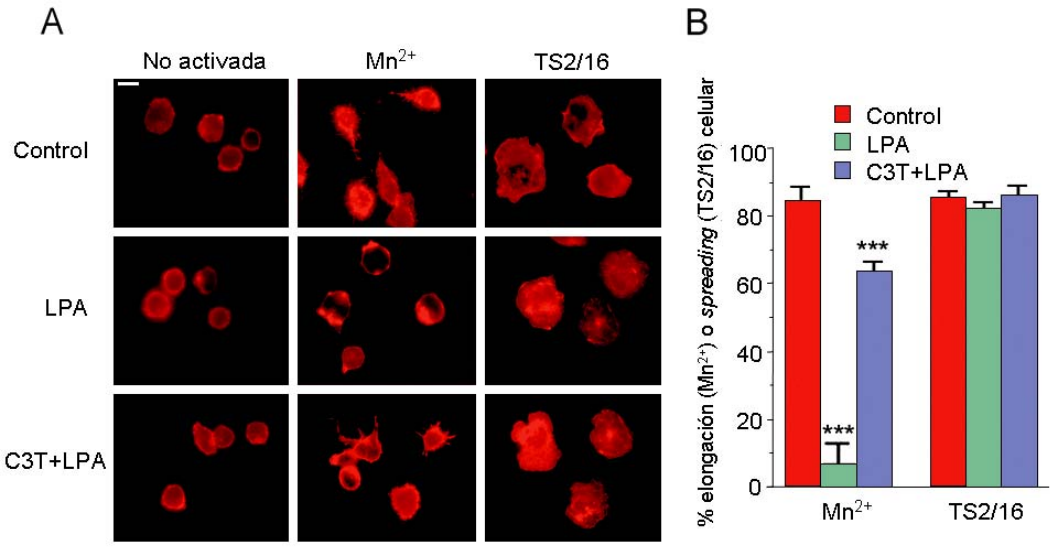

Figura 31. Efecto de la activación exógena de RhoA en la reorganización del citoesqueleto de células Jurkat tras la activación de la integrina α4β1 con Mn^{2+} y TS2/16. A: Las células Jurkat con o sin una incubación previa durante toda la noche con 50 µg/ml C3T, se trataron con Mn^{2+} (1 mM) o con TS2/16 (5 µg/ml) y luego fueron incubadas con 1 µM de LPA durante 60 min. Las células se dejaron en adhesión sobre FN-H89 durante 60 min a 37ºC, y posteriormente fueron fijadas y teñidas con faloidina-TRITC. Las células control en este caso fueron tratadas con Mn^{2+} o TS2/16 pero no recibían más tratamiento. Barra, 10 µm. **B**: Cuantificación del efecto del LPA o C3T+LPA sobre el patrón morfológico inducido por el Mn^{2+} (polarización) o el Acm TS2/16 *(spreading)*. Los valores representan la media de 4 ensayos con sus desviaciones estándar. ***, indica diferencias estadísticamente significativas con respecto al control ($p \leq 0.001$).

Para confirmar la implicación de RhoA en estos procesos, se realizó una activación endógena de las células mediante transfecciones transitorias con construcciones constitutivamente activas (V14RhoA) o dominantes negativas (N19RhoA) fusionadas a la GFP. Como se muestra en la figura 32, la sobre-expresión

de V14RhoA en células Jurkat adheridas al fragmento FN-H89 inhibía en un 90% la morfología polarizada inducida por el Mn^{2+}, mientras que en las células activadas con el Acm TS2/16, no tenía ningún efecto. Además la supresión de la actividad de RhoA, por la transfección transitoria con N19RhoA, daba lugar a una morfología polarizada en un 65% de las células, mientras que no tenía ningún efecto sobre la morfología inducida por el Acm TS2/16 (figura 32).

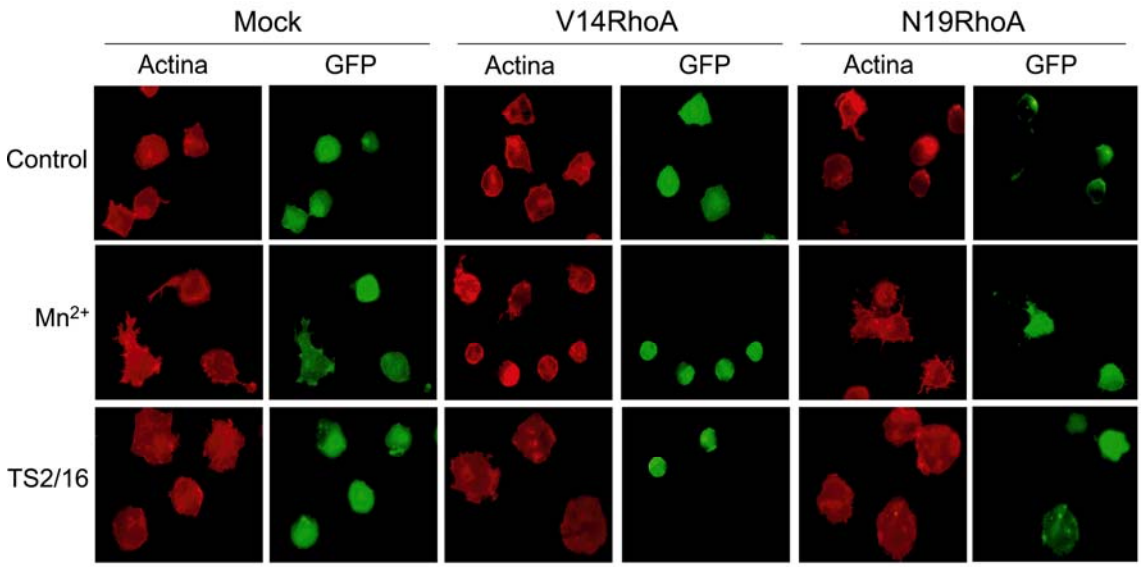

Figura 32: Regulación endógena de RhoA. Las células Jurkat fueron transfectadas transitoriamente con el vector PEGFP-C1 vacío (mock), con el mutante activo V14RhoA-GFP, o con el mutante dominante negativo N19RhoA-GFP. Las células no activadas (control) o activadas con Mn^{2+} (1 mM) o TS2/16 (5 µg/ml) se adhirieron a FN-H89 durante 60 min, se fijaron y se tiñeron con faloidina-TRITC (rojo). Las células transfectadas se visualizaron por GFP (verde). El experimento se repitió 3 veces con resultados equiparables.

Otra de las GTPasas implicadas en la reorganización del citoesqueleto de actina, es la GTPasa Rac1. La sobreexpresión de V12Rac1 (constitutivamente activa) en las células Jurkat y su posterior adhesión al sustrato FN-H89, induce también una inhibición (70%) en la morfología polarizada observada tras el tratamiento con Mn^{2+}, pero no afecta a la morfología extendida observada tras el tratamiento con el Acm TS2/16 (figura 33). Sin embargo, y de acuerdo con los resultados obtenidos con RhoA, la transfección con N17Rac1 (dominante negativo) no afecta la polarización celular inducida por Mn^{2+} y no tiene ningún efecto sobre la morfología extendida causada por el Acm TS2/16 (figura 33).

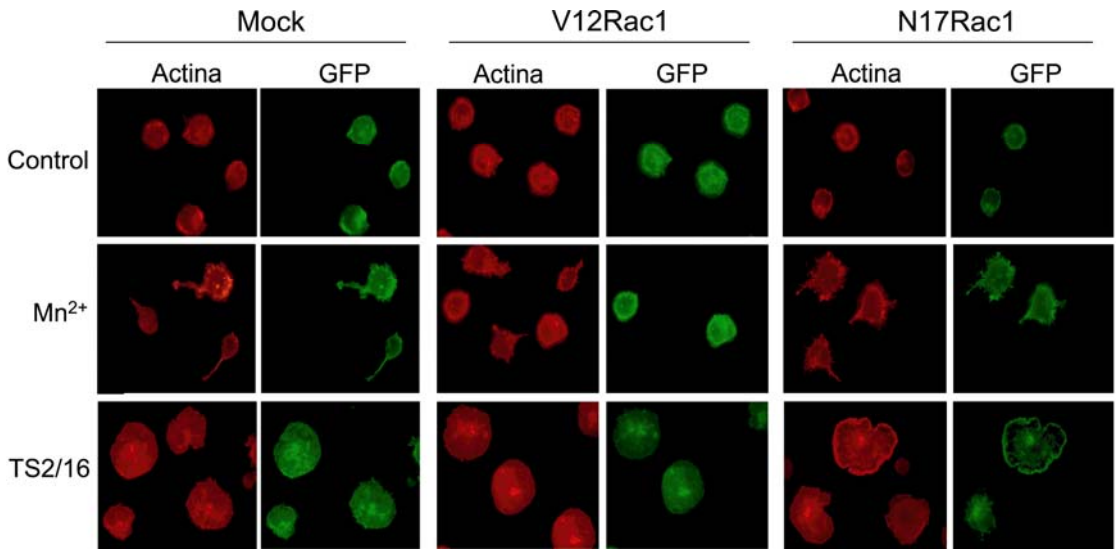

Figura 33: Regulación endógena de Rac1. Las células Jurkat fueron transfectadas transitoriamente con el vector PEGFP-C1 vacío (mock), con el mutante activo V12Rac1-GFP, o con el mutante dominante negativo N17Rac1-GFP. Las células no activadas (control) o activadas con Mn^{2+} (1 mM) o TS2/16 (5 µg/ml) se adhirieron a FN-H89 durante 60 min, se fijaron y se tiñeron. El citoesqueleto de actina se tiñó con faloidina-TRITC (rojo) y las células transfectadas se visualizaron por GFP (verde). El experimento se repitió 3 veces con resultados equiparables.

Las diferentes activaciones de la integrina α4β1 y su posterior adhesión a FN-H89 dan lugar a una distinta regulación de RhoA y Rac1.

Una vez comprobada la implicación de RhoA y Rac1 en el proceso, quisimos establecer el papel de RhoA y Rac1 en la morfología polarizada o extendida de las células T. Con esta finalidad se realizaron ensayos de arrastre (*pull-down*) por afinidad usando las proteínas de fusión C21 y PAK fusionadas a la GST, que unen solamente RhoA y Rac1 en estado activado (GTP). Los lisados de células Jurkat, previamente tratadas o no con los diferentes agentes activadores de la integrina α4β1 y adheridas sobre FN-H89, se preincubaron con las proteínas de fusión, y se analizaron por SDS-PAGE y *western blotting* con los Acms anti-RhoA o anti-Rac1. Como se puede observar en la figura 34, los niveles de RhoA tras la activación de la integrina con Mn^{2+} o con el Acm TS2/16 no presentan grandes diferencias con respecto a las células no tratadas (control), excepto a los 5 min, en el caso de la activación con TS2/16, donde hay una disminución de la activación de RhoA. Sin embargo, la activación de Rac1 sí presenta una diferente regulación dependiendo del tratamiento que se le dé a la célula. El tratamiento con Mn^{2+} da lugar a una disminución muy significativa ($p \leq 0.01$) de la activación de Rac1 durante los 20 primeros minutos de adhesión, seguida de un

aumento muy significativo ($p \leq 0.01$) que se sostiene durante el resto del ensayo. Sin embargo el Acm TS2/16 induce un incremento progresivo en la actividad de Rac1, el cual es muy significativo ($p \leq 0.01$) a los 60 min de adhesión con respecto a las células no tratadas. No se estudiaron tiempos más largos porque el efecto de la diferente reorganización del citoesqueleto de actina según el estímulo que activase la integrina α4β1 era muy claro a los 60 min.

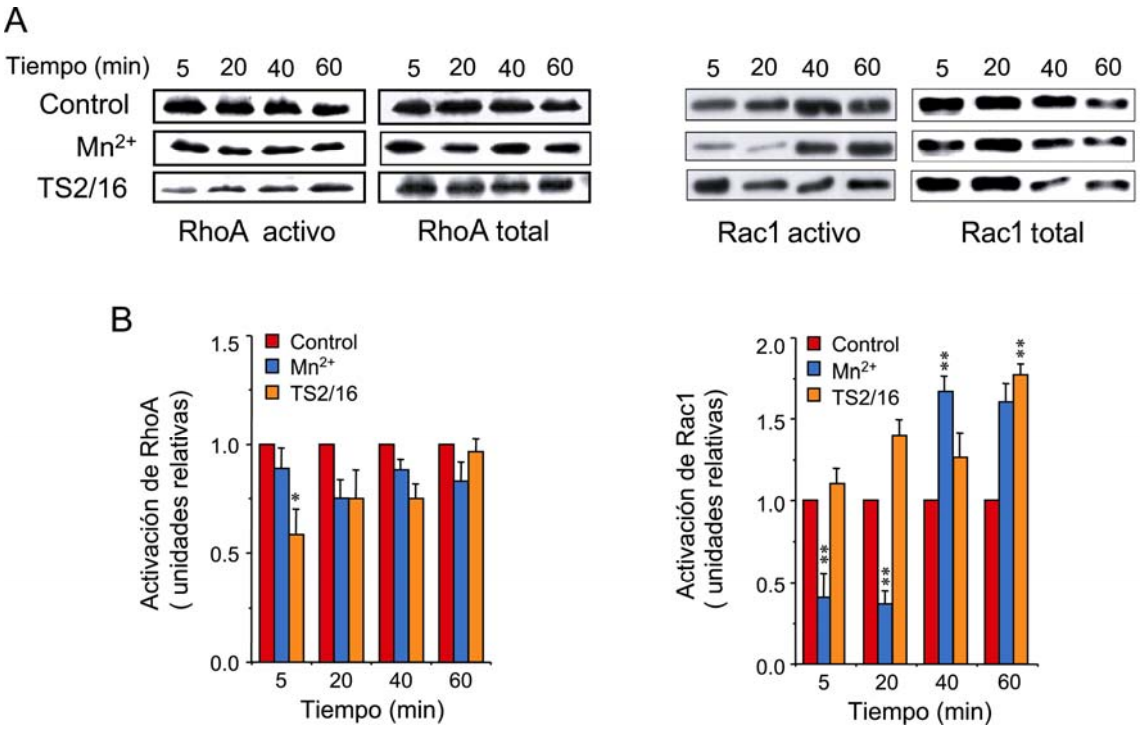

Figura 34. **Regulación de RhoA y Rac1 tras la activación de la integrina α4β1 por Mn^{2+} o TS2/16**. **A**: Las células Jurkat ($30x10^6$ células/punto) fueron privadas de suero durante tres horas, y posteriormente fueron activadas o no con Mn^{2+} (1 mM) o TS2/16 (5 μg/ml). Tras la activación se adhirieron a FN-H89 durante el tiempo indicado y posteriormente fueron lisadas en tampón RIPA, siendo los lisados clarificados por centrifugación. Estos lisados se incubaron con C21-GST o PAK-GST, para RhoA y Rac1 respectivamente, junto con glutation-agarosa durante toda la noche. Tanto la fracción unida como la GTPasa total, fueron eluídas hirviendo las muestras en tampón de carga y posteriormente fueron analizados por western blotting. **B**: Cuantificación de los niveles relativos de RhoA y Rac1 activado, para cada tiempo (media de 3 ensayos con sus respectivas desviaciones estándar). Los niveles de las células no tratadas fueron normalizados a 1. El análisis estadístico se refiere al grado de activación de las GTPasas en las células activadas con respecto a las células no tratadas (control) (*, $p \leq 0.05$; **, $p \leq 0.01$).

Los diferentes estímulos que activan la integrina α4β1 dan lugar a una distinta fosforilación de Pyk-2.

Es bien sabido que la interacción de la integrina α4β1 con VCAM-1 o con un Acm anti-α4 induce fosforilación de Pyk-2 (van Seventer *et al*. 1998; Gismondi *et al*. 2003). Asimismo, se conoce la localización de esta molécula durante el proceso de *spreading* o de motilidad inducido por integrinas (Rodríguez-Fernández *et al*. 1999; Vicente-Manzanares and Sánchez-Madrid 2004). A partir de estas premisas se quiso determinar cual era el estado de Pyk-2 tras las diferentes activaciones de la integrina α4β1. Para ello se midió el grado de activación (fosforilación) de Pyk-2 en lisados de células Jurkat no tratadas (control) o tratadas con los diferentes agentes estimuladores y posteriormente adheridas a FN-H89 durante diferentes tiempos. Como se observa en la figura 35 (A y B), los niveles de fosforilación de Pyk-2 en células donde la integrina no está activada pero si adherida a FN-H89, son muy bajos a todos los tiempos estudiados. Sin embargo la activación de la integrina con agentes que provocan una polarización celular (Mn^{2+}, SDF-1α o el Acm anti-CD3) y su posterior adhesión a FN-H89 aumenta la fosforilación de Pyk-2, observándose el máximo a los 30-45 min de adhesión. Este incremento es estadísticamente significativo ($p \leq 0.05$ o $p \leq 0.01$) para los tres estímulos y a todos los tiempos testados, excepto para el tratamiento con SDF-1α a 60 min.

Por otro lado, en la figura 35 (A y B) observamos que la activación con SDF-1α (o con el Acm anti-CD3) de células Jurkat en suspensión, también induce incremento en la fosforilación de Pyk-2 a los 30 minutos, siendo este incremento significativo para SDF1-α ($p \leq 0.05$). Sin embargo ese incremento es inferior en un 50% al obtenido tras la adhesión de estas mismas células a FN-H89. Estos resultados, junto con el hecho de que FN-H89 es un pobre inductor de fosforilación de Pyk-2 en células no tratadas (figura 35), sugieren que además de un efecto sinergístico entre α4β1 y el CD3 (van Seventer *et al*. 1998), la activación de la integrina por ligación de CD3 o por SDF-1α, también juega un papel en la fosforilación de Pyk-2. Compatibles con estos resultados son los obtenidos tras el tratamiento con el Acm anti-α4 HP2/1 o con toxina pertúsica, inhibidores de α4 y de la señalización inducida por CXCR4 (receptor de SDF-1α) respectivamente. En éstos se observa una reducción de los niveles de fosforilación de Pyk-2 hasta niveles constitutivos (figura 35 C y D).

Por el contrario, la activación de la α4β1 por agentes que provocan la morfología extendida (aplastada), como el Acm TS2/16, y su posterior adhesión a

FN-H89, no producía un aumento de la fosforilación de Pyk-2. La activación con PMA producía una fosforilación intermedia, alcanzando su máximo de activación a los 30 min (figura 35 A y B). Estos resultados indican que existe una diferente regulación de la fosforilación de Pyk-2, tras el tratamiento con diferentes agentes activadores de la integrina α4β1, y esta respuesta se correlaciona con la respuesta migratoria o estacionaria que presentan las células T.

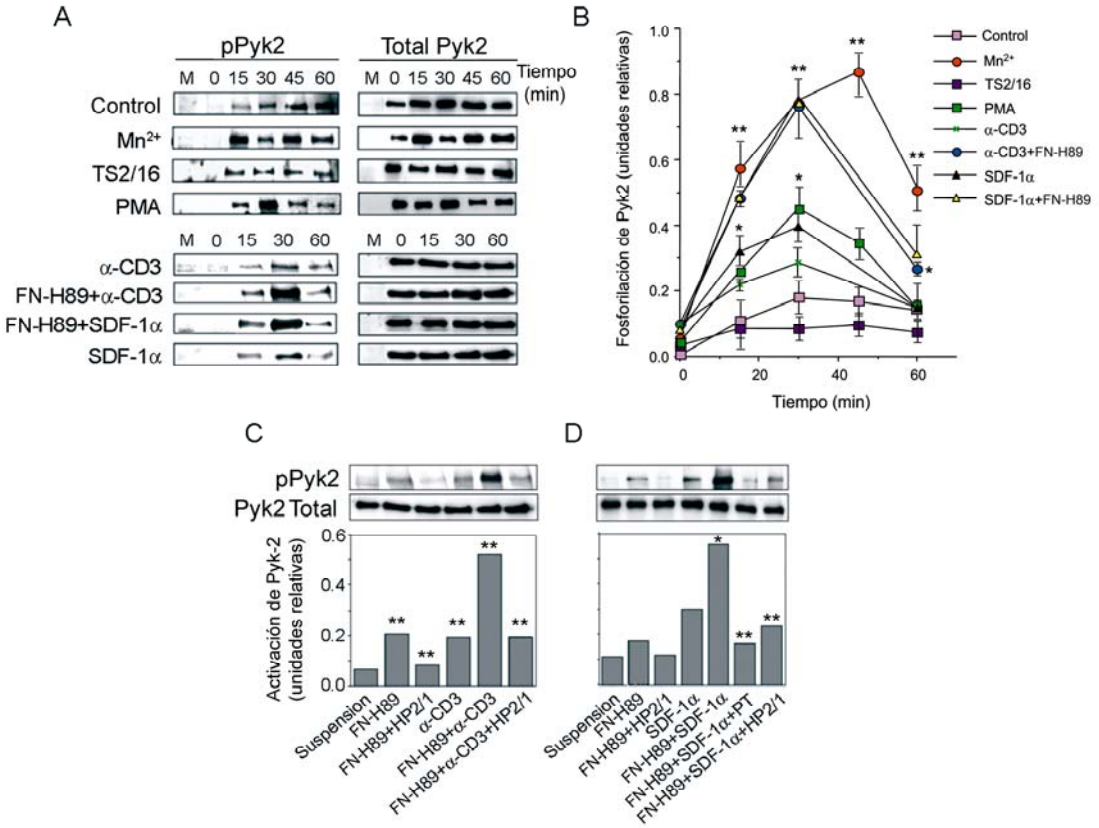

Figura 35. Efecto de las diferentes activaciones de la integrina α4β1 en la fosforilación de Pyk-2.
A: Células Jurkat ($10x10^6$/condición) activadas o no con Mn^{2+} (0.3 mM), TS2/16 (5 μg/ml), PMA (50 ng/ml), o SDF-1α (150 ng/ml) se añadieron a placas de 6 pocillos cubiertas con FN-H89 (8 μg/ml). Las células no activadas también se añadieron a placas cubiertas con FN-H89 (8 μg/ml) + Acm anti-CD3 (α-CD3, 0.1 μg/ml) o con el Acm anti-CD3 (0.1 μg/ml) sólo. A los tiempos de adhesión indicados las células fueron lisadas e inmunoprecipitadas frente a Ac específicos frente a Pyk-2. Posteriormente fueron analizados por SDS-PAGE y *western blotting*. M indica mock (no incubadas con anti-Pyk2). **B**: Cuantificación de los niveles de fosforilación de Pyk-2 (pPyk2) para cada condición, realizada por la normalización de los valores con respecto a la proteína total. Estos valores muestran la media de 4 ensayos independientes con sus respectivas desviaciones estándar. El análisis estadístico se refiere al grado de fosforilación de Pyk-2 en las células activadas con respecto a las células no tratadas (control) (**, $p \leq 0.01$; ***, $p \leq 0.001$). **C**: Determinación de la fosforilación de Pyk-2 tras 30 minutos de adhesión a FN-H89, FN-H89+anti-CD3 o anti-CD3 sólo, de las células pretratadas o no con el Acm HP2/1 (anti-α4). **D**: Determinación de la fosforilación de Pyk-2 tras 30 minutos de adhesión a FN-H89 o BSA (para SDF-1α) de las células pretratadas o no con el Acm HP2/1 (anti-α4) o con toxina pertúsica (PT, 10 ng/ml). Los valores en C y D muestran la media de 3 ensayos independientes con sus respectivas desviaciones estándar. * y ** indican diferencias estadísticamente significativas con respecto a las células en suspensión ($p \leq 0.05$ y $p \leq 0.01$, respectivamente)

3. Papel del dominio Hep III de FN en la formación de matrices de FN

El fragmento FNIII4-5 (dominio Hep III de FN) inhibe el ensamblaje de la matriz de fibronectina.

Los resultados expuestos establecen que tanto el fragmento FN-H89 (dominio Hep II), como el fragmento FNIII4-5 (dominio Hep III), inducen una reorganización similar del citoesqueleto de actina. Por otra parte, resultados anteriores de nuestro laboratorio (Moyano *et al.*, 1999) indicaban otras homologías funcionales entre ambos dominios de FN, como la capacidad de mediar adhesión celular a través de su interacción con la integrina α4β1 y con PG. Así, hemos identificado previamente la secuencia WTTPRAQITGYRLTVGLTRR en la repetición III5 de la FN (sitio HBP/III5), que media adhesión a través de PGCS y que es homóloga a la secuencia WQPPRARITGY de la repetición III14 (sitio FN-C/H V). También se identificó la secuencia KLDAPT en la misma repetición III5 de la FN (sitio H2), que media adhesión a través de la integrina α4β1 activada y que es homóloga a la secuencia IDAPS de la repetición III14 (sitio H1) (figura 36).

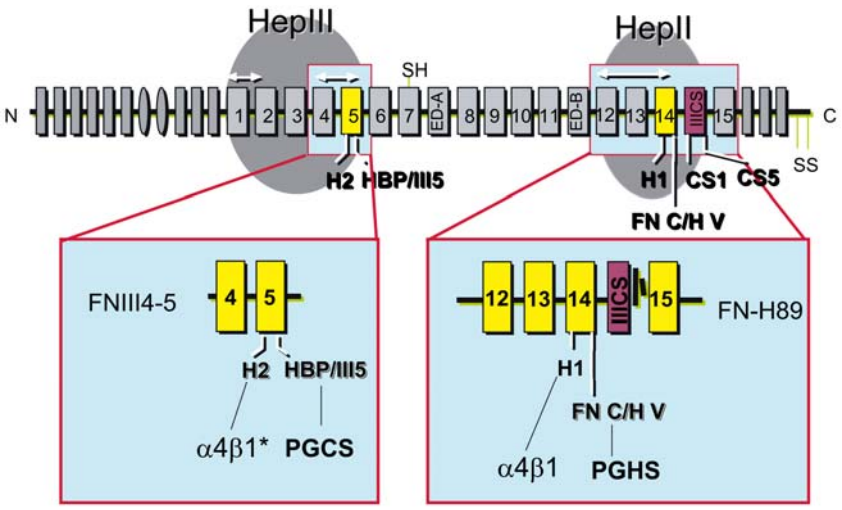

Figura 36. Esquema comparativo de los fragmentos recombinantes FNIII4-5 y FN-H89 utilizados. Los fragmentos recombinantes son indicados por sus correspondientes repeticiones estructurales, especificando en negrita sus sitios activos de adhesión, y con líneas en negrita la unión a sus receptores.* significa estado activado de la integrina.

También hemos demostrado previamente que HBP/III5 (como FN-C/H-V) aumenta la formación de fibras de estrés y adhesiones focales inducidas por la integrina α5β1 en células de melanoma (Moyano *et al*., 2003b). Dado que el dominio Hep II está implicado en la formación de matrices de FN (Bultmann *et al.*, 1998; Santas *et al.*, 2002) y tiene muchas similitudes funcionales y estructurales con el dominio Hep III, estudiamos a continuación el posible papel del dominio Hep III en el proceso de fibrilogénesis de FN. En primer lugar se estudió su papel en la formación de matriz a partir de FN exógena. Para ello se incubaron fibroblastos humanos, durante toda la noche con FN plasmática (4 μg/ml), en presencia de cicloheximida (CHX), y en presencia o ausencia de 200 μg/ml de diferentes fragmentos de FN (figura 37). En concreto del fragmento proteolítico de 70 kDa (amino terminal), del fragmento recombinante FNIII4-5 o del fragmento proteolítico de 80 kDa, analizándose en todos los casos la formación de fibrillas de FN por inmunofluorescencia.

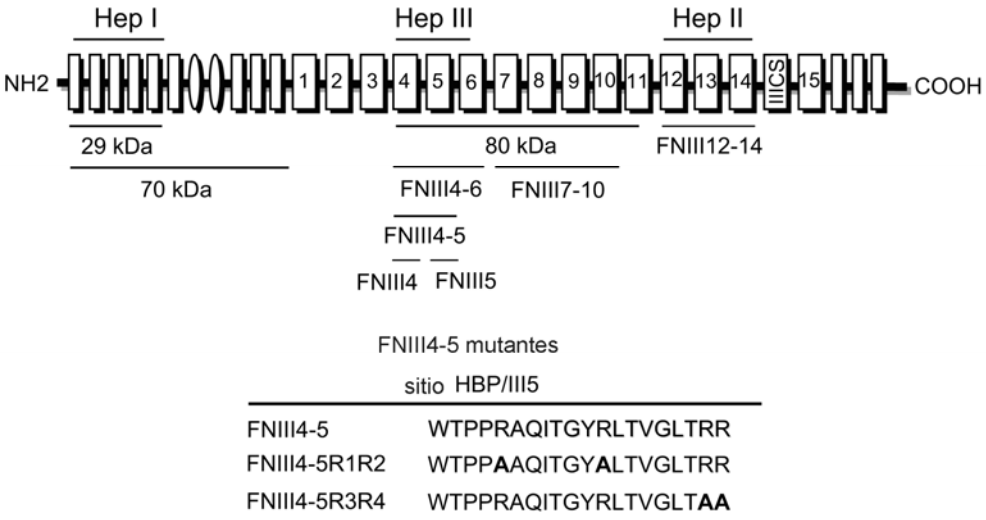

Figura 37. Esquema de un monómero de la FN plasmática (cadena A) y de los fragmentos recombinantes y proteolíticos utilizados. Los fragmentos proteolíticos son indicados por sus correspondientes pesos moleculares, mientras que los fragmentos recombinantes contenidos en el dominio Hep III están marcados como FNIII, especificando en negrita los residuos mutados en algunos de los fragmentos.

Los resultados obtenidos mostraban una buena formación de matriz de FN cuando los fibroblastos estaban en presencia de FN plasmática sóla (figura 38 A), y un bloqueo de esta matriz tanto en presencia del fragmento de 70 kDa (región que es una conocida competidora de la fibrilogénesis) (McDonald *et al*., 1987) (figura 38 B), como en

presencia del fragmento recombinante FNIII4-5 (figura 38 C). Sin embargo, el fragmento de 80 kDa, que también contiene la región III4-5, no inhibía la fibrilogénesis de FN (figura 38 D).

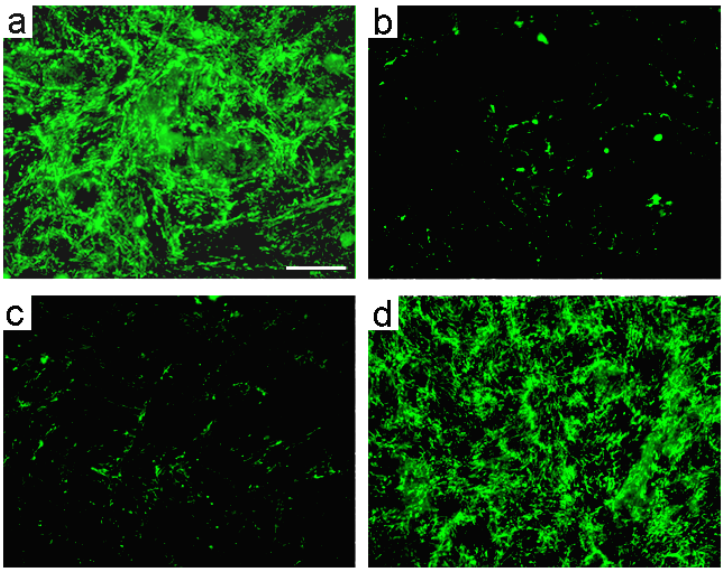

Figura 38. **Inhibición de la formación de la matriz de fibronectina exógena por los fragmentos de 70 kDa y FNIII4-5.** Los fibroblastos tratados con CHX (25 µg/ml) fueron plaqueados sobre FN e incubados toda la noche con 4 µg/ml de FN plasmática sola (a), o en combinación con 200 µg/ml del fragmento de 70 kDa (b), del fragmento FNIII4-5 (c), o del fragmento de 80 kDa (d). Las células fueron fijadas e incubadas con un Ac policlonal anti-FN, siendo posteriormente incubadas con un Ac anti-IgG de conejo conjugado a rodamina. Barra, 50 µm

El fragmento FNIII4-5 también inhibía la formación de matriz a partir de FN endógena. Como se muestra en la figura 39, las células incubadas en ausencia de CHX, son capaces de ensamblar su propia matriz de manera eficiente (figura 39 A). La incubación con el fragmento de 70 kDa o con FNIII4-5 inhibía casi por completo esta formación (figura 39 B y C).

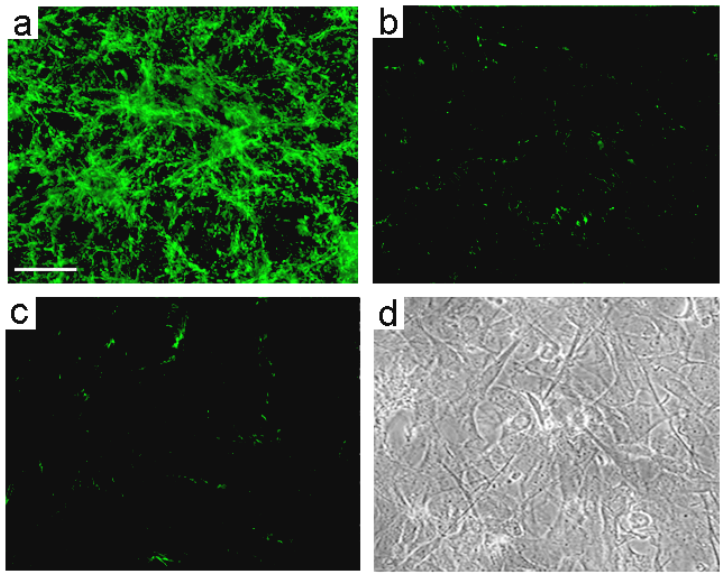

Figura 39. **Inhibición de la formación de la matriz de fibronectina endógena por los fragmentos de 70 kDa y FNIII4-5.** Los fibroblastos fueron plaqueados sobre FN e incubados toda la noche con 4 µg/ml de FN plasmática sola (a), o en combinación con 200 µg/ml del fragmento de 70 kDa (b), del fragmento FNIII4-5 (c). Una imagen de la monocapa celular obtenida por contraste de fase se muestra en (d). Las células fueron fijadas e incubadas con un Ac policlonal anti-FN, siendo posteriormente incubadas con un Ac anti-IgG de conejo conjugado a rodamina. Barra, 50 µm

Este efecto inhibitorio del fragmento FNIII4-5 a nivel de inmunofluorescencia se pudo confirmar y cuantificar estudiando el papel de este fragmento en la incorporación de ^{125}I-FN a una monocapa de fibroblastos. Como se muestra en la figura 40, el fragmento FNIII4-5 inhibía la unión de FN a las células de forma dosis dependiente, con una $IC_{50} < 10^{-7}$ M . Como era de esperar el fragmento de 70 kDa también inhibía esta unión ($IC_{50} < 10^{-8}$ M). En el mismo ensayo el fragmento proteolítico de 80 kDa, no inhibía la incorporación de ^{125}I-FN a fibroblastos (figura 40). Dado que la región III4-5 está incluida en este fragmento de 80 kDa (figure 37) estos resultados sugerían una actividad críptica del fragmento FNIII4-5.

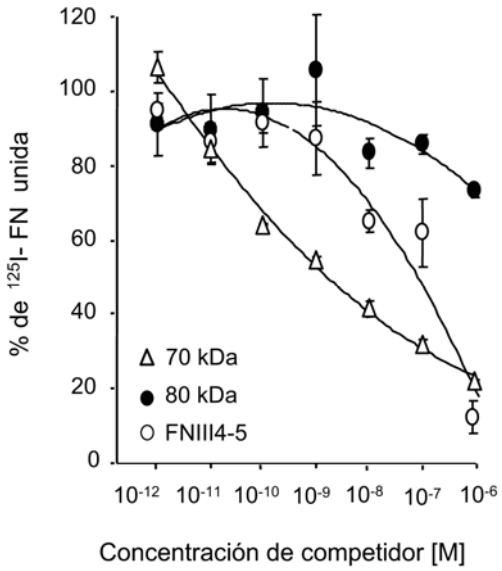

Figura 40. Inhibición de la incorporación de ^{125}I-FN a fibroblastos por varios fragmentos de FN. Los fibroblastos (3 x 10^4 células/punto) fueron plaqueados durante 24 ó 48 h a 37^0C e incubados posteriormente con ^{125}I-FN (2.7 x 10^6 cpm/ml) en presencia o ausencia de los fragmentos de 80 kDa, 70 kDa, y FNIII4-5 durante 3 h. La actividad especifica de la ^{125}I-FN era 3.8 x 10^7 cpm/µg.

Caracterización de los sitios implicados en el efecto inhibitorio del fragmento FNIII4-5 en el ensamblaje de la matriz de FN.

Una vez visto que el fragmento recombinante FNIII4-5 tenía un papel inhibitorio en la formación de matrices de FN, nos planteamos conocer las diferentes razones que pueden causar este efecto. Establecimos dos premisas: 1) FNIII4-5 puede bloquear la interacción entre la superficie celular y la región de 70 kDa de FN, crítica para el proceso de fibrilogénesis y 2) FNIII4-5 puede prevenir la interacción FN-FN utilizada para polimerizar las fibrillas. Para estudiar la primera premisa y también determinar si las secuencias activas previamente identificadas en la región III4-5 de FN (Moyano *et al.,* 1999), contribuían al efecto inhibitorio de esta región en la formación de la matriz de FN, se utilizaron una serie de fragmentos recombinantes derivados del FNIII4-5 original que contenían mutaciones en la secuencia HBP/III5 (ver figura 37).

Los fibroblastos tratados con CHX se incubaron sobre FN completa en presencia de FN plasmática sóla o en combinación con 200 µg/ml de los fragmentos mutados FNIII4-5R1R2 y FNIII4-5R3R4, así como del propio fragmento FNIII4-5 y del fragmento relacionado FNIII4-6 (figura 37), y se analizaron los resultados por inmunofluorescencia (figura 41).

Como se muestra en la figure 41 C el fragmento FNIII4-6 inhibía la formación de la matriz de FN tan eficientemente como el FNIII4-5 (D), sugiriendo por tanto que los residuos implicados en este efecto no son crípticos en el fragmento FNIII4-6. El fragmento FNIII4-5R1R2 (E) también inhibía la fibrilogénesis de FN, indicando que las 2 primeras argininas (R1R2) del sitio HBP/III5, no están implicados en este proceso. Por el contrario con la mutación FNIII4-5R3R4 (F) se eliminaba por completo el efecto inhibitorio de FNIII4-5, por lo tanto las 2 últimas argininas (R3R4) si desempeñan un papel importante en este proceso.

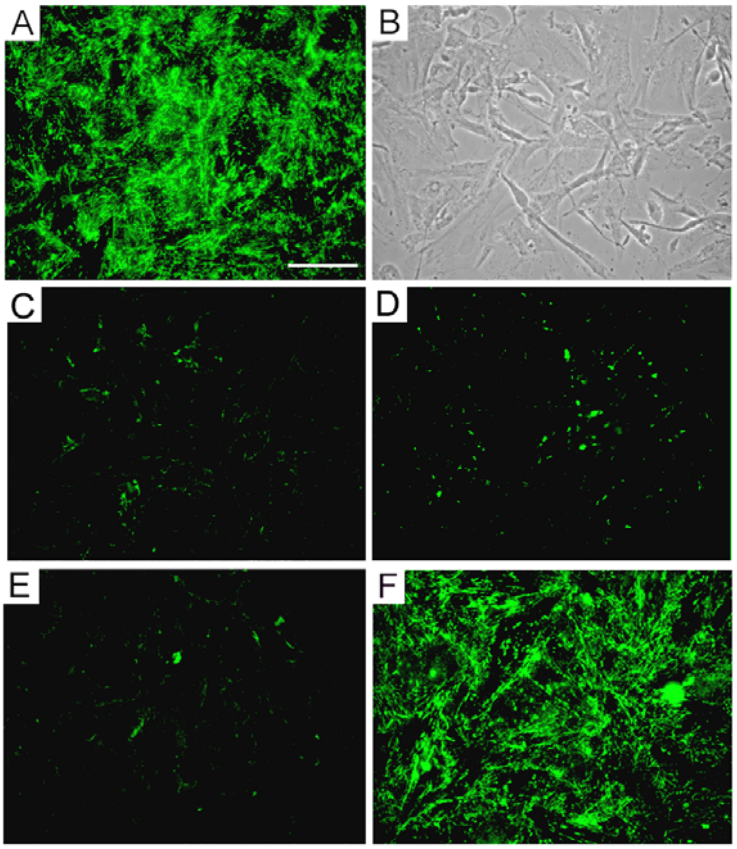

Figura 41. **Efecto de los fragmentos recombinantes FNIII4-5, FN-III4-6 y de las mutaciones en el sitio HBP/III5 de FNIII4-5 en el ensamblaje de la matriz de FN.** Los fibroblastos tratados con CHX (25 µg/ml) fueron plaqueados sobre 10 µg/ml de FN e incubados toda la noche con 4 µg/ml de FN plasmática sóla (A), o en combinación con 200 µg/ml del fragmento FNIII4-6 (C), FNIII4-5 (D), FNIII4-5R1R2 (E), o FNIII4-5R3R4 (F). Una imagen de la monocapa celular obtenida por contraste de fase se muestra en (B). Las células fueron fijadas e incubadas con un Ac policlonal anti-FN, y posteriormente fueron incubadas con Ac anti-IgG de conejo conjugado a rodamina. Barra, 20 µm

Para corroborar estos resultados obtenidos por inmunofluorescencia, quisimos testar la capacidad de estos fragmentos en la incorporación de ^{125}I-FN a una monocapa de fibroblastos. Como muestra la figura 42 A, el mutante FNIII4-5R1R2 es tan buen

inhibidor como el fragmento de 70 kDa, con una $IC_{50} < 10^{-7}$ M, mientras que el mutante FNIII4-5R3R4 no compite por la unión de ^{125}I-FN. El fragmento FNIII4-6 bloqueaba parcialmente la unión, alcanzando sólo el 45% de inhibición.

Por otro lado, sabemos que la región amino terminal de la molécula de FN está implicada en fibrilogénesis de FN, siendo el fragmento proteolítico de 29 kDa representativo de esta región (figura 37). Para determinar si FNIII4-5 inhibía la fibrilogénesis porque competía de forma directa con las interacciones del fragmento 29 kDa con la superficie celular, estudiamos el papel de los fragmentos FNIII4-5, FNIII4-5 R1R2, FNIII4-5 R3R4 y FNIII4-6 en la incorporación de ^{125}I-29 kDa (5.5 x10^6 cpm/ml) a una monocapa de fibroblastos (ver figura 42 B). Los resultados son muy similares a los obtenidos con la incorporación de ^{125}I-FN. Todos los fragmentos a excepción del FNIII4-5R3R4 bloquean la incorporación de ^{125}I-29 kDa a la monocapa celular.

El conjunto de estos resultados sugieren que las argininas tercera y cuarta (R3R4) del sitio HBP/III5 son requeridas para esta capacidad inhibitoria del fragmento FNIII4-5, mientras que las dos primeras argininas del sitio HBP/III5 no juegan un papel relevante en este proceso.

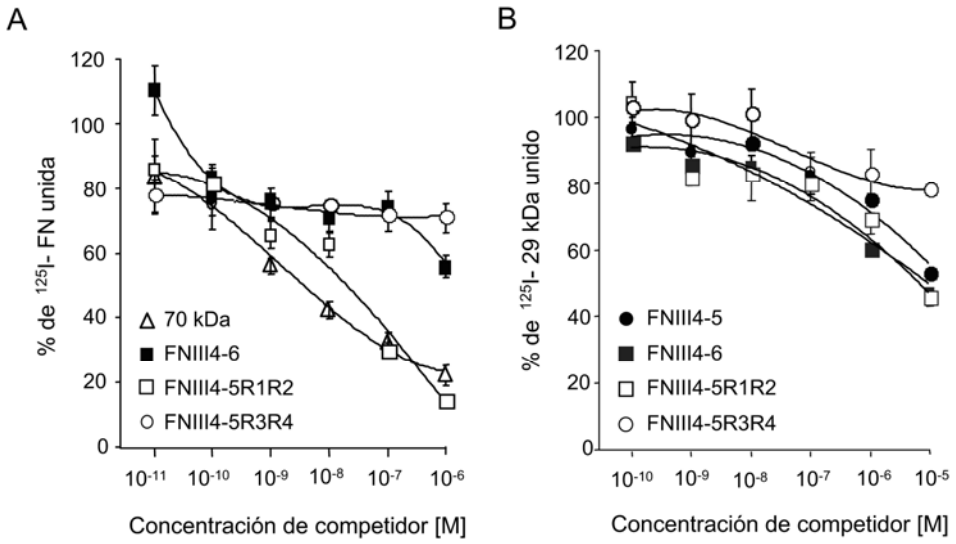

Figura 42. Inhibición de la incorporación de ^{125}I-FN y ^{125}I-29kDa a una monocapa celular de fibroblastos por varios fragmentos de FN. Los fibroblastos (3 x 10^4 células/punto) fueron plaqueados durante 24 o 48 h a 37^{0}C e incubados con ^{125}I-FN (panel A) o ^{125}I-29kDa (panel B) en presencia o ausencia de los fragmentos no marcados de 70 kDa, FNIII4-5, FN-III4-6, FNIII4-5R1R2, y FNIII4-5R3R4 durante 3 h. La actividad específica de ^{125}I-FN era 3.7x 10^7 cpm/µg y la de ^{125}I-29kDa era 1 x 10^8 cpm/µg. Los valores representan la media de 3 ensayos.

El fragmento FNIII4-5 interacciona consigo mismo y con fragmentos derivados de la región amino terminal de la FN.

Para comprobar la segunda premisa, es decir si el fragmento FNIII4-5 inhibía el ensamblaje de la matriz por interacción directa con la región amino terminal de la FN (fundamental para la fibrilogénesis), utilizamos un biosensor óptico. En primer lugar se inmovilizaron el fragmento de 70 kDa o la molécula de FN completa sobre cubetas de CMD, y se midió la unión del fragmento FNIII4-5 soluble. Como se observa en la figura 43 (A y B) existe una unión dosis dependiente y una respuesta muy similar en ambas condiciones. A la misma concentración molar del fragmento soluble, sobre FN la respuesta alcanza los 2594 arc/seg y sobre el fragmento de 70 kDa, los 3128 arc/seg. Sin embargo el fragmento 80 kDa soluble no se unía a FN ni al fragmento de 70 kDa, lo que de nuevo sugería una localización críptica de los residuos de FNIII4-5 implicados en esta unión. Para comparar esta capacidad de unión a FN del FNIII4-5 (Hep III), con la interacción ya conocida entre el dominio Hep II y la región amino terminal de FN, lo que hicimos fue medir la unión del fragmento FNIII12-14 (Hep II). Se observó unión tanto a FN como a 70 kDa, lo que estaba de acuerdo con resultados previos (Bultmann et al., 1998). La respuesta era similar, 2295 arc/seg y 2550 arc/seg, a FN y 70 kDa respectivamente, e inferior a la de FNIII4-5 a la misma concentración molar (figura 43 A y B).

Se analizó también si el fragmento FNIII4-5 inmovilizado era capaz de unir los fragmentos de 70 kDa y de 29 kDa añadidos de forma soluble. Como se muestra en la figura 43 C, el fragmento de 29 kDa soluble se unía a FNIII4-5 de manera dosis dependiente, mientras que el fragmento de 70 kDa no se unía a ninguna de las concentraciones testadas (no mostrado). Esto sugería que la interacción de FNIII4-5 con la región amino terminal de FN era sensible a la conformación del amino terminal. Además, el fragmento FN-III4-5 inmovilizado también unía el propio FNIII4-5 soluble indicando la presencia de un sitio de auto-asociación en esta región. Como en el caso de la FN o el fragmento de 70 kDa inmovilizados, el fragmento de 80 kDa no se unía al FNIII4-5 inmovilizado (figura 43 C).

Para confirmar que estas interacciones de FNIII4-5 eran específicas para la región amino terminal de la FN, se utilizó el fragmento FNIII7-10, que representa a la región central de la FN (ver figura 37). Como se muestra en la figura 43 D, ni el fragmento FNIII4-5 soluble, ni el de 29kDa, se unían a FNIII7-10 inmovilizado. La presencia del

fragmento FNIII7-10 en la cubeta del biosensor, se comprobó utilizando un Ac anti-FN, que se unía de forma dosis dependiente (figura 43 D)

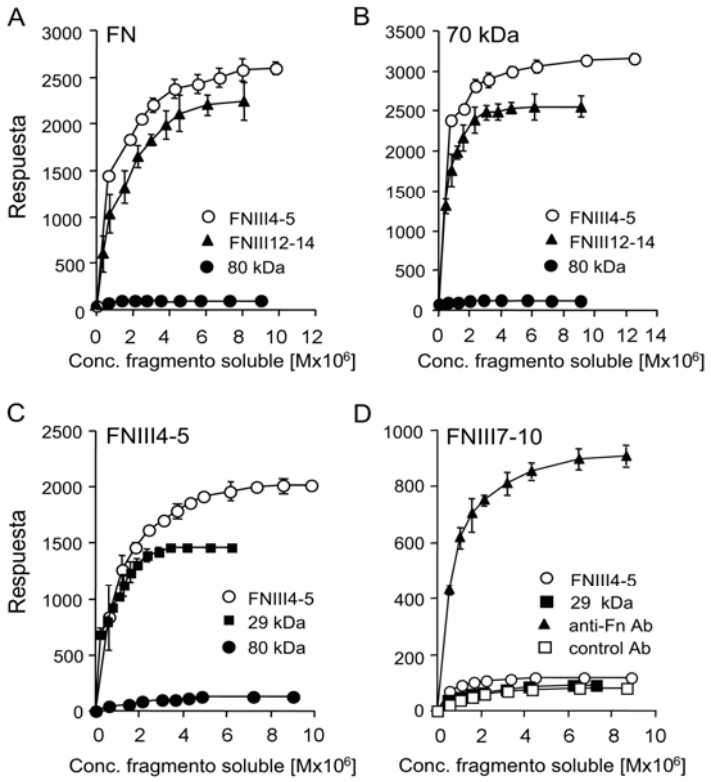

Figura 43. **Unión del fragmento FNIII4-5 soluble a FN completa o a los fragmentos 70 kDa, FNIII7-10 o FNIII4-5 inmovilizados.** La FN y el resto de fragmentos utilizados fueron equilibrados en el buffer 10 mM Tris, 50 mM NaCl, pH 7.5. Fueron inmovilizados en cubetas de doble-cavidad con CMD, utilizando un biosensor óptico IAsysPlus. Tras la inmovilización se fueron añadiendo paulatinamente los fragmentos solubles monitorizando la respuesta (arc/seg) hasta saturación, representándose la unión a FN (A), a 70 kDa (B), a FNIII4-5 (C) y a FNIII7-10 (D). Estos valores representan la media de al menos 3 ensayos.

Caracterización de los sitios de interacción con la FN y de auto-asociación de la región III4-5.

La falta de unión del fragmento de 80 kDa observada en la figura 43, sugería que los sitios de unión a FN contenidos en la región FNIII4-5 eran crípticos en este fragmento más grande. Para confirmar esto, se estudió la unión del fragmento FNIII4-6 soluble sobre los fragmentos inmovilizados de 70 kDa y FNIII4-5 o sobre la FN completa. Como se muestra en la figura 44, a la misma concentración molar, la unión del fragmento FNIII4-6 a FN completa es 10 veces inferior con respecto a FNIII4-5 (301 arc/seg frente a 2988) (figura 44 A). La unión del fragmento FNIII4-6 soluble a 70 kDa o FNIII4-5 inmovilizados, era algo mejor, pero todavía 5 y 3 veces inferior,

respectivamente comparado con la unión de FNIII4-5 a estos sustratos (figura 44 B y C).

De igual forma se analizó el comportamiento de otros dos fragmentos recombinantes de FN, el FNIII4 y el FNIII5, lo que podría dar una indicación sobre la necesidad de la presencia de ambas repeticiones para que el fragmento FNIII4-5 se uniera a FN. Los resultados obtenidos muestran como el fragmento FNIII4 no se une ni a FN completa (figura 44 A) ni a 70 kDa (figura 44 B) ni a FNIII4-5 (figura 44 C) a ninguna de las concentraciones testadas. El fragmento FNIII5, si se une, aunque esta unión es 11.5, 12.5 y 5.4 veces inferior respectivamente con respecto a la unión de FNIII4-5 sobre los mismos sustratos, a una misma concentración molar (figura 44 A, B y C).

Estos resultados indican que los sitios de unión a la FN en el fragmento FNIII4-5 están crípticos en fragmentos largos de FN y que es necesario que la región III4-5 esté integra, para que se de esta actividad.

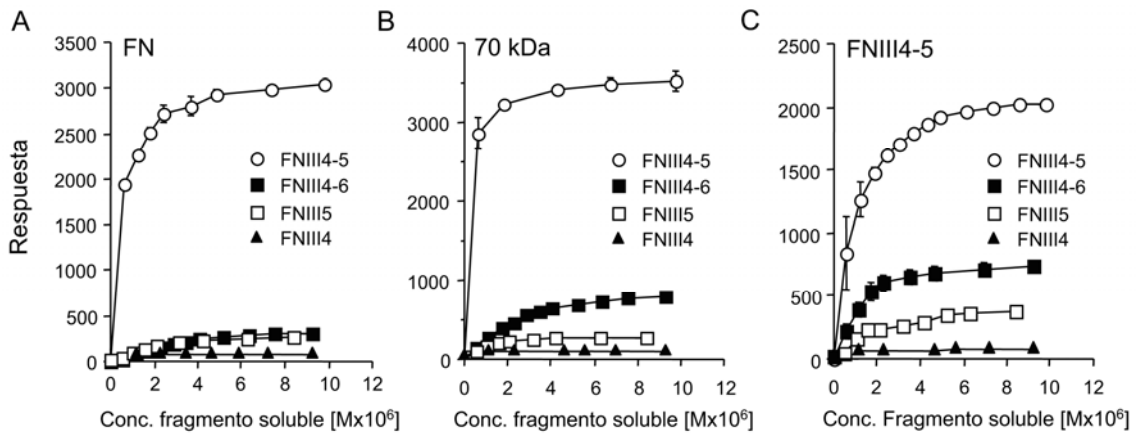

Figura 44. **Unión de los diferentes fragmentos recombinantes solubles que contienen la región III4-5 a FN completa, o a los fragmentos 70 kDa y FNIII4-5.** La FN y los fragmentos fueron inmovilizados en cubetas de CMD; tras esto se añadieron concentraciones crecientes de los fragmentos solubles FNIII4-5, FNIII4-6, FNIII4, o FNIII5 sobre la FN completa inmovilizada (A), sobre el fragmento de 70 kDa (B) o sobre FN-III4-5 (C) monitorizando la señal. Estos valores representan la media de al menos 3 ensayos.

Para determinar la relevancia de las secuencias activas de HBP/III5 ya mencionadas, en la unión del fragmento FNIII4-5 a sí mismo y a FN, se utilizaron como ligandos solubles varios fragmentos de FNIII4-5 mutados. Como se observa en la figura 45, la sustitución de los 2 primeros residuos de arginina del sitio HBP/III5 (FNIII4-5R1R2) por 2 residuos de alanina, bloqueaba completamente la unión a la FN completa,

a 70 kDa y a FNIII4-5. En cambio la sustitución de los dos últimos residuos de arginina por alanina (FNIII4-5R3R4), no bloqueaba esta unión (figura 45).

Estos resultados indican que los 2 primeros residuos de arginina en HBP/III5 (R1R2) están implicados en la unión del fragmento FNIII4-5 a sí mismo, a FN completa y al fragmento proteolítico de 70 kDa.

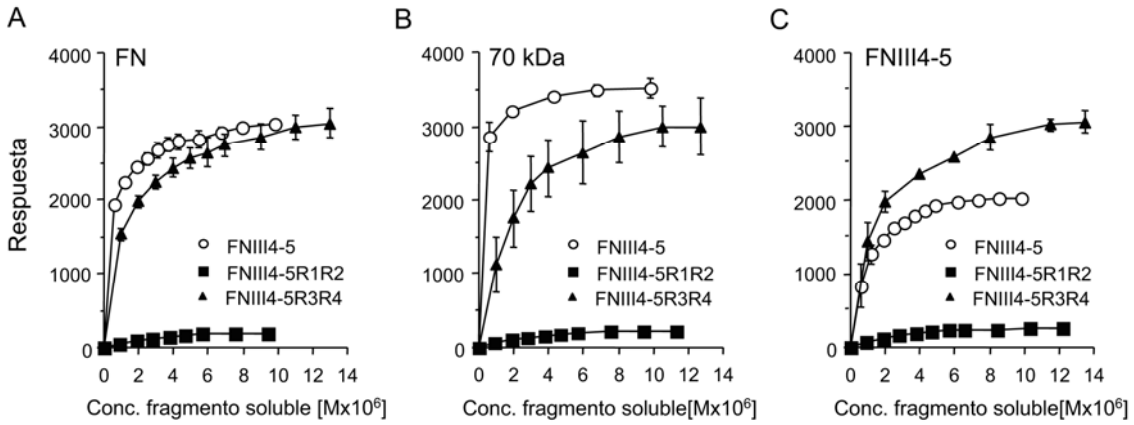

Figura 45. **Efecto de las mutaciones específicas del fragmento FNIII4-5 sobre la unión a FN, 70 kDa o FN-III4-5 inmovilizados.** La FN y los fragmentos fueron inmovilizados en cubetas de CMD; tras esto se añadieron concentraciones crecientes de los fragmentos solubles FNIII4-5, FNIII4-5R1R2, o FNIII4-5R3R4 sobre la FN completa inmovilizada (A), sobre el fragmento de 70 kDa (B) o sobre FNIII4-5 (C) monitorizando la señal. Estos valores representan la media de al menos 3 ensayos.

Relevancia fisiológica de alteraciones en la formación de la matriz de fibronectina.

Para estudiar las posibles funciones fisiológicas que puede tener la pérdida de la capacidad de ensamblaje de matriz de FN, hemos analizado lo que ocurre en líneas celulares de cáncer renal deficientes o no en el gen supresor de tumores von Hippel-Lindau (VHL).

Conocemos a través de la bibliografía que la pérdida de una adecuada matriz de FN influye en la transformación celular y en la tumorogénesis in vivo (Mack *et al.*, 2003); que el gen supresor de tumores von Hippel-Lindau está implicado en la deposición de la matriz extracelular (Ohh *et al.*, 1998; Esteban-Barragan *et al.,* 2002); que en las células de cáncer renal VHL(-) la pérdida del ensamblaje de la matriz de FN promueve y mantiene la angiogénesis tumoral (Tang et al., 2006). Partiendo de estas premisas, se analizó a nivel de inmunofluorescencia la formación de matrices de FN en presencia o ausencia de FN exógena en diferentes líneas celulares de cáncer renal. Se

sabe que la adición exógena de FN no reestablece el ensamblaje de FN en las células 786-O VHL(-) (Esteban-Barragan *et al,*. 2002). Por ello se utilizó esta línea junto a otras tres líneas adicionales RCC4, RCC10 y UMRC, para estos estudios. Como se muestra en la figura 46 ninguna las células VHL(-) aún en presencia de FN exógena, forman fibras de FN, indicando que su incapacidad para ensamblar FN no es consecuencia de una baja disponibilidad de FN. Hay que destacar que en las células UMRC VHL(+) sólo se forma matriz en presencia de FN exógena, por lo que en este caso en particular, la baja secreción de FN sí podría contribuir a la pérdida la matriz de FN (figura 46).

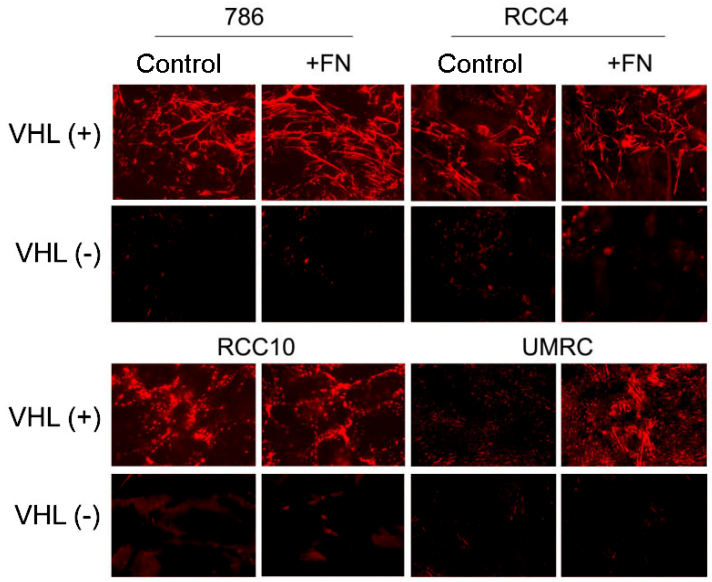

Figura 46. Análisis comparativo de la organización de la matriz de FN en las células de cáncer renal (RCC) en presencia de FN exógena. Células 786-O, RCC4, RCC10 y UMRC, fueron crecidas hasta la confluencia en placas precubiertas de FN (10 μg/ml) o sin precubrir (control). Después de 3-4 días las células se lisaron y se analizó el ensamblaje de la FN por inmunofluorescencia indirecta usando un Ac policlonal anti-FN.

Los trabajos previos de otros investigadores han atribuido la pérdida de la capacidad para formar matriz de las células VHL(-) a la baja expresión de FN por estas células (Clifford *et al.,* 2001). Asimismo, se ha atribuido a un mal procesamiento de la FN, de manera que la forma anómala podría acumularse e interferir con la FN normal no permitiendo su ensamblaje (Ohh *et al.,* 1998). En resultados no mostrados, hemos encontrado que las células VHL(-) producen niveles normales de FN y que ésta es funcional, por tanto estas hipótesis no parecen ser la razón de la incapacidad de las células VHL(-) para ensamblar FN.

Por otro lado, las células VHL(-), forman menos fibras de estrés que las VHL(+) (Calzada *et al.,* 2006), por lo que se estudió si la familia de las GTPasas podría estar implicada en este proceso. En concreto se estudio la GTPasa RhoA la cual está implicada en el proceso de formación de fibras de estrés.

En primer lugar se realizaron los ensayos de arrastre (*pull-down*) en la línea celular 786-O. Como se muestra en la figura 47 la curva de activación de la GTPasa RhoA es diferente en las células VHL(-) y VHL(+). Las células VHL(+) muestran una actividad basal de RhoA, que incrementa progresivamente hasta las 72 horas, mientras que las VHL(-) tienen menor actividad basal y presentan un aumento transitorio a las 24 horas que no se mantiene a tiempos más largos. Por lo tanto la ruta de señalización de RhoA podía jugar un papel en las alteraciones funcionales observadas en las células VHL (-).

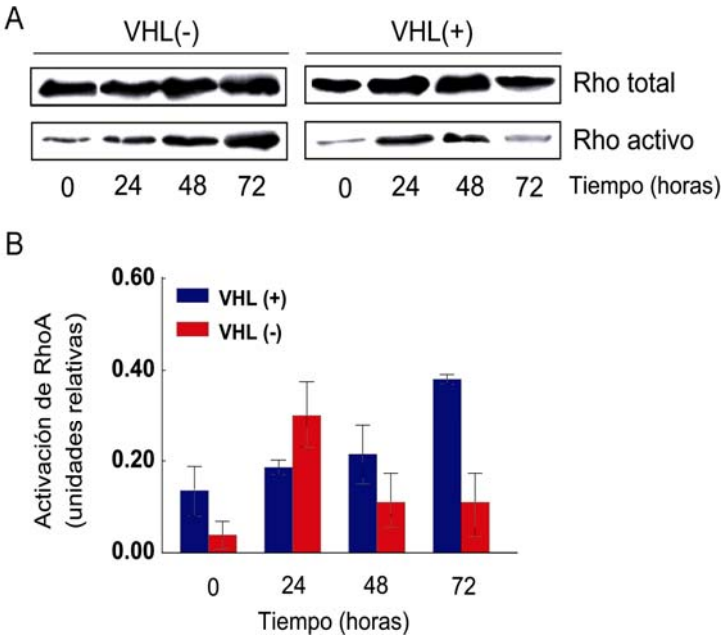

Figura 47. Estado de activación de RhoA en células 786-O. A: Las células ($7x10^6$) VHL(+) o VHL(-) fueron incubadas 3 horas en ausencia de suero, considerando el tiempo 0 como nivel basal de activación de RhoA. Las células fueron mantenidas en cultivo durante 24, 48 y 72 horas. Después de cada tiempo, las células fueron lisadas y el lisado se incubó toda la noche con C21-GST. La fracción unida (activa) y la total fueron analizadas por western blotting usando un Acm anti-RhoA. La figura muestra un experimento representativo de tres realizados. **B**: Cuantificación de los niveles relativos de RhoA activado, para cada tiempo (media de 3 ensayos, con sus desviaciones estándar).

Para determinar la posible causa(s) del defecto de activación de RhoA, y dado que uno de los inhibidores de RhoA es p190RhoGAP (Arthur and Burridge, 2001), se estudió la activación de p190RhoGAP en estas células, por ensayos de inmunoprecipitación. Como se muestra en la figura 48 p190RhoGAP se encuentra activo (fosforilado) en las células VHL(-), pero no en las VHL(+).

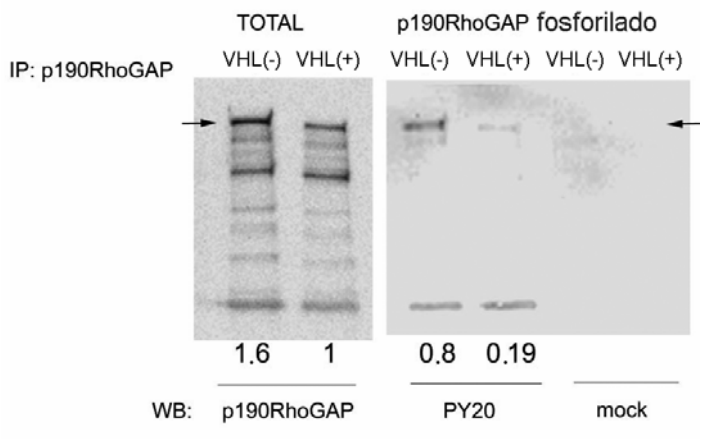

Figura 48. Análisis de la fosforilación de p190RhoGAP en las células 786-O VHL(+) y VHL(-). Las células fueron crecidas con medio completo, privándolas de suero durante 3 horas. A partir del lisado celular ($7x10^6$ células/punto) se inmunoprecipitó p190RhoGAP. El total fué analizado por *western-blot* usando un Acm anti-p190RhoGAP, y el fosforilado fue analizado por un Acm anti-fosfotirosina (PY20). El *mock* en este caso representa la unión de las bolitas de proteína-G a un Ac no específico. La cuantificación de las cantidades relativas de p190RhoGAP total o fosforilado se indica bajo cada carril. La figura muestra un experimento representativo de tres. Las flechas indican la banda correspondiente a p190RhoGAP.

Se analizó también por inmunofluorescencia lo que ocurría tras el tratamiento de las células con un activador de RhoA (LPA) o un inhibidor de ROCK (efector de RhoA), el Y-27632. Como se muestra en la figura 49 el tratamiento con LPA daba lugar a un incremento en la formación de fibras de FN en las VHL(+) y a formación de fibras en las VHL(-), mientras que el tratamiento con Y-27632 provocaba la inhibición del ensamblaje de matriz de FN en las células VHL(+).

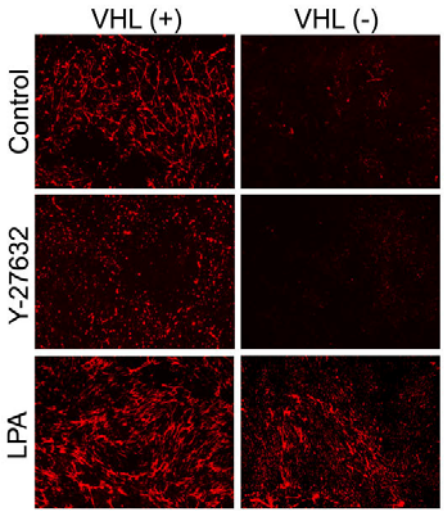

Figura 49. Activación exógena de RhoA en células RCC. Células 786-O fueron cultivadas 3-4 días en presencia o ausencia del inhibidor Y-27632 (5 μM) o del activador LPA (6 μM), siendo el control las células sin tratar. Las células fueron fijadas e incubadas posteriormente con un Ac policlonal anti-FN, posteriormente fueron lavadas y marcadas con un Ac anti-IgG de conejo generado en cabra y asociado a Rodamina Red™-X.

Para confirmar el papel de RhoA en la incapacidad de las VHL(-) para ensamblar FN, se realizaron transfecciones con los mutantes constitutivamente activos (Q63LRhoA) y dominante negativo (N19RhoA) de esta GTPasa. La expresión del

mutante dominante negativo de RhoA en células VHL(+), daba lugar a una disminución en el ensamblaje de la FN y la expresión del mutante constitutivamente activo de RhoA en VHL(-), restablecía la capacidad de ensamblar la matriz de FN (figura 50).

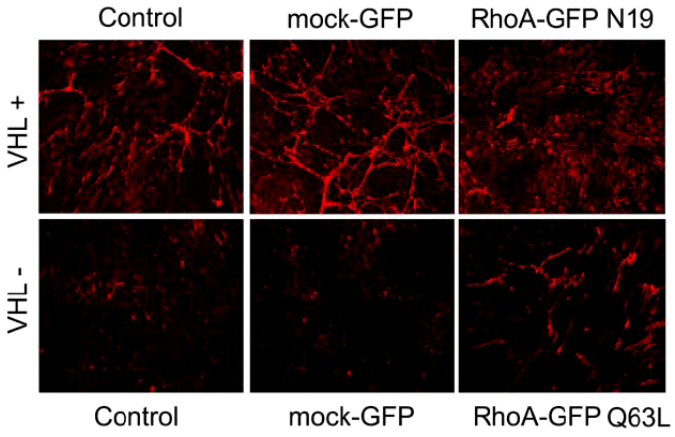

Figura 50. Efecto de la expresión de las construcciones dominante negativa (N19RhoA) y constitutivamente activa (Q63LRhoA) en células 786-O. Las células fueron infectadas con un vector de expresión retroviral GFP sólo (mock) o con las construcciones N19RhoA o Q63LRhoA. Estas células ($2x10^5$) fueron crecidas durante 3-4 días a 37ºC, 5% CO_2, se fijaron y se incubaron con un Ac policlonal anti-FN, posteriormente fueron lavadas y marcadas con un Ac anti-IgG de conejo generado en cabra y asociado a Rodamina Red™-X. En la figura se muestra un ensayo representativo de al menos tres.

Estos resultados aportan un mecanismo para explicar, al menos parcialmente, la pérdida de la capacidad de ensamblaje de la matriz de FN en las células de cáncer renal deficientes en el gen supresor de tumores von Hippel-Lindau (VHL). Este mecanismo consistiría en una activación deficiente de la GTPasa RhoA, y esto podría ser debido a la activación constitutiva de p190RhoGAP en estas células.

Discusión

En la primera parte de esta tesis doctoral se han estudiado las consecuencias funcionales de las distintas activaciones de la integrina α4β1 tras la unión a sus ligandos (los dominios IIICS, Hep II y Hep III de FN y la proteína VCAM-1), y también algunas de las rutas de señalización que pueden estar implicadas en dichas respuestas. Este trabajo muestra por primera vez la existencia de una diferente reorganización del citoesqueleto de actina dependiente del estímulo utilizado para activar la integrina α4β1. Numerosos artículos han descrito que existen múltiples formas de activación de la integrina α4β1 y que la activación de α4β1 da lugar a un incremento en la adhesión celular y en la afinidad y/o avidez por su ligando (Sánchez-Aparicio *et al.,* 1993; Masumoto and Hemler, 1993; Chen *et al.,* 1999). En esta tesis doctoral se ha demostrado que la activación de α4β1 por Mn^{2+}, por el Acm CD3 o por SDF-1α, da lugar a una morfología polarizada, mientras que la activación por TS2/16 o PMA da lugar a una morfología aplastada ("*spreading*"). Asimismo, estas respuestas no están restringidas sólo a la línea celular Jurkat, ni a células T, sino que también ocurren en otros tipos celulares. El hecho de que se dé una respuesta u otra no parece depender de la naturaleza interna (*inside-out*) (CD3, SDF-1α, PMA) o externa (*outside-in*) (Mn^{2+}, TS2/16) del estímulo. Tampoco depende de una modulación específica de la actividad de la integrina: afinidad frente a avidez ("*clustering*"), ya que por ejemplo PMA mayoritariamente incrementa la avidez, mientras que otros activadores utilizados en este trabajo que daban lugar a un mismo tipo de respuesta, como el Acm anti-β1 TS2/16, incrementan la afinidad de la integrina (Hogg *et al.,* 2003; Pribila *et al.,* 2004). Por tanto parece ser que son los factores intrínsecos asociados a cada estímulo los causantes de las diferentes respuestas.

Es interesante destacar que al igual que ocurría a nivel de adhesión celular (Moyano *et al.,* 1999), el tratamiento de las células Jurkat con condroitinasa ABC inhibía parcialmente la reorganización del citoesqueleto observada tras la activación de α4β1 con Mn^{2+}, pero no afectaba a la respuesta causada tras la activación con TS2/16. De igual forma, en células activadas con Mn^{2+}, el Acm HP2/1 (anti-α4) reducía parcialmente la adhesión celular y el porcentaje de células que presentaban una morfología elongada, mientras que HP2/1 inhibía totalmente la adhesión inducida por activación con el Acm TS2/16.

Nuestros resultados confirman por tanto que cuando la integrina se activa por Mn^{2+}, ésta requiere la cooperación de PG (tipo condroitín-sulfato (PGCS) en este caso),

tanto para la adhesión a sus ligandos como para la posterior reorganización del citoesqueleto. Por el contrario, cuando la integrina α4β1 se activa por el Acm TS2/16, no es necesaria dicha cooperación, para realizar sus funciones. Por tanto, el papel de α4β1 y PGCS en la reorganización del citoesqueleto es claramente dependiente del tipo de activación (Mn^{2+} o TS2/16) de la integrina.

La respuesta polarizada observada tras la activación de α4β1 vía CD3, es distinta a lo publicado previamente (Hyduk and Cybulsky, 2002). En ese estudio, la coinmovilización de los Acm anti-CD3 y anti-α4 daba lugar a polimerización cortical de actina, como la que inducía el Acm anti-CD3 por si sólo, frente a la formación de extensiones o filopodios que inducía el Acm anti-α4. La explicación a esta discrepancia podría ser que en nuestro trabajo hemos utilizado bajas concentraciones del Acm anti-CD3, suficientes para activar a la integrina, pero no para dar otro tipo de señalización. En apoyo a esta explicación se ha visto que la integrina LFA-1 requiere una concentración mucho más baja del Acm-anti-CD3 para su activación que para inducir proliferación celular (Mueller *et al.,* 2004).

Las dos morfologías observadas reflejaban un fenotipo migratorio (células polarizadas) frente a un fenotipo de adhesión fuerte (células aplastadas). De hecho la posición del MTOC tras la activación con Mn^{2+} coincide con lo descrito en células migratorias (Vicente-Manzanares and Sánchez-Madrid, 2004). Sin embargo, a nivel de videomicroscopía no observamos de forma muy clara este efecto migratorio tras las activaciones con Mn^{2+}, SDF-1α o el Acm anti-CD3, sino más bien un ligero aumento de la migración. Esto es probablemente debido a que bajo estas condiciones, la integrina α4β1 se encuentra muy activada y está fuertemente unida a su ligando. Esto estaría de acuerdo con algunos trabajos previos donde se muestra que la activación de la integrina por Mn^{2+} o TS2/16 (o activaciones similares a éstas), bloquea la migración celular e induce un aumento en la fuerza de adhesión a su sustrato (Kuijpers *et al.,* 1993; Rodríguez-Fernández *et al.,* 1999). No obstante en los videos se confirman claramente las dos morfologías observadas en los ensayos de citoesqueleto, así como diferencias en la actividad de la membrana celular, que son dependientes del estímulo que active a la integrina α4β1.

Debido a que tanto los niveles de α4β1 activada como de la concentración de ligando, pueden variar dependiendo de las condiciones fisiológicas particulares que se den en cada momento, hemos estudiado el efecto de diferentes concentraciones de

activadores y ligandos de α4β1. En todos los casos se ha observado que la morfología polarizada daba lugar a migración celular y la morfología aplastada daba lugar a una fuerte adhesión y a una mayor resistencia al "*detachment*" bajo condiciones de flujo.

En su conjunto, los resultados obtenidos en esta primera parte de la tesis doctoral nos permiten establecer que la integrina α4β1 puede inducir diferentes respuestas en células T, dependiendo de la activación específica que reciba. También hemos visto que los dos tipos de respuesta celular observados, requieren de una diferente señalización intracelular. Es el caso de la GTPasas RhoA y Rac1, de las cuales es conocida su función en la reorganización del citoesqueleto (Ridley, 2001; Burridge and Wennerberg, 2004). La activación de RhoA inhibía la polarización celular y la migración, lo que estaría de acuerdo con publicaciones previas referidas a otras integrinas leucocitárias (Rodríguez-Fernández *et al.,* 2001; Vicente-Manzanares and Sánchez-Madrid, 2004). Por el contrario, nuestros resultados también indican que la respuesta que daba lugar a una morfología aplastada y a una inhibición de la migración, es independiente de RhoA.

Se ha demostrado que el *crosslinking* de α4β1 en suspensión con anticuerpos o ligandos en células NK (Gismondi *et al.,* 2003), o en células dependientes de IL-3 (Kanda *et al.,* 2003) activa a la GTPasa Rac1. Por otra parte, Rac1 activo regula la adhesión y el *spreading* celular mediado parcialmente por la integrina α4β1 (D´Souza-Schorey *et al.,* 1998). En el presente trabajo mostramos por primera vez una regulación diferencial de Rac1 en células T, dependiente de si la activación de la integrina α4β1 da lugar a una respuesta migratoria (morfología polarizada) o a una adhesión fuerte (morfología aplastada). Los estímulos que daban lugar a una morfología aplastada llevan asociados una moderada y progresiva activación de Rac1, y la respuesta celular que originan es independiente de la actividad inicial de Rac1. Esto estaría de acuerdo con la falta de efecto de los mutantes constitutivamente activos (V12Rac1) a nivel de reorganización del citoesqueleto. En cambio las activaciones que daban lugar a una morfología polarizada, requieren de una baja actividad inicial de Rac1, lo cual podría ser necesario para que ocurra esa polarización celular. Estos resultados correlacionan con el efecto observado en los ensayos de inmunofluorescencia para el mutante V12Rac1, y están de acuerdo con publicaciones previas referidas a otras integrinas como LFA-1 (Sánchez-Martín *et al.,* 2004) o la integrina α5β1 (Del Pozo *et al.,* 1999). Por lo tanto, se podría asumir que una vez que la célula se ha polarizado, la actividad de

Rac1 puede aumentar, sin afectar al nivel de reorganización del citoesqueleto. El mecanismo implicado en la inactivación transitoria de Rac1 a tiempos cortos todavía no se conoce, pero una posible explicación sería la activación de un GAP específico, como ocurre con la inactivación de RhoA mediada por α4β1 en células de melanoma (Moyano *et al.,* 2003b)

Existen varias moléculas que están implicadas en las etapas iniciales de la señalización por integrinas. En esta tesis se ha estudiado la regulación de la tirosín-quinasa Pyk-2. Esta molécula es muy abundante en células Jurkat y está implicada en motilidad celular, reorganización del citoesqueleto y señalización (Avraham *et al.,* 2000). Pyk-2 se activa por autofosforilación, y ésta puede ser inducida por diferentes estímulos incluyendo quimioquinas, la integrina α4β1 o el receptor de células T (Ganju *et al.,* 1998; Kanda *et al.,* 2003; Rose *et al.,* 2002). Nuestros resultados muestran una clara diferencia en el grado de fosforilación de Pyk-2 dependiendo del estímulo que se utilice para activar a la integrina α4β1. Así, existe una buena correlación entre inducción de una morfología polarizada y niveles altos de fosforilación de Pyk-2. Esto sugiere que Pyk-2 puede ser esencial para la polarización y migración de células T mediada por α4β1. Por el contrario, los resultados con activaciones que daban lugar a una respuesta de adhesión firme, muestran una modesta fosforilación de Pyk-2. Esta es por tanto la primera evidencia de un diferente grado de fosforilación de Pyk-2 en respuesta a las diferentes activaciones de α4β1. Pyk-2 puede además asociarse a proteínas como paxilina o Vav (GEF de Rac1), y éstas son fosforiladas en tirosina tras la activación de la integrina (Gismondi *et al.,* 2003). De acuerdo con estos datos y aunque no lo mostramos en esta tesis doctoral, hemos encontrado tanto paxilina como Vav en lisados de células T, independientemente del tipo de activación dado a la integrina α4β1. El posible papel que juegan Vav y/o paxilina en esta diferente respuesta celular dependiente del estímulo utilizado para activar α4β1, es actualmente desconocido.

Tomados en su conjunto, estos resultados sugieren que la integrina α4β1 presenta una nueva propiedad, consistente en su capacidad para dar lugar a dos tipos de respuestas celulares distintas, dependiendo del estímulo que la active. Además estas respuestas llevan asociada una diferente señalización intracelular. Nuestros estudios *in vitro* probablemente representan condiciones fisiológicas en que por ejemplo el tratamiento con quimioquinas, activa la integrina α4β1 e induce migración linfocitaria.

Este proceso es esencial en homeostasis, en el proceso de extravasación a los tejidos y en la respuesta inflamatoria. Esta forma de activación de la integrina conllevaría una baja actividad de RhoA, altos niveles de fosforilación de Pyk-2 y una regulación dual de Rac-1. Por otra parte en los tejidos, los linfocitos pueden recibir otro tipo de señales, como la activación de la PKC, que también activa la integrina α4β1, pero induciría una adhesión firme y una morfología celular "aplastada". Esta forma de activación de α4β1 sería independiente de RhoA, de Pyk-2 y del estado inicial de Rac1. Otro ejemplo puede ser la migración de los linfocitos en los tejidos, que podría estar dirigida por la activación del receptor de células T, que también activa la integrina α4β1. En esta situación α4β1 puede contribuir a la respuesta iniciada por el antígeno, y que conlleva señales de parada o de migración en células T (Dustin, 2004). El inicio de una u otra respuesta, vendría determinado por el estímulo específico que reciba la integrina α4β1 en una determinada localización.

En la primera parte de esta tesis, también hemos demostrado que la diferente reorganización del citoesqueleto de actina en respuesta a diferentes activaciones de α4β1, era similar para células adheridas al dominio Hep III (fragmento FNIII4-5) o al dominio Hep II (fragmento FN-H89) de FN. En estudios anteriores de nuestro laboratorio, se había visto que entre los dominios Hep III y Hep II existe una homología funcional y estructural (Moyano *et al.*, 1997, 1999, 2003b). En base a estas similitudes, y dado que el dominio Hep II está implicado en fibrilogénesis de FN (Bultman *et al.,* 1998), nos planteamos si el dominio Hep III podría jugar un papel en la formación de matrices de FN.

En la segunda parte de la tesis hemos descrito una nueva propiedad biológica del dominio Hep III, consistente en su implicación en el proceso de formación de matrices de FN. Hemos identificado dos secuencias específicas dentro de la región específica III4-5 que median: 1) asociación de la molécula de FN a sí misma y 2) ensamblaje de fibrillas de FN. Estas secuencias se localizan dentro de la repetición III5, en concreto dentro del sitio conocido como HBP/III5 (WTPPRAQITGYRLTVGLTRR) de unión a PGCS (Moyano *et al.,* 1999). La secuencia implicada en la unión de la región III4-5 a sí misma o a la región amino terminal de la FN, requiere los residuos de arginina R994 y R1001 (llamados R1R2 a lo largo de la tesis). La secuencia implicada en el proceso de fibrilogénesis de FN requiere de los residuos de arginina R1008 y R 1009 (llamados R3R4). Es decir, existen dentro del dominio III4-5 dos sitios con actividades diferentes.

La actividad de estos dos sitios parece estar regulada por la conformación que presente el dímero de FN.

La capacidad de unión del fragmento recombinante FNIII4-5 a FN no está presente en fragmentos más largos, como el fragmento proteolítico de 80 kDa o el fragmento recombinante FNIII4-6. Esto sugiere que los residuos R1R2 se encuentran total o parcialmente escondidos en la FN o en fragmentos grandes de FN. Esta propiedad, también está ausente o muy reducida en las repeticiones individuales FNIII4 y FNIII5, lo que sugiere que la disposición espacial de los residuos de arginina en el fragmento FNIII4-5, es importante. Asimismo, esta capacidad de interacción con FN también depende, al menos parcialmente, de la conformación que presente la región amino terminal de la FN. Nuestros resultados muestran el fragmento FNIII4-6 se une mejor al fragmento proteolítico de 70 kDa (representativo de la región amino terminal de la FN), que a la molécula de FN completa. De esta forma, el dominio III4-5 parece tener un comportamiento similar al de otras regiones que unen FN, incluyendo las repeticiones III1 y III12-14, cuya actividad también es críptica (Wierzbicka-Patynowski and Schwarzbauer, 2003; Mao and Schwarzbauer, 2005).

Todos estos resultados sugieren que la capacidad de unión a FN de la región III4-5, no juega un papel en las interacciones con la superficie celular que ocurren al comienzo del proceso de fibrilogénesis, ya que éstas preceden a los cambios conformacionales necesarios para exponer los sitios crípticos de FN (Baneyx et *al.,* 2002). Una vez expuestos, los residuos R1R2 pueden proporcionar sitios de unión adicionales para las fibrillas de FN ya formadas, contribuyendo así a su elongación y estabilización.

A diferencia de los residuos R1R2, la actividad de los residuos R3R4 en fibrilogénesis se encuentra presente tanto en el fragmento FNIII4-5 como en el FNIII4-6. Aunque la estructura cristalográfica de la región III4-5 todavía no está resuelta, podría aproximarse a partir de la estructura conocida de las repeticiones III12-14 (Sharma *et al.,* 1999), ya que todas las repeticiones de tipo III en FN presentan una estructura de hélice-β similar. De esta forma el residuo R1 encontrado en la secuencia PRAQI de la repetición III5 se localizaría en una región relativamente estrecha entre las repeticiones, por lo que estaría críptico. En cambio, los residuos R3R4 encontrados en la secuencia GLTRR de III5 estarían expuestos al otro lado de la molécula (Sharma *et al.,* 1999). Otro apoyo para esta hipótesis, proviene de los resultados previos de nuestro laboratorio (Moyano *et al.,* 2003a, 2003b), donde vimos que los residuos R3R4 son

activos en fragmentos largos de FN, y promueven la formación de fibras de estrés y adhesiones focales, así como la activación de RhoA en células de melanoma. Las fuerzas contráctiles que se generan tras la activación de RhoA y la formación de fibras de estrés juegan un papel importantísimo en el proceso de fibrilogénesis de FN (Zhang *et al*., 1994; Zhong *et al*., 1998). Estas fuerzas ejercen una tensión sobre el dímero de FN, de forma que le provoca un cambio conformacional, quedando expuestos los sitios crípticos de unión a otros sitios de la FN (como los residuos R1R2 del dominio III4-5), que se utilizan finalmente para el paso del dímero de FN a fibrillas (Wierzbicka-Patynowski and Schwarzbauer, 2003). Por tanto, de nuestros resultados se deduce que las dos funciones presentes en la región III4-5 parecen ser independientes la una de la otra y dependientes del tipo de conformación que presente el dímero de FN.

El receptor celular que interacciona con los residuos R3R4 del dominio III4-5 no se conoce actualmente. Sin embargo, un candidato muy razonable puede ser un sindecano o cualquier otro PG. Los miembros de la familia de los sindecanos se unen al dominio Hep II de la FN, que también regula la fibrilogénesis e interacciona con la región amino terminal de la FN (Bultmann *et al.,* 1998; Woods, 2001). Además, se ha visto que la mutación de un sindecano tipo 2 previene la formación de matrices de FN en células CHO (Klass *et al.,* 2000). También, se ha descrito (Hocking et al., 1999) que el dominio de unión a heparina de la vitronectina bloquea el ensamblaje de la matriz de FN, y esto parece estar mediado por proteoglicanos de tipo heparán-sulfato (PGHS) que inducen señalización intracelular. Asimismo, sabemos que los dominios de unión a heparina juegan un papel importante en el ensamblaje de la laminina 5 para formar matriz (Tsubota *et al.,* 2005). Otro dato que puede apoyar nuestra hipótesis es que en muchos tipos celulares que forman matrices de FN, la activación del mecanismo de contractibilidad, requiere de la cooperación entre integrinas y PG (Couchman and Woods, 1999). La interacción con ambos receptores sería necesaria para activar RhoA y/o proveer a las células de fuerzas contráctiles que permitan la exposición de sitios crípticos (Zhong *et al.,* 1998).

Todo esto podría explicar por qué el fragmento FNIII4-5 soluble, es capaz de inhibir la fibrilogénesis de FN. Este proceso requiere de al menos dos receptores de superficie celular, de forma que el dímero de FN pueda estirarse y exponer sus sitios de unión a FN. Si el fragmento FNIII4-5 (a través de sus residuos R3R4) ocupa a uno de estos receptores, incluso si se indujera activación de RhoA, se bloquearía el proceso de fibrilogénesis, ya que la FN sólo estaría unida a un receptor y las fuerzas contráctiles no

serían capaces de abrir la molécula y exponer los sitios crípticos (como R1R2) (ver figura 51).

El siguiente esquema (figura 51) pretende explicar el papel dual del dominio Hep III en la fibrilogénesis de FN.

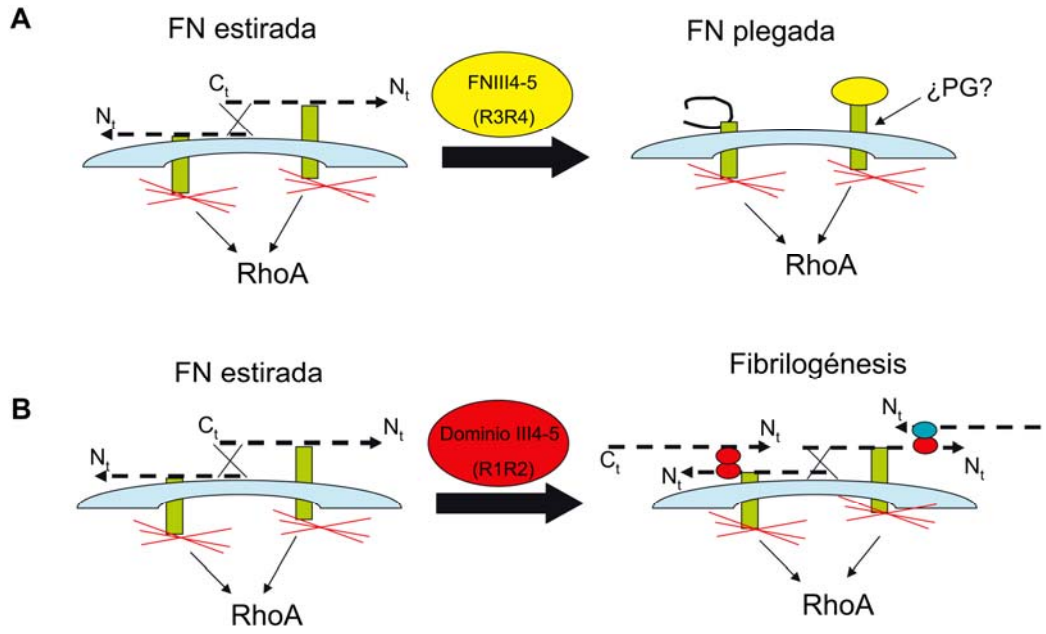

Figura 51. **Modelo propuesto para el papel del dominio Hep III (región III4-5) en fibrilogénesis.** **A**: La unión del fragmento FNIII4-5 soluble a uno de los dos receptores de superficie celular implicados en fibrilogénesis, por ejemplo un PG (¿sindecano?), a través de su secuencia R3R4, inhibe la fibrilogénesis de FN, pese a que pueda inducir activación de RhoA. **B**: Tras la activación de RhoA, se generan fuerzas contráctiles que provocan el cambio conformacional de la FN. Se exponen nuevos sitios de unión a la molécula de FN, como la secuencia R1R2, lo que facilita la interacción de la región III4-5, con la región amino terminal y con ella misma, en otras moléculas de FN. De esta forma contribuye al proceso de fibrilogénesis.

En apoyo al papel de la región III4-5 en fibrilogénesis descrito en esta tesis, existen estudios previos donde se ha mutado la molécula de FN, eliminando su región III1-7 (Scheler *et al* 1996). Este mutante era capaz de ensamblar fibras de FN, pero la progresión de la matriz era mucho más lenta que con la FN normal, e iba precedida de la formación de agregados insolubles en la superficie celular. Aunque el tamaño tan grande de la delección presente en este mutante pueda suponer un problema para poder llegar a conclusiones definitivas, estos resultados sugieren un papel regulatorio de la región III1-7 en la fibrilogénesis de FN. Sin embargo, en otro trabajo (Sechler *et al.*, 2001) la pérdida de la región III4-5, no afectaba la fibrilogénesis. Esto podría explicarse porque la función reguladora ejercida por el dominio III4-5, esté compensada en este

caso por otras regiones de la molécula de FN implicadas en la regulación de la fibrilogénesis (Mao and Schwarzbauer, 2005; Wierzbicka-Patynowki *et al.,* 2003). Por ejemplo podría estar compensada por el dominio Hep II de la FN, que también está implicado en fibrilogénesis (Bultmann *et al.,* 1998) y que como mostramos en los resultados de esta tesis, se une tan eficientemente como el dominio Hep III a FN completa o al fragmento de 70 kDa. Por lo tanto, las diferentes regiones de la molécula de FN, que juegan un papel en la interacción FN-FN, parecen representar mecanismos alternativos, pero que a la vez son redundantes para el proceso de fibrilogénesis. Esta redundancia no es sorprendente, ya que en el contexto de la relevancia que tiene para la célula el proceso de fibrilogénesis, las fibrillas de FN (a diferencia de otras matrices como las de colágeno) crecen en todas las direcciones, y con variedad de tamaños. De esta forma tendría sentido la existencia de múltiples sitios de autoasociación, que estarían disponibles dependiendo de la conformación de la FN o de los sitios ya ocupados.

A pesar de los numerosos trabajos publicados sobre las regiones implicadas en fibrilogénesis de FN, los mecanismos que la controlan este proceso son bastante desconocidos. En trabajos anteriores se han sugerido algunos mecanismos que pueden contribuir a la polimerización de FN y al ensamblaje de la matriz, como son la formación de interacciones muy estables proteína-proteína (Chen and Mosher, 1996) y/o la formación de puentes disulfuro debidos a la actividad disulfuro isomerasa inherente a la FN (Langenbanch and Sottile, 1999). Como en el caso de otras regiones de FN implicadas en fibrilogénesis, el mecanismo exacto con el cual el fragmento recombinante FNIII4-5 contribuye a este proceso todavía no se conoce. En esta tesis describimos dos nuevas propiedades del dominio III4-5: unión a la FN y regulación de la fibrilogénesis. Estas funciones probablemente ocurren a diferentes tiempos y parecen ser independientes la una de la otra. Así los residuos R3R4 pueden regular las rutas de señalización en los primeros pasos de la fibrilogénesis, pudiendo inhibirla o activarla dependiendo de que estos residuos se encontraran en fragmentos o en la FN completa. Los residuos R1R2, que en principio se encuentran crípticos en el dímero de FN, una vez expuestos podrían favorecer la propagación de las fibrillas de FN y su estabilización, aportando nuevos (alternativos) sitios de unión a FN. El dominio III4-5 puede jugar por tanto un papel dual, tanto inhibitorio como activador en el proceso de fibrilogénesis.

En este trabajo se muestra por primera vez que el dominio Hep III, representado por las repeticiones III4-5, está implicado en la interacción entre moléculas de FN y en el ensamblaje de matrices de FN, contribuyendo así a la regulación de los múltiples procesos biológicos que son dependientes de la interacción célula-matriz de FN, como migración, expresión génica, proliferación, y otros muchos, entre los que quiero destacar el proceso de transformación oncogénica. La relevancia biológica del proceso de fibrilogénesis de FN la hemos querido plasmar en esta tesis doctoral con el ejemplo del cáncer renal.

Las células de cáncer renal (RCC) que son deficientes en el gen supresor de tumores de von Hippel Lindau (VHL(-)), presentan una pérdida de su capacidad para la formación de matrices de FN, y además promueven y mantienen la angiogénesis tumoral permitiendo la infiltración de los tumores a los vasos (Kurban *et al.,* 2006). Considerando la importancia de los procesos de crecimiento tumoral, en esta tesis doctoral nos planteamos el estudio de las posibles causas de este fallo de las células RCC VHL(-) en la capacidad para formar su propia matriz de FN. Publicaciones previas (Esteban-Barragan *et al.,* 2002) han mostrado que no existe correlación entre la capacidad de ensamblaje de la FN y la capacidad de producción de ésta. Por otra parte, se ha propuesto que la interacción entre el VHL y la FN podría ser necesaria para el ensamblaje de fibrillas de FN (Ohh *et al.,* 1998; Clifford SC *et al.,* 2001). Sin embargo, no está claro el mecanismo por el cual VHL estaría mediando esta interacción. Algunos de nuestros resultados (no presentados en esta tesis) parecen sugerir que no siempre es necesaria la interacción VHL-FN para que ocurra el ensamblaje de la matriz de FN. Otra posibilidad podría ser que VHL regule indirectamente el ensamblaje de la matriz de FN, lo que puede dar lugar a modificaciones post-traduccionales que inhabiliten la formación de fibrillas de FN. Con respecto a esta hipótesis se ha propuesto que la FN extracelular en las células VHL(-) está degradada, quizá por el incremento en la activación de las metaloproteinasas como MMP2 (Kurban *et al.,* 2006). Esta degradación de la matriz en las células VHL(-) es una explicación razonable a la pérdida de matriz en estas células. Sin embargo no está claro si el VHL regula directamente la actividad de las MMPs, o si es un efecto secundario debido a la transformación de la célula.

El hecho de que ni siquiera en presencia de FN exógena, las células VHL(-) puedan formar esta matriz de FN, nos hace pensar que quizá algunos eventos intracelulares, como la reorganización del citoesqueleto de actina y la contractibilidad

celular, pueden estar regulando el proceso de fibrilogénesis en las células VHL(+). De hecho las células VHL(-) no forman estructuras propias relacionadas con la reorganización del citoesqueleto y la contractibilidad (Kamada *et al.,* 2001; Esteban-Barragan *et al.,* 2002; Calzada *et a.,* 2006). Todas estas publicaciones apoyan nuestros resultados, donde hemos visto, que la pérdida de la capacidad para formar matrices de FN de las células VHL(-), puede ser debida a la deficiente activación de RhoA, que es una GTPasa muy importante en la reorganización del citoesqueleto (Zhong *et al.,* 1998; Ridley., 2001). Sin embargo, todavía no está bien establecida la relación entre VHL y las RhoGTPasas, y es posible que VHL regule RhoA de manera indirecta, a través de una interacción secundaría de VHL con otra proteína. Por ejemplo, VHL se une a varias isoformas atípicas de PKCs (Iturrioz *et al.,* 2006; Pal S *et al.,* 1997) y estas isoformas están implicadas en el control de la polaridad celular, formación de contactos focales, fibras de estrés y organización de los filamentos de actina (Harrington *et al.*, 2005; Coghlan *et al.,* 2000). Estos a su vez están implicados en la actividad de las RhoGTPasas. Por ejemplo en células endoteliales, una PKC atípica fosforila Rho-GDI y Rho-GEF induciendo la activación de RhoA (Pang and Bitur, 2005) y en este mismo tipo celular, la PKC_{δ} interacciona con p190RhoGAP (Harrington *et al.,* 2005). Nuestros resultados muestran que las células VHL(-) presentan un incremento en el grado de fosforilación de p190RhoGAP. Esto estaría de acuerdo con la hipótesis de que la interacción de VHL con las PKC atípicas, regula la actividad de RhoA a través de la modulación del estado de fosforilación de sus inhibidores tales como los factores Rho-GDI y Rho-GAP, o sus activadores como Rho-GEF.

Los resultados de esta última parte de la tesis doctoral sugieren que las células RCC VHL(-) tienen alterada la señalización intracelular que regula la contractibilidad celular, ya que presentan una activación constitutiva de p190RhoGAP, lo que explicaría los bajos niveles de RhoA activo en estas células. Ya que RhoA controla la formación de matrices de FN, esto podría explicar la incapacidad de las células RCC VHL(-) para ensamblar dichas matrices.

Conclusiones

1. **La activación de α4β1 con Mn^{2+}, el Acm anti-CD3, o SDF-1α, da lugar a una morfología celular elongada, inducción de migración celular y a una señalización intracelular donde Pyk2 está altamente fosforilado, RhoA no está activo y Rac1 presenta una regulación dual.**

2. **La activación de α4β1 con PMA o el Acm TS2/16, da lugar a una morfología aplastada, a una inhibición de la migración celular y a una señalización intracelular independiente de Pyk2 y RhoA pero dependiente de la activación de Rac1.**

3. **La integrina α4β1, por tanto, puede dar lugar a dos tipos de respuestas celulares diferentes. Estas respuestas se observan tras la adhesión a cualquiera de los ligandos de α4β1 en FN: dominios Hep II, Hep III y IIICS, o a la proteína endotelial VCAM-1.**

4. **El dominio Hep III de FN contiene dos nuevas funciones no identificadas previamente: unión a FN y regulación del ensamblaje de matrices de FN. Ambas funciones están mediadas por residuos de arginina diferentes.**

5. **Los residuos implicados en unión a FN (R1R2) son crípticos y requieren un cambio conformacional previo de la FN para exponerse y contribuir a la elongación y estabilización de las fibrillas de FN.**

6. **Los residuos implicados en regulación de la fibrilogénesis (R3R4) están expuestos en FN y probablemente median señalización intracelular a través de receptores tipo sindecano. Los fragmentos que contienen estos residuos inhiben la formación de matrices de FN.**

7. **Una explicación (al menos parcial) de la incapacidad de las células RCC VHL(-) para ensamblar la matriz de FN es la deficiente activación de RhoA, que podría ser debida a la fosforilación constitutiva de p190RhoGAP presente en estas células.**

Bibliografía

Adams, J.C., and Watt, F.M. (1993). Regulation of development and differentiation by the extracellular matrix. Development *117*, 1183-1198.

Aguirre, K.M., McCormick, R.J., and Schwarzbauer, J.E. (1994). Fibronectin self-association is mediated by complementary sites within the amino-terminal one-third of the molecule. J Biol Chem *269*, 27863-27868.

Alon, R., Kassner, P.D., Carr, M.W., Finger, E.B., Hemler, M.E., and Springer, T.A. (1995). The integrin VLA-4 supports tethering and rolling in flow on VCAM-1. J Cell Biol *128*, 1243-1253.

Altevogt, P., Hubbe, M., Ruppert, M., Lohr, J., von Hoegen, P., Sammar, M., Andrew, D.P., McEvoy, L., Humphries, M.J., and Butcher, E.C. (1995). The alpha 4 integrin chain is a ligand for alpha 4 beta 7 and alpha 4 beta 1. J Exp Med *182*, 345-355.

Amano, M., Fukata, Y., and Kaibuchi, K. (2000). Regulation and functions of Rho-associated kinase. Exp Cell Res *261*, 44-51.

Arroyo, A.G., Garcia-Pardo, A., and Sanchez-Madrid, F. (1993). A high affinity conformational state on VLA integrin heterodimers induced by an anti-beta 1 chain monoclonal antibody. J Biol Chem *268*, 9863-9868.

Arroyo, A.G., Sanchez-Mateos, P., Campanero, M.R., Martin-Padura, I., Dejana, E., and Sanchez-Madrid, F. (1992). Regulation of the VLA integrin-ligand interactions through the beta 1 subunit. J Cell Biol *117*, 659-670.

Arthur, W.T., and Burridge, K. (2001). RhoA inactivation by p190RhoGAP regulates cell spreading and migration by promoting membrane protrusion and polarity. Mol Biol Cell *12*, 2711-2720.

Auckhill, I., Joshi, P., Yan, Y., and Erickson, H.P. (1993). Cell- and heparin-binding domains of the hexabrachion arm identified by tenascin expression proteins. J Biol. Chem *268*, 2542-2553.

Avraham, H., Park, S.Y., Schinkmann, K., and Avraham, S. (2000). RAFTK/Pyk2-mediated cellular signalling. Cell Signal *12*, 123-133.

Avraham, S., London, R., Fu, Y., Ota, S., Hiregowdara, D., Li, J., Jiang, S., Pasztor, L.M., White, R.A., Groopman, J.E., and et al. (1995). Identification and characterization of a novel related adhesion focal tyrosine kinase (RAFTK) from megakaryocytes and brain. J Biol Chem *270*, 27742-27751.

Baneyx, G., Baugh, L., and Vogel, V. (2002). Fibronectin extension and unfolding within cell matrix fibrils controlled by cytoskeletal tension. Proc Natl Acad Sci U S A *99*, 5139-43.

Bar-Sagi, D., and Hall, A. (2000). Ras and Rho GTPases: a family reunion. Cell *103*, 227-238.

Bartolome, R.A., Sanz-Rodriguez, F., Robledo, M.M., Hidalgo, A., and Teixido, J. (2003). Rapid up-regulation of alpha4 integrin-mediated leukocyte adhesion by transforming growth factor-beta1. Mol Biol Cell *14*, 54-66.

Bayless, K.J., Meininger, G.A., Scholtz, J.M., and Davis, G.E. (1998). Osteopontin is a ligand for the alpha4beta1 integrin. J Cell Sci *111 (Pt 9)*, 1165-1174.

Beauvais-Jouneau, A., Delouvee, A., Craig, S.E., Humphries, M.J., Thiery, J.P., and Dufour, S. (1997). Direct role of the carboxy-terminal cell-binding domain of fibronectin in neural crest cell motility. Exp Cell Res *233*, 1-10.

Bednarczyk, J.L., and McIntyre, B.W. (1992). Expression and ligand-binding function of the integrin alpha 4 beta 1 (VLA-4) on neural-crest-derived tumor cell lines. Clin Exp Metastasis *10*, 281-290.

Bernards, A., and Settleman, J. (2004). GAP control: regulating the regulators of small GTPases. Trends Cell Biol *14*, 377-385.

Boudreau, N.J., and Jones, P.J. (1999). Extracellular Matrix and integrin signalling: the same of things to come. Biochemical Journal *339*, 481-488.

Braga, V.M. (2002). Cell-cell adhesion and signalling. Curr Opin Cell Biol *14*, 546-556.

Bultmann, H., Santas, A.J., and Peters, D.M.P. (1998). Fibronectin Fibrillogenesis Involves the Heparin II BInding Domain of Fibronectin. Journal of Biological Chemistry *273*, 2601-2609.

Burridge, K., and Wennerberg, K. (2004). Rho and Rac take center stage. Cell *116*, 167-179.

Butcher, E.C., and Picker, L.J. (1996). Lymphocyte homing and homeostasis. Science *272*, 60-66.

Calderwood, D.A., Shattil, S.J., and Ginsberg, M.H. (2000). Integrins and actin filaments: reciprocal regulation of cell adhesion and signaling. J Biol Chem *275*, 22607-22610.

Calzada, M. J., Esteban, M. A., Feijoo-Cuaresma, M., Castellanos, C., Naranjo-Suarez, S., Temes, E., Mendez, F., Yanez-Mo, M., Ohh, M., and O. Landazuri, M. (2006). "von Hippel-Lindau tumor suppressor protein regulates the assembly of intercellular junctions in renal cancer cells through hypoxia-inducible factor-independent mechanisms". Cancer Res *66*, 1553-60.

Campanero, M.R., Pulido, R., Ursa, M.A., Rodriguez-Moya, M., de Landazuri, M.O., and Sanchez-Madrid, F. (1990). An alternative leukocyte homotypic adhesion mechanism, LFA-1/ICAM-1-independent, triggered through the human VLA-4 integrin. J Cell Biol *110*, 2157-2165.

Carman, C.V., and Springer, T.A. (2003). Integrin avidity regulation: are changes in affinity and conformation underemphasized? Curr Opin Cell Biol *15*, 547-556.

Chan, B.M., Kassner, P.D., Schiro, J.A., Byers, H.R., Kupper, T.S., and Hemler, M.E. (1992). Distinct cellular functions mediated by different VLA integrin alpha subunit cytoplasmic domains. Cell *68*, 1051-1060.

Chan, J.R., and Cybulsky, M.I. (2004). Detection of high-affinity alpha4-integrin upon leukocyte stimulation by chemoattractants or chemokines. Methods Mol Biol *239*, 261-268.

Chan, J.R., Hyduk, S.J., and Cybulsky, M.I. (2003). Detecting rapid and transient upregulation of leukocyte integrin affinity induced by chemokines and chemoattractants. J Immunol Methods *273*, 43-52.

Chen, H., and Mosher, D.F., (1996). Formation of sodium dodecyl sulfate-stable fibronectin multimers. Failure to detect products of thiol-disulfide exchange in cyanogen bromide or limited acid digests of stabilized matrix fibronectin. J. Biol. Chem. *271*, 9084-9089.

Chen, LL., Whitty, A., Lobb, RR., Adams, SP., and Pepinsky, RB. (1999). Multiple activation states of integrin α4β1 detected through their different affinities for a small molecule ligand. J Biol Chem *274*, 13167-13175.

Chen, W.T., Hasegawa, E., Hasegawa, T., Weinstock, C., and Yamada, K.M. (1985). Development of cell surface linkage complexes in cultured fibroblasts. J Cell Biol *100*, 1103-1114.

Christopher, R.A., Kowalczyk, A.P., and McKeown-Longo, P.J. (1997). Localization of fibronectin matrix assembly sites on fibroblasts and endothelial cells. J Cell Sci *110* (Pt 5), 569-581.

Clifford, S.C., Cockman, M.E., Smallwood, A.C., Mole, D.R., Woodward, E.R., Maxwell, P.H., Ratcliffe, P.J., and Maher, E.R. (2001). "Contrasting effects on HIF-1alpha regulation by disease-causing pVHL mutations correlate with patterns of tumourigenesis in von Hippel-Lindau disease." Hum Mol Genet *10*, 1029-38.

Coghlan, MP., Chou, MM., and Carpenter, CL. (2000). Atypical protein kinases Clambda and -zeta associate with the GTP-binding protein Cdc42 and mediate stress fiber loss. Mol Cell Biol *20*, 2880-9.

Couchman, J.R., and Woods, A., (1999). Syndecan-4 and integrins: combinatorial signaling in cell adhesion. J. Cell Sci. 112, 3415-3420.

Dallas, S.L., Miyazono, K., Skerry, T.M., Mundy, G.R., and Bonewald, L.F. (1995). Dual role for the latent transforming growth factor-beta binding protein in storage of latent TGF-beta in the extracellular matrix and as a structural matrix protein. J Cell Biol *131*, 539-549.

Dedhar, S. (1999). Integrins and signal transduction. Curr Opin Hematol *6*, 37-43.

De la Fuente, MT., Casanova, B., Garcia-Gila, M., Silva, A., and Garcia-Pardo, A. (1999). Fibronectin interaction with alpha4beta1 integrin prevents apoptosis in B cell

chronic lymphocytic leukemia: correlation with Bcl-2 and Bax. Leucemia *13*, 266-74.

De la Fuente, MT., Casanova, B., Moyano, JV., Garcia-Gila, M., Sanz, L., Garcia-Marco, J., Silva, A., and Garcia-Pardo, A. (2002). Engagement of alpha4beta1 integrin by fibronectin induces in vitro resistance of B chronic lymphocytic leukemia cells to fludarabine.
J Leukoc Biol *71*, 495-502.

Del Pozo, M.A., Vicente-Manzanares, M., Tejedor, R., Serrador, J.M., and Sanchez-Madrid, F. (1999). Rho GTPases control migration and polarization of adhesion molecules and cytoskeletal ERM components in T lymphocytes. Eur J Immunol *29*, 3609-3620.

DeMali, K.A., Wennerberg, K., and Burridge, K. (2003). Integrin signaling to the actin cytoskeleton. Curr Opin Cell Biol *15*, 572-582.

Dikic, I., Tokiwa, G., Lev, S., Courtneidge, S.A., and Schlessinger, J. (1996). A role for Pyk2 and Src in linking G-protein-coupled receptors with MAP kinase activation. Nature *383*, 547-550.

Dillon, S.T., y Feig L.A. (1995). Purification and assay of recombinant C·transferase. Methods Enzymol *256*, 174-184.

Dominguez-Jimenez, C., Sanchez-Aparicio, P., Albar, J.P., and Garcia-Pardo, A. (1996). The alpha 4 beta 1 fibronectin ligands CS-1, Hep II, and RGD induce different intracellular events in B lymphoid cells. Comparison with the effects of the endothelial ligand VCAM-1. Cell Adhes Commun *4*, 251-267.

D'Souza-Schorey, C., Boettner, B., and Van Aelst, L. (1998). Rac regulates integrin-mediated spreading and increased adhesion of T lymphocytes. Mol Cell Biol *18*, 3936-3946.

Edlund, S., Landstrom, M., Heldin, C.H., and Aspenstrom, P. (2002). Transforming growth factor-beta-induced mobilization of actin cytoskeleton requires signaling by small GTPases Cdc42 and RhoA. Mol Biol Cell *13*, 902-914.

Eisenmann, K.M., McCarthy, J.B., Simpson, M.A., Keely, P.J., Guan, J.L., Tachibana, K., Lim, L., Manser, E., Furcht, L.T., and Iida, J. (1999). Melanoma chondroitin sulphate proteoglycan regulates cell spreading through Cdc42, Ack-1 and p130cas. Nat Cell Biol *1*, 507-513.

Elices, M.J., Osborn, L., Takada, Y., Crouse, C., Luhowskyj, S., Hemler, M.E., and Lobb, R.R. (1990). VCAM-1 on activated endothelium interacts with the leukocyte integrin VLA-4 at a site distinct from the VLA-4/fibronectin binding site. Cell *60*, 577-584.

Emsley, J., Knight, C.G., Farndale, R.W., Barnes, M.J., and Liddington, R.C. (2000). Structural basis of collagen recognition by integrin alpha2beta1. Cell *101*, 47-56.

Etienne-Manneville, S., and Hall, A. (2002). Rho GTPases in cell biology. Nature *420*, 629-635.

Esteban-Barragan, M.A., Avila, P., Alvarez-Tejado, M., Gutierrez, M.D., García-Pardo, A., Sanchez-Madrid, F., and O. Landazuri, M. (2002). "Role of the von Hippel-Lindau tumor suppressor gene in the formation of beta1-integrin fibrillar adhesions." Cancer Res *62*, 2929-36.

Fogerty, F.J., Akiyama, S.K., Yamada, K.M., and Mosher, D.F. (1990). Inhibition of Binding of Fibronectin to Matrix Assembly Sites by Anti-Integrin(a5b1)Antibodies. Journal of Cell Biology *111*, 699-708.

Ganju, R.K., Brubaker, S.A., Meyer, J., Dutt, P., Yang, Y., Qin, S., Newman, W., and Groopman, J.E. (1998). The alpha-chemokine, stromal cell-derived factor-1alpha, binds to the transmembrane G-protein-coupled CXCR-4 receptor and activates multiple signal transduction pathways. J Biol Chem *273*, 23169-23175.

Garcia-Gila, M., Lopez Martin, EM., and Garcia-Pardo, A. (2002). Adhesion to fibronectin via alpha4 integrin (CD49d) protects B cells from apoptosis induced by serum deprivation but not via IgM or Fas/Apo-1 receptors. Clin Exp Immunol *127*, 455-62.

Garcia-Pardo, A., Ferreira, O.C., Valinsky, J., and Bianco, C. (1989). Fibronectin receptors of mononuclear phagocytes: binding characteristics and biochemical isolation. Exp Cell Res *181*, 420-431.

Garcia-Pardo, A., and Ferreira, O.C. (1990). Adhesion of human T-lymphoid cells to fibronectin is mediated by two different fibronectin domains. Immunology *69*, 121-126.

Garcia-Pardo, A., Pearlstein, E., and Frangione, B. (1983). Primary structure of human plasma fibronectin. Journal of Biological Chemistry *258*, 12670-12674

Garcia-Pardo, A., Rostagno, A., and Franfione, B (1987). Primary structure of human plasma fibronectin. Characterization of a 38 kDa domain containing the C-terminal heparin-binding site (Hep III site) and a region of molecular heterogeneity. Biochem J *241*, 923-8.

Geiger, B., Bershadsky, A., Pankov, R., and Yamada, K.M. (2001). Transmembrane crosstalk between the extracellular matrix-cytoskeleton crosstalk. Nat Rev Mol Cell Biol *2*, 793-805.

Giancotti, F.G., and Ruoslahti, E. (1999). Integrin signaling. Science *285*, 1028-1032.

Gismondi, A., Jacobelli, J., Strippoli, R., Mainiero, F., Soriani, A., Cifaldi, L., Piccoli, M., Frati, L., and Santoni, A. (2003). "Proline-rich tyrosine kinase 2 and Rac activation by chemokine and integrin receptors controls NK cell transendothelial migration." J Immunol *170*, 3065-73.

Grayson, M.H., Van der Vieren, M., Sterbinsky, S.A., Michael Gallatin, W., Hoffman, P.A., Staunton, D.E., and Bochner, B.S. (1998). Alpha d beta2 integrin is expressed on

human eosinophils and functions as an alternative ligand for vascular cell adhesion molecule 1 (VCAM-1). J Exp Med *188*, 2187-2191.

Gregory, P., Kraemer, E., Zurcher, G., Gentinetta, R., Rohrbach, V., Brodbeck, U., Andres, A.C., Ziemiecki, A., and Butikofer, P. (2005). GPI-specific phospholipase D (GPI-PLD) is expressed during mouse development and is localized to the extracellular matrix of the developing mouse skeleton. Bone *37*, 139-147.

Guan, J.L., and Hynes, R.O (1990). Lymphoid cells recognize an alternatively spliced segment of fibronectin via the integrin receptor alpha 4 beta 1. Cell *60*, 53-61.

Gui, L., Wojciechowski, K., Gildner, C.D., Nedelkovska, H., and Hocking, D.C. (2006). Identification of the heparin-binding determinants within fibronectin repeat III1: role in cell spreading and growth. J Biol Chem *281*, 34816-34825.

Harrington, EO., Shannon, CJ., Morin, N., Rowlett, H., Murphy, C., and Lu, Q. (2005). PKCdelta regulates endothelial basal barrier function through modulation of RhoA GTPase activity. Exp Cell Res *308*, 407-21.

Haskell, M.D., Nickles, A.L., Agati, J.M., Su, L., Dukes, B.D., and Parsons, S.J. (2001). Phosphorylation of p190 on Tyr1105 by c-Src is necessary but not sufficient for EGF-induced actin disassembly in C3H10T1/2 fibroblasts. J Cell Sci *114*, 1699-1708.

Hemler, M.E., Elices, M.J., Parker, C., and Takada, Y. (1990). Structure of the integrin VLA-4 and its cell-cell and cell-matrix adhesion functions. Immunol Rev *114*, 45-65.

Hemler, M.E., Kassner, P.D., and Chan, B.M. (1992). Functional roles for integrin alpha subunit cytoplasmic domains. Cold Spring Harb Symp Quant Biol *57*, 213-220.

Hocking, D.C., Sottile, J., and McKeown-Longo, P.J. (1994). Fibronectin´s III-1 Module Contains a Conformation-dependent Binding Site for the Amino-terminal Region of Fibronectin. Journal of Biological Chemistry *269*, 19183-19191.

Hocking, D.C., Sottile, J., Reho, T., Fässler, R., McKeown-Longo, P.J., 1999. Inhibition of fibronectin matrix assembly by the heparin-binding domain of vitronectin. J. Biol. Chem. 274, 27257-27264.

Hogg, N., Laschinger, M., Giles, K., and McDowall, A.(2003). T-cell integrins: more than just sticking points. J Cell Sci *116*, 4695-4705.

Hughes, P.E., and Pfaff, M. (1998). Integrin affinity modulation. Trends Cell Biol *8*, 359-364.

Humphries, JD., and Humphries, MJ. (2007). CD14 is a ligand for the integrin alpha4beta1.FEBS Lett *581*, 757-63.

Humphries, M.J (2000). Integrin structure. Biochem Soc Trans *28*, 311-39.

Humphries, M.J., Komoriya, A., Akiyama, S.K., Olden, K., and Yamada, K.M. (1987). Identification of two distinct regions of the type III connecting segment of human

plasma fibronectin that promote cell type-specific adhesion. J Biol Chem *262*, 6886-6892.

Hurley, R.W., McCarthy, J.B., and Verfaillie, C.M. (1995). Direct adhesion to bone marrow stroma via fibronectin receptors inhibits hematopoietic progenitor proliferation. J Clin Invest *96*, 511-519.

Hyduk, SJ., and Cybulsky, MI. (2002). α4 integrin signaling activates phosphatidylinositol 3-kinase and stimulates T cell adhesion to intercellular adhesion molecule-1 to a similar extent as CD3, but induces a distinct rearrangement of the actin cytoskeleton. J Immunol *168*, 696-704.

Hynes, R.O. (1986). Fibronectins. Sci Am *254*, 42-51.

Hynes, R.O. (1987). Integrins: a family of cell surface receptors. Cell *48*, 549-554.

Hynes, R.O. (1990). Fibronectins. Springer-Verlang Inc., New York.

Hynes, R.O. (1992). Integrins: versatility, modulation, and signaling in cell adhesion. Cell *69*, 11-25.

Hynes, R.O. (2002). Integrins: bidirectional, allosteric signaling machines. Cell *110*, 673-687.

Hynes, R.O., and Zhao, Q. (2000). The evolution of cell adhesion. J Cell Biol *150*, 89-96.

Iida, J., Meijne, A.M., Oegema, T.R., Jr., Yednock, T.A., Kovach, N.L., Furcht, L.T., and McCarthy, J.B. (1998). A role of chondroitin sulfate glycosaminoglycan binding site in alpha4beta1 integrin-mediated melanoma cell adhesion. J Biol Chem *273*, 5955-5962.

Iida, J., Meijne, A.M., Spiro, RC., Roos, E., Furcht, L.T., and McCarthy, J.B. (1995). Spreading and focal contact formation of human melanoma cells in response to the stimulation of both melanoma-associated proteoglycan (NG2) and alpha 4 beta 1 integrin.Cancer Res *55*, 2177-85.

Iida, J., Skubitz, A.P., Furcht, L.T., Wayner, E.A., and McCarthy, J.B. (1992). Coordinate role for cell surface chondroitin sulfate proteoglycan and alpha 4 beta 1 integrin in mediating melanoma cell adhesion to fibronectin. J Cell Biol *118*, 431-444.

Ingber, D. (1999). How cells (might) sense microgravity. Faseb J *13 Suppl*, S3-15.

Isberg, R.R., and Leong, J.M. (1990). Multiple beta 1 chain integrins are receptors for invasin, a protein that promotes bacterial penetration into mammalian cells. Cell *60*, 861-871.

Isobe, T., Hisaoka, T., Shimizu, A., Okuno, M., Aimoto, S., Takada, Y., Saito, Y., and Takagi, J. (1997). Propolypeptide of von Willebrand factor is a novel ligand for very late antigen-4 integrin. J Biol Chem *272*, 8447-8453.

Issekutz, A.C., Ayer, L., Miyasaka, M., and Issekutz, T.B. (1996). Treatment of established adjuvant arthritis in rats with monoclonal antibody to CD18 and very late activation antigen-4 integrins suppresses neutrophil and T-lymphocyte migration to the joints and improves clinical disease. Immunology *88*, 569-576.

Iturrioz, X., Durgan, J., Calleja, V., Larijani, B., Okuda, H., Whelan, R., and Parker, PJ.(2006)**.** The von Hippel-Lindau tumour-suppressor protein interaction with protein kinase C delta. Biochem J *397*, 109-20

Jakubowski, A., Rosa, M.D., Bixler, S., Lobb, R., and Burkly, L.C. (1995). Vascular cell adhesion molecule (VCAM)-Ig fusion protein defines distinct affinity states of the very late antigen-4 (VLA-4) receptor. Cell Adhes Commun *3*, 131-142.

Johnston, B., Issekutz, T.B., and Kubes, P. (1996). The alpha 4-integrin supports leukocyte rolling and adhesion in chronically inflamed postcapillary venules in vivo. J Exp Med *183*, 1995-2006.

Kamada, M., Suzuki, K., Kato, Y., Okuda, H., and Shuin, T. (2001) von Hippel-Lindau protein promotes the assembly of actin and vinculin and inhibits cell motility. Cancer Res *61*, 4184-9.

Kanda, E., Jin, Z-H., Mizuchi, D., Arai, A., and Miura, O. (2003). Activation of Rac and tyrosine phosphorylation of cytokine receptors induced by cross-linking of integrin α4β1 and cell adhesion in hematopoietic cells. Biochem Biophys Res Comm *301*, 934-940.

Kassner, P.D., and Hemler, M.E. (1993). Interchangeable alpha chain cytoplasmic domains play a positive role in control of cell adhesion mediated by VLA-4, alpha 4 beta 1 integrin. J Exp Med *178*, 649-660.

Kassner, P.D., Kawaguchi, S., and Hemler, M.E. (1994). Minimum alpha chain cytoplasmic tail sequence needed to support integrin-mediated adhesion. J Biol Chem *269*, 19859-19867.

Katagiri, K., Maeda, A., Shimonaka, M., and Kinashi, T. (2003). RAPL, a Rap1-binding molecule that mediates Rap1-induced adhesion through spatial regulation of LFA-1. Nat Immunol *4*, 741-748.

Katagiri, K., Shimonaka, M., and Kinashi, T. (2004). Rap1-mediated lymphocyte function-associated antigen-1 activation by the T cell antigen receptor is dependent on phospholipase C-gamma1. J Biol Chem *279*, 11875-11881.

Katagiri, T., Takahashi, T., Sasaki, T., Nakamura, S., and Hattori, S. (2000). Protein-tyrosine kinase Pyk2 is involved in interleukin-2 production by Jurkat T cells via its tyrosine 402. J Biol Chem *275*, 19645-19652.

Kim, M., Carman, C.V., and Springer, T.A. (2003). Bidirectional transmembrane signaling by cytoplasmic domain separation in integrins. Science *301*, 1720-1725.

Kinashi, T. (2005). Intracellular signalling controlling integrin activation in lymphocytes. Nat Rev Immunol *5*, 546-559.

Kinashi, T., and Katagiri, K. (2005). Regulation of immune cell adhesion and migration by regulator of adhesion and cell polarization enriched in lymphoid tissues. Immunology *116*, 164-171.

Klass, C.M., Couchman, J.R., Woods, A., (2000). Control of extracellular matrix assembly by syndecan-2 proteoglycan. J. Cell Science 113, 493-506.

Kornblihtt, A.R., Umezawa, K., Vibe-Pedersen, K., and Baralle, F.E. (1985). Primary structure of human fibronectin: differential splicing may generate at least 10 polypeptides from a single gene. Embo J *4*, 1755-1759.

Kuijpers, TW., Mul, EP., Blom, M., Kovach, NL., Gaeta, FC., Tollefson, V., Elices, MJ., and Harlan, JM. (1993). Freezing adhesion molecules in a state of high-avidity binding blocks eosinophil migration.J Exp Med *178*, 279-84.

Kurban, G., Hudon, V., Duplan, E., Ohh, M., and Pause, A. (2006). Characterization of a von Hippel Lindau pathway involved in extracellular matrix remodeling, cell invasion, and angiogenesis. Cancer Res *66*, 1313-1319.

Langenbach, K.J., Sottile, J., (1999). Identification of protein-disulfide isomerase activity in fibronectin. J. Biol. Chem. 274, 7032-7038.

Laudanna, C., Campbell, J.J., and Butcher, E.C. (1996). Role of Rho in chemoattractant-activated leukocyte adhesion through integrins. Science *271*, 981-983.

Laudanna, C., Campbell, J.J., and Butcher, E.C. (1997). Elevation of intracellular cAMP inhibits RhoA activation and integrin-dependent leukocyte adhesion induced by chemoattractants. J Biol Chem *272*, 24141-24144.

Lee, J.O., Rieu, P., Arnaout, M.A., and Liddington, R. (1995). Crystal structure of the A domain from the alpha subunit of integrin CR3 (CD11b/CD18). Cell *80*, 631-638.

Lev, S., Moreno, H., Martinez, R., Canoll, P., Peles, E., Musacchio, J.M., Plowman, G.D., Rudy, B., and Schlessinger, J. (1995). Protein tyrosine kinase PYK2 involved in Ca(2+)-induced regulation of ion channel and MAP kinase functions. Nature *376*, 737-745.

Liddington, R.C., and Ginsberg, M.H. (2002). Integrin activation takes shape. J. Cell Biol. *158*, 833-839.

Lobb, R.R., and Hemler, M.E. (1994). The pathophysiologic role of alpha 4 integrins in vivo. J Clin Invest *94*, 1722-1728.

Mack, F.A., Rathmell, W.K., Arsham, A.M., Gnarra, J., Keith, B., and Simon, M.C. (2003). "Loss of pVHL is sufficient to cause HIF dysregulation in primary cells but does not promote tumor growth." Cancer Cell *3*, 75-88.

Madaule, P., and Axel, R. (1985). A novel ras-related gene family. Cell *41*, 31-40.

Mao, Y., and Schwarzbauer, J.E. (2005). Fibronectin fibrillogenesis, a cell-mediated matrix assembly process. Matrix Biol *24*, 389-399.

Martin, K.H., Slack, J.K., Boerner, S.A., Martin, C.C., and Parsons, J.T. (2002). Integrin connections map: to infinity and beyond. Science *296*, 1652-1653.

Masumoto, A., and Hemler, ME. (1993). Multiple activation states of VLA-4. Mechanistic differences between adhesion to CS1/fibronectin and to vascular cell adhesion molecule-1. J Biol Chem *268*, 228-234.

McDonald, J.A., Quade, B.J., Broekelmann, T.J., LaChance, R., Forsman, K., Hasegawa, E., and Akiyama, S. (1987). Fibronectin´s Cell-adhesive Domain and Amino-terminal Matrix Assembly Domain Participate in Its Assembly into Fibroblast Pericellular Matrix. Journal of Biological Chemistry *262*, 2957-2967.

McKeown-Longo, P.J., and Mosher, D.F. (1985). Interaction of the 70,000-mol-wt Amino -terminal Fragment of Fibronectin with the Matrix-assembly Receptor of Fibroblasts. Journal of Cell Biology *100*, 364-374.

Mercurius, K.O., and Morla, A.O. (2001). Cell adhesion and signaling on the fibronectin I st type III repeat;requesite roles for cell surface proteoglycans and integrins. BMC Cell Biology *2*, 18.

Midwood, K.S., Mao, Y., Hsia, H.C., Valenick, L.V., and Schwarzbauer, J.E. (2006). Modulation of Cell-Fibronectin Matrix Interactions during Tissue Repair. J Invest Dermatol *126* Suppl, 73-78.

Midwood, K.S., Williams, L.V., and Schwarzbauer, J.E. (2004). Tissue repair and the dynamics of the extracellular matrix. Int J Biochem Cell Biol *36*, 1031-1037.

Mittelbrunn, M., Molina, A., Escribese, M.M., Yanez-Mo, M., Escudero, E., Ursa, A., Tejedor, R., Mampaso, F., and Sanchez-Madrid, F. (2004). VLA-4 integrin concentrates at the peripheral supramolecular activation complex of the immune synapse and drives T helper 1 responses. Proc Natl Acad Sci U S A *101*, 11058-11063.

Mooradian, D.L., McCarthy, J.B., Skubitz, A.P.N., Cameron, J.D., and Furcht, L.T. (1993). Invest. Opthalmol. & Visual Sci *34*, 153-164.

Mosher, D.F. (1993). Current opinion structural biology *3*, 214-222.

Mostafavi-Pour, Z., Askari, J.A., Parkinson, S.J., Parker, P.J., Ng, T.T., and Humphries, M.J. (2003). Integrin-specific signaling pathways controlling focal adhesion formation and cell migration. J Cell Biol *161*, 155-167.

Mostafavi-Pour, Z., Askari, J.A., Whittard, J.D., and Humphries, M.J. (2001). Identification of a novel heparin-binding site in the alternatively spliced IIICS region of fibronectin: roles of integrins and proteoglycans in cell adhesion to fibronectin splice variants. Matrix Biol *20*, 63-73.

Mould, A.P., and Humphries, M.J. (1991). Identification of a novel recognition sequence for the integrin alpha 4 beta 1 in the COOH-terminal heparin-binding domain of fibronectin. Embo J *10*, 4089-4095.

Mould, A.P., Askari, J.A., Barton, S., Kline, AD., McEwan, PA., Craig, S.E., and Humphries, M.J. (2002). Integrin activation involves a conformational change in the alpha 1 helix of the beta subunit A-domain. J Biol Chem *277*, 19800-5.

Mould, A.P., Askari, J.A., Craig, S.E., Garrat, A.N., Clements, J., and Humphries, M.J. (1994). Integrin α4β1-mediated melanoma cell adhesion and migration on vascular cell adhesion molecule (VCAM-1) and the alternatively spliced IIICS region of fibronectin. J Biol Chem *269*, 27224-27230.

Moyano, J.V., Carnemolla, B., Albar, J.P., Leprini, A., Gaggero, B., Zardi, L., and Garcia-Pardo, A. (1999). Cooperative role for activated alpha4 beta1 integrin and chondroitin sulfate proteoglycans in cell adhesion to the heparin III domain of fibronectin. Identification of a novel heparin and cell binding sequence in repeat III5. J Biol Chem *274*, 135-142.

Moyano, J.V., Carnemolla, B., Dominguez-Jimenez, C., Garcia-Gila, M., Albar, J.P., Sanchez-Aparicio, P., Leprini, A., Querze, G., Zardi, L., and Garcia-Pardo, A. (1997). Fibronectin type III5 repeat contains a novel cell adhesion sequence, KLDAPT, which binds activated alpha4beta1 and alpha4beta7 integrins. J Biol Chem *272*, 24832-24836.

Moyano, J.V., Maqueda, A., Albar, J.P., and Garcia-Pardo, A. (2003a). A synthetic peptide from the heparin-binding domain III (repeats III4-5) of fibronectin promotes stress-fiber and focal-adhesion formation in melanoma cells. Biochem J *371*, 565-571.

Moyano, J.V., Maqueda, A., Casanova, B., and Garcia-Pardo, A. (2003b). Alpha4beta1 integrin/ligand interaction inhibits alpha5beta1-induced stress fibers and focal adhesions via down-regulation of RhoA and induces melanoma cell migration. Mol Biol Cell *14*, 3699-3715.

Mueller, KL., Daniels, MA., Felthauser, A., Kao, C., Jameson, SC., and Shimizu, Y. (2004). LFA-1 integrin-dependent T cell adhesion is regulated by both Ag specificity and sensitivity. J Immunol *173*, 2222-2226.

Nakahara, H., Mueller, S.C., Nomizu, M., Yamada, Y., Yeh, Y., and Chen, W.T. (1998). Activation of beta1 integrin signaling stimulates tyrosine phosphorylation of p190RhoGAP and membrane-protrusive activities at invadopodia. J Biol Chem *273*, 9-12.

Neish, A.S., Williams, A.J., Palmer, H.J., Whitley, M.Z., and Collins, T. (1992). Functional analysis of the human vascular cell adhesion molecule 1 promoter. J Exp Med *176*, 1583-1593.

Nobes, C.D., and Hall, A. (1995). Rho, rac, and cdc42 GTPases regulate the assembly of multimolecular focal complexes associated with actin stress fibers, lamellipodia, and filopodia. Cell *81*, 53-62.

Ohh, M., Yauch, R.L., Lonergan, K.M., Whaley, J.M., Stemmer-Rachamimov, A.O., Louis, D.N., Gavin, B.J., Kley, N., Kaelin, W.G., Jr., and Iliopoulos, O. (1998). The von Hippel-Lindau tumor suppressor protein is required for proper assembly of an extracellular fibronectin matrix. Mol Cell *1*, 959-968.

Okigaki, M., Davis, C., Falasca, M., Harroch, S., Felsenfeld, D.P., Sheetz, M.P., and Schlessinger, J. (2003). Pyk2 regulates multiple signaling events crucial for macrophage morphology and migration. Proc Natl Acad Sci U S A *100*, 10740-10745.

Osborn, L., Hession, C., Tizard, R., Vassallo, C., Luhowskyj, S., Chi-Rosso, G., and Lobb, R. (1989). Direct expression cloning of vascular cell adhesion molecule 1, a cytokine-induced endothelial protein that binds to lymphocytes. Cell *59*, 1203-1211.

Ostergaard, H.L., Lou, O., Arendt, C.W., and Berg, N.N. (1998). Paxillin phosphorylation and association with Lck and Pyk2 in anti-CD3- or anti-CD45-stimulated T cells. J Biol Chem *273*, 5692-5696.

Pal, S., Claffey, KP., Dvorak, HF., and Mukhopadhyay, D. (1997). The von Hippel-Lindau gene product inhibits vascular permeability factor/vascular endothelial growth factor expression in renal cell carcinoma by blocking protein kinase C pathways. J Biol Chem *272*, 27509-12

Pang H.,and Bitar, KN. (2005). Direct association of RhoA with specific domains of PKC-alpha. Am J Physiol Cell Physiol *289*, 982-93.

Peters, D.M., and Mosher, D.F. (1987). Localization of cell surface sites involved in fibronectin fibrillogenesis. J. Cell Biol. *104*, 121-130.

Plow, E.F., Haas, T.A., Zhang, L., Loftus, J., and Smith, J.W. (2000). Ligand binding to integrins. J Biol Chem *275*, 21785-21788.

Porter, J.C., and Hogg, N. (1998). Integrins take partners: cross-talk between integrins and other membrane receptors. Trends Cell Biol *8*, 390-396.

Pribila, J.T., Quale, A.C., Mueller, K.L., and Shimizu, Y. (2004). Integrins and T cell-mediated immunity. Annu Rev Immunol *22*, 157-180.

Raftopoulou, M., and Hall, A. (2004). Cell migration: Rho GTPases lead the way. Dev Biol *265*, 23-32.

Ridley A. (2001). Rho family proteins: coordinating cell responses. Trends Cell Biol *11*, 471-477.

Ridley, AJ., and Hall, A.(1992). The small GTP-binding protein rho regulates the assembly of focal adhesions and actin stress fibers in response to growth factors. Cell *70*, 389-99.

Ridley, A.J., Paterson, H.F., Johnston, C.L., Diekmann, D., and Hall, A. (1992). The small GTP-binding protein rac regulates growth factor-induced membrane ruffling. Cell *70*, 401-410.

Ridley, A.J., Self, A.J., Kasmi, F., Paterson, H.F., Hall, A., Marshall, C.J., and Ellis, C. (1993). rho family GTPase activating proteins p190, bcr and rhoGAP show distinct specificities in vitro and in vivo. Embo J *12*, 5151-5160.

Rodriguez-Fernandez, J.L., Gomez, M., Luque, A., Hogg, N., Sanchez-Madrid, F., and Cabanas, C. (1999). The interaction of activated integrin lymphocyte function-associated antigen 1 with ligand intercellular adhesion molecule 1 induces activation and redistribution of focal adhesion kinase and proline-rich tyrosine kinase 2 in T lymphocytes. Mol Biol Cell *10*, 1891-1907.

Rodriguez-Fernandez, J.L., Sanchez-Martin, L., Rey, M., Vicente-Manzanares, M., Narumiya, S., Teixido, J., Sanchez-Madrid, F., and Cabanas, C. (2001). Rho and Rho-associated kinase modulate the tyrosine kinase PYK2 in T-cells through regulation of the activity of the integrin LFA-1. J Biol Chem *276*, 40518-40527.

Rose, D.M., Han, J., and Ginsberg, M.H. (2002). Alpha4 integrins and the immune response. Immunol Rev *186*, 118-124.

Sadahira, Y., Yoshino, T., and Monobe, Y. (1995). Very late activation antigen 4-vascular cell adhesion molecule 1 interaction is involved in the formation of erythroblastic islands. J Exp Med *181*, 411-415.

Sanchez-Aparicio, P., Dominguez-Jimenez, C., and Garcia-Pardo, A. (1994). Activation of the alpha 4 beta 1 integrin through the beta 1 subunit induces recognition of the RGDS sequence in fibronectin. J Cell Biol *126*, 271-279.

Sanchez-Aparicio, P., Ferreira Junior, O.C., and Garcia-Pardo, A. (1993). Alpha 4 beta 1 recognition of the Hep II domain of fibronectin is constitutive on some hemopoietic cells but requires activation on others. J Immunol *150*, 3506-3514.

Sander, E.E., ten Klooster, J.P., van Delft, S., van der Kammen, R.A., y Collard, J.G. (1999). Rac downregulates Rho activity: reciprocal balance between both GTPases determines cellular morphology and migratory behaviour. J Cell Biol *147*, 1009-1021.

Sanjay, A., Houghton, A., Neff, L., DiDomenico, E., Bardelay, C., Antoine, E., Levy, J., Gailit, J., Bowtell, D., Horne, W.C., and Baron, R. (2001). Cbl associates with Pyk2 and Src to regulate Src kinase activity, alpha(v)beta(3) integrin-mediated signaling, cell adhesion, and osteoclast motility. J Cell Biol *152*, 181-195.

Santas, A.J., Peterson, J.A., Halbleib, J.L., Craig, S.E., Humphries, M.J., and Peters, D.M.P. (2002). Alternative Splicing of IIICS Domain in Fibronectin Governs the Role of the Heparin II Domain in Fibrillogenesis and Cell Spreading. Journal of Biological Chemistry *277*, 13650-13658.

Saoncella, S., Echtermeyer, F., Denhez, F., Nowlen, J.K., Mosher, D.F., Robinson, S.D., Hynes, R.O., and Goetinck, P.F. (1999). Syndecan-4 signals cooperatively with integrins in a Rho-dependent manner in the assembly of focal adhesions and actin stress fibers. Proc Natl Acad Sci USA *96*, 2805-2810.

Schmidt, A., and Hall, A. (2002). Guanine nucleotide exchange factors for Rho GTPases: turning on the switch. Genes Dev *16*, 1587-1609.

Schmidt, A., Schmelzle, T., and Hall, M.N. (2002). The RHO1-GAPs SAC7, BEM2 and BAG7 control distinct RHO1 functions in Saccharomyces cerevisiae. Mol Microbiol *45*, 1433-1441.

Schwartz, M.A., and Ginsberg, M.H. (2002). Networks and crosstalk: integrin signalling spreads. Nat Cell Biol *4*, 65-68.

Schwartz, M.A., and Shattil, S.J. (2000). Signaling networks linking integrins and rho family GTPases. Trends Biochem Sci *25*, 388-391.

Schwarzbauer, J.E. (1991). Identification of the fibronectin sequences required for assembly of a fibrillar matrix. J Cell Biol *113*, 1463-1473.

Schwarzbauer, J.E., Patel, R.S., Fonda, D., and Hynes, R.O. (1987). Multiple sites of alternative splicing of the rat fibronectin gene transcript. Embo J *6*, 2573-2580.

Schwarzbauer, J.E., Tamkun, J.W., Lemischka, I.R., and Hynes, R.O. (1983). Three different fibronectin mRNAs arise by alternative splicing within the coding region. Cell *35*, 421-431.

Sechler, J.L., Rao, H., Cumiskey, A.M., Vega-Colón, I., Smith, M.S., Murata, T., and Schwarzbauer, J.E. (2001). A novel fibronectin binding site required fot fibronectin fibril growth during matrix assembly. Journal of Cell Biology *154*, 1081-1088.

Sechler, J.L., Takada, Y., and Schwarzbauer, J.E., (1996). Altered rate of fibronectin matrix assembly by deletion of the first type III repeats. J Cell Biol *134*, 573-583.

Sharma, A., Askari, J.A., Humphries, M.J., Jones, E.Y., and Stuart, D.I. (1999). Crystal structure of a heparin- and integrin-binding segment of human fibronectin. Embo J *18*, 1468-1479.

Shimizu, Y., Rose, D.M., and Ginsberg, M.H. (1999). Integrins in the immune system. Adv Immunol *72*, 325-380.

Singer, II, Scott, S., Kawka, D.W., Kazazis, D.M., Gailit, J., and Ruoslahti, E. (1988). Cell surface distribution of fibronectin and vitronectin receptors depends on substrate composition and extracellular matrix accumulation. J Cell Biol *106*, 2171-2182.

Sironi, M., Sciacca, F.L., Matteucci, C., Conni, M., Vecchi, A., Bernasconi, S., Minty, A., Caput, D., Ferrara, P., Colotta, F., and et al. (1994). Regulation of endothelial and mesothelial cell function by interleukin-13: selective induction of vascular cell adhesion molecule-1 and amplification of interleukin-6 production. Blood *84*, 1913-1921.

Soede, R.D., Zeelenberg, I.S., Wijnands, Y.M., Kamp, M., and Roos, E. (2001). Stromal cell-derived factor-1-induced LFA-1 activation during in vivo migration of T cell hybridoma cells requires Gq/11, RhoA, and myosin, as well as Gi and Cdc42. J Immunol *166*, 4293-4301.

Springer, T.A. (1997). Folding of the N-terminal, ligand-binding region of integrin alpha-subunits into a beta-propeller domain. Proc Natl Acad Sci U S A *94*, 65-72.

Stein, J.V., Soriano, S.F., M'Rini, C., Nombela-Arrieta, C., de Buitrago, G.G., Rodriguez-Frade, J.M., Mellado, M., Girard, J.P., and Martinez, A.C. (2003). CCR7-mediated physiological lymphocyte homing involves activation of a tyrosine kinase pathway. Blood *101*, 38-44.

Stewart, M., and Hogg, N. (1996). Regulation of leukocyte integrin function: affinity vs. avidity. J Cell Biochem *61*, 554-561.

Swerlick, R.A., Lee, K.H., Li, L.J., Sepp, N.T., Caughman, S.W., and Lawley, T.J. (1992). Regulation of vascular cell adhesion molecule 1 on human dermal microvascular endothelial cells. J Immunol *149*, 698-705.

Takada, Y., Elices, M.J., Crouse, C., and Hemler, M.E. (1989). The primary structure of the alpha 4 subunit of VLA-4: homology to other integrins and a possible cell-cell adhesion function. Embo J *8*, 1361-1368.

Takagi, J., Petre, B.M., Walz, T., and Springer, T.A. (2002). Global conformational rearrangements in integrin extracellular domains in outside-in and inside-out signaling. Cell *110*, 599-511.

Takai, Y., Sasaki, T., and Matozaki, T. (2001). Small GTP-binding proteins. Physiol Rev *81*, 153-208.

Tang, N., Mack, F., Haase, V.H., Simon M.C., and Johnson, R.S. (2006). "pVHL function is essential for endothelial extracellular matrix deposition." Mol Cell Biol *26*, 2519-30.

Taooka, Y., Chen, J., Yednock, T., and Sheppard, D. (1999). The integrin alpha9beta1 mediates adhesion to activated endothelial cells and transendothelial neutrophil migration through interaction with vascular cell adhesion molecule-1. J Cell Biol *145*, 413-420.

Teixidó, J., Parker, C.M., Kassner, P.D., and Hemler, M.E. (1992). Functional and structural analysis of VLA-4 integrin alpha 4 subunit cleavage. J Biol Chem *267*, 1786-1791.

Teixidó, J., and Sánchez-Madrid, F. (1993). Structure and function of the VLA-4 integrin. Lymphocyte Adhesion Molecules, G. Landes C, 54.

Toker, A., and Cantley, L.C. (1997). Signalling through the lipid products of phosphoinositide-3-OH kinase. Nature *387*, 673-676.

Tsubota, Y., Yasuda, C., Kariya, Y., Ogawa, T., Hirosaki, T., Mizushima, H., Miyazaki, K., 2005. Regulation of biological activity and matrix assembly of laminin-5 by COOH-terminal, LG4-5 domain of α3 chain. J Biol Chem 280, 14370-14377.

Uchiyama, H., Barut, B.A., Chauhan, D., Cannistra, S.A., and Anderson, K.C. (1992). Characterization of adhesion molecules on human myeloma cell lines. Blood *80*, 2306-2314.

Uchiyama, H., Barut, B.A., Mohrbacher, A.F., Chauhan, D., and Anderson, K.C. (1993). Adhesion of human myeloma-derived cell lines to bone marrow stromal cells stimulates interleukin-6 secretion. Blood *82*, 3712-3720.

van Seventer, G.A., Mullen, M.M., and van Seventer, J.M. (1998). Pyk2 is differentially regulated by beta1 integrin- and CD28-mediated co-stimulation in human CD4+ T lymphocytes. Eur J Immunol *28*, 3867-3877.

Verfaillie, C.M., McCarthy, J.B., and McGlave, P.B. (1992). Mechanisms underlying abnormal trafficking of malignant progenitors in chronic myelogenous leukemia. Decreased adhesion to stroma and fibronectin but increased adhesion to the basement membrane components laminin and collagen type IV. J Clin Invest *90*, 1232-1241.

Vicente-Manzanares, M., and Sanchez-Madrid, F. (2004). Role of the cytoskeleton during leukocyte responses. Nat Rev Immunol *4*, 110-122.

Vinogradova, O., Velyvis, A., Velyviene, A., Hu, B., Haas, T., Plow, E., and Qin, J. (2002). A structural mechanism of integrin alpha(IIb)beta(3) "inside-out" activation as regulated by its cytoplasmic face. Cell *110*, 587-597.

Wayner, E.A., Garcia-Pardo, A., Humphries, M.J., McDonald, J.A., and Carter, W.G. (1989). Identification and characterization of the T lymphocyte adhesion receptor for an alternative cell attachment domain (CS-1) in plasma fibronectin. J Cell Biol *109*, 1321-1330.

Wherlock, M., and Mellor, H. (2002). The Rho GTPase family: a Racs to Wrchs story. J Cell Sci *115*, 239-240.

Whittaker, C.A., and Hynes, R.O. (2002). Distribution and evolution of von Willebrand/integrin A domains: widely dispersed domains with roles in cell adhesion and elsewhere. Mol Biol Cell *13*, 3369-3387.

Wierzbicka-Patynowski, I., and Schwarzbauer, JE. (2003). The ins and outs of fibronectin matrix assembly. J Cell Sci *16 (Pt 16)*, 3269-76.

Wittchen, E.S., van Buul, J.D., Burridge, K., and Worthylake, R.A. (2005). Trading spaces: Rap, Rac, and Rho as architects of transendothelial migration. Curr Opin Hematol *12*, 14-21.

Woods, A., (2001). Syndecans: transmembrane modulators of adhesion and matrix assembly. J Clin Invest.107, 935-941.

Woods, A., and Couchman, J.R. (1992). Protein kinase C involvement in focal adhesion formation. Journal of Cell Science, 277-290.

Woods, A., and Couchman, J.R. (1998). Syndecans: synergistic activators of cell adhesion. Trends Cell Biol, 189-192.

Woods, A., McCarthy, J.B., Furcht, L.T., and Couchman, J.R. (1993). A synthetic peptide from the COOH-terminal heparin-binding domain of fibronectin promotes focal adhesion formation. Mol Biol Cell *4*, 605-613.

Worthylake, R.A., and Burridge, K. (2001). Leukocyte transendothelial migration: orchestrating the underlying molecular machinery. Curr Opin Cell Biol *13*, 569-577.

Xiong, J.P., Stehle, T., Diefenbach, B., Zhang, R., Dunker, R., Scott, D.L., Joachimiak, A., Goodman, S.L., and Arnaout, M.A. (2001). Crystal structure of the extracellular segment of integrin alpha Vbeta3. Science *294*, 339-345.

Xiong, W., and Parsons, J.T. (1997). Induction of apoptosis after expression of PYK2, a tyrosine kinase structurally related to focal adhesion kinase. J Cell Biol *139*, 529-539.

Xu, J., Wang, F., Van Keymeulen, A., Herzmark, P., Straight, A., Kelly, K., Takuwa, Y., Sugimoto, N., Mitchison, T., and Bourne, H.R. (2003). Divergent signals and cytoskeletal assemblies regulate self-organizing polarity in neutrophils. Cell *114*, 201-214.

Yabkowitz, R., Dixit, V.M., Guo, N., Roberts, D.D., and Shimizu, Y. (1993). Activated T-cell adhesion to thrombospondin is mediated by the alpha 4 beta 1 (VLA-4) and alpha 5 beta 1 (VLA-5) integrins. J Immunol *151*, 149-158.

Yamada, K.M., Pankov, R., and Cukierman, E. (2003). Dimensions and dynamics in integrin function. Braz J Med Biol Res *36*, 959-966.

Yang, J.T., Rayburn, H., and Hynes, R.O. (1995). Cell adhesion events mediated by alpha 4 integrins are essential in placental and cardiac development. Development *121*, 549-560.

Yu, H., Li, X., Marchetto, G.S., Dy, R., Hunter, D., Calvo, B., Dawson, T.L., Wilm, M., Anderegg, R.J., Graves, L.M., and Earp, H.S. (1996). Activation of a novel calcium-dependent protein-tyrosine kinase. Correlation with c-Jun N-terminal kinase but not mitogen-activated protein kinase activation. J Biol Chem *271*, 29993-29998.

Zamir, E., Katz, B.Z., Aota, S., Yamada, K.M., Geiger, B., and Kam, Z. (1999). Molecular diversity of cell-matrix adhesions. J Cell Sci *112 (Pt 11)*, 1655-1669.

Zhang, B., Zhang, Y., Wang, Z., and Zheng, Y. (2000). The role of Mg2+ cofactor in the guanine nucleotide exchange and GTP hydrolysis reactions of Rho family GTP-binding proteins. J Biol Chem *275*, 25299-25307.

Zhang, Q., Checovich, W.J., Peters, D.M., Albrecht, R.M., Mosher, D.F., (1994). Modulation of cell surface fibronectin assembly sites by lysophosphatidic acid. J. Cell Biol. 127, 1447-1459.

Zhang, Q., and Mosher, D.F. (1996). Cross-linking of the NH2-terminal Region of Fibronectin to Molecules of Large Apparent Molecular Mass. Journal of Biological Chemistry *271*, 33284-33292.

Zhao, J., Zheng, C., and Guan, J. (2000). Pyk2 and FAK differentially regulate progression of the cell cycle. J Cell Sci *113 (Pt 17)*, 3063-3072.

Zhong, C., Chrzanowska-Wodnicka, M., Brown, J., Shaub, A., Belkin, AM., and Burridge, K. (1998). Rho-mediated contractility exposes a cryptic site in fibronectin and induces fibronectin matrix assembly. J Cell Biol 141,539-51

Anexos

ANEXOS

Publicaciones del autor relacionadas con el trabajo de tesis:

Alfredo Maqueda, José V. Moyano, M.Dolores Gutiérrez-López, Susana Ovalle, José M.Rodríguez-Frade, Carlos Cabañas, and Ángeles García-Pardo. "*Activation pathways of α4β1 integrin leading to distinct T cell cytoskeleton reorganization, Rac1 regulation and Pyk2 phosphorylation"*. Journal of Cellular Physiology 2006 207(3) 746-756.……..……...***ANEXO I***.

Alfredo Maqueda, José V. Moyano, Donna M. Peters and Ángeles García-Pardo. "*Two novel functions for fibronectina heparin III binding domain (type III4-5 repeats): Self-association and involvement in fibronectin fibrillogenesis"*. Matrix Biology 2007. En revisión……..***ANEXO II***.

Mónica Feijoó-Cuaresma, Fernando Méndez, **Alfredo Maqueda,** Miguel Esteban-Barragán, Salvador Naranjo, María C Castellanos, Mercedes Hernández del Cerro, Angeles García-Pardo, María J. Calzada and Manuel Ortiz de Landázuri**. "***The Lack of Fibronectin Matrix Assembly in the von Hippel-Lindau Protein Defective Renal Cancer Cells is Partly Due to a Deficient Activation of the GTPase RhoA"***.** Cancer Research 2007. En revisión.…….....***ANEXO III***.

Moyano, J.V., **Maqueda, A**., Albar, J.P., and García-Pardo, A. "*A synthetic peptide from the heparin-binding domain III (repeats III4-5) of fibronectin promotes stress fiber and focal adhesión formation in melanoma cells"***.** Biochemical Journal 2003 (371) 565-571……..……..…….....***ANEXO IV***.

Moyano, J. V., **Maqueda, A.**, Casanova, B., and García-Pardo, A. "*α4β1 integrin/ligand interaction inhibits α5β1–induced stress fiber and focal adhesions via downregulation of RhoA and induces melanoma cell migration"***.** Molecular Biology of the Cell 2003 (14) 3699-3715…….…….....***ANEXO V***.

CD con material adicional……...……***ANEXO VI.***

Anexo I

JOURNAL OF CELLULAR PHYSIOLOGY 207:746–756 (2006)

Activation Pathways of α4β1 Integrin Leading to Distinct T-Cell Cytoskeleton Reorganization, Rac1 Regulation and Pyk2 Phosphorylation

ALFREDO MAQUEDA,[1] JOSÉ V. MOYANO,[1] M. DOLORES GUTIÉRREZ-LÓPEZ,[2] SUSANA OVALLE,[2] JOSÉ M. RODRÍGUEZ-FRADE,[3] CARLOS CABAÑAS,[2] AND ANGELES GARCIA-PARDO[1]*

[1]*Departamento de Inmunología, Centro de Investigaciones Biológicas, CSIC, Madrid, Spain*
[2]*Instituto de Farmacología y Toxicología, CSIC-UCM, Madrid, Spain*
[3]*Centro Nacional de Biotecnología, CSIC, Madrid, Spain*

α4β1 integrin is highly expressed in lymphocytes and is essential in hematopoiesis, extravasation, and the inflammatory response. α4β1 can be activated by intracellular signals elicited upon T-cell activation by phorbol esters, CD3 crosslinking, or certain chemokine/receptor interactions (inside-out activation). Divalent cations or certain anti- β1 mAbs (i.e., TS2/16) can also bind and activate integrins directly (outside-in activation). In both cases, activation results in increased adhesion and/or affinity for ligands. It is not known if these various stimuli produce the same or different post-adhesion events. To address this, we have studied the cytoskeleton organization and intracellular signaling following activation of α4β1 in Jurkat cells and in human T-lymphoblasts. Treatment with Mn^{2+}, α-CD3 mAb or the chemokine SDF-1α followed by attachment to the fibronectin fragment H89 or the endothelial molecule VCAM-1 (α4β1 ligands), resulted in cell polarization and migration. In contrast, activation with PMA or TS2/16 induced cell spreading and strong adherence. Video microscopy and Transwell analyses confirmed these results, which correlated with different resistance to detachment under flow. Activation of the small GTPase RhoA or transfection with the constitutively active mutants V14RhoA or V12Rac1, abolished the α4β1-induced cell polarization but did not affect cell spreading. Moreover, Rac1 activity was distinctly modulated by agents that induce a polarized or spread phenotype. The tyrosine kinase Pyk2 was highly phosphorylated upon induction of cell polarity but not during cell spreading. These results reveal novel properties of α4β1 integrin, namely the ability to trigger two types of T-cell cytoskeletal response with different signaling requirements. J. Cell. Physiol. 207: 746–756, 2006. © 2006 Wiley-Liss, Inc.

T-cell interactions with the extracellular matrix and vascular endothelium are mainly mediated by the integrin family of receptors, which are heterodimers composed of two subunits, α and β (Hogg et al., 2003; Pribila et al., 2004). These interactions must be dynamic and transient so that lymphocytes can extravasate, respond to an inflammatory signal from injured tissue, search for antigens within lymphoid tissues, or engage in firm adhesion to perform the immune response (Pribila et al., 2004). To allow this, lymphocyte integrins undergo rapid and highly regulated transitions between different states of activation. Integrin activation consists in a conformational change which separates the α and β cytoplasmic tails and extends the integrin. This can be induced by intracellular signals triggered by engagement of other cell surface receptors (inside-out activation) (Liddington and Ginsberg, 2002; Takagi and Springer, 2002; Travis et al., 2003; Mould and Humphries, 2004; Kinashi, 2005). Certain chemokines such as SDF-1α, PMA, or PDBu phorbol esters, as well as crosslinking of the CD3 complex, are well-known inside-out integrin activators (reviewed by Kinashi, 2005).

Integrins can also be activated from outside the cell by divalent cations (mostly Mn^{2+}) or certain anti-β mAbs, which induce the active conformation by binding to the integrin extracellular domains and exposing the ligand binding sites (outside-in activation) (Kovach et al., 1992; van de Wiel-van Kemenade et al., 1992; Arroyo et al., 1993; Faull et al., 1994). Integrin activation by intracellular or extracellular stimuli enhances cell adhesion and in some cases, increases the affinity of integrins for their ligands (Faull et al., 1994; Hogg et al., 2003; Mould and Humphries, 2004).

α4β1, a major integrin in lymphocytes, is the receptor for the extracellular matrix and bone marrow stroma component fibronectin (Fn), and for vascular cell adhesion molecule-1 (VCAM-1) in endothelium, thus playing a key role in hematopoiesis and lymphocyte

This article includes Supplementary Material available from the authors upon request or via the Internet at http://www.interscience.wiley.com/jpages/0021-9541/suppmat.

A. Maqueda and S. Ovalle were supported by I3P predoctoral fellowships from CSIC/European Union Social Fund; J.V. Moyano was supported by a fellowship from GlaxoSmithKline; M.D. Gutiérrez-López was supported by a postdoctoral fellowship from MEC.

Contract grant sponsor: Ministerio de Educación y Ciencia (MEC), Spain; Contract grant number: SAF2003-00824; Contract grant sponsor: MMA Foundation, Madrid, Spain (to A.G.P.); Contract grant sponsor: MEC (to C.C.); Contract grant number: SAF2004-01715.

José V. Moyano's present address is Northwestern University, Chicago, Illinois, USA.

*Correspondence to: Angeles Garcia-Pardo, Centro de Investigaciones Biológicas, CSIC, Ramiro de Maeztu 9, 28040 Madrid, Spain. E-mail: agarciapardo@cib.csic.es

Received 10 October 2005; Accepted 5 January 2006

DOI: 10.1002/jcp.20624

extravasation (Rose et al., 2002). α4β1 also provides co-stimulatory signals for T-cell activation and differentiation and plays a role during the interaction of T-cells with antigen presenting cells (Mittelbrunn et al., 2004; Pribila et al., 2004). Regulation of the activity of α4β1 is therefore crucial for the development and function of the immune system and the inflammatory response. In previous studies using Mn^{2+} and the anti-β1 mAb TS2/16, we and others have defined multiple states of α4β1 activation with different affinities for its ligands (Masumoto and Hemler, 1993; Sánchez-Aparicio et al., 1993; Chen et al., 1999). It is also established that the constitutive activity of α4β1 differs among different cell types, that constitutive and activated α4β1 recognize different ligands in Fn, and that Mn^{2+} and TS2/16 activate α4β1 by distinct mechanisms (Masumoto and Hemler, 1993; Sánchez-Aparicio et al., 1993, 1994; Moyano et al., 1997). Similarly, CD3 crosslinking and SDF-1α increase α4β1 affinity while PMA increase adhesion by enhancing spreading (Faull et al., 1994; Sanz-Rodríguez et al., 2001; Chan and Cybulsky, 2004).

These previous studies on the initial steps of ligand binding and cell adhesion, indicate that the various stimuli regulate α4β1 activity differently. It is not known if these stimuli also induce different α4β1-mediated post-adhesion events, such as cell migration and intracellular signaling. The family of the small Rho GTPases, which includes RhoA and Rac1, regulates cytoskeleton organization and plays an important role in lymphocyte migration (Hogg et al., 2003; Vicente-Manzanares and Sánchez-Madrid, 2004). Likewise, the tyrosine kinase Pyk2 is also involved in cell migration and provides a link between integrin-mediated adhesion and Rho GTPases (Wittchen et al., 2005). In certain cell systems, constitutive α4β1 activates Rac1 and Pyk2 (van Seventer et al., 1998; Gismondi et al., 2003) and it is not known how activation of α4β1 by different agents affects this property. To clarify these issues, in the present report we have studied the cytoskeletal response of T-cells upon α4β1 activation by different stimuli and adhesion to its ligands.

MATERIALS AND METHODS

Antibodies, reagents, and recombinant proteins

mAbs TS2/16 (anti-β1, integrin activating), Alex 1/4 (anti-β1, non-activating), HP2/1 (anti-α4, function blocking), and anti-HLA were obtained from Dr. Francisco Sánchez-Madrid (Hospital de la Princesa, Madrid, Spain); mAbs to RhoA (sc-418) and α-tubulin (sc-5286), and polyclonal Abs to Pyk2 (C-19, sc-1515) were purchased from Santa Cruz Biotechnology, Inc., (Santa Cruz, CA); mAb to Rac1 was from BD Biosciences Europe (Erembodegem, Belgium); mAb to CD3 was from Serotec (Oxford, UK); mAb to phosphotyrosine PY20 was from Biomol Research Laboratories, Inc., (Plymouth Meeting, PA). Lysophosphatidic acid (LPA) and PMA were purchased from Sigma (St. Louis, MO). SDF-1α was from R&D Systems (Minneapolis, MN). The Fn fragment H89 containing the CS-1 ligand for α4β1 integrin, was obtained from Dr. Martin Humphries (University of Manchester, UK) and prepared as described (Mould et al., 1994). VCAM-1 was provided by Dr. Roy Lobb (Albor Biologics, Inc., Westwood, MA); C3 transferase (C3) was obtained from Dr. Alan Hall (University College, London, UK) and purified as described (Dillon and Feig, 1995). Green fluorescent protein (GFP) fused to active (V14RhoA, V12Rac1) or dominant negative (N19RhoA, N17Rac1) mutants were gifts from Dr. Francisco Sánchez-Madrid.

Cells and cell treatments

The human T-cell line Jurkat was obtained from Dr. Margarita López-Trascasa (Hospital La Paz, Madrid, Spain). Human T-lymphoblasts were prepared as previously described (Rodríguez-Fernández et al., 1999). Prior to all assays (except when indicated) cells were serum-starved for 3 h. Cell viability was assessed by trypan blue exclusion. Integrin activation was performed in 10 mM HEPES, 1% BSA, Tris-buffered saline (Mn^{2+} treatment), or RPMI (all other conditions). Cells were incubated with Mn^{2+} (0.2–2 mM), TS2/16 (0.1–5 μg/ml) or PMA (5–50 ng/ml) for 20 min at 37°C. For activation via CD3 crosslinking, cells were incubated at 4°C with 20 μg/ml anti-CD3 mAb for 30 min, and goat Abs to mouse IgG (Dako A/S, Glostrup, Denmark) for 5 min. Alternatively, mAb anti-CD3 (0.1–2 μg/ml) was co-immobilized with H89 or VCAM-1 and used as adhesion substrate. SDF-1α activation (150 ng/ml) was performed for 1 min at 37°C.

Cell detachment assays

Petri dishes were spotted overnight with H89 (5 μg/ml in PBS), blocked with 0.5% BSA and assembled as the lower wall of a parallel flow chamber (IQUUM, Boston, MA), mounted on an inverted microscope (LEICA DMIL) equipped with a CCD camera (LEICA DC 100). Jurkat cells (1×10^6/ml) were perfused through the chamber at a flow rate of 1 dyn/cm^2 in serum-free medium. Cells were allowed to attach to the substrate and the number of cells remaining bound at increasing flow rates (0.5–6 dyn/cm^2) was determined.

Assessment of cell migration

For video microscopy analyses, serum-starved Jurkat cells untreated or treated with the various stimuli, were added to 35-mm dishes coated with 1.2 μg/ml H89 fragment, H89+anti-CD3 mAb, or anti-CD3 alone. Images were acquired every 30 s over a period of 1 h using a Leica DM-IRE2 microscope equipped with a digital camera. Videos were compiled using the VideoMach software. Migrating cells were quantitated from the videos by five independent investigators.

Cell migration was also analyzed using 5 μm-pore Transwell filters (Costar Corp., Cambridge, MA) coated with 8 μg/ml VCAM-1, or VCAM-1+anti-CD3 mAb (or the same for H89). Cells (2×10^5) untreated or treated with the various stimuli were added to the upper chamber, and 100 ng/ml SDF-1α in 600 μl of medium was added to the lower chamber. Migrated cells were quantitated after 7 h at 37°C by flow cytometry.

Analysis of RhoA/Rac1 activity and Pyk2 phosphorylation

RhoA and Rac1 pull-down assays were performed exactly as described (Moyano et al., 2003). For analysis of Pyk2, untreated or treated 10×10^6 cells were added to six-well plates previously coated with 8 μg/ml H89, 0.1 μg/ml anti-CD3 mAb, or both. At different times attached cells were lysed in RIPA buffer and Pyk2 immunoprecipitated from the lysates. Phoshorylated Pyk2 was detected by Western blotting using PY20 mAb and HRP-labeled secondary Ab. Protein bands were visualized with ECL Supersignal West Femto (Pierce, Rockford, IL) and quantified on a densitometer (Molecular Dynamics, Sunnyvale, CA) using the Quantity-One™ program (Bio-Rad Laboratories, Hercules, CA).

Online supplementary material

The methodology for immunofluorescence assays, cell transfection, and statistical analyses, as well as seven videos documenting the migration of untreated Jurkat cells (video 1), treated with Mn^{2+} (video 2), SDF-1α (video 3), TS2/16 (video 4), PMA (video 5), H89+anti-CD3 mAb (video 6), or anti-CD3 mAb alone (video 7), are available on the Journal of Cellular Physiology website (http://www.interscience.wiley.com/jpages-0021-9541/suppmat).

RESULTS

Activation of α4β1 integrin by different stimuli results in distinct T-cell cytoskeleton organization

It is well established that activation of integrins, including α4β1, in T-cells increases adhesion to their ligands (reviewed by Pribila et al., 2004). In agreement with this, treatment of Jurkat cells with Mn^{2+}, TS2/16

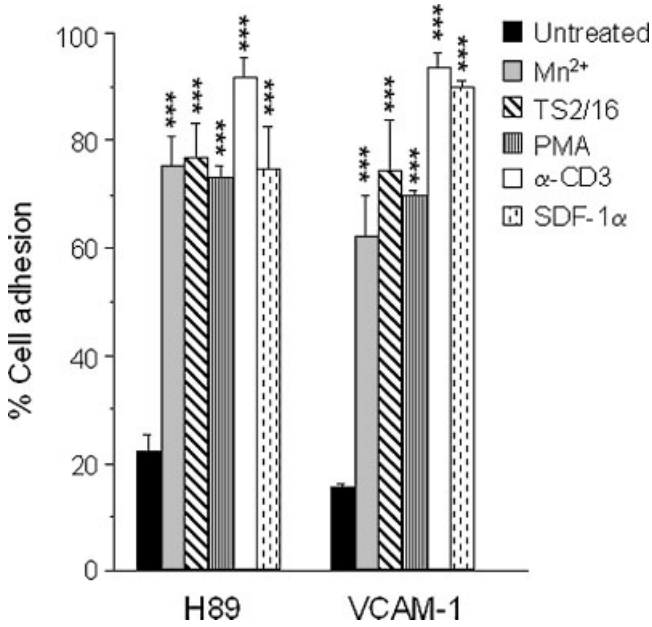

Fig. 1. Increased cell adhesion to the H89 Fn fragment and VCAM-1 by different activators of α4β1 integrin. Jurkat cells were untreated or treated for 30 min at 37°C with either 1 mM Mn^{2+}, 5 μg/ml TS2/16, 50 ng/ml PMA, 20 μg/ml anti-CD3 mAb, or for 1 min with 150 ng/ml SDF-1α. Cells (6×10^4/well) were added to wells previously coated with H89 (3 μg/ml) or VCAM-1 (2.3 μg/ml); after 45 min (2 min for SDF-1α treatment), attached cells were stained with 0.1% toluidine-blue and quantitated by determining the absorbance at 620 nm on a microplate reader. Values represent the average of three different experiments with duplicate determinations. Bars represent standard deviations. ***$P \leq 0.001$, compared to untreated cells.

mAb, PMA, SDF-1α, or CD3 crosslinking, clearly resulted in significant ($P \leq 0.001$) increased adhesion to the Fn fragment H89 and to VCAM-1 (Fig. 1). To determine the effect of these various stimuli on α4β1-mediated post-adhesion events, we first analyzed the pattern of actin organization following adhesion of Mn^{2+}- or TS2/16-treated Jurkat cells (outside-in activation) to H89 or VCAM-1 (8 and 5 μg/ml respectively). Treatment with Mn^{2+} induced an elongated morphology, where a cell body and a cytoplasmic projection were clearly visible in approximately 80% of cells (Fig. 2A). However, treatment with TS2/16 resulted in a very different pattern, with cells showing significant rounded spreading and formation of lamellipodia on both substrata (85% of cells, Fig. 2A). Identical results where obtained when other concentrations of H89 (range 0.6–15 μg/ml) or VCAM-1 (range 0.3–10 μg/ml) were used (data not shown), ruling out an effect of the substrate in the differential response. The effect of TS2/16 was due to its activation properties, since the control anti-β1 mAb Alex 1/4 did not induce spreading of Jurkat cells on either H89 or VCAM-1 (Fig. 2A). Cells attached to poly-D-lysine (p-Lys) remained unaffected by all these conditions, confirming the specificity of the α4β1-mediated response (Fig. 2A).

To further confirm that a cytoskeleton rearrangement was involved in the morphologies observed, we analyzed the microtubule organization upon cell treatment with Mn^{2+} or TS2/16 and attachment to the H89 fragment. As shown in Fig. 2B, the MTOC (microtubule organizing center) had a central position in 90% of untreated cells, in agreement with their round morphology (Rodríguez-Fernández et al., 1999; Vicente-Manzanares and Sánchez-Madrid, 2004). Upon activation of α4β1 with Mn^{2+}, the MTOC moved to the rear of the cell and located at the proximal region of the cytoplasmic projection (in 85% of cells, Fig. 2B), a characteristic feature of polarized cells (Rodríguez-Fernández et al., 1999; Vicente-Manzanares and Sánchez-Madrid, 2004). However, on TS2/16 treated cells, the MTOC remained at a central position in 90% of cells (Fig. 2B). Identical results were obtained for cells attached to VCAM-1 (data not shown). Moreover, cytochalasin D (Sigma) inhibited both the polarized and spread morphologies, thus establishing that the distinct patterns observed were dependent on actin reorganization.

To determine if primary T-cells also showed a distinct cytoskeletal response depending of the outside-in activation stimulus, we performed similar experiments using human T-lymphoblasts. As shown in Figure 2C, Mn^{2+} induced a polarized morphology on approximately 65% of T-cells attached to H89 (or VCAM-1, not shown), while TS2/16 induced enhanced spreading in 75% of cells. Therefore, the observed differential response was not restricted to a particular cell line, but was a general feature of T-lymphocytes.

Interestingly, inside-out activation of α4β1 also rendered different cytoskeleton rearrangement depending on the stimulus used. As shown in Figure 3A, treatment of T-lymphoblasts with PMA, followed by adhesion to the H89 fragment resulted in rounded spreading resembling that observed upon TS2/16 treatment, in approximately 75% of cells. However activation of α4β1 by co-immobilizing 0.1 μg/ml anti-CD3 mAb with H89 resulted in a polarized morphology as observed for Mn^{2+} activation (70% of cells, Fig. 3A). Similar results were obtained with Jurkat cells attached to H89 or VCAM-1. As shown in Figure 3B, Jurkat cells showed enhanced spreading upon PMA treatment (80% of cells) or polarization (68% of cells) after activation by co-immobilizing anti-CD3 mAb with H89 or VCAM-1. Identical results were obtained upon CD3 crosslinking in suspension, followed by adhesion to these substrata (data not shown). The observed cytoskeleton rearrangement was due to α4β1 integrin since cells plated on immobilized anti-CD3 mAb alone at 0.1 μg/ml, attached poorly and remained round (Fig. 3B). Co-immobilization of anti-CD3 mAb at this concentration with H89, increased Jurkat cell adhesion from 15% to 77% (data not shown), confirming that anti-CD3 mAb at 0.1 μg/ml was activating α4β1. Cells attached to a control anti-HLA mAb alone or in combination with H89 or VCAM-1 did not reorganize the cytoskeleton and remained as untreated cells (Fig. 3B). Since Jurkat cells and T-lymphoblasts showed similar differential responses to the various stimuli that activate α4β1, subsequent studies were performed using the Jurkat T-cell line.

To confirm that the two distinct morphological patterns observed did not represent different stages of the same process, we first increased the time of adhesion of cells treated with 1 mM Mn^{2+} or 0.1 μg/ml anti-CD3 mAb up to 3 h and this did not cause its progression to the TS2/16- or PMA-induced morphology (data not shown). Second, we studied the effect of different concentrations of the various stimuli. As shown in Figure 3C, Mn^{2+} or anti-CD3 mAb did not induce a spread pattern at any of the concentrations tested, but resulted in polarization in 55%, 65%, and 80% of cells for 0.2, 0.5, and 2 mM Mn^{2+} respectively; likewise, 75% of cells were polarized in response to 0.5, 1, or 2 μg/ml of anti-CD3 mAb. Moreover, lowering the concentration

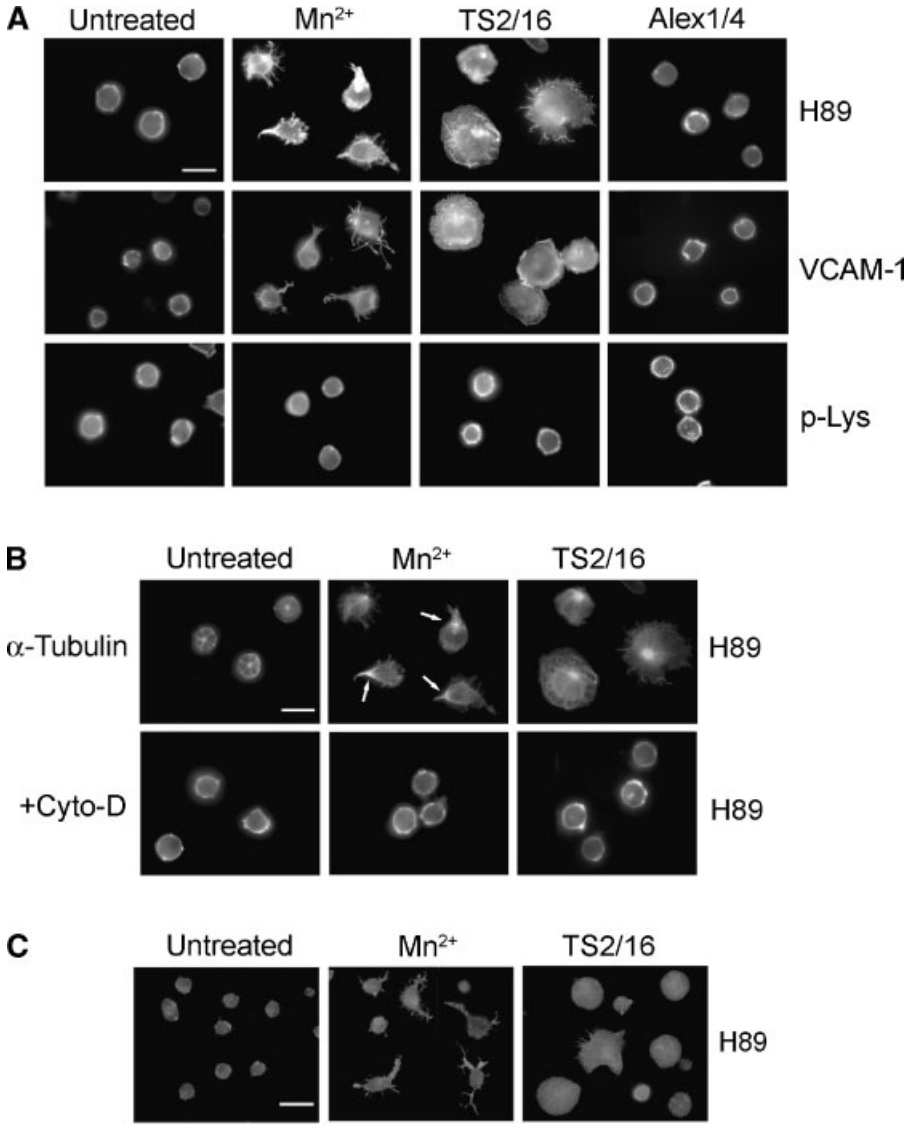

Fig. 2. Effect of different outside-in α4β1 integrin activators on T-cell cytoskeleton reorganization. **A**: 80×10^3 Jurkat cells were untreated or treated with 1 mM Mn^{2+}, 5 μg/ml TS2/16, or the control Ab Alex 1/4 (5 μg/ml), and added to glass coverslips previously coated with 8 μg/ml H89, 5 μg/ml VCAM-1 or 10 μg/ml pLys. F-actin was visualized after 1 h with TRITC-phalloidin. A representative experiment out of six performed is shown. **B**: Jurkat cells untreated or treated with Mn^{2+} or TS2/16 were added to glass coverslips coated with H89. After 1 h, microtubule organization was visualized with anti-α-tubulin mAb and FITC-labeled secondary Ab. In a separate experiment cells were incubated with 4 μg/ml cytochalasin D (Cyto-D) prior to Mn^{2+} or TS2/16 stimulation. Representative of three experiments. **C**: T-lymphoblasts (80×10^3) were untreated or treated with Mn^{2+} or TS2/16 and added to glass coverslips coated with H89 (8 μg/ml). After 1 h, actin was visualized as explained. Representative of three experiments. Bar, 10 μm.

of TS2/16 (0.1–2 μg/ml) or PMA (5–25 ng/ml) did not result in cell polarization and 70%–85% of cells remained spread in both conditions (Fig. 3C). Thus the differential cell response observed was specific for a particular agonist and did not depend on the strength of the stimulus.

α4β1 activation stimuli that induce T-cell polarization, but not those that promote cell spreading, also induce cell migration and lower resistance to detachment under flow

Because polarization is a characteristic of migrating lymphocytes, we first analyzed by video microscopy if Jurkat cells were differentially induced to migrate or adhere firmly depending of the α4β1 activation stimuli. Cells untreated or treated with Mn^{2+}, TS2/16, PMA, or SDF-1α were added to H89-coated dishes and monitored for 1 h. The concentration of H89 in these assays was adjusted to 1.2 μg/ml, since high concentrations of substrate prevented T-cell migration, as previously documented in several cell systems (Crisa et al., 1996; Shenoy et al., 2001). To monitor the CD3 effect, untreated cells were added to H89+anti-CD3 mAb, or anti-CD3-coated dishes respectively. Figure 4A displays four representative frames for each condition taken at different times during the assay. As observed in this figure, the kinetics of response to the different treatments was very similar and morphological changes were already evident after 15–20 min. Video 1 (see supplemental material) shows that untreated cells were highly motile and 23% of cells displayed random migration (Fig. 4B). All α4β1 activation treatments reduced cell migration compared to untreated cells ($P \leq 0.01$ or $P \leq 0.001$, Fig. 4B), but there were important differences with respect to the various stimuli. Upon activation of α4β1 with 0.2 mM Mn^{2+}, migration was clearly evident on 12% of cells (Fig. 4B) and active polarization on approximately 55% (video 2). SDF-1α treatment

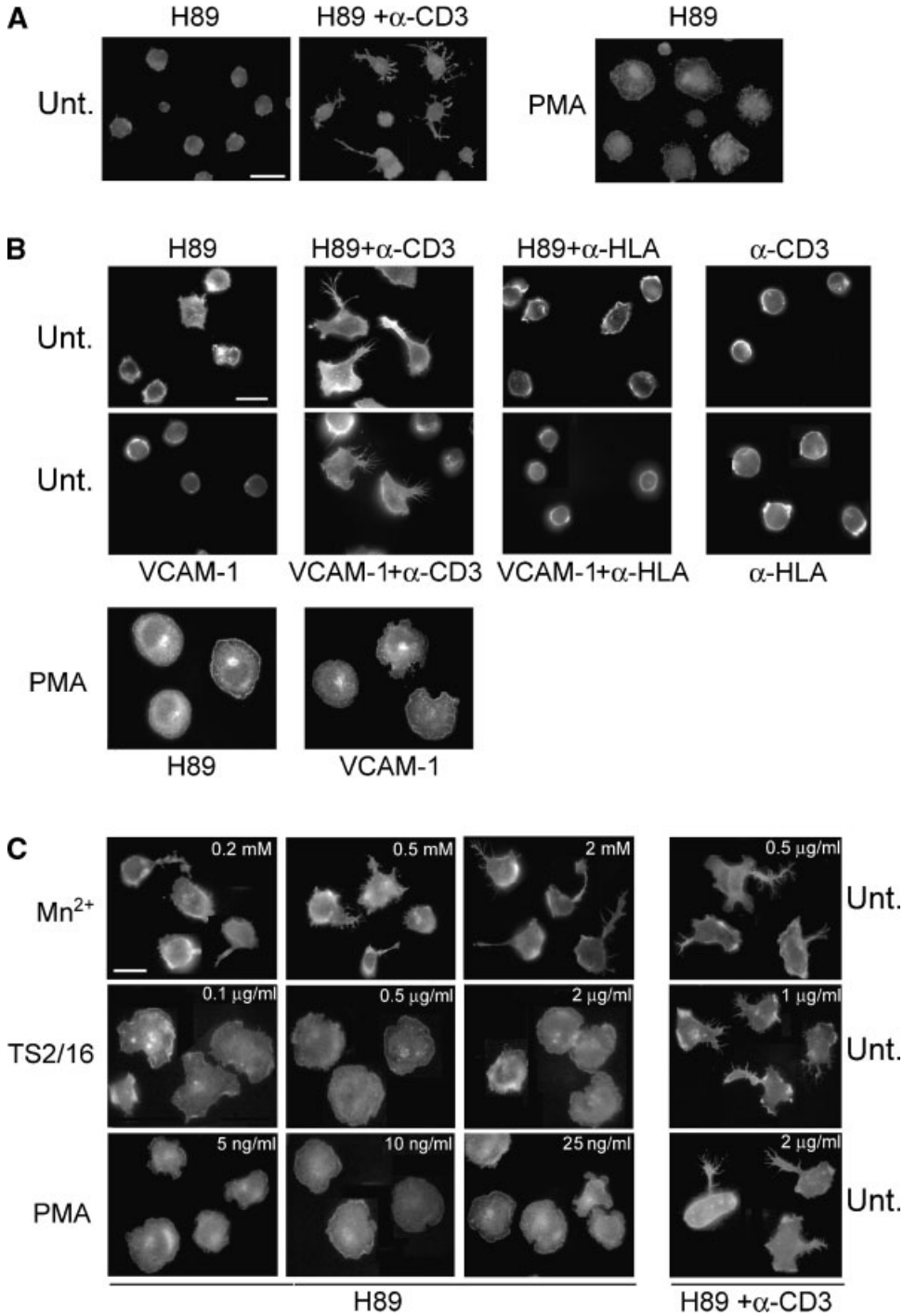

Fig. 3. Effect of different inside-out α4β1 integrin activators on T-cell cytoskeleton reorganization. **A**: T-lymphoblasts (80×10^3) were untreated or treated with PMA and added to glass coverslips coated with H89 (8 μg/ml). Untreated cells were also added to coverslips coated with a mixture of H89 + α-CD3 (8 μg/ml/0.1 μg/ml). F-actin was visualized as explained. Representative of three experiments. **B**: 80×10^3 Jurkat cells were untreated or treated with PMA and added to glass coverslips coated with H89 or VCAM-1. Untreated cells were also added to coverslips coated with mixtures of H89/α-CD3 or VCAM-1/α-CD3. Control mixtures were H89/α-HLA or VCAM-1/α-HLA. Immobilized α-CD3 or α-HLA mAbs alone were also used as controls. A representative experiment out of five performed is shown. **C**: Jurkat cells were treated with the indicated concentrations of the various stimuli, and added to glass coverslips coated with H89. Untreated cells were added to coverslips coated with H89 plus the indicated concentrations of α-CD3. F-actin was visualized as explained. Representative results from one out of three experiments performed. Bar, 10 μm.

also induced migration on 14% of cells (video 3 and Fig. 4B). Treatment with TS2/16 (video 4) abolished cell migration (Fig. 4B) and approximately 70% of cells displayed enhanced spreading and active lamella-type projections around the cell surface. PMA induced a mixed pattern, where approximately 75% of cells spread and formed active lamellipodia (video 5) and 6% were migrating cells (Fig. 4B). Approximately 60% of untreated cells added to mixed substrata of H89+anti-CD3 mAb or after CD3 crosslinking in suspension (data not shown), were polarized (video 6) and 11% were migrating cells (Fig. 4B). Cell elongation and migration

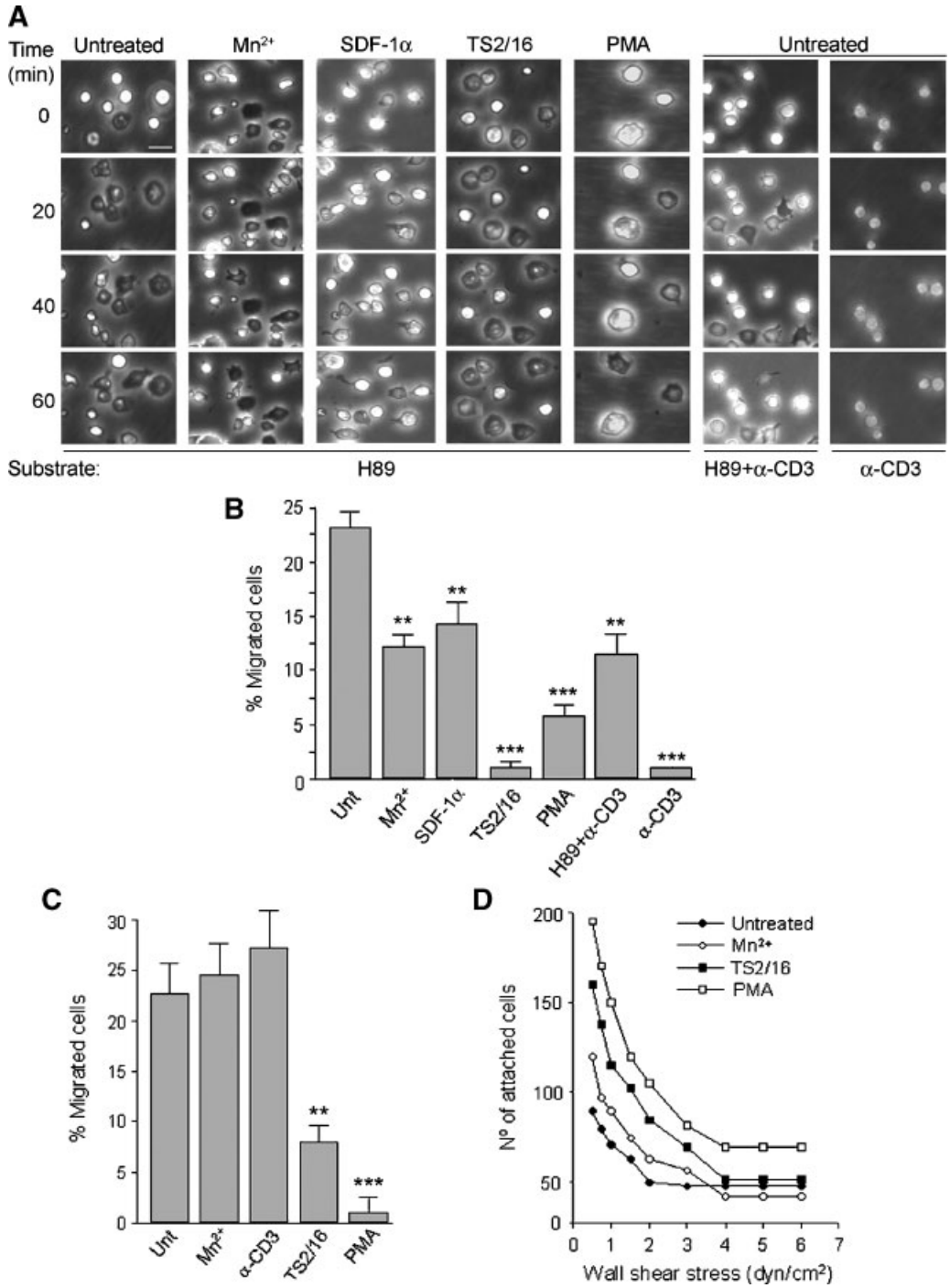

Fig. 4. Differential effect of the various α4β1 activation stimuli on T-cell migration and detachment under flow. **A**: Jurkat cells (5×10^5) were untreated or treated with Mn^{2+}, SDF-1α, TS2/16, or PMA, and added to coverslips coated with the indicated substrata. Coverslips were placed on a thermally controlled plate and photographed every 30 s for 1 h. Four representative times are shown for each condition. See online material for the corresponding videos. Bar, 10 μm. **B**: Migrating cells on H89 or anti-CD3 mAb (control) and under each of the stimulating conditions stated in A, were visually quantitated from the videos and are shown as the percentage of total cells in each video ± standard deviations. $^{**}P \leq 0.01$; $^{***}P \leq 0.001$, compared to untreated cells. **C**: Jurkat cells (2×10^5) untreated or stimulated were added to the upper chamber of 5 μm-pore Transwell filters previously coated with 8 μg/ml VCAM-1. Untreated cells were also added to filters coated with mixtures of VCAM-1/α-CD3 (8 μg/ml/0.1 μg/ml). SDF-1α (100 ng/ml) was added to the lower chamber. Migrated cells were quantitated after 7 h at 37°C by flow cytometry and are expressed as the percentage of total cellular input. Values represent the average of three independent experiments, and bars represent standard deviations. $^{**}P \leq 0.01$; $^{***}P \leq 0.001$, compared to untreated cells. **D**: Effect of the various stimuli that activate α4β1 on resistance to detachment under flow. Plastic dishes were spotted with 5 μg/ml H89 and placed on a flow chamber. Jurkat cells (1×10^6/ml) untreated or treated with 0.2 mM Mn^{2+}, 5 μg/ml TS2/16 or 50 ng/ml PMA, were perfused through the chamber at 1 dyn/cm^2 in serum-free medium. After 2 min, flow was stopped and cells allowed to attach for 10 min and quantitated. Flow was restored and increased every 60 s as indicated. Resistance to detachment was determined by counting the cells that remained bound after each interval. A representative experiment out of two performed is shown.

was mediated by α4β1 since cells added to anti-CD3 mAb alone, remained round and did not migrate (video 7 and Fig. 4B).

We also studied the migratory response using Transwell filters coated with 8 μg/ml VCAM-1 or VCAM-1+anti-CD3 Ab. As shown in Figure 4C, in the presence of low concentrations of Mn^{2+} (0.2 mM) or anti-CD3 (0.1 μg/ml), the percentage of migrated cells was similar or slightly higher than that of untreated cells. In contrast, TS2/16 (5 μg/ml) or PMA (10 ng/ml) significantly inhibited cell migration ($P = 0.002$ and $P = 0.0004$ respectively), in agreement with earlier reports (reviewed in Pribila et al., 2004). As observed, the effects of Mn^{2+} and anti-CD3 mAb were quantitatively different in Transwell assays (Fig. 4C) and when cells were monitored by video microscopy (Fig. 4B). This is probably due to the different measuring technique employed and not to the specific substrata (H89 vs. VCAM-1) used in Figures 4B and C, since identical results were obtained when Transwell filters were coated with 8 μg/ml H89 (data not shown). In spite of the quantitative difference, in both types of assays Mn^{2+} and anti-CD3 clearly induced cell migration, acting very differently than TS2/16 or PMA (Fig. 4B and C). Altogether these results established that activation of α4β1 leads to a migratory or stationary phenotype, depending on the specific stimulus.

We next studied whether the differential biological response to the various α4β1 activation stimuli was also observed under dynamic/physiological conditions. Jurkat cells, untreated or treated with Mn^{2+}, TS2/16, or PMA, were allowed to bind to H89 (5 μg/ml) for 10 min and their resistance to detachment under increasing shear flow was determined. Activation of α4β1 with either treatment increased this resistance with respect to untreated cells (Fig. 4C), in agreement with an increased cell adhesion strength. However, cells treated with Mn^{2+}, an agent that induces cell polarization and migration, showed lower resistance to detachment than cells treated with PMA or TS2/16, agents that induce cell spreading and firm adhesion (Fig. 4C). Identical results were obtained when the coating concentration of H89 was 1.2 μg/ml (data not shown). These results therefore establish that the differential response induced by the various agents that activate α4β1 integrin, is also observed under physiological conditions of flow.

Activation of RhoA and Rac1 interferes with the α4β1-induced T-cell polarization and migration, but does not affect induction of cell spreading

Cytoskeleton reorganization and migration are regulated by members of the RhoA family of small GTPases (Burridge and Wennerberg, 2004). To determine whether RhoA was involved in the signaling pathways induced by the different α4β1 activation stimuli, we first performed exogenous activation of RhoA with 1 μM LPA and subsequent cell adhesion to H89. As shown in Figure 5A for Mn^{2+} or TS2/16 activation, LPA had a dramatic effect on cells treated with Mn^{2+}, with almost complete (88% of cells) and significant ($P \leq 0.001$) disappearance of the elongated morphology (Fig. 5A,B). Incubation of cells with the RhoA inhibitor C3 (50 μg/ml) prior to LPA treatment, reverted the LPA effect resulting in partial recovery of cell elongations on 65% of Mn^{2+}-treated cells (Fig. 5A,B). In contrast, LPA or C3 did not affect the cytoskeletal pattern of TS2/16-treated or untreated cells (Fig. 5A,B). Identical results were obtained for anti-CD3 (loss of polarization) or PMA (no effect) treated cells (data not shown).

To further establish that an active RhoA selectively affected cell polarization, we transfected Jurkat cells with GFP-V14RhoA or GFP-N19RhoA and studied the cytoskeletal organization upon α4β1 activation and adhesion to the H89 fragment. Transfection with an empty vector coupled to GFP had no effect on either condition (Fig. 5C). The presence of constitutively active V14RhoA however, prevented cell elongation in Mn^{2+} treated cells (90% of transfected cells, Fig. 5C). V14RhoA did not affect the morphological pattern induced by TS2/16 (Fig. 5C), in agreement with the LPA results. Moreover, suppression of RhoA activity by transfection with N19RhoA resulted in a polarized morphology in response to Mn^{2+} treatment (65% of cells). As observed for LPA or V14RhoA transfectants, N19RhoA had no effect on TS2/16-treated cells (Fig. 5C).

We also transfected Jurkat cells with the constitutively active V12Rac1 or dominant negative N17Rac1, and studied the cytoskeletal response after activation of α4β1 with various stimuli. Figure 6 shows that transfection with V12Rac1 abolished cell polarization (induced by Mn^{2+}) on 70% of transfected cells, but did not affect the spreading induced by TS2/16. As observed for RhoA, suppression of Rac1 activity by transfection with N17Rac1 resulted in cell polarization upon Mn^{2+} treatment. N17Rac1 had no effect on the spread morphology induced by TS2/16 (Fig. 6).

Distinct regulation of RhoA and Rac1 by α4β1 activating agents that induce a polarized or spread morphology

To further establish the role of RhoA and Rac1 in the polarized or spread T-cell morphology, we performed affinity-binding assays using the C21-GST or PAK-GST fusion proteins which only bind active RhoA and Rac1 respectively (Ren et al., 1999; Sander et al., 1999). Lysates from serum starved Jurkat cells, untreated or treated with the model activators Mn^{2+} or TS2/16 and plated on H89-coated wells for different times, were analyzed for RhoA and Rac1 activity. Figure 7 shows that after treatment with either Mn^{2+} or TS2/16 the levels of active RhoA did not significantly vary with respect to untreated cells, except for the 5 min time of TS2/16 activation, where values were slightly lower. However, Rac1 activity was distinctly regulated upon Mn^{2+} or TS2/16 activation. Treatment with Mn^{2+} resulted in a very significant ($P \leq 0.01$) decrease in Rac1 activity during the initial 20 min of adhesion (Fig. 7A,B), after which Rac1 activity increased and remained high for the rest of the assay. TS2/16 however, induced a progressive increase in Rac1 activity, which was statistically significant ($P \leq 0.01$) after 60 min of adhesion (Fig. 7A,B).

Differential phosphorylation of Pyk2 by the various stimuli that activate α4β1 integrin

Pyk2 is phosphorylated upon engagement of α4β1 integrin by VCAM-1 or anti-α4 antibodies (van Seventer et al., 1998; Gismondi et al., 2003) and redistributes during integrin-triggered cell spreading and motility (Rodríguez-Fernández et al., 1999; Vicente-Manzanares and Sánchez-Madrid, 2004). To determine whether the different stimuli that activate α4β1 distinctly regulated Pyk2, we measured Pyk2 phosphorylation in lysates of Jurkat cells treated with the various agents and attached to H89 for different times. In untreated cells, adhesion to H89 resulted in very low levels of Pyk2 phosphorylation at all times studied (Fig. 8A,B). However, treatment with Mn^{2+}, anti-CD3 mAb or SDF-1α

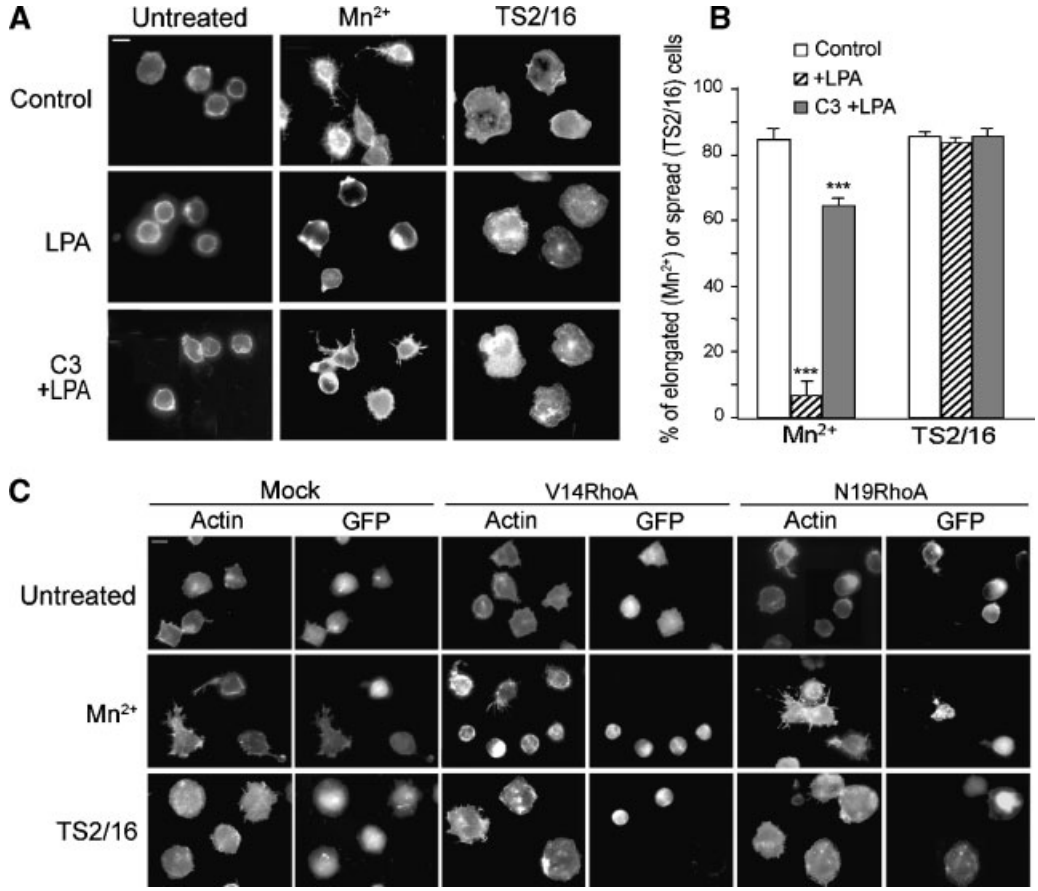

Fig. 5. Effect of RhoA activation on the Mn^{2+} and TS2/16-induced Jurkat cytoskeleton rearrangement. **A**: Jurkat cells with or without previous incubation with 50 μg/ml C3 were treated with Mn^{2+} or TS2/16, and then with 1 μM LPA for 60 min. Cells were added to H89-coated coverslips and after 60 min fixed and stained with TRITC-phalloidin. Control cells were activated with Mn^{2+} or TS2/16 but received no further treatment. Bar, 10 μm. **B**: Quantitation of the effect of LPA or C3+LPA on the morphological pattern induced by Mn^{2+} (polarization) or TS2/16 (spreading). Values are the mean of four different experiments and bars correspond to standard deviations. $^{***}P \leq 0.001$, compared to control cells. **C**: Jurkat cells were transiently transfected with empty vector (mock), GFP-V14RhoA, or GFP-N19RhoA, and untreated or treated with Mn^{2+} or TS2/16. Cells were added to H89-coated coverlips and after 1 h, fixed and stained with TRITC-phalloidin. Transfected cells were visualized by GFP fluorescence. A representative experiment out of three performed is shown. Bar, 10 μm.

followed by adhesion to H89, dramatically increased Pyk2 phosphorylation, with a maximum after 30–45 min (Fig. 8A,B). This increase was statistically significant ($P \leq 0.05$ or $P \leq 0.01$) for all three stimuli and for all times studied, with the exception of SDF-1α treatment after 60 min (Fig. 8B). Treatment of suspended cells with SDF-1α also induced Pyk2 phosphorylation for the initial 30 min of the assay ($P \leq 0.05$, Fig. 8A,B), in

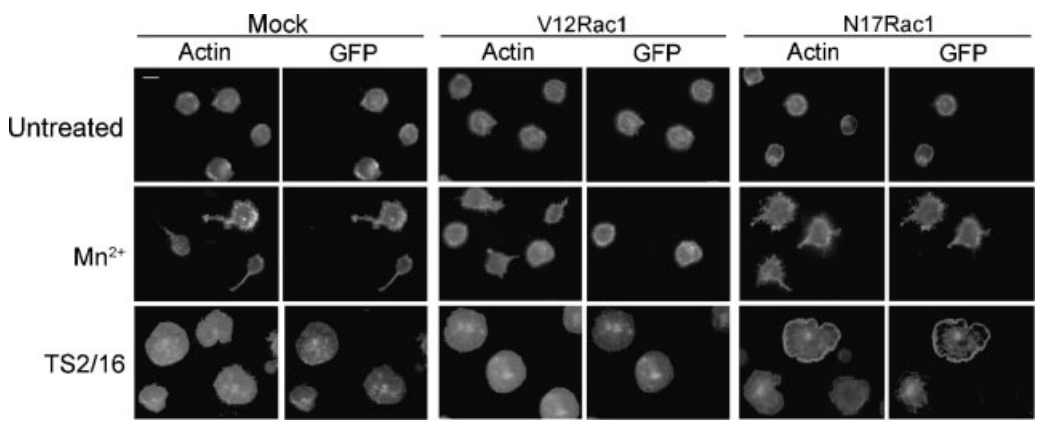

Fig. 6. Effect of Rac1 activation on the Mn^{2+} and TS2/16-induced Jurkat cytoskeleton rearrangement. Jurkat cells were transiently transfected with the empty vector (mock), GFP-V12Rac1, or GFP-N17Rac1, and untreated or treated with Mn^{2+} or TS2/16. Cells were added to H89-coated coverlips and after 1 h, fixed and stained with TRITC-phalloidin. Transfected cells were visualized by GFP fluorescence. Representative of two experiments. Bar, 10 μm.

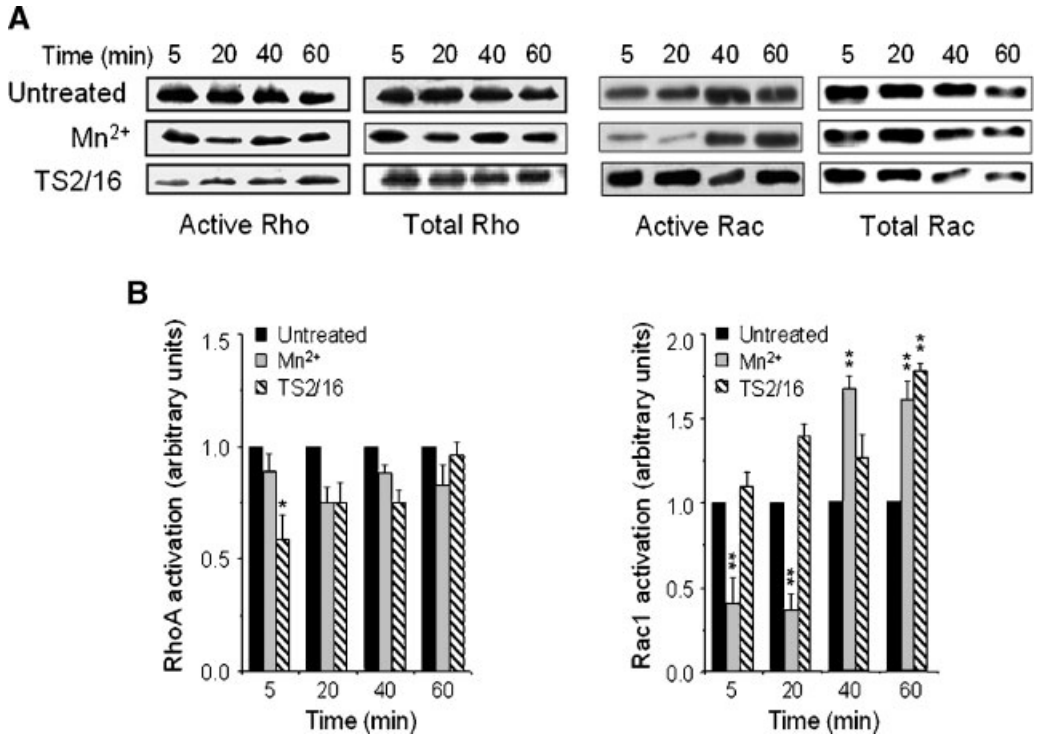

Fig. 7. Regulation of RhoA and Rac1 activity upon α4β1 integrin activation by Mn^{2+} or TS2/16. **A**: Serum-starved Jurkat cells untreated or treated with Mn^{2+} or TS2/16 were added to H89-coated wells (10×10^6 cells/condition) and lysed after the indicated times. Lysates were incubated with C21-GST or PAK-GST for RhoA and Rac1 respectively, and bound and total RhoA and Rac1 analyzed by Western blotting. A representative experiment out of three performed is shown. **B**: Quantitation of the relative levels of active RhoA and Rac1 for each time (average of three experiments). The levels of untreated cells were normalized to 1. Bars represent standard deviations. $^*P \leq 0.05$; $^{**}P \leq 0.01$, compared to untreated cells.

agreement with previous reports (Ganju et al., 1998); however, the maximal levels attained were approximately 50% lower than upon adhesion to H89 (Fig. 8A,B). Since H89 by itself is a poor inducer of Pyk2 phosphorylation in untreated cells (Fig. 8A,B) these results suggested that besides the reported synergistic effect of α4β1 and CD3 (van Seventer et al., 1998), activation of the integrin by CD3 crosslinking (or SDF-1α) also plays a role in the observed Pyk2 phosphorylation. Consistent with this, the anti-α4 mAb HP2/1 or pertussis toxin, an inhibitor of the SDF-1α receptor signaling, reduced Pyk2 phosphorylation to constitutive levels (Fig. 8C,D).

Interestingly, activation of α4β1 by TS2/16 did not induce Pyk-2 phosphorylation above the levels of untreated cells (Fig. 8A,B). Activation with PMA resulted in intermediate levels of Pyk2 phosphorylation, also maximal after 30 min (the only value statistically significant, $P \leq 0.05$) and approximately 50% lower than those produced by Mn^{2+} or the combination of adhesion to H89 and either SDF-1α or anti-CD3 (Fig. 8A,B). Altogether these results revealed a distinct regulation of Pyk2 by the different agents that activate α4β1, in correlation with induction of a migratory or stationary T-cell response.

DISCUSSION

Many previous reports have clearly established that α4β1 exists in multiple activation forms and that activation of α4β1 results in increased cell adhesion and affinity/avidity for its ligands (Masumoto and Hemler, 1993; Sánchez-Aparicio et al., 1993; Chen et al., 1999). Our present study shows for the first time that the subsequent cytoskeletal response is different depending of the stimulus used to activate α4β1. Induction of a polarized or spread morphology was independent of the internal or external nature of the stimulus and of the modulation of affinity versus clustering of the integrin (Hogg et al., 2003; Pribila et al., 2004). The specific effect must therefore be due to factors intrinsic to each stimulus. The polarized response obtained upon activation of α4β1 via CD3, differs from a previous report (Hyduk and Cybulsky, 2002) in which the effect of anti-CD3 mAbs prevailed over the effect of anti-α4 mAbs when both were co-immobilized. This discrepancy could be explained by the very low concentration of anti-CD3 mAb used in our study, which is sufficient to activate α4β1 but probably no other signaling. In support of this, activation of LFA-1 integrin required much lower concentration of anti-CD3 than induction of cell proliferation (Mueller et al., 2004). Since the levels of α4β1 stimuli and ligands also vary according to the particular physiological situation, we have tested different concentrations of Mn^{2+}, anti-CD3 mAb, H89 or VCAM-1 and show in the present study, that the polarized morphology resulted in cell migration and the spread morphology in strong adhesion, with higher resistance to detachment under flow. Our results establish that α4β1 may elicit either response in T-cells, depending of the specific activation signal received.

Importantly, we have found that the two functional responses elicited by activation of α4β1, required different intracellular signaling. This was the case for the small GTPases RhoA and Rac1, with a well-known function on cytoskeleton organization (Ridley, 2001; Burridge and Wennerberg, 2004). Crosslinking of α4β1 in suspension with antibodies or ligands was shown to

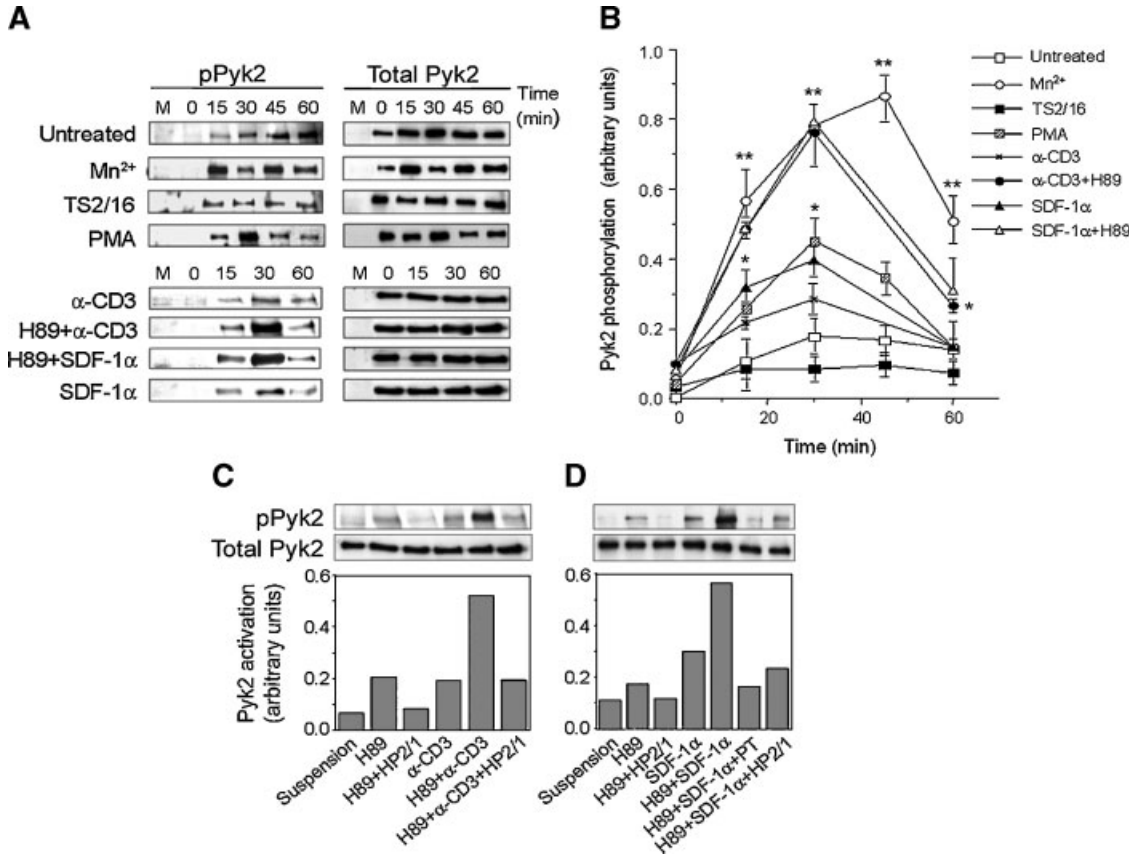

Fig. 8. Effect of α4β1 integrin activation by different pathways on Pyk2 phosphorylation. **A**: Jurkat cells (10×10^6/condition) untreated or treated with Mn^{2+}, TS2/16, PMA, or SDF-1α, were added to six-well plates previously coated with H89. Untreated cells were also added to wells coated with H89 + α-CD3 mAb. At the indicated times cells were lysed and Pyk-2 immunoprecipitated with specific Abs, and analyzed by SDS–PAGE and Western blotting. M indicates mock (no anti-Pyk2 Ab). **B**: The levels of phosphorylated Pyk2 (pPyk2) for each condition were determined by normalizing with respect to total protein. Values represent the average of four independent experiments, and bars represent standard deviations. $^*P \leq 0.05$; $^{**}P \leq 0.01$, compared to untreated cells. **C**: Cells with or without previous incubation with HP2/1 (anti-α4 subunit) were added to wells coated with the indicated substrata. After 30 min, Pyk2 phosphorylation was determined as explained. **D**: Cells with or without previous incubation with HP2/1 or pertussis toxin (PT, 10 ng/ml) were either untreated or treated with SDF-1α (150 ng/ml) and added to wells coated with H89 or BSA (SDF-1α lane). After 30 min, Pyk2 phosphorylation was analyzed. A representative experiment out of two performed for C and D, with identical results, is shown.

activate Rac1 in NK cells (Gismondi et al., 2003) and IL3-dependent cells (Kanda et al., 2003). Active Rac1 also regulated T-cell adhesion and spreading that was partly mediated by α4β1 integrin (D'Souza-Schorey et al., 1998). We now show for the first time that Rac1 is differentially regulated in T-cells, depending on whether activation of α4β1 results in cell migration or adhesion and spreading. Cell spreading was accompanied by a moderate Rac1 activation and was independent of the initial Rac1 activity, in agreement with the lack of effect of the constitutively active mutant V12Rac1. In contrast, induction of cell polarization and migration required initial low Rac1 activity, which may be necessary for cell elongation to occur and correlates with the results showing that V12Rac1 prevents cell polarization. This is also in agreement with our recent findings showing that V12Rac1 prevented the polarization induced by LFA-1 (Sánchez-Martín et al., 2004), and with another report in which cell polarization was triggered by α5β1 integrin ligation (Del Pozo et al., 1999). Our results suggest that once the polarization is established, Rac1 activity may increase without affecting the cytoskeletal response. The mechanism involved in the transient Rac1 inactivation is presently unknown.

Several other molecules are involved in the early events triggered by integrin engagement. We have studied the regulation of the tyrosine kinase Pyk2, which is very abundant in Jurkat cells and is involved in cell motility, cytoskeleton rearrangement and downstream signaling (Avraham et al., 2000). We have found a clearly distinct Pyk2 phosphorylation depending on the stimulus used to activate α4β1. Moreover, our results show a good correlation between induction of a polarized phenotype and high levels of Pyk2 phosphorylation, suggesting that phosphorylation of Pyk2 may be essential for α4β1-mediated T-cell polarization and migration. These data are in contrast with the modest Pyk2 activation observed during α4β1-mediated cell spreading. To our knowledge, this is the first evidence of a differential Pyk2 phosphorylation in response to α4β1 activation.

In summary, the present report reveals novel properties of α4β1 integrin, namely the ability to trigger two types of T-cell cytoskeletal response involving different intracellular signaling. Our in vitro studies likely represent the physiological situation in which specific stimuli such as chemokines, will activate α4β1 and induce lymphocyte migration, which is essential in homeostasis, during extravasation into tissues, and in inflammatory responses. This pathway of α4β1 activation, involves low RhoA activity and high levels of Pyk2 phosphorylation, as well as a bimodal regulation of Rac1. Once within tissues, lymphocytes may receive

other signals, such as PKC activation, which also activate α4β1 but induce strengthening of adhesion and cell spreading independently of RhoA, initial Rac1 activity or Pyk2. Lymphocytes also migrate within tissues and this may be driven by activation of the T-cell receptor, which in turn activates α4β1. In this situation, α4β1 may also contribute to the antigen-driven response which provides a stop or go signal for T-cells (Dustin, 2004). Initiation of one or another biochemical pathway by α4β1 will therefore be determined by the specific stimuli present at a given location. Our findings represent a novel level of regulation of the T-cell post-adhesion physiological response mediated by α4β1 integrin.

ACKNOWLEDGMENTS

We thank all mentioned investigators for gifts of constructs and antibodies; Dr. Pedro Lastres for help with the flow cytometry analyses; and Mercedes Hernández del Cerro for excellent technical assistance.

LITERATURE CITED

Arroyo AG, Garcia-Pardo A, Sánchez-Madrid F. 1993. A high affinity conformational state on VLA integrin heterodimers induced by an anti-beta 1 chain monoclonal antibody. J Biol Chem 268:9863–9868.

Avraham H, Park SY, Schinkmann K, Avraham S. 2000. RAFTK/Pyk2-mediated cellular signalling. Cell Signal 12:123–133.

Burridge K, Wennerberg K. 2004. Rho and Rac take center stage. Cell 116:167–179.

Chan JR, Cybulsky ML. 2004. Detection of high-affinity α4 integrin upon leukocyte stimulation by chemoattractants or chemokines. Meth Mol Biol 239:261–268.

Chen LL, Whitty A, Lobb RR, Adams SP, Pepinsky RB. 1999. Multiple activation states of integrin α4β1 detected through their different affinities for a small molecule ligand. J Biol Chem 274:13167–13175.

Crisa L, Cirulli V, Ellisman MH, Ishii JK, Elices MJ, Salomon DR. 1996. Cell adhesion and migration are regulated at distinct stages of thymic T cell development: The roles of fibronectin, VLA-4 and VLA-5. J Exp Med 184:215–228.

D'Souza-Schorey C, Boettner B, van Aelst L. 1998. Rac regulates integrin-mediated spreading and increased adhesion of T lymphocytes. Mol Cell Biol 18:3936–3946.

Del Pozo MA, Vicente-Manzanares M, Tejedor R, Serrador JM, Sánchez-Madrid F. 1999. Rho GTPases control migration and polarization of adhesion molecules and cytoskeletal ERM components in T lymphocytes. Eur J Immunol 29:3609–3620.

Dillon ST, Feig LA. 1995. Purification and assay of recombinant C3 transferase. Meth Enzymol 256:174–184.

Dustin ML. 2004. Stop and go traffic to tune T cell responses. Immunity 21:305–314.

Faull RJ, Kovach NL, Harlan JM, Ginsberg MH. 1994. Stimulation of integrin-mediated adhesion of T lymphocytes and monocytes: Two mechanisms with divergent biological consequences. J Exp Med 179:1307–1316.

Ganju RK, Brubaker SA, Meyer J, Dutt P, Yang Y, Qin S, Newman W, Groopman JE. 1998. The α-chemokine, stromal cell-derived factor-1α, binds to the transmembrane G-protein-coupled CXCR-4 receptor and activates multiple signal transduction pathways. J Biol Chem 273:23169–23175.

Gismondi A, Jacobelli J, Strippoli R, Mainiero F, Soriani A, Cifaldi L, Piccoli M, Frati L, Santoni A. 2003. Proline-rich tyrosine kinase 2 and Rac activation by chemokine and integrin receptors controls NK cell transendothelial migration. J Immunol 170:3065–3073.

Hogg N, Laschinger M, Giles K, McDowall A. 2003. T-cell integrins: More than just sticking points. J Cell Sci 116:4695–4705.

Hyduk SJ, Cybulsky MI. 2002. α4 integrin signaling activates phosphatidylinositol 3-kinase and stimulates T cell adhesion to intercellular adhesion molecule-1 to a similar extent as CD3, but induces a distinct rearrangement of the actin cytoskeleton. J Immunol 168:696–704.

Kanda E, Jin Z-H, Mizuchi D, Arai A, Miura O. 2003. Activation of Rac and tyrosine phosphorylation of cytokine receptors induced by cross-linking of integrin α4β1 and cell adhesion in hematopoietic cells. Biochem Biophys Res Comm 301:934–940.

Kinashi T. 2005. Intracellular signaling controlling integrin activation in lymphocytes. Nature Rev Immunol 5:546–559.

Kovach NL, Carlos TM, Yee E, Harlan JM. 1992. A monoclonal antibody to beta 1 integrin (CD29) stimulates VLA-dependent adherence of leukocytes to human umbilical vein endothelial cells and matrix components. J Cell Biol 116:499–509.

Liddington RC, Ginsberg MH. 2002. Integrin activation takes shape. J Cell Biol 158:833–839.

Masumoto A, Hemler ME. 1993. Multiple activation states of VLA-4. Mechanistic differences between adhesion to CS1/fibronectin and to vascular cell adhesion molecule-1. J Biol Chem 268:228–234.

Mittelbrunn M, Molina A, Escribese MM, Yañez-Mo M, Escudero E, Ursa A, Tejedor R, Mampaso F, Sánchez-Madrid F. 2004. VLA-4 integrin concentrates at the peripheral supramolecular activation complex of the immune synapse and drives T helper 1 responses. Proc Natl Acad Sci USA 101:11058–11063.

Mould AP, Humphries MJ. 2004. Regulation of integrin function through conformational complexity: Not simply a knee-jerk reaction? Curr Op Cell Biol 16:544–551.

Mould AP, Askari JA, Craig SE, Garrat AN, Clements J, Humphries MJ. 1994. Integrin α4β1-mediated melanoma cell adhesion and migration on vascular cell adhesion molecule-1 (VCAM-1) and the alternatively spliced IIICS region of fibronectin. J Biol Chem 269:27224–27230.

Moyano JV, Carnemolla B, Domínguez-Jiménez C, García-Gila M, Albar JP, Sánchez-Aparicio P, Leprini A, Querzé G, Zardi L, Garcia-Pardo A. 1997. Fibronectin type III5 repeat contains a novel cell adhesion sequence, KLDAPT, which binds activated α4β1 and α4β7 integrins. J Biol Chem 272:24832–24836.

Moyano JV, Maqueda A, Casanova B, Garcia-Pardo A. 2003. α4β1 integrin/ligand interaction inhibits α5β1-induced stress fibers and focal adhesions via down-regulation of RhoA and induces melanoma cell migration. Mol Biol Cell 14:3699–3715.

Mueller KL, Daniels MA, Felthauser A, Kao C, Jameson SC, Shimizu Y. 2004. LFA-1 integrin-dependent T cell adhesion is regulated by both Ag specificity and sensitivity. J Immunol 173:2222–2226.

Pribila JT, Quale AC, Mueller KL, Shimizu Y. 2004. Integrins and T cell-mediated immunity. Ann Rev Immunol 22:157–180.

Ren X-D, Kiosses WB, Schwartz MA. 1999. Regulation of the small GTP-binding protein Rho by cell adhesion and the cytoskeleton. EMBO J 18:578–585.

Ridley A. 2001. Rho family proteins: Coordinating cell responses. Trends Cell Biol 11:471–477.

Rodríguez-Fernández JL, Gómez M, Luque A, Hogg N, Sánchez-Madrid F, Cabañas C. 1999. The interaction of activated integrin lymphocyte function-assocated antigen 1 with ligand intercellular adhesion molecule 1 induces activation and redistribution of focal adhesion kinase and proline-rich tyrosine kinase 2 in T lymphocytes. Mol Biol Cell 10:1891–1907.

Rose DM, Han J, Ginsberg MH. 2002. α4 integrins and the immune response. Immunol Rev 186:118–124.

Sánchez-Aparicio P, Ferreira OC, Garcia-Pardo A. 1993. α4β1 recognition of the Hep II domain of fibronectin is constitutive on some hemopoietic cells but requires activation on others. J Immunol 150:3506–3514.

Sánchez-Aparicio P, Domínguez-Jiménez C, Garcia-Pardo A. 1994. Activation of the α4β1 integrin through the β1 subunit induces recognition of the RGDS sequence in fibronectin. J Cell Biol 126:271–279.

Sánchez-Martín L, Sánchez-Sánchez N, Gutiérrez-López MD, Rojo AI, Vicente-Manzanares M, Pérez-Alvarez MJ, Sánchez-Mateos P, Bustelo XR, Cuadrado A, Sánchez-Madrid F, Rodríguez-Fernández JL, Cabañas C. 2004. Signaling through the leukocyte integrin LFA-1 in T cells induces a transient activation of Rac1 that is regulated by Vav and PI3K/Akt-1. J Biol Chem 279:16194–16205.

Sander EE, ten Klooster JP, van Delft S, van der Kammen RA, Collard JG. 1999. Rac downregulates Rho activity: Reciprocal balance between both GTPases determines cellular morphology and migratory behavior. J Cell Biol 147:1009–1022.

Sanz-Rodríguez F, Hidalgo A, Teixidó J. 2001. Chemokine stromal cell-derived factor-1α modulates VLA-4 integrin-mediated multiple myeloma cell adhesion to CS-1/fibronectin and VCAM-1. Blood 15:346–351.

Shenoy PS, Uniyal S, Miura K, McColl C, Oravecz T, Morris VL, Chan BM. 2001. Beta1 integrin-extracellular matrix protein interaction modulates the migratory response to chemokine stimulation. Biochem Cell Biol 79:399–407.

Takagi J, Springer TA. 2002. Integrin activation and structural rearrangement. Immunol Rev 186:141–163.

Travis MA, Humphries JD, Humphries MJ. 2003. An unraveling tale of how integrins are activated from within. Trends Pharmacol Sci 24:192–197.

van de Wiel-van Kemenade E, van Kooyk Y, de Boer AJ, Huijbens RJ, Weder P, van de Kasteele W, Melief CJ, Figdor CG. 1992. Adhesion of T and B lymphocytes to extracellular matrix and endothelial cells can be regulated through the beta subunit of VLA. J Cell Biol 117:461–470.

van Seventer GA, Mullen MM, van Seventer JM. 1998. Pyk2 is differentially regulated by β1 integrin- and CD28-mediated co-stimulation in human $CD4^+$ T lymphocytes. Eur J Immunol 28:3867–3877.

Vicente-Manzanares M, Sánchez-Madrid F. 2004. Role of the cytoskeleton during leukocyte responses. Nat Rev Immunol 4:110–122.

Wittchen ES, van Buul JD, Burridge K, Worthylake RA. 2005. Trading spaces: Rap, Rac, and Rho as architects of transendothelial migration. Curr Op Hematol 12:14–21.

Anexo II

Two novel functions for fibronectin heparin III binding domain (types III4-5 repeats): self-association and involvement in fibronectin fibrillogenesis

Alfredo Maqueda[a], José V. Moyano[a]*, Mercedes Hernández del Cerro[a], Donna M. Peters[b], and Angeles Garcia-Pardo[a#]

[a]Departamento de Fisiopatología Celular y Molecular, Centro de Investigaciones Biológicas, CSIC, Ramiro de Maeztu 9, 28040 Madrid, Spain, and [b]Department of Pathology and Laboratory Medicine, University of Wisconsin Medical School, 1300 University Avenue/6590 MSC, Madison, Wisconsin 53706

Key words: Fibronectin heparin III-binding domain, matrix assembly, fibronectin self-association, FNIII4-5 fragment, HBP/III5 site

*Present address: Dept. of Medicine – Endocrinology, Northwestern University, Chicago, IL, USA

#Corresponding author: Departamento de Fisiopatología Celular y Molecular, Centro de Investigaciones Biológicas, CSIC, Ramiro de Maeztu 9, 28040 Madrid, Spain. Phone: 34-91-537 3112, ext. 4430; Fax: 34-91-536 0432; E-Mail: agarciapardo@cib.csic.es

Abstract

Fibronectin matrix assembly involves interactions among various regions of the molecule, which contribute to elongation and stabilization of the fibrils. In this study, we show that the heparin III domain of fibronectin (repeats III4-5) participates in fibronectin

fibrillogenesis. The recombinant fragment FNIII4-5 blocked fibronectin fibril formation and ^{125}I-fibronectin incorporation into cell layers, as effectively as the 70 kDa fragment, a well known competitor in these assays. Binding assays using a biosensor revealed that FNIII4-5 bound fibronectin and the amino-terminal 70 kDa and 29 kDa fragments. It also bound to itself, indicating a previously unidentified self-association site in repeats III4-5. These interactions were specific since FNIII4-5 did not bind to the FNIII7-10 fragment, representing a central region in fibronectin. The fibronectin-binding property of the III4-5 domain, but not its matrix assembly inhibitory function, was apparently cryptic in larger fragments. By mutating the arginine residues in the WTPPRAQITGYRLTVGLTRR proteoglycan-binding sequence (HBP/III5 site) of FNIII4-5 (Moyano et al., J. Biol. Chem. 274: 135, 1999), we found that the first two arginine residues in HBP/III5 were involved in the fibronectin-binding property of FNIII4-5, while the last two arginine residues in HBP/III5 were required for inhibition of matrix assembly and ^{125}I-fibronectin binding to cell layers. These results established that fibronectin III4-5 repeats constitute a novel region involved in fibronectin self-association and fibrillogenesis. Both properties appear to function independently from each other, depending on the conformation of the fibronectin dimer.

1. Introduction

The extracellular matrix (ECM) is essential for cell adhesion, migration, differentiation and growth (Hynes, 1990; Adams and Watt, 1993; Boudreau and Jones, 1999). A major component of the ECM are fibronectin (Fn) fibrils. The assembly of Fn into fibrils is a multi-step process that involves the disruption of intramolecular Fn-Fn interactions and the subsequent unfolding of Fn to reveal cryptic Fn-Fn binding sites involved in fibrillogenesis (Hynes, 1990; Mosher, 1993; Mao and Schwarzbauer, 2005). The unfolding of Fn is initiated by interactions with cell surface molecules such as $\alpha 5\beta 1$ integrin and LAMMs (McDonald et al., 1987; Fogerty et al., 1990; Zhang and Mosher, 1996).

Several Fn domains that participate in fibrillogenesis have been identified. The most critical domain is the amino-terminal repeats I1-5, which are essential for Fn fibrillogenesis since recombinant Fn lacking this region does not assemble into fibrils (Schwarzbauer, 1991). Moreover, 29 kDa and 70 kDa fragments containing this amino-terminal region, block Fn fibrillogenesis (McDonald et al., 1987; McKeown-Longo and Mosher, 1985). Other regions of Fn involved in fibrillogenesis include the III1, III2, III9-10, and III12-14 repeats (Mao and Schwarzbauer, 2005; McKeown-Longo and Mosher, 1985; Aguirre et al., 1994; Hocking et al., 1994; Bultmann et al., 1998; Sechler et al., 2001). The III9-10 domain is an integrin-binding site involved in the initial cell surface steps of fibrillogenesis (McDonald et al., 1987; Fogerty et al., 1990). The III1, III2, and III12-14 repeats all bind to the I1-5 domain and the addition of fragments containing these regions inhibit Fn fibril formation (McKeown-Longo and Mosher, 1985; Aguirre et al., 1994; Hocking et al., 1994; Bultmann et al., 1998). The Fn binding site located in III1 is cryptic (Hocking et al., 1994) while the activity of III12-14 repeats appears to be determined by the adjacent alternatively spliced IIICS region (Santas et al., 2002). The role of these various domains is still unknown. They are believed to modulate Fn-Fn interactions during the elongation and stabilization of Fn fibrils. Fn fibrillogenesis therefore involves multiple, apparently redundant, interactions, which may provide alternative mechanisms to regulate the formation and/or activity of fibronectin fibrils.

It is interesting that most Fn regions that participate in fibrillogenesis bind heparin and proteoglycans (Hynes, 1990). The III12-14 region is the heparin II (Hep II) binding domain and the I1-5 repeats constitute the Hep I binding domain (Hynes, 1990). The III1 repeat also binds heparin and proteoglycans (Mercurius and Morla, 2001; Gui et al., 2006) and appears to be part of the central, low affinity Hep III domain, which also comprises the III4-6 repeats (Hynes, 1990). Using recombinant fragments encompassing the III4-5 and III4-6 repeats, we previously identified the WTPPRAQITGYRLTVGLTRR sequence in the III5 repeat (HBP/III5 site), which

binds proteoglycans and mediates cell adhesion (Moyano et al., 1999). This sequence is highly homologous to WQPPRARITGY (FN-C/H V site) found in the Hep II domain, which also mediates cell adhesion by binding to proteoglycans (Mooradian et al., 1993). The HBP/III5 sequence, like the FN-C/H V site (Woods et al., 1993), also enhances the formation of stress fibers and focal adhesions induced via α5β1 integrin (Moyano et al., 2003a). Since the Hep III and Hep II domains appear to be functionally similar, we hypothesized that the Hep III domain may also participate in Fn fibrillogenesis. Using the recombinant fragments FNIII4-5 and FNIII4-6 in matrix assembly and protein binding assays, we show that the HBP/III5 site in repeat III5 constitutes a previously unidentified region in Fn that is involved in fibrillogenesis.

2. Results

2.1. The FNIII4-5 fragment, containing the heparin III domain of fibronectin, inhibits the assembly of fibronectin into matrix

To determine whether the Hep III region could participate in Fn fibrillogenesis, we examined the assembly of Fn fibrils in the presence or absence of the FNIII4-5 fragment that contains the Hep III domain (Fig. 1). In agreement with our previous reports (Bultmann et al., 1998; Santas et al., 2002), cycloheximide-treated fibroblasts formed numerous Fn fibrils upon incubation overnight with plasma Fn (Fig. 2Aa). As expected, the 70 kDa amino-terminal fragment blocked fibril formation (Fig. 2Ab). The FNIII4-5 fragment also inhibited Fn fibril formation as efficiently as the 70 kDa fragment (Fig. 2Ac), suggesting a role for the Hep III domain in this process. In contrast, the 80 kDa fragment (see Fig. 1) did not affect Fn matrix assembly (Fig. 2Ad), thus confirming the specificity of the inhibitory effect of the FNIII4-5 fragment.

We also studied whether the FNIII4-5 fragment blocked the assembly of endogenous Fn. To this end, fibroblasts were incubated overnight without cycloheximide and in the presence or absence of the FNIII4-5 or 70 kDa fragments. As

shown in Fig. 2B, cells assembled their own endogenous Fn quite efficiently (Fig. 2Ba) and this was inhibited by incubation with the 70 kDa (Fig. 2Bb) or FNIII4-5 (Fig. 2Bc) fragments. Again, the 80 kDa fragment had no effect (not shown). These results indicated that the Hep III domain is involved in the assembly of both endogenous as well as exogenously added Fn.

2.2. The FNIII4-5 fragment interacts with itself and with amino-terminal-derived Fn fragments

There are two possible ways for the FNIII4-5 fragment to inhibit Fn fibrillogenesis. First, it could prevent Fn-Fn interactions used to polymerize fibrils. Second, it could block the cell surface interactions with the 70 kDa region of Fn critical for fibrillogenesis. To explore the possibility that the FNIII4-5 fragment inhibited Fn matrix assembly by directly interacting with Fn regions involved in fibrillogenesis, we used a biosensor to measure the binding of soluble FNIII4-5 to immobilized Fn or the 70 kDa fragment on sensor chips. As shown in Figure 3A & B, the FNIII4-5 domain bound to Fn and the 70 kDa fragment in a dose-dependent manner. At the same molar concentration, soluble FNIII4-5 bound equally well to immobilized Fn and immobilized 70 kDa fragment (2594 and 3128 arc sec respectively). In contrast, the 80 kDa fragment (see Fig. 1) did not bind to Fn or the 70 kDa fragment in these assays (Fig. 3A & B).

To compare this Fn-binding property of the FNIII4-5 fragment (Hep III domain) with the previously described interactions between the Hep II domain and the amino-terminal region of Fn, we tested the binding of the FNIII12-14 fragment (see Fig. 1) in this system. In agreement with our previous results (Bultmann et al., 1998), FNIII12-14 bound to immobilized Fn or 70 kDa fragment (Fig. 3A & B) and the binding response was similar (2295 arc sec for Fn and 2550 arc sec for 70 kDa) to that attained by FNIII4-5, at the same molar concentration. The binding affinity of FNIII12-14 for Fn (K_D=1.4 μM) and 70 kDa (K_D=0.42 μM) was also in the same range as that of FNIII4-5 (K_D=0.8 μM and 0.31 μM for Fn and 70 kDa, respectively). Therefore, the interaction of

the Hep III and Hep II domains with Fn or the Fn amino-terminal region appears to be similar.

We next tested the ability of soluble 70 kDa fragment to bind to immobilized FNIII4-5, to determine if the binding observed was merely an artifact caused by the denaturation of the absorbed 70 kDa fragment. Surprisingly, the soluble 70 kDa fragment did not bind to immobilized FNIII4-5 at any of the concentrations tested (up to 8 μM, data not shown). However, a soluble, smaller, 29 kDa fragment contained within the 70 kDa fragment, did bind to immobilized FNIII4-5 in a dose–dependent manner (Fig. 3C). This suggested that the interaction between the amino terminus of Fn and FNIII4-5 was valid, although sensitive to the conformation of the amino terminus. This result also showed that the binding site in the 70 kDa fragment was contained within the region of Fn previously identified to be critical for fibrillogenesis (Schwarzbauer, 1991). The immobilized FNIII4-5 also bound soluble FNIII4-5 in a dose-dependent manner (Fig. 3C), indicating the presence of a self-association site in this region, as previously suggested (Carnemolla et al., 1996). As in the case of immobilized Fn and the 70 kDa fragment, the soluble 80 kDa fragment did not bind to immobilized FNIII4-5 (Fig. 3C).

To further confirm the specificity of the above interactions, we immobilized a fragment corresponding to the central region of Fn (FNIII7-10, see Fig. 1) and tested the binding of soluble FNIII4-5 or 29 kDa fragments. As shown in Fig. 3D, neither of these fragments bound to FNIII7-10 at any concentration tested. The soluble FNIII12-14 fragment also failed to bind to immobilized FNIII7-10 (data not shown). The presence of the FNIII7-10 fragment on the biosensor chip was confirmed using a polyclonal anti-Fn antibody which bound to FNIII7-10 in a dose-dependent manner, while a control, irrelevant, polyclonal antibody did not bind (Fig. 3D).

2.3. Further characterization of Fn-binding sites in FNIII4-5

The preceding results with the 80 kDa fragment suggested that the Fn-binding sites in the III4-5 region were masked in this larger fragment. To demonstrate this, we

compared the binding of FNIII4-5 and the larger FNIII4-6 fragment (see Fig. 1) to immobilized Fn, the 70 kDa fragment, or the FNIII4-5 fragment. As shown in Figure 4A, at the same molar concentration and at saturation, binding of the FNIII4-6 fragment to immobilized Fn was 10-fold lower than binding of the FNIII4-5 fragment (301 *vs* 2988 arc sec, respectively). Soluble FNIII4-6 bound slightly better to immobilized 70 kDa or FNIII4-5 fragments, but again the response was 5-fold and 3-fold lower, respectively compared to FNIII4-5 at the same molar concentration (Fig. 4B & C).

Binding studies using smaller recombinant fragments comprising either repeat III4 or III5, revealed that the Fn-binding sites in FNIII4-5 required the presence of both repeats. The FNIII4 repeat did not bind to immobilized Fn, 70 kDa or FNIII4-5 fragments at any concentration tested (Fig. 4) and the binding of the FNIII5 fragment to these substrata was 11.5, 12.5 and 5.4-fold lower respectively, than the corresponding binding of FNIII4-5, at the same molar concentration (Fig. 4 A-C). None of these fragments bound to immobilized FNIII7-10 (data not shown). These results, therefore, indicated that the Fn-binding sites in FNIII4-5 are cryptic in larger fragments and require the integrity of the III4-5 region.

To determine the sequences involved in the interaction of FNIII4-5 with itself and with the amino-terminus of Fn, we performed binding studies using two FNIII4-5 fragments containing mutations in the HBP/III5 proteoglycan binding site (Fig. 1). Substitution of the first two arginine residues in the HBPIII5 sequence by alanine residues (FNIII4-5R1R2 mutant) completely blocked binding of FNIII4-5 to Fn, 70 kDa or FNIII4-5 fragments (Fig. 5A-C). In contrast, mutating the last two arginine residues of HBP/III5 (FNIII4-5R3R4 mutant) did not prevent binding of FNIII4-5 to these substrata (Fig. 5A-C). These results indicated that the first two arginine residues in HBP/III5 were involved in the interaction of FNIII4-5 with itself, Fn, or the 70 kDa fragment.

2.4. Sites involved in the Fn matrix assembly inhibitory activity of FNIII4-5

We next studied whether the matrix assembly-inhibitory activity of FNIII4-5 had the same or different requirements as the Fn-binding property of this fragment. To this end,

we performed matrix assembly assays in the presence or absence of FNIII4-6 or FNIII4-5. Figure 6C & D shows that both FNIII4-6 and FNIII4-5 fragments were efficient inhibitors of Fn fibrillogenesis, suggesting that the residues involved in fibrillogenesis were not cryptic in FNIII4-6, as were the residues involved in Fn-Fn interactions. We next tested the effect of mutating the arginine residues in the HBP/III5 sequence on the matrix assembly activity of FNIII4-5. Figure 6E & F shows that the FNIII4-5R1R2 mutant inhibited Fn fibril formation as efficiently as the parental FNIII4-5 region (Fig. 6E), indicating that the first two arginine residues in HBP/III5 were not important for the matrix inhibitory effect of FNIII4-5. However, mutations affecting the R3R4 residues (FNIII4-5R3R4 mutant) completely abolished the inhibitory activity of FNIII4-5 (Fig. 6F), and matrix assembly was similar to the control (Fig. 6A).

We next measured the effect of FNIII4-5 and FNIII4-5 mutants on fibrillogenesis using the established matrix assembly assay with ^{125}I-labeled Fn and confluent cell layers of fibroblasts. As shown in Figure 7A, the FNIII4-5 fragment inhibited binding of ^{125}I-Fn to cell layers in a dose-dependent manner ($IC_{50} < 10^{-7}$ M). As expected, the 70 kDa fragment also inhibited binding of ^{125}I-Fn in these assays ($IC_{50} < 10^{-8}$ M), and the 80 kDa fragment had no inhibitory effect. We then tested the ability of the other fragments to inhibit the binding of Fn to the cell surface. As shown in Figure 7B, the FNIII4-5R1R2 mutant was as good inhibitor as the 70 kDa fragment and also blocked binding of ^{125}I-Fn ($IC_{50} < 10^{-7}$), indicating that the arginines at these positions are not involved in inhibiting fibrillogenesis. In contrast, the FNIII4-5R3R4 mutant did not compete for the binding of ^{125}I-Fn to cell layers (Fig. 7B), in agreement with the results shown in Figure 6. Not surprisingly, the FNIII4-6, which bound poorly to Fn (Fig. 4A), was a poor inhibitor of ^{125}I-Fn binding to the cell surface and only partially blocked (45% inhibition) ^{125}I-Fn binding.

Since FNIII4-5 also bound to the 29 kDa amino-terminal region of Fn (Fig 3C), we reasoned that FNIII4-5 might block fibrillogenesis (Fig. 6D) because it could interfere with the cell surface interactions with the 29 kDa domain of Fn (McKeown-

Longo and Mosher, 1985). To test this, we measured the effect of the FNIII4-5, FNIII4-6 and FNIII4-5 mutants on the interaction of the ^{125}I-29 kDa fragment with cell layers. As shown in Fig 7C, all the fragments with the exception of the FNIII4-5R3R4 mutant blocked binding of the ^{125}I-29 kDa fragment (IC_{50} =10^{-5}). Altogether these results suggest that the R3R4 arginine residues of FNIII4-5 are required for the ability of this fragment to block Fn fibrillogenesis and that the R1R2 arginines are involved in FNIII4-5 self-association or binding to the amino-terminal region of Fn.

3. Discussion

In this study, we have established that the Hep III domain (III4-5 repeats) is a novel region in Fn that participates in Fn self-association and assembly of Fn fibrils. We have identified two distinct sequences that mediate these properties. The sequence involved in self-association promotes binding between the III4-5 repeats as well as binding to the amino-terminal I1-5 repeats of Fn, and requires the arginine residues R994 and R1001 (called R1R2 in this report). The sites involved in Fn fibrillogenesis are the arginine residues R1008 and R1009 (R3R4 in this report). Both sequences are located in the Fn III5 repeat. Thus, there appears to be two distinct sites and functions within the III4-5 domain.

The activity of these two sites appears to be regulated by the conformation of the Fn dimer. Thus, the Fn binding property of FNIII4-5 was absent in the larger 80 kDa or FNIII4-6 fragments suggesting that the R1R2 residues are totally or partially buried in Fn or large Fn fragments. This property was also absent or highly reduced in the individual III4 or III5 repeats, suggesting that the spatial arrangement of the arginine residues in the III4-5 region is important. These results suggest that the Fn-binding property of the III4-5 domain does not play a role in the cell surface interactions involved in the initiation of Fn fibrils, since these interactions are believed to precede the conformational changes needed to expose the Fn-Fn binding sites used for fibrillogenesis. Such changes apparently take place during initiation of Fn

fibrillogenesis, upon binding of Fn to the cell surface (Baneyx et al., 2002). Thus, the Fn III4-5 domain appears to behave in a similar manner as the previously reported Fn binding regions, including the III1 and III12-14 repeats, whose activity is also cryptic (Wierzbicka-Patynowski and Schwarzbauer, 2003; Mao and Schwarzbauer, 2005). Once exposed, the R1R2 residues may provide additional binding sites to already formed Fn fibrils, and contribute to their elongation and/or stabilization.

In contrast to the R1R2 sites involved in Fn-binding, the matrix assembly activity of the R3R4 residues was present in both the FNIII4-5 and FNII4-6 fragments. The crystal structure of the Fn III4-5 region has not been solved. However, it can be approached from the known structure of the Fn III12-14 repeats (Sharma et al., 1999), since all type III repeats in Fn follow a similar β-strand arrangement. Accordingly, the R1 residue found in the PRAQI sequence of repeat III5 would be located in a relatively tight inter-repeat interface and thus would be expected to be cryptic. While the R3R4 residues found in the GLTRR sequence of this repeat would be exposed on the other side of the molecule (Sharma et al., 1999).

The R3R4 residues may regulate signaling events which control the assembly of Fn fibrils (Fig. 8). In support of this, we have previously shown that the GLTRR sequence is active in the context of large Fn fragments and regulates stress fiber formation and the activation of RhoA in melanoma cells (Moyano et al., 2003a, 2003b). The contractile forces generated by activated RhoA and actin stress fibers play a critical role in regulating Fn fibrillogenesis (Zhang et al., 1994; Zhong et al., 1998). These forces are believed to exert tension onto the compact Fn dimer, thereby exposing cryptic Fn-Fn binding sites (such as the R1R2 residues in repeats III4-5) that are eventually used to cross-link Fn dimers into fibrils (Wierzbicka-Patynowski and Schwarzbauer, 2003).

The cell surface molecules interacting with the R3R4 residues in the Fn III4-5 domain are presently unknown. However, since the III4-5 domain is a heparin-binding region, a reasonable candidate is syndecan or another proteoglycan. Members of the

syndecan family bind to the Hep II domain in Fn, which also regulates fibril formation and interacts with the amino-terminus of Fn (Bultmann et al., 1998, and this report). In addition, mutation of syndecan-2 prevented fibril formation in CHO cells (Klass et al., 2000). Moreover, the heparin-binding domain of vitronectin has been shown to block Fn matrix assembly and this apparently involved heparan-sulfate proteoglycans at the cell surface and intracellular signaling (Hocking et al., 1999). Likewise, heparin-binding domains were recently shown to play an important role in the assembly of laminin-5 onto a matrix (Tsubota et al., 2005).

As already shown for many cell types that make Fn fibrils, activation of the contractile mechanisms requires cooperative signaling events between integrins and cell surface proteoglycans (Couchman and Woods, 1999; Woods, 2001). Interactions with both these cell surface receptors would be necessary to either activate RhoA and/or provide the contractile forces that expose Fn-Fn binding sites (Zhong et al., 1998). It is this later process that probably accounts for how the FNIII4-5 fragment is able to prevent fibrillogenesis. This step requires that Fn be bound to at least two cell surface molecules so that the Fn dimer can be unfolded to expose Fn-Fn binding sites. If the the FNIII4-5 fragment was bound to one of these two cell surface molecules, even if RhoA is activated, fibril formation would be blocked because Fn would only be tethered to one cell surface site, thereby disabling the contractile forces from unfolding the compact dimer (see proposed model in Fig. 8).

A role for the Fn III4-5 domain in Fn fibrillogenesis is supported by a previous report showing that a recombinant Fn lacking repeats III1-7 assembled much slower into fibrils than native Fn, and this was preceded by formation of insoluble aggregates at the cell surface (Sechler et al., 1996). Although the large size of the deletion present on this mutant makes it difficult to draw definitive conclusions, these results suggested a regulatory role for this region in matrix assembly. It is not clear why another study found that a recombinant Fn lacking the III4-5 repeats, assembled normally into a matrix (Sechler et al., 2001). One possible explanation is that the regulatory function

exerted by the Fn III4-5 domain, is compensated by other regions in Fn (Mao and Schwarzbauer, 2005). For example, it could be compensated by the Hep II domain, which we previously showed to be involved in Fn fibrillogenesis (Bultmann et al., 1998) and as we show here, binds as efficiently as FNIII4-5 to Fn or the 70 kDa fragment. Thus, the various regions of Fn, known to participate in Fn-Fn interactions, appear to represent alternative but redundant mechanisms of Fn matrix formation. These multiple I1-5 binding sites in Fn may have an important biological role in fibrillogenesis progression and stabilization of the growing fibrils, because they would provide alternative sites of interactions that could be necessary to promote fibril thickening and branching. We believe that the apparent redundancy of interactions between several Fn domains is not surprising. Fn is a crucial molecule in the organism and Fn matrices control many important cellular functions. Equally important is the fact that the Fn matrix is not formed by well-ordered and length-controlled fibrils as it is the case of collagen matrices for example. The Fn fibrils grow in all directions and the fibrils vary in length, thickness, etc. In this context, it would make sense that multiple self-association sites exist, and that these sites may only be available depending on the Fn conformation or the sites already occupied.

In spite of an extensive literature and the early identification of some of the modules involved on Fn fibrillogenesis, the mechanisms that control this process are still largely unknown. It has been suggested that formation of highly stable protein-protein interactions (Chen and Mosher, 1996) or/and disulfide bond formation due to the inherent disulfide isomerase activity of Fn (Langenbach and Sottile, 1999), may contribute to Fn polymerization and matrix assembly. As in the case of the previously identified modules involved in fibrillogenesis, the exact mechanism by which the Fn III4-5 region contributes to matrix assembly is presently unknown. Nevertheless, our present report establishes that the two novel properties of the III4-5 domain (Fn binding and regulation of fibrillogenesis), may function at different times and independently from each other. While the R3R4 residues may regulate signaling pathways at the early

steps of fibrillogenesis, the R1R2 residues, which require previous unfolding of the Fn molecule, would contribute to fibril propagation and stabilization by providing additional or alternative Fn-binding sites.

In summary, our present findings are the first to show that Fn III4-5 repeats are involved in Fn-Fn interactions and Fn matrix assembly, therefore contributing to the regulation of the many biological processes (migration, gene expression, proliferation, etc) which are dependent on cellular interactions with Fn matrices. Furthermore, these studies further support that cooperative cell surface signaling events are needed for the regulation of Fn matrices.

4. Experimental procedures

4.1. Proteolytic and recombinant fragments of fibronectin

Figure 1 illustrates all the Fn fragments used in this study. The proteolytic 29 kDa (I1-I5 repeats) and 80 kDa (III4-III11 repeats) fragments were obtained by tryptic digestions of human plasma Fn, as previously described (García-Pardo et al., 1983, 1989). The 70 kDa (I1-I9 + II1-II2 repeats) proteolytic fragment was prepared by cathepsin D digestion of Fn as reported (Peters and Mosher, 1987). The recombinant fragments FNIII4-6, FNIII4-5, FNIII4, FNIII5, FNIII4-5R1R2, FNIII4-5R3R4, FNIII7-10 and FNIII12-14 were prepared as described (Moyano et al., 1999, 2003a, Bultmann et al., 1998).

4.2. Binding assays

Binding interactions between Fn and fragments or between different Fn fragments were analysed using an IAsysPlus optical biosensor (Labsystems Affinity Sensors, Cambridge, UK). Fn, 70 kDa, FNIII4-5, or FNIII7-10 fragments in 10 mM Tris, 50 mM NaCl, pH 7.5, were immobilized on carboxymethyl dextran (CMD) dual-well cuvettes following instructions from the manufacturer. Increasing amounts of soluble fragments, in the same Tris/NaCl buffer, were added stepwise to the cuvette containing the immobilized substrata, and the response (arc sec) monitored until saturation was

reached. Samples and cuvettes were maintained at 22^{0}C and each measurement was repeated at least three times.

4.3. Immunofluorescence microscopy

These assays were performed as previously described (Bultmann et al., 1998; Santas et al., 2002). Briefly, human fibroblasts were plated at confluence onto glass coverslips previously coated with 10 μg/ml Fn. Cells were allowed to attach for 1 h in DMEM with 7.5% FBS, before replacing the medium with serum-free media. After 3 h, this medium was replaced by serum-free medium containing 4 μg/ml Fn and 25 μg/ml cycloheximide, and cells were incubated overnight at 37^{0}C in the presence or absence of 200 μg/ml of the various fragments. For inhibition of endogeneous Fn matrix assembly, Fn and cycloheximide were not added to the medium. Cell layers were washed with PBS, fixed with 4% paraformaldehyde, and incubated with polyclonal anti-Fn antibodies (A. García-Pardo, unpublished), followed by rhodamine-conjugated goat antibodies to rabbit IgG. Fn fibrils were visualized on a epifluorescence axioplan microscope (Zeiss, Oberkochen, Germany). At least six different random fields for each condition were photographed with a CCD camera (Photometrics Inc., Tucson, AZ). Final images were composed based on blinded evaluations by three different investigators.

4.4. Fibronectin matrix assembly assay

Matrix assembly assays were performed as described (Bultmann et al., 1998; Santas et al., 2002). Briefly, human foreskin fibroblasts (3 x 10^4 cells/well) were grown for 24 or 48 h in 96-well plates. Cell layers were washed and then incubated for 3 h at 37^{0}C with ^{125}I-Fn or ^{125}I-29 kDa fragment in serum-free medium, in the presence or absence of the various cold competitors. The cultures were washed and wells were broken apart and counted in a γ-counter.

Acknowledgements

We thank Drs. Germán Rivas and Carlos Alfonso (Centro de Investigaciones Biológicas, Madrid) for expert advice and help with the binding experiments. This work was supported by Grants SAF2003-00824, from the Ministerio de Educación y Ciencia; PI060400, from the Instituto de Salud Carlos III, Madrid, Spain; and by a grant from the Fundación de Investigación Médica Mutua Madrileña (Madrid, Spain) (to A. García-Pardo), as well as by National Institutes of Health grant EY012515 (to D.M. Peters). A. Maqueda was supported by an I3P predoctoral fellowship from CSIC/European Union Social Fund; J.V. Moyano was supported by a fellowship from GlaxoSmithKline.

References

Adams, J.C., Watt, F.M., 1993. Regulation of development and differentiation by the extracellular matrix. Development 117, 1183-1198.

Aguirre, K.M., McCormick, R.J., Schwarzbauer, J.E., 1994. Fibronectin self-association is mediated by complementary sites within the amino-terminal one-third of the molecule. J. Biol. Chem. 269, 27863-27868.

Baneyx, J., Baugh, L., Vogel, V., 2002. Fibronectin extension and unfolding within cell matrix fibrils controlled by cytoskeletal tension. Proc. Natl. Acad. Sci. USA. 99, 5139-5143.

Boudreau, N.J., Jones, P.J., 1999. Extracellular matrix and integrin signalling: the shape of things to come. Biochem. J. 339, 481-488.

Bultmann, H., Santas, A.J., Peters, D.M.P., 1998. Fibronectin fibrillogenesis involves the heparin II binding domain of fibronectin. J. Biol. Chem. 273, 2601-2609.

Carnemolla, B., Leprini, A., Querze, G., Urbini, S., and Zardi, L., 1996. Novel self-association fibronectin sites. Biochem. Cell Biol. 74, 745-748.

Chen H., Mosher, D.F., 1996. Formation of sodium dodecyl sulfate-stable fibronectin multimers. Failure to detect products of thiol-disulfide exchange in cyanogen

bromide or limited acid digests of stabilized matrix fibronectin. J. Biol. Chem. 271, 9084-9089.

Couchman, J.R., Woods, A., 1999. Syndecan-4 and integrins: combinatorial signaling in cell adhesion. J. Cell Sci. 112, 3415-3420.

Fogerty, F.J., Akiyama, S.K., Yamada, K.M., Mosher, D.F., 1990. Inhibition of binding of fibronectin to matrix assembly sites by anti-integrin (alpha 5 beta 1) antibodies. J. Cell Biol. 111, 699-708.

Garcia-Pardo, A., Pearlstein, E., Frangione, B., 1983. Primary structure of human plasma fibronectin. The 29,000-dalton NH2-terminal domain. J. Biol. Chem. 258, 12670-12674.

Garcia-Pardo, A., Ferreira, O.C., Valinsky, J.E., Bianco, C., 1989. Fibronectin receptors of mononuclear phagocytes: binding characteristics and biochemical isolation. Exp. Cell Res. 181, 420-431.

Gui, L., Wojciechowski, K., Gildner, C.D., Nedelkovska, H., Hocking, D.C., 2006. Identification of the heparin-binding determinants within fibronectin repeat III_1. J. Biol. Chem. 281, 34816-34825.

Hocking, D.C., Sottile, J., McKeown-Longo, P.J., 1994. Fibronectin's III-1 module contains a conformation-dependent binding site for the amino-terminal region of fibronectin. J. Biol. Chem. 269, 19183-19187.

Hocking, D.C., Sottile, J., Reho, T., Fässler, R., McKeown-Longo, P.J., 1999. Inhibition of fibronectin matrix assembly by the heparin-binding domain of vitronectin. J. Biol. Chem. 274, 27257-27264.

Hynes, R.O., 1990. Fibronectins. Springer-Verlag Inc., New York.

Klass, C.M., Couchman, J.R., Woods, A., 2000. Control of extracellular matrix assembly by syndecan-2 proteoglycan. J. Cell Science 113, 493-506.

Langenbach, K.J., Sottile, J., 1999. Identification of protein-disulfide isomerase activity in fibronectin. J. Biol. Chem. 274, 7032-7038.

Mao, Y., Schwarzbauer, J.E., 2005. Fibronectin fibrillogenesis, a cell-mediated matrix assembly process. Matrix Biol. 24, 389-399.

McDonald, J.A., Quade, B.J., Broekelmann, T.J., LaChance, R., Forsman, K., Hasegawa, E., Akiyama, S., 1987. Fibronectin's cell-adhesive domain and an amino-terminal matrix assembly domain participate in its assembly into fibroblast pericellular matrix. J. Biol. Chem. 262, 2957-2967.

McKeown-Longo, P.J., Mosher, D.F., 1985. Interaction of the 70,000-mol-wt amino-terminal fragment of fibronectin with the matrix-assembly receptor of fibroblasts. J. Cell Biol. 100, 364-374.

Mercurius, K.O., Morla, A.O., 2001. Cell adhesion and signaling on the fibronectin 1st type III repeat; requisite roles for cell surface proteoglycans and integrins. BMC Cell Biol. 2, 18.

Mooradian, D.L., McCarthy, J.B. Skubitz, A.P.N., Cameron, J.D., Furcht, L.T. 1993. Characterization of FN-C/H-V, a novel synthetic peptide from fibronectin that promotes rabbit corneal epithelial cell adhesion, spreading, and motility. Invest. Opthalmol. & Visual Sci. 34, 153-164.

Mosher, D.F., 1993. Assembly of fibronectin into extracellular matrix. Curr. Op. Struct. Biol. 3, 214-222.

Moyano, J.V., Carnemolla, B., Albar, J.P., Leprini, A., Gaggero, B., Zardi, L., Garcia-Pardo, A., 1999. Cooperative role for activated $\alpha 4\beta 1$ integrin and chondroitin sulfate proteoglycans in cell adhesion to the heparin III domain of fibronectin. Identification of a novel heparin and cell binding sequence in repeat III5. J. Biol. Chem. 274, 135-142.

Moyano, J.V., Maqueda, A., Albar, J.P., Garcia-Pardo, A., 2003a. A synthetic peptide from the heparin-binding domain III (repeats III4-5) of fibronectin promotes stress-fibre and focal-adhesion formation in melanoma cells. Biochem. J. 371, 565-571.

Moyano, J.V., Maqueda, A., Casanova, B., Garcia-Pardo, A., 2003b. $\alpha 4\beta 1$ integrin/ligand interaction inhibits $\alpha 5\beta 1$-induced stress fibers and focal adhesions

via down-regulation of RhoA and induces melanoma cell migration. Mol. Biol. Cell. 14, 3699-3715.

Peters, D.M., Mosher, D.F., 1987. Localization of cell surface sites involved in fibronectin fibrillogenesis. J. Cell Biol. 104, 121-130.

Santas, A.J., Peterson, J.A., Halbleib, J.L., Craig, S.E., Humphries, M.J., Peters, D.M.P., 2002. Alternative splicing of the IIICS domain in fibronectin governs the role of the heparin II domain in fibrillogenesis and cell spreading. J. Biol. Chem. 277, 13650-13658.

Schwarzbauer, J.E., 1991. Identification of the fibronectin sequences required for assembly of a fibrillar matrix. J. Cell Biol. 113, 1463-1473.

Sechler, J.L., Takada, Y., and Schwarzbauer, J.E., 1996. Altered rate of fibronectin matrix assembly by deletion of the first type III repeats. J. Cell Biol. 134, 573-583.

Sechler, J.L., Rao, H., Cumiskey, A.M., Vega-Colón, I., Smith, M.S., Murata, T., Schwarzbauer, J.E., 2001. A novel fibronectin binding site required for fibronectin fibril growth during matrix assembly. J. Cell Biol. 154, 1081-1088.

Sharma, A., Askari, J.A., Humphries, M.J., Ivonne-Jones, E., Stuart, D.I., 1999. Crystal structure of a heparin- and integrin-binding segment of human fibronectin. EMBO J. 18, 1468-1479.

Tsubota, Y., Yasuda, C., Kariya, Y., Ogawa, T., Hirosaki, T., Mizushima, H., Miyazaki, K., 2005. Regulation of biological activity and matrix assembly of laminin-5 by COOH-terminal, LG4-5 domain of α3 chain. J. Biol. Chem. 280: 14370-14377.

Wierzbicka-Patynowski, I., Schwarzbauer, J.E., 2003. The ins and outs of fibronectin matrix assembly. J. Cell Science 116, 3269-3276.

Woods, A., McCarthy, J.B., Furcht, L.T., Couchman, J.R., 1993. A synthetic peptide from the COOH-terminal heparin-binding domain of fibronectin promotes focal adhesion formation. Mol. Biol. Cell. 4, 605-613.

Woods, A., 2001. Syndecans: transmembrane modulators of adhesion and matrix assembly. J Clin Invest.107, 935-941.

Zhang, Q., Checovich, W.J., Peters, D.M., Albrecht, R.M., Mosher, D.F., 1994. Modulation of cell surface fibronectin assembly sites by lysophosphatidic acid. J. Cell Biol. 127, 1447-1459.

Zhang, Q., Mosher, D.F., 1996. Cross-linking of the NH2-terminal region of fibronectin to molecules of large apparent molecular mass. Characterization of fibronectin assembly sites induced by the treatment of fibroblasts with lysophosphatidic acid. J. Biol. Chem. 271, 33284-33292.

Zhong, C., Chrzanowska-Wodnicka, M., Brown, J., Shaub, A., Belkin, A.M., Burridge, K., 1998. Rho-mediated contractility exposes a cryptic site in fibronectin and induces fibronectin matrix assembly. J. Cell Biol. 141, 539-551.

Figure legends

Figure 1. Schematic drawing of a monomer of plasma Fn and the Fn fragments used in this study. The three types of homology repeats are shown with the type III repeats numbered. The position of the heparin binding domains (Hep I, Hep II and Hep III) is indicated. The proteolytic fragments used are indicated below, with their corresponding molecular mass. Recombinant fragments containing the Hep III domain (FNIII4-6, FNIII4-5, FNIII4, FNIII5), the central cell-binding domain (FNIII7-10), and the Hep II domain (FNIII12-14), as well as the various mutations performed in the FNIII4-5 fragment are also shown. The specific mutated residues are indicated in bold type.

Figure 2. Inhibition of fibronectin fibrillogenesis by 70 kDa or FNIII4-5 fragments. A) Cycloheximide-treated fibroblasts plated on Fn were incubated overnight with 4 μg/ml (9×10^{-9} M) plasma Fn alone (a), or in combination with 200 μg/ml of 70 kDa (2.8×10^{-6} M) (b), FNIII4-5 (7.1×10^{-6} M) (c), or 80 kDa (2.5×10^{-6} M) (d) fragments. B) Fibroblasts plated on Fn were incubated overnight without cycloheximide or soluble plasma Fn, in the absence (a) or presence of 70 kDa (b) or FNIII4-5 (c) fragments. A phase image of the cell layer is shown in (d). Cell cultures were fixed and incubated with a rabbit polyclonal anti-fibronectin Ab, followed by rhodamine-conjugated goat Abs to rabbit IgG. As a negative control, cell cultures were incubated in parallel with secondary Abs alone. In these instances, no immunofluorescence was detected (data not shown). Images show the results from a representative experiment out of five performed. Bar, 50 μm.

Figure 3. Binding of soluble FNIII4-5 fragment to immobilized Fn, 70 kDa, FNIII4-5, or FNIII7-10 fragments. Fn or fragments in 10 mM Tris, 50 mM NaCl, pH 7.5 were immobilized on CMD dual-well cuvettes using an IAsysPlus optical biosensor. Increasing concentrations of the indicated soluble fragments were added and the response (arc sec), representing the binding to Fn (A), 70 kDa fragment (B), FNIII4-5

fragment (C), or FNIII7-10 fragment (D) was monitored until saturation was reached. Binding of a polyclonal anti-Fn antibody or a control antibody is also shown in (D). Samples and cuvettes were maintained at 22^0 C and values represent the average of three different experiments. Error bars indicate standard deviations.

Figure 4. Binding of various soluble recombinant fragments containing the III4-5 region to immobilized Fn, 70 kDa or FNIII4-5. Fn or fragments were immobilized on CMD dual-well cuvettes as described for Fig. 3. Increasing concentrations of soluble FNIII4-5, FNIII4-6, FNIII4, or FNIII5 fragments were added and binding to immobilized Fn (A), 70 kDa (B), or FNIII4-5 (C) was monitored as explained. Values represent the average of at least three different experiments and error bars indicate standard deviations.

Figure 5. Effect of specific mutations on FNIII4-5 on its binding to immobilized Fn, 70 kDa or FNIII4-5. Fn or fragments were immobilized on CMD dual-well cuvettes as described for Fig. 4. Increasing amounts of FNIII4-5 or the indicated mutants were added and binding to Fn (A), 70 kDa (B), or FNIII4-5 (C), was monitored as explained. Values represent the average of at least three different experiments and error bars indicate standard deviations.

Figure 6. Effect of FNIII4-5, FNIII4-6 and FNIII4-5 mutants on Fn matrix assembly. Cycloheximide-treated fibroblasts plated on 10 μg/ml (2.2×10^{-8} M) Fn were incubated overnight with 4 μg/ml (9×10^{-9} M) plasma Fn alone (A), or in combination with 200 μg/ml of FNIII4-6 (4.7×10^{-6} M) (C), FNIII4-5 (7.1×10^{-6} M) (D), FNIII4-5R1R2 (7.1×10^{-6} M) (E), or FNIII4-5R3R4 (7.1×10^{-6} M) (F) fragments. A phase image of the cell layer is shown in (B). Cell cultures were fixed and incubated with a polyclonal anti-Fn Ab, followed by rhodamine-conjugated goat Abs to rabbit IgG. As a negative control, cell cultures were incubated in parallel with secondary Abs alone. In these instances, no immunofluorescence was detected (data not shown). Images from a representative experiment out of four performed are shown. Bar, 20 μm.

Figure 7. Inhibition of ^{125}I-labeled Fn or ^{125}I-labeled 29 kDa fragment binding to matrix-deprived fibroblasts by various Fn fragments. Fibroblasts (3 x 10^4 cells/well) plated for 24 or 48 h at 37^0 C were incubated with ^{125}I-fibronectin (2.7 x 10^6 cpm/ml) in the absence or presence of 80 kDa, 70 kDa or FNIII4-5 fragments (A) or FNIII4-6, FNIII4-5R1R2, or FNIII4-5R3R4 fragments (B) for 3 h. Fibroblasts were also incubated for 3 h with ^{125}I-29 kDa fragment (5.5 x 10^6 cpm/ml) in the presence of the indicated fragments (C). The specific activity was 3.8 x 10^7 cpm/μg and 1 x 10^8 cpm/μg for ^{125}I-Fn and ^{125}I-29 kDa fragment, respectively. Values represent the average of three different experiments each with duplicate measurements, and bars indicate standard errors. Curves (A-C) are third order regression lines.

Figure 8. Summary and proposed model for the role of the Fn III4-5 region in Fn matrix assembly. A) The schematic positions of the four arginine residues in the WTPPRAQITGYRLTVGLTRR sequence of repeat III5 are shown. The native sequence mediates both Fn binding and matrix assembly. Replacing the R1R2 residues in FNIII4-5 with alanine, abolishes Fn binding but does not affect its role in Fn matrix assembly. Conversely, replacing the R3R4 residues with alanine, blocks the effect of this region in Fn fibrillogenesis. B) The assembly of Fn into fibrils involves the unfolding of Fn dimers (dashed lines) at the cell surface. This requires interactions with at least two receptors (white rectangles) at the cell surface as well as activation of RhoA in order for tension to be generated. The FNIII4-5 fragment may block Fn fibrillogenesis because even though it may activate RhoA, its binding to the cell surface prevents Fn from being tethered at two sites, and thus tension cannot be generated to expose Fn-Fn binding sites used during fibrillogenesis.

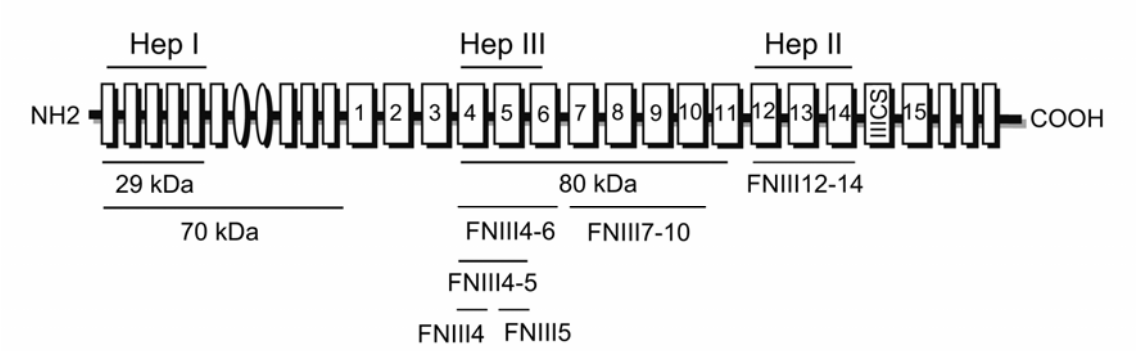

FNIII4-5 mutants

	HBP/III5 site
FNIII4-5	WTPPRAQITGYRLTVGLTRR
FNIII4-5R1R2	WTPP**A**AQITGY**A**LTVGLTRR
FNIII4-5R3R4	WTPPRAQITGYRLTVGLT**AA**

Figure 1

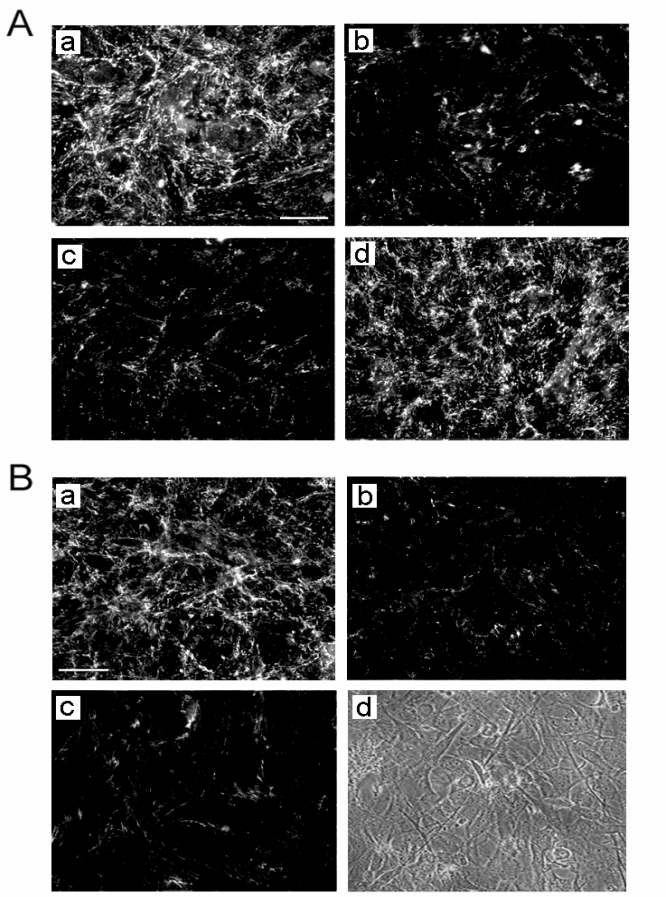

Figure 2

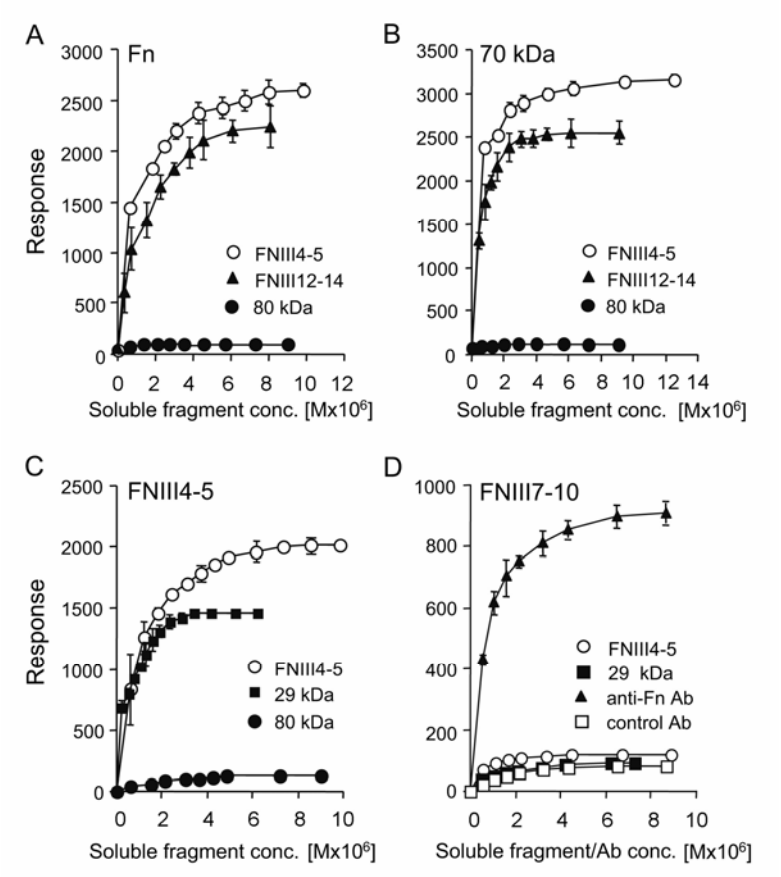

Figure 3

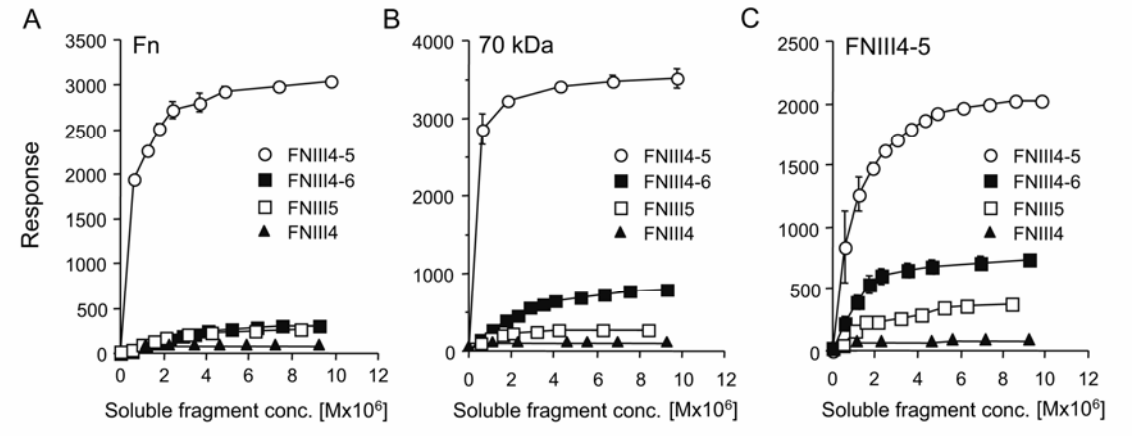

Figure 4

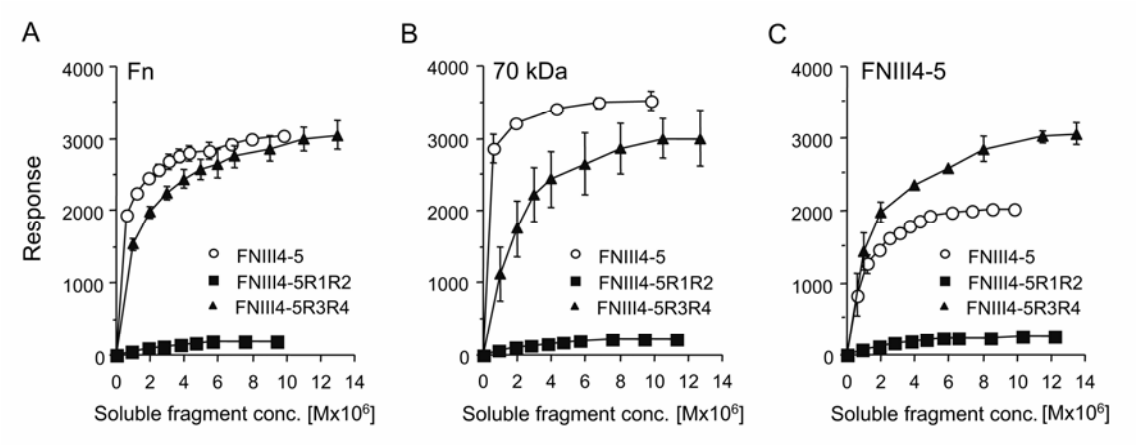

Figure 5

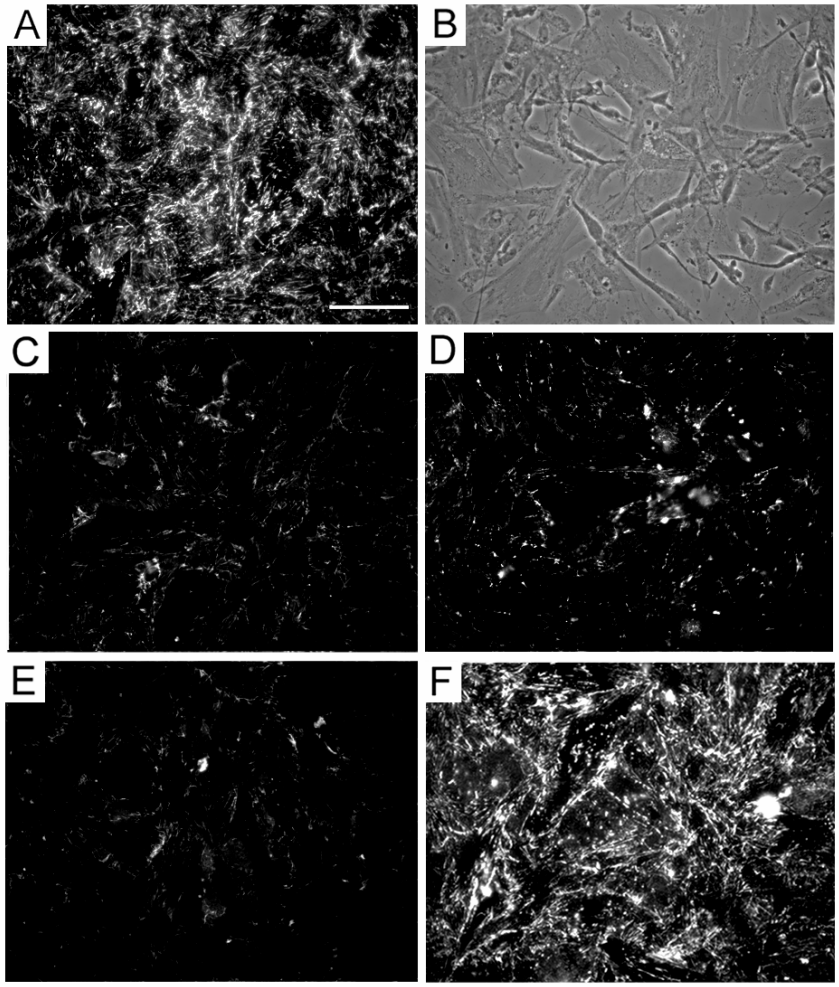

Figure 6

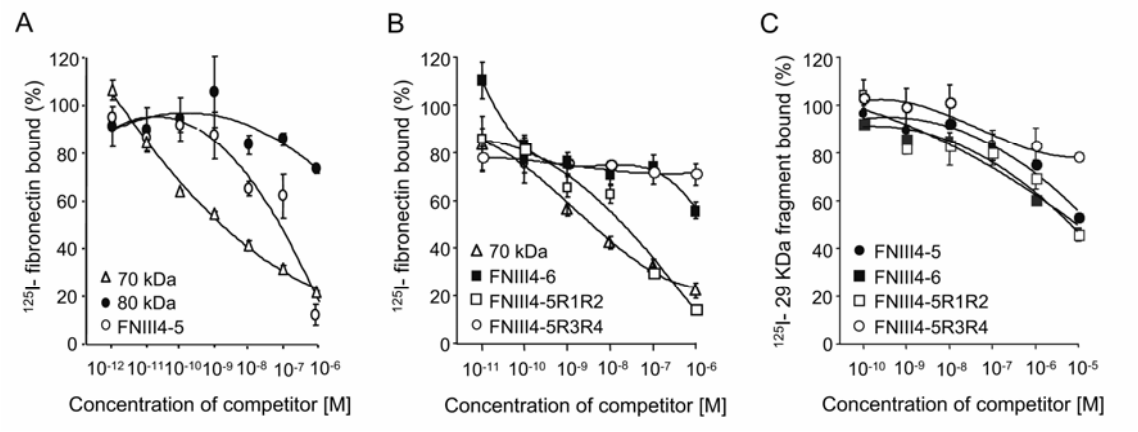

Figure 7

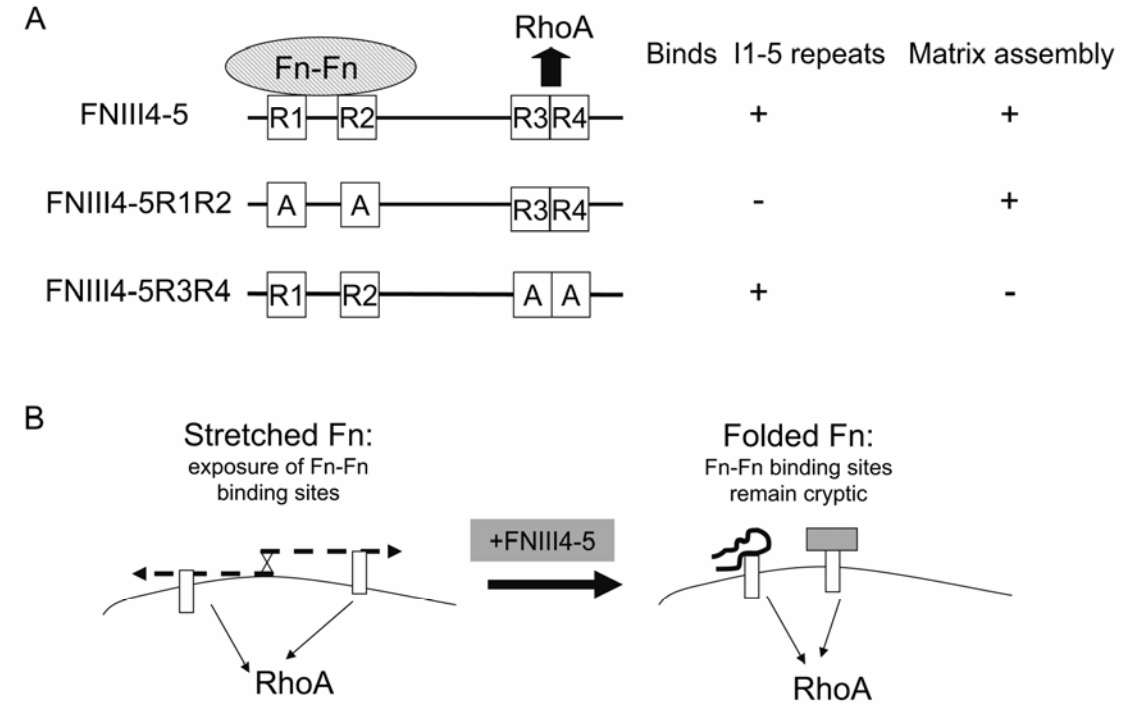

Figure 8

Anexo III

The Lack of Fibronectin Matrix Assembly in the von Hippel-Lindau Protein Defective Renal Cancer Cells is Partly Due to a Deficient Activation of the GTPase RhoA.

Mónica Feijóo-Cuaresma[1*], Fernando Méndez[1*], Alfredo Maqueda[2], Miguel A. Esteban[3], Salvador Naranjo[1], María C Castellanos[1], Mercedes Hernández del Cerro[2], Angeles García-Pardo[2], María J. Calzada[1,&] and Manuel O. Landázuri[1,&].

[1]From Servicio de Inmunología, Hospital de la Princesa, Departamento de Medicina, Universidad Autónoma de Madrid; Diego de León 62, 28006 Madrid (Spain). [2]Departamento de Inmunología, Centro de Investigaciones Biológicas, CSIC, 28006 Madrid. [3]Renal Section, Imperial College, Hammersmith Campus, London, (UK).

Acknowledgments:
SAF2004-00824 from Ministerio de Educación y Ciencia (Manuel O. Landazuri); María C Castellanos and Salvador Naranjo were supported by RECAVA C03/01; MEC, Contratos Ramón y Cajal (María J. Calzada). SAF2003-00824 from MEC and the Fundación de Investigación Médica Mutua Madrileña (A. Garcia-Pardo). A Maqueda was supported by an I3P fellowship from CSIC/European Union Social Fund. UAM/Comunidad Autónoma de Madrid grant 06/CSB/002 (Maria J. Calzada); We thank Dr. Luis del Peso and Dr. Elisa Temes for critical reading of this manuscript.

Request for reprints: María J. Calzada, Hospital de la Princesa, Diego de León 62, 28006, Madrid, Spain. E-mail: mcalzada.hlpr@salud.madrid.org

Note: * These authors contributed equally to this work; **&** These senior authors contributed equally to this work.
Running Title: Role of RhoA on FN matrix defects of VHL (-) RCC cells
Key words: VHL, Renal Cancer Cells, extracellular matrix, fibronectin, RhoA GTPase.

Words: 5000

ABSTRACT

Loss of a proper fibronectin matrix influences cellular transformation and tumorigenesis in vivo. The von Hippel-Lindau tumor suppressor gene (*vhl*) regulates extracellular matrix deposition. In VHL negative renal cancer cells, VHL (-), the lack of fibronectin matrix assembly has been described to promote and maintain tumor angiogenesis allowing vessels to infiltrate tumors. Therefore, and considering the importance of this process in tumor growth, the aim of our studies was to understand why VHL (-) renal cancer cells fail to form a proper extracellular matrix. Our results showed that VHL (-) cells did not have a defect in fibronectin production, and that fibronectin produced by these cells was equally functional in matrix assembly as that produced by VHL (+) cells. Since these VHL (-) cells fail to form β1 integrin fibrillar adhesions and have a diminished organization of actin stress fibers, we studied if the small GTPase family was taking part in this process. We found that activation of a member of this family, the RhoA GTPase, was defective in VHL (-) cells and this was possibly mediated by an increased activation of its inhibitor, p190RhoGAP. Additionally, the expression of a dominant negative RhoA mutant in VHL (+) cells decreased the assembly of fibronectin, while the expression of constitutively active RhoA in VHL (-) cells resulted in formation of a fibronectin matrix. These results strongly suggest an important role for RhoA in some of the defects observed in renal cancer cells.

INTRODUCTION

The von Hippel-Lindau disease is an autosomal dominant hereditary cancer syndrome caused by germ line mutations of the *vhl* tumor suppressor gene (1). The VHL protein (VHL) plays an important role in the oxygen-sensing pathway and its best known function is to promote the ubiquitination and subsequent elimination by the proteasome of the hypoxia-inducible transcription factors HIF1α and HIF2α (2, 3). Loss of VHL leads to activation of the HIF pathway in normoxia (4), which in turn leads to excessive transcription of HIF-α target genes, including the angiogenic factor VEGF (5). Despite the latter provides an explanation for the high vascularization of VHL (-) tumors, it remains unclear how loss of VHL leads to renal cancer.

A recent study has suggested that in fibrosarcoma tumor models, additional genetic changes other than dysregulation of HIF are necessary for the induction of tumorigenesis (6). Indeed, other VHL functions independent of the regulation of HIF have been reported. These include regulation of cell motility and invasivity (7-9); stability of microtubules (10, 11); maintenance of an epithelial-like cell shape and monolayer organization (12-17) and dysregulation of proteins related to cell cycle and apoptosis (18, 19). Additionally, a link between the role of VHL in renal cancer cell (RCC) tumorigenesis and activation of the tumor suppressor p53 has also been reported (20). Adequate interaction of cells with the surrounding matrix regulates essential aspects of normal cell function, and breakdown of the basement membrane occurs in cancer progression and is often associated with solid tumors (21). With regard to RCC tumors we and others have shown that RCC cells lacking VHL fail to organize a normal extracellular fibronectin (FN) matrix (13, 22, 23). Therefore the lack of a proper cell matrix might be involved in the aggressive behaviour of VHL (-) tumors. In addition it has been recently shown that highly angiogenic tumors are not only dependent on the

VHL-HIF 2α degradation pathway, but are also a consequence upon loss of a proper extracellular matrix assembly (24). On the other hand, it has also been reported that VHL physically interacts with intracellular FN in vivo (22, 25, 26). This interaction, that seems to be critical for the proper extracellular FN assembly (22), is lost in almost all naturally occurring VHL mutants (1). Extracellular matrix assembly is a complex multi-step process, which first requires binding of FN to cell surface integrins, mostly α5β1, (27). Additionally other events such as actin stress fibers formation and cell contraction are required for the progressive ordination into detergent insoluble fibers (28). These processes are mediated by the small Ras-type GTPase member RhoA (29, 30). In this respect, we have reported the inability of VHL (-) cells to form β1 fibrillar adhesions (13) and intracellular actin stress fibers (15), and other authors have shown that these cells also lack of proper assembly of actin and vinculin, which promotes actin stress fiber formation (8).

Although expression of VHL is necessary for proper extracellular matrix assembly, the mechanism by which VHL mediates this process is poorly understood. To approach this, we have evaluated the levels and functionality of the FN produced by VHL (+) and VHL (–) cells. We have also studied the role of the signalling pathway that controls formation of actin stress fibers and cell contraction, as well as the state of integrin activation, in the regulation of FN matrix assembly in VHL (+) and VHL (–) cells. Our results demonstrated that FN expression levels in VHL (+) and (-) cells showed no correlation with the ability to assemble a FN matrix and that VHL (-) cells expressed functional FN that was properly assembled by VHL (+) cells. Additionally, we found that the lack of FN matrix in VHL (-) cells was partly due to sustained down-regulation of RhoA activity via p190RhoGAP increased activation. These results provide an insight into novel mechanisms altered in VHL (-) renal cancer cells.

MATERIALS AND METHODS

Cell culture. Cell lines used have been previously described (15). 786-O cells and subclones stably producing wild type VHL (WT8), or empty vector (RC3) (31), VHL L188V (32), VHL(RRR) and VHL(KRR) (33), parental RCC4 and RCC10 and subclones stably producing wild type VHL (34), were all maintained in RPMI 1640 medium with GLUTAMAX-I (Invitrogen) supplemented with 10% fetal bovine serum (FBS) (Linus) and grown at 37ºC with 5% CO_2. Parental UMRC cells and the stable VHL transfectants were provided by Dr. Michael Lerman and Dr. Sergey Ivanov (Laboratory of Immunobiology, NCI, Frederick, MD). VHL type 2A (Y112H) and 2B (C162F) mutants were provided by Dr. Michael Ohh (University of Toronto, Canada).

Antibodies and reagents. Polyclonal anti-FN antibody was from Sigma. Anti-RhoA (clone 26C4, SC-418) was from Santa Cruz Biotechnology (Santa Cruz, CA), anti-p190RhoGAP from Upstate, NY, and anti-phospho tyrosine antibody PY20 was from Biomol. LPA and 2,3-butanedione -monoxime (BDM) from Sigma, and the Rho kinase inhibitor Y-27632 was from Calbiochem.

Isolation of DOC-soluble and insoluble material. Cells were cultured in 6-well plates with RPMI 1640 and GLUTAMAX-I (Invitrogen) supplemented with 5% FN-free FBS. Cells were washed with ice–cold PBS and lysed in 200 µl DOC lysis buffer (2% deoxycholate, 20 mM Tris-HCl, pH 8.8, 2 mM PMSF, 2 mM EDTA and Roche protease inhibitors mix). DOC-insoluble material isolated by centrifugation (15,000g, 20 min, 4ºC) was solubilized in 200 µl of SDS solubilizing buffer (1% SDS, 25 mM Tris-HCl, pH 8.0, 2 mM PMSF, 2 mM EDTA and Roche protease inhibitors mix). Total lysates were recovered by adding 200 µl of RIPA lysis buffer. Aliquots of DOC-insoluble material and total lysates were electrophoresed and transferred to nitrocellulose membranes. Immunolabeling was detected by enhanced

chemiluminescence (Amersham Pharmacia Biotechnology, Piscataway, NJ) and visualized with a digital luminescent image analyzer (Fujifilm LAS-1000 CH).

Immunofluorescence microscopy. Immunofluorescence staining was performed as previously described (13). Briefly, cells were grown for three days on uncoated or FN (10 μg/ml) coated coverslips. Cells were cultured in RPMI/10% FBS-FN free and detached with 0.5% Triton X-100 and 20 mM NH4OH/PBS. Coverslips were fixed with 3% paraformaldehyde and washed with TBS-0.5% Tween-20. Non specific binding sites were blocked with TNB (0.1 M Tris-HCl, 0.15 M NaCl, 0.5% blocking reagent) for 20 min at 37ºC. Coverslips were incubated with polyclonal anti-FN antibody for 1 hour at 37ºC, washed and incubated with the secondary antibody Rhodamine Red™-X goat anti-rabbit IgG (Molecular Probes, Inc. Eugene, OR) for 30 min at 37ºC, and washed with TBS-T. Cells were briefly washed with distilled water, and mounted with Mowiol. For RhoA activation we incubated the cells with 6 μM Lysophosphatidic Acid (LPA), which induces actin stress fibers formation. For RhoA inhibition cells were incubated with 5 μM Y-27632 (an inhibitor of the RhoA downstream effector, ROCK), or with 15 mM 2,3-butanedione-monoxime or BDM (an inhibitor of actin-myosin interaction). Preparations were analyzed with a Leica DMR photomicroscope (Leica Microsystems) equipped with QFISH software.

Quantitative Real Time PCR analysis. Cells were grown to confluence in 100-mm culture dishes, and total cellular RNA was isolated using the Ultraspec RNA Isolation System (Biotecx Laboratories, Houston, TX). Total RNA (2 μg/sample) was reverse-transcribed to cDNA (Improm II RT, Promega, Madison, WI). Quantitative RNA analysis protocol and primers pairs for β-actin have been described elsewhere (35). FN primers used were 5´-AGGATTACCGGCTACAT-3´ (forward) and 5´-GTGACGAAAGGGGTCT-3´ (reverse). The number of copies of the studied gene in

each sample was extrapolated from the corresponding standard curve with the software. The gene copy number was normalized to the amount of β-actin.

Purification of secreted FN from VHL (+) and VHL (-) cells. Cells were grown in T175 flasks with RPMI media containing 10% FN-depleted serum and maintained in a shaking platform at 37ºC. Conditioned media (500 ml/each cell type) was collected after 4-5 days and loaded into a gelatine-agarose (Sigma) affinity column. FN was eluted with 4M urea and dialyzed against PBS.

Cell adhesion assay: FN purified from VHL (+) or (-) cells, was absorbed at 5 μg/ml onto maxisorb 96 well plates (Costar). The wells were aspirated, and the plates were blocked with 1% BSA/PBS for 30 min. Cells ($20x10^3$/well) were resuspended in M199/0.1% BSA and incubated for 1 h at 37°C in 5% CO_2. After washing with PBS cells were fixed with 1% glutaraldehyde/PBS and stained with 1% crystal violet/PBS. Cells were washed with distilled water and the plate read by an ORION-2 plate reader at 590 nm.

RhoA Activity Assay. RhoA activity was measured using a GST-rhotekin-Rho binding domain (GST-C21) a gift of Dr. John Collard (The Netherlands Cancer Institute, Amsterdam, The Netherlands). Briefly, a total of 7×10^6 cells were lysed in RIPA lysis buffer. After centrifugation (20000g, 15 min, 4ºC), equal amounts of protein from the supernatant were incubated overnight at 4ºC with beads coated with GST-C21. Beads were washed and bound protein was eluted by boiling in Laemmli buffer. Total and bound RhoA subject to electrophoresis and transferred to nitrocellulose membranes were detected using an anti-RhoA mAb followed by HRP-conjugated anti-mouse IgG antibody (Dako) and visualized with ECL Super-Signal West Pico kit (Pierce, Rockford, IL). For statistical purposes, gels from active and total RhoA normalized with

respect to the loading control were subjected to densitometric analysis and analyzed using the Quantity-One^{TM} program (BIO-RAD).

Analysis of p190RhoGAP Phosphorylation. VHL (+) and (-) RCC cells (6 x 10^6) were lysed in 500 µl RIPA buffer. 15 µl of the supernatant were used for analysis of total protein and the remaining was incubated overnight at 4°C with protein G-agarose beads (Pierce) coated with 4 µg of anti-p190RhoGAP mAb (Upstate, NY) or with the IgG1 anti-CD45 T200 antibody (mock). Beads were washed with RIPA buffer, and bound proteins extracted by boiling in Laemmli buffer, subject to electrophoresis and transferred into nitrocellulose membranes. Phosphorylated proteins were detected using PY20 mAb followed by an HRP-labelled secondary antibody. Protein bands were quantitated as above.

Retroviral Infection. Constructs of a constitutive active form (RhoA Q63L) or a dominant negative form (RhoA N19) of RhoA were kindly provided by Dr. Silvio Gutkind (Bethesda, MD). These constructions were subcloned into the BamH1/EcoR1 site of the retroviral vector pLZR IRES-GFP. 786-O cells infection was performed as we described previously (15)

RESULTS

The comparative study of FN mRNA and protein expression levels in VHL (+) and VHL (-) RCC cells reveals no correlation with the ability to assemble a FN matrix.

Failure to assemble a proper FN matrix by VHL (-) RCC cells has been attributed to a decreased expression of this protein and/or to the lack of FN interaction with VHL (22, 25, 26). To determine whether this was a general phenomenon in RCCs, we first analyzed the FN mRNA and protein levels in several RCC cell lines and in cells with different VHL mutations corresponding to type 2A, 2B and 2C phenotype of the VHL disease**.** These included the mutants Y112H (type 2A), C162F (type 2B), L188V (type 2C), and a nonneddylateable version of VHL termed RRR, or the control termed KRR (33), all of them on the RRC 786-O background. Remarkably, FN mRNA levels measured by quantitative RT-PCR were significantly lower in 786-O and UMRC VHL (+) cells than in their corresponding VHL (-) counterparts (Figure 1A). Likewise, FN mRNA levels in the various VHL mutants were higher when compared to the corresponding levels in 786-O VHL (+) cells (Figure 1A). In contrast, in RCC10 cells FN mRNA expression was always higher in VHL (+) versus VHL (-) cells (Figure 1A). It is worth mentioning that FN mRNA levels in RCC10 cells, both VHL (+) and (-), were significantly higher compared to the other cell lines.

We also analyzed FN protein levels in cell lysates or deoxycholate insoluble fractions derived from all these cell types. In agreement with the mRNA data, VHL (-) and mutants derived from 786-O parental cells, consistently showed higher FN protein expression than 786-O VHL (+) cells (Figure 1B). Since VHL (-) cells do not assemble FN, the FN encountered in the DOC insoluble fraction could be due to FN interacting with other cytoskeletal proteins. In contrast, RCC4, RCC10 and UMRC VHL (-) cells had lower FN protein levels than their VHL (+) counterparts, both in lysates and in

DOC insoluble fractions (Figure 1B). Altogether these results indicated a heterogeneous expression of FN on the various VHL (+) and VHL (-) RCC cells and most important, that lack of matrix assembly by VHL (-) cells could not always be attributed to low levels of FN on these cells.

To further confirm the above conclusion, we analyzed the assembly of FN matrix either in the absence or presence of exogenous FN. We have previously reported that addition of exogenous FN did not re-establish assembly in 786-O VHL (-) cells (13). In this report we analyzed the assembly in three additional cell lines, RCC4, RCC10 and UMRC and in addition in the type 2A, 2B and 2C VHL mutants described above. Our results showed that VHL (-) cells cultured on uncoated or FN coated coverslips did not form visible FN fibers, indicating that FN availability is not exclusively responsible for their incapability to form a matrix (Figure 2A). Interestingly, VHL (+) but not VHL (-) UMRC cells, only formed a visible matrix when cultured on exogenous FN (Figure 2A), indicating that, in this particular case, low secretion of FN (see Figure 1A,B) might be responsible for the lack of FN matrix in this VHL expressing cell line. Additionally, none of the three different mutants, type 2A, 2B or 2C, were able to assemble FN even when it was exogenously added (Figure 2B). These results further supported our previous findings showing that FN production did not correlate with its assembly.

Fibronectin produced by VHL (-) cells is functional and normally assembled by VHL (+) cells.

It has also been suggested that the failure to assemble FN by VHL (-) cells could be due to the presence of malfolded or malprocessed FN, which accumulates extracellularly and interferes with normal FN for its assembly (22, 36). However it is not clear whether

FN interaction with VHL is necessary for its assembly. On the other hand it is interesting to note that the L188V type 2C mutant although capable of interacting with FN (26) failed to assemble it into fibrils (our results and (25, 33)). Moreover, the hypothesis of FN modification by VHL does not agree with our previously reported observations (13) and our current results (Figure 2) showing that exogenously added FN does not improve matrix assembly by VHL (-) cells.

To clarify these issues, we purified FN from the conditioned media of the different VHL (+) and (-) cell lines and first compared its capability to bind to its receptor, the α5β1 integrin, and to form fibrils. The proper expression and functionality of this integrin is necessary for FN assembly into fibrils in many cell types (27). We and others have shown that the defect on FN matrix assembly in VHL (-) cells is not attributable to a decreased integrin expression or activation (12, 13). Adhesion experiments on a collagen type I matrix indicate that VHL (+) and (-) cells similarly attach to this substrate (12). Therefore we next sought to analyze if α5β1 integrin was functional and able to attach to immobilized FN. We performed cell adhesion experiments on FN coated plates, using FN purified from VHL (+) and VHL (-) cell conditioned media. As shown in Figure 3A, all cell lines showed similar levels of adhesion to FN from either source and this was independent of their VHL status. These results indicated that the lack of FN assembly by VHL (-) cells is not due to a decreased α5β1 integrin activity and that FN synthesized from VHL (-) is able to mediate cell adhesion as efficiently as that synthesized by VHL (+) cells.

We also compared the ability of FN purified from the conditioned media of VHL (+) and VHL (-) cells to assemble into fibrils. Our results confirmed that VHL (-) RCCs did not assemble a FN matrix, even in the presence of exogenous FN from VHL (+) cells (Figure 3B). In contrast, VHL (+) RCCs consistently formed a FN matrix when

cultured either on FN purified from their own conditioned medium or from that of VHL (-) cells (Figure 3B). UMRC VHL (+) cells were a good read out control, since they barely produce FN and hence they do not assemble it unless we provide them with exogenous FN. As shown in Figure 3B, UMRC VHL (+) cells showed a similar assembly pattern when cultured on FN from VHL (+) or VHL (-) cells. Therefore these results confirmed that FN produced by VHL (-) cells, does not interfere with normal FN function in VHL (+) cells. Additionally, they clearly indicated that FN secreted by VHL (-) cells is fully functional and able to be assembled by VHL (+) cells.

Activation of the small GTPase RhoA is defective in VHL (-) cells.

We have previously shown that VHL (-) cells fail to assemble proper β1 fibrillar adhesions, and have a diminished organization of actin stress fibers (13, 15). Therefore the lack of proper formation of actin stress fibers and cell contraction could explain the defective assembly of FN by VHL (-) cells, since these events are required for the exposure of cryptic sites in FN and its progressive ordination into detergent insoluble fibers (30). It is also well established that the GTP-binding protein RhoA mediates the formation of actin stress fibers and regulates cellular functions such as cell adhesion and contractility (37). Furthermore, inhibitors of RhoA-mediated cellular contractility prevent FN assembly into fibrils (29), and a constitutive active form of RhoA restores the assembly of FN into fibrils in cells lacking active β1 integrins (38). According to this, we hypothesized that RhoA activation and/or function could be defective in VHL (-) cells.

To determine whether RhoA was directly involved in FN matrix assembly in RCC, we first performed immunofluorescence experiments to analyze the assembly of FN by 786-O VHL (+) and VHL (-) RCC cells in the presence of inhibitors or activators

of the RhoA signalling pathway. In the presence of Y-27632 or 2-3-BDM, inhibitors of RhoA downstream effectors, we found that the assembly of FN was completely abolished in VHL (+) cells (Figure 4A and data not shown). Interestingly, stimulation of RhoA by LPA resulted in increased FN fibers formation in VHL (+) cell cultures and induction of a few FN fibers by VHL (-) cells (Figure 4A). We next performed RhoA activity assays using the C21-GST fusion protein. We evaluated RhoA activity at time zero and after 24, 48 and 72 hours in culture. As shown in Figure 4B and 4C, VHL (+) cells showed a basal RhoA activity which progressively increased over time during the 72 hours of the assay. In contrast, VHL (-) cells had very low basal RhoA activity, which transiently increased upon 24 hour culture, but was not sustained for longer times. (Figure 4B). These results suggested that the RhoA signalling pathway was playing a role on the functional alterations observed on VHL (-) cells.

Constitutive activation of RhoA stimulates FN assembly by VHL (-) cells.

To obtain further evidence for the involvement of RhoA in the lack of FN assembly in VHL (-) cells, we introduced a recombinant constitutively active (GFP RhoA-Q63L) or a dominant negative (GFP RhoA-N19) RhoA form in VHL (-) and VHL (+) cells respectively. The efficiency of cell infection was 98% as evaluated by flow cytometry and the expression of RhoA was increased at least three times (Supplementary Figure 1). Three days after infection, we analyzed changes on cell morphology and observed that infection of VHL (+) cells with GFP RhoA-N19 did not induce phenotypic alterations (data not shown). In contrast, infection of VHL (-) cells with GFP RhoA-Q63L, induced an epithelial cytoarchitecture that resembled that of VHL (+) cells, while infection with the empty vector did not have any effect (Supplementary Figure 2). We next analyzed whether infection with these mutants induced alterations in the assembly

of FN. Immunofluorescence experiments with VHL (+)/GFP RhoA-N19 cells revealed a decrease of FN fibrils when compared to the control VHL (+) cells or with cells infected with the empty vector (Figure 5, top). In contrast, infection of VHL (-) cells with GFP RhoA-Q63L stimulated the assembly of FN into fibers, while infection with the empty vector had no effect (Figure 5, bottom). Altogether these results further supported the conclusion that the inability of VHL (-) cells to properly assemble a FN matrix is due, at least in part, to an impaired activation of RhoA.

Down-regulation of RhoA activity in VHL (-) RCC cells correlates with increased p190RhoGAP phosphorylation.

The small Rho-GTPases can switch from an active form (bound to GTP) to inactive form (bound to GDP). They associate with factors that regulate this process, such as the guanine nucleotide exchange factors (GEFs), GDP dissociation inhibitor (GDI) or the GTP-ase-activating proteins (GAPs) that promote hydrolysis of GTP to GDP and then inhibit the small Rho-GTPases (37). Down-regulation of RhoA activity has been correlated with activation of p190RhoGAP by phosphorylation (39). Therefore we asked whether the decreased RhoA activity encountered in VHL (–) cells was due to an increased activation of p190RhoGAP. To this end, p190RhoGAP was immunoprecipitated from lysates of cells cultured for 72 hours, time at which we observed the lowest RhoA activity in VHL (-) cells (see Figure 4B), and analyzed for tyrosine phosphorylation. As shown in Figure 6, densitometric analysis showed that both total and phosphorylated p190RhoGAP were increased in VHL (-) cells with respect to VHL (+) cells (1.6-fold and 4.2-fold respectively). Thus, the net increase of phosphorylated/total p190RhoGAP in VHL (-) versus VHL (+) cells was 2.6-fold

(Figure 6). These results indicated that the enhanced phosphorylation of p190RhoGAP in VHL (-) cells probably explains the decreased RhoA activity in these cells.

DISCUSSION

In VHL (-) RCC cells the lack of FN assembly has been shown to promote and maintain tumor angiogenesis allowing vessels to infiltrate tumors (23). Considering the importance of this process in tumor growth, the aim of our studies was to understand why VHL (-) RCC cells fail to form a proper extracellular matrix. An altered integrin expression-function or insufficient FN synthesis could account for this defect. However, we previously demonstrated (13) that integrin expression or function did not significantly differed in VHL (+) or VHL (-) cells, and we also have confirmed that FN production did not correlated with its assembly. With respect to this, some RCCs tumors accumulated FN in the tumor cell cytoplasm, and little or none in the stroma (36), suggesting a defective transport and secretion of FN that could account for the lack of FN assembly by these cells. However our previous results using cultured cells, showed no evidence of intracellular accumulation of FN (13). Additionally, recent studies have demonstrated no important differences between total or secreted FN in VHL tumor cells (23). These findings support our present results showing that FN secreted by VHL (+) and VHL (-) cells is equally functional.

Several authors have shown that VHL interacts with FN, and this interaction seems to be necessary for its assembly into fibrils (22, 25, 26). However, it remains unclear how VHL mediates this process. Given the role of VHL in proteasomal-mediated degradation, Ohh et al (22) propose that VHL may exert a role in the removal of abnormally processed FN molecules, therefore involving FN regulation at the post-transcriptional level. These authors also suggest that the intracellular accumulation and secretion of this abnormal FN underlie the defective matrix phenotype observed on VHL (-) RCC cells. In contrast to this hypothesis, our present experiments showed that purified FN from VHL (-) cells was functional and assembled by VHL (+) cells.

Furthermore, VHL (-) cells were unable to assemble exogenously added FN produced by VHL (+). With respect to the VHL-FN interaction requirement for FN fibril formation (25), we showed in this report that the type 2C VHL mutant that preserves the property of binding to FN (26) failed to assemble it into fibrils. These results suggested that VHL-FN interaction is not always necessary to support FN assembly. Additionally, most of the FN molecules are secreted to the extracellular matrix, and thus only a small portion of FN could interact with VHL. Interestingly though, these authors (22) support the idea that FN-VHL interaction could occur in the endoplasmic reticulum during ER-mediated export of FN to the cell surface. Another possibility is that VHL indirectly regulates FN assembly, which could be post-transcriptionally modified resulting in the inability to form fibrils. In this respect, it has been proposed that extracellular FN in VHL (-) cells is degraded by the increased activation of metalloproteinases such as MMP2 (23). Therefore degradation of FN matrix in VHL (-) cells is a reasonable explanation for the lack of matrix in these cells. However, it remains unclear whether VHL directly regulates MMPs activity or this is a secondary effect of cell transformation. Additionally, the fact that even in the presence of an excess of extracellular FN, VHL (-) cells failed to form a proper matrix, let us think that other intracellular events such as cytoskeleton reorganization and cell contractility might be regulating the assembly of FN in VHL (+) cells. In this regard, VHL (-) cells do not form proper structures related to cytoskeleton organization and cell contractility (8, 13, 15). These facts support our present observations showing that the lack of FN assembly in VHL (-) cell is partly caused by a deficient activation of the small GTPase RhoA, which on the other hand is an important regulator of cell cytoskeleton organization (29, 37). However, since no relationship between VHL and Rho-GTPases has been established to date, it is unclear how VHL regulates this process.

One possibility is that VHL regulates Rho-GTPases indirectly, through a second VHL interacting protein. For example, VHL binds to several isoforms of atypical PKCs (40, 41) such as PKCλ, whose activated form is then ubiquitinated and thus its cellular activity reduced (42). It is also known that atypical PKCs are involved in the control of cell polarity, focal contact integrity, actin filament organization and stress fibers formation (43, 44), and these effects probably involve regulation of the activity of the Rho family of small GTPases. According to this, in endothelial cells one atypical PKC phosphorylates Rho-GDI and Rho-GEF and induces RhoA activation (45-47). Moreover, PKCδ was shown to interact with p190RhoGAP in endothelial cells (43). It is therefore possible that VHL interaction with atypical PKCs regulates the activity of Rho-GTPases by modulating the phosphorylation state of RhoA inhibitors such as GDI and GAP factors or the Rho-GEF activator. This hypothesis is in agreement with our present results showing an increased p190Rho-GAP phosphorylation in VHL (-) cells.

In summary, our present study demonstrates that FN production and function is not deficient in VHL (-) cells but rather, that altered intracellular signals regulating cell contractility, are responsible for the inability of these cells to assemble a FN matrix. Our results are the first to provide a mechanism that explains some of the defects observed in VHL (-) cells. However the precise role of VHL on this mechanism remains to be established.

REFERENCES

1. Kaelin WG, Jr. Molecular basis of the VHL hereditary cancer syndrome. Nat Rev Cancer 2002;2:673-82.
2. Ivan M, Kondo K, Yang H, et al. HIFalpha targeted for VHL-mediated destruction by proline hydroxylation: implications for O2 sensing. Science 2001;292:464-8.
3. Jaakkola P, Mole DR, Tian YM, et al. Targeting of HIF-alpha to the von Hippel-Lindau ubiquitylation complex by O2-regulated prolyl hydroxylation. Science 2001;292:468-72.
4. Maxwell PH, Wiesener MS, Chang GW, et al. The tumour suppressor protein VHL targets hypoxia-inducible factors for oxygen-dependent proteolysis. Nature 1999;399:271-5.
5. Maher ER ,Kaelin WG, Jr. von Hippel-Lindau disease. Medicine (Baltimore). 1997;76:381-91.
6. Mack FA, Rathmell WK, Arsham AM, et al. Loss of pVHL is sufficient to cause HIF dysregulation in primary cells but does not promote tumor growth. Cancer Cell 2003;3:75-88.
7. Koochekpour S, Jeffers M, Wang PH, et al. The von Hippel-Lindau tumor suppressor gene inhibits hepatocyte growth factor/scatter factor-induced invasion and branching morphogenesis in renal carcinoma cells. Mol Cell Biol 1999;19:5902-12.
8. Kamada M, Suzuki K, Kato Y, Okuda H, Shuin T. von Hippel-Lindau protein promotes the assembly of actin and vinculin and inhibits cell motility. Cancer Res 2001;61:4184-9.
9. Hsu T, Adereth Y, Kose N, Dammai V. Endocytic function of von Hippel-Lindau tumor suppressor protein regulates surface localization of fibroblast growth factor receptor 1 and cell motility. J Biol Chem. 2006;281:12069-80.
10. Hergovich A, Lisztwan J, Barry R, Ballschmieter P, Krek W. Regulation of microtubule stability by the von Hippel-Lindau tumour suppressor protein pVHL. Nat Cell Biol 2003;5:64-70.
11. Bluyssen HA, Lolkema MP, van Beest M, et al. Fibronectin is a hypoxia-independent target of the tumor suppressor VHL. FEBS Lett 2004;556:137-42.
12. Davidowitz EJ, Schoenfeld AR, Burk RD. VHL induces renal cell differentiation and growth arrest through integration of cell-cell and cell-extracellular matrix signaling. Mol Cell Biol 2001;21:865-74.
13. Esteban-Barragan MA, Avila P, Alvarez-Tejado M, et al. Role of the von Hippel-Lindau tumor suppressor gene in the formation of beta1-integrin fibrillar adhesions. Cancer Res 2002;62:2929-36.
14. Lewis MD ,Roberts BJ. Role of nuclear and cytoplasmic localization in the tumour-suppressor activity of the von Hippel-Lindau protein. Oncogene 2003;22:3992-7.
15. Calzada MJ, Esteban MA, Feijoo-Cuaresma M, et al. von Hippel-Lindau tumor suppressor protein regulates the assembly of intercellular junctions in renal cancer cells through hypoxia-inducible factor-independent mechanisms. Cancer Res 2006;66:1553-60.

16. Esteban MA, Tran MG, Harten SK, et al. Regulation of E-cadherin expression by VHL and hypoxia-inducible factor. Cancer Res 2006;66:3567-75.
17. Krishnamachary B, Zagzag D, Nagasawa H, et al. Hypoxia-inducible factor-1-dependent repression of E-cadherin in von Hippel-Lindau tumor suppressor-null renal cell carcinoma mediated by TCF3, ZFHX1A, and ZFHX1B. Cancer Res 2006;66:2725-31.
18. Kim M, Yan Y, Lee K, Sgagias M, Cowan KH. Ectopic expression of von Hippel-Lindau tumor suppressor induces apoptosis in 786-O renal cell carcinoma cells and regresses tumor growth of 786-O cells in nude mouse. Biochem Biophys Res Commun. 2004;320:945-50.
19. Bindra RS, Vasselli JR, Stearman R, Linehan WM, Klausner RD. VHL-mediated hypoxia regulation of cyclin D1 in renal carcinoma cells. Cancer Res 2002;62:3014-9.
20. Roe JS, Kim H, Lee SM, et al. p53 stabilization and transactivation by a von Hippel-Lindau protein. Mol Cell 2006;22:395-405.
21. Hanahan D ,Weinberg RA. The hallmarks of cancer. Cell 2000;100:57-70.
22. Ohh M, Yauch RL, Lonergan KM, et al. The von Hippel-Lindau tumor suppressor protein is required for proper assembly of an extracellular fibronectin matrix. Mol Cell 1998;1:959-68.
23. Kurban G, Hudon V, Duplan E, Ohh M, Pause A. Characterization of a von Hippel Lindau pathway involved in extracellular matrix remodelling, cell invasion, and angiogenesis. Cancer Res 2006;66:1313-9.
24. Tang N, Mack F, Haase VH, Simon MC, Johnson RS. pVHL function is essential for endothelial extracellular matrix deposition. Mol Cell Biol 2006;26:2519-30.
25. Hoffman MA, Ohh M, Yang H, et al. von Hippel-Lindau protein mutants linked to type 2C VHL disease preserve the ability to downregulate HIF. Hum Mol Genet 2001;10:1019-27.
26. Clifford SC, Cockman ME, Smallwood AC, et al. Contrasting effects on HIF-1alpha regulation by disease-causing pVHL mutations correlate with patterns of tumourigenesis in von Hippel-Lindau disease. Hum Mol Genet 2001;10:1029-38.
27. Hynes RO. Integrins: versatility, modulation, and signaling in cell adhesion. Cell 1992;69:11-25.
28. Wierzbicka-Patynowski I ,Schwarzbauer JE. The ins and outs of fibronectin matrix assembly. J Cell Sci 2003;116:3269-76.
29. Zhong C, Chrzanowska-Wodnicka M, Brown J, et al. Rho-mediated contractility exposes a cryptic site in fibronectin and induces fibronectin matrix assembly. J Cell Biol 1998;141:539-51.
30. Zhang Q, Magnusson MK, Mosher DF. Lysophosphatidic acid and microtubule-destabilizing agents stimulate fibronectin matrix assembly through Rho-dependent actin stress fibbers formation and cell contraction. Mol Biol Cell 1997;8:1415-25.
31. Iliopoulos O, Kibel A, Gray S, Kaelin WG, Jr. Tumour suppression by the human von Hippel-Lindau gene product. Nat Med 1995;1:822-6.
32. Ohh M, Takagi Y, Aso T, et al. Synthetic peptides define critical contacts between elongin C, elongin B, and the von Hippel-Lindau protein. J Clin Invest 1999;104:1583-91.

33. Stickle NH, Chung J, Klco JM, et al. pVHL modification by NEDD8 is required for fibronectin matrix assembly and suppression of tumor development. Mol Cell Biol 2004;24:3251-61.
34. Krieg M, Haas R, Brauch H, et al. Up-regulation of hypoxia-inducible factors HIF-1alpha and HIF-2alpha under normoxic conditions in renal carcinoma cells by von Hippel-Lindau tumor suppressor gene loss of function. Oncogene 2000;19:5435-43.
35. Naranjo-Suarez S, Castellanos MC, Alvarez-Tejado M, et al. Down-regulation of hypoxia-inducible factor-2 in PC12 cells by nerve growth factor stimulation. J Biol Chem 2003;278:31895-901.
36. He Z, Liu S, Guo M, Mao J, Hughson MD. Expression of fibronectin and HIF-1alpha in renal cell carcinomas: relationship to von Hippel-Lindau gene inactivation. Cancer Genet Cytogenet 2004;152:89-94.
37. Ridley AJ. Rho family proteins: coordinating cell responses. Trends Cell Biol 2001;11:471-7.
38. Cali G, Mazzarella C, Chiacchio M, et al. RhoA activity is required for fibronectin assembly and counteracts beta1B integrin inhibitory effect in FRT epithelial cells. J Cell Sci 1999;112:957-65.
39. Arthur WT, Petch LA, Burridge K. Integrin engagement suppresses RhoA activity via a c-Src-dependent mechanism. Curr Biol 2000;10:719-22.
40. Iturrioz X, Durgan J, Calleja V, et al. The von Hippel-Lindau tumour-suppressor protein interaction with protein kinase C delta. Biochem J 2006;397:109-20.
41. Pal S, Claffey KP, Dvorak HF, Mukhopadhyay D. The von Hippel-Lindau gene product inhibits vascular permeability factor/vascular endothelial growth factor expression in renal cell carcinoma by blocking protein kinase C pathways. J Biol Chem 1997;272:27509-12.
42. Okuda H, Saitoh K, Hirai S, et al. The von Hippel-Lindau tumor suppressor protein mediates ubiquitination of activated atypical protein kinase C. J Biol Chem 2001;276:43611-7.
43. Harrington EO, Shannon CJ, Morin N, et al. PKC delta regulates endothelial basal barrier function through modulation of RhoA GTPase activity. Exp Cell Res 2005;308:407-21.
44. Coghlan MP, Chou MM, Carpenter CL. Atypical protein kinases Clambda and -zeta associate with the GTP-binding protein Cdc42 and mediate stress fibers loss. Mol Cell Biol 2000;20:2880-9.
45. Pang H ,Bitar KN. Direct association of RhoA with specific domains of PKC-alpha. Am J Physiol Cell Physiol 2005;289:C982-93.
46. Mehta D, Rahman A, Malik AB. Protein kinase C-alpha signals rho-guanine nucleotide dissociation inhibitor phosphorylation and Rho activation and regulates the endothelial cell barrier function. J Biol Chem 2001;276:22614-20.
47. Holinstat M, Mehta D, Kozasa T, Minshall RD, Malik AB. Protein kinase Calpha-induced p115RhoGEF phosphorylation signals endothelial cytoskeletal rearrangement. J Biol Chem 2003;278:28793-8.

FIGURE LEGENDS

Figure 1. Comparative study of FN mRNA and protein levels in several VHL (+) and VHL (-) RCC cells. A) FN gene transcription levels in 786-O, RCC4, UMRC, RCC10, and VHL mutants were determined by quantitative real time PCR. FN mRNA levels were normalized to beta-actin and the number of copies were extrapolated from the corresponding standard curve expressed in ng/μl. Values represent the average from three different experiments ($P \leq 0.05$). **B)** FN endogenous levels were determined by western blots. Total cell lysates or deoxycholate insoluble fractions were immunoblotted with an anti-FN polyclonal Ab. A representative experiment is shown.

Figure 2. Comparative analysis of FN matrix organization in RCCs and VHL mutants in the presence of exogenous FN. A) 786-O, RCC4, RCC10 and UMRC RCC cells and their counterparts expressing VHL were grown to confluence on uncoated or FN (10 μg/ml) coated coverslips. After 3-4 days cells were lysed and FN matrix was analyzed by indirect immunofluorescence using a polyclonal anti-FN antibody. **B)** Type 2A (Y112H), 2B (C162F) and 2C (L188V, RRR and control KRR) VHL mutants were grown under the same conditions as in A and FN matrix was analyzed after 4 days of cell culture. The images shown are representative of at least three experiments.

Figure 3. Functional evaluation of FN purified from VHL (+) and VHL (-) RCC cells. A) Cell adhesion on FN purified from VHL (+) and VHL (-) cells conditioned media using gelatine-agarose affinity matrices. Cells ($2x10^4$/well) were incubated on 96-well FN (5 μg/ml) coated plates during 1 h at 37ºC in 5% CO_2, fixed and stained as described in materials and methods. Attached cells were then quantitated at 590 nm.

The average from three different experiments is represented. **B)** FN assembly was analyzed by indirect immunofluorescence staining. 786-O, RCC4, RCC10 and UMRC ($2x10^5$ cells) were plated on uncoated or FN (10 μg/ml) coated coverslips, using FN purified from VHL (+) or VHL (-) cells. After 3-4 days of culture at 37ºC and 5% CO_2, FN matrix formation was analyzed with a conventional immunofluorescence microscope. A representative experiment of at least four performed is shown.

Figure 4. RhoA activation state in VHL (+) and (-) RCC cells. A) 786-O RCC cells were cultured for 3-4 days in the absence or presence of the RhoA signalling inhibitor, Y27632 (5 μM) or the activator LPA (6 μM). FN matrix formation was analyzed by immunofluorescence experiments performed as described in materials and methods. **B)** 786-O VHL (+) and VHL (-) cells ($7x10^6$) were incubated for three hours in serum free media and this was considered as time cero for basal levels of RhoA activity. Cells were then maintained in culture for an additional period of 24, 48 and 72 hours. After each time point, cells were lysed and the lysates were incubated overnight with C21-GST. Bound and total RhoA was analyzed by western blot using an anti-RhoA mAb; a representative experiment is shown and the average of three different experiments of VHL (+) (grey bars) and VHL (-) (black bars) is represented; ($P \leq 0.05$).

Figure 5. Effect of expressing a recombinant dominant negative or constitutively active RhoA in VHL (+) and (-) cells. FN matrix formation by 786-O VHL (+) and VHL (-) cells infected with a retroviral vector expressing GFP alone or with a dominant negative (RhoA N19) or a constitutively active (RhoA Q63L) mutants respectively was analyzed by indirect immunofluorescence. Cells ($2x10^5$ cells) were grown for 3-4 days

at 37ºC and 5% CO_2, and FN matrix was detected with a polyclonal anti-FN antibody. A representative experiment of at least three performed is shown.

Figure 6. Analysis of p190RhoGAP phosphorylation state in VHL (+) and VHL (-) RCC cells. 786-O VHL (+) and VHL (-) cell were grown for 72 hours in complete media, then serum starved for three hours and p190RhoGAP was immunoprecipitated from cell lysates ($7x10^6$). Total p190RhoGAP constitutive expression was analyzed by western blot using a specific anti-p190RhoGAP mAb, and phosphorylated p190RhoGAP was measured with the anti-phosphotyrosine mAb PY20. Mock; protein G-agarose beads bound to a non-specific Ab. Quantitation (arbitrary units) of the relative amounts of total p190RhoGAP and phospho-p190RhoGAP are indicated under each band. A representative experiment out of three performed is shown.

Supplementary Figure 1. **VHL (+) and VHL (-) cells infection with a constitutively active or dominant negative RhoA mutants.** 786-O cells and their VHL (+) counterparts were infected with a retroviral vector expressing GFP alone or with a constitutively active (RhoA-Q63L) or dominant negative (RhoA N19) RhoA mutants. Three days after infection GFP counts were measured by flow-cytometry and the protein over-expression was analyzed by western blot using an anti-RhoA mAb.

Supplementary Figure 2. Changes on VHL (-) cells morphology after infection with a constitutively active RhoA mutant. 786-O cells were infected with a retroviral vector expressing GFP alone or with a constitutively active (RhoA-Q63L) mutant. One week after infection 786-O cells were grown to confluence and changes on cell morphology were analyzed with a phase contrast microscope.

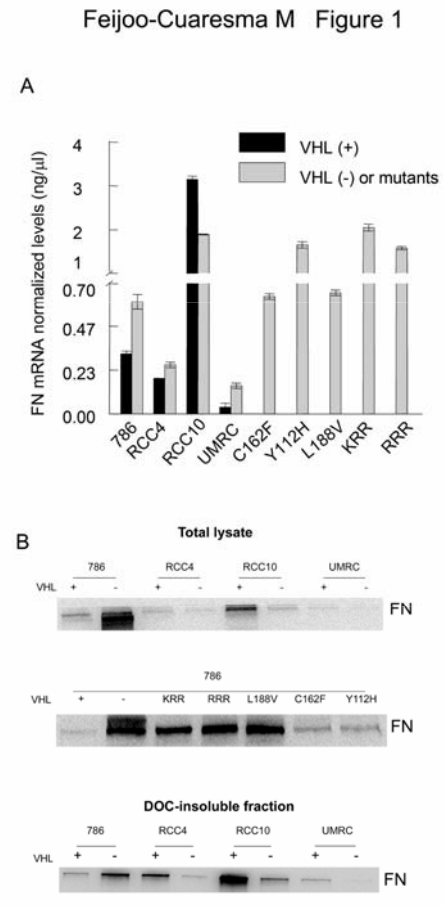

Fijoo-Cuaresma M Figure 2

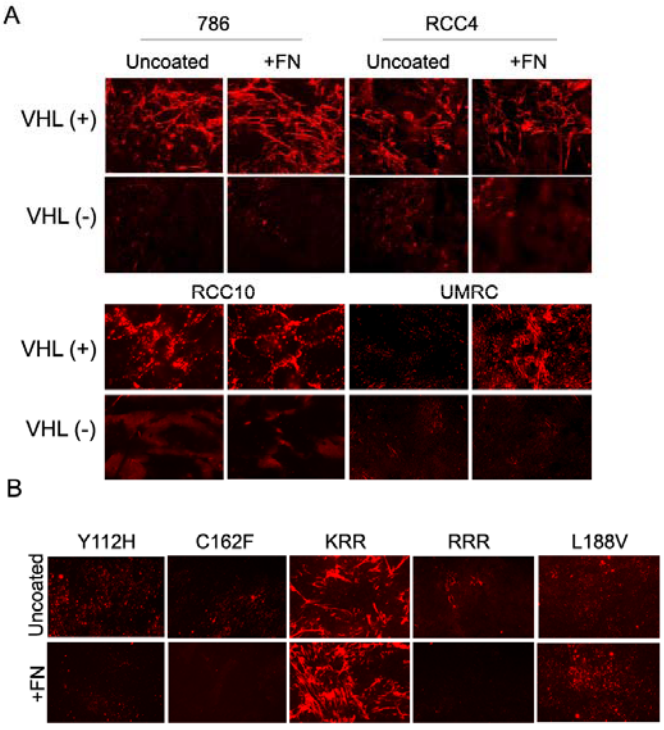

Feijoo-Cuaresma M Figure 3

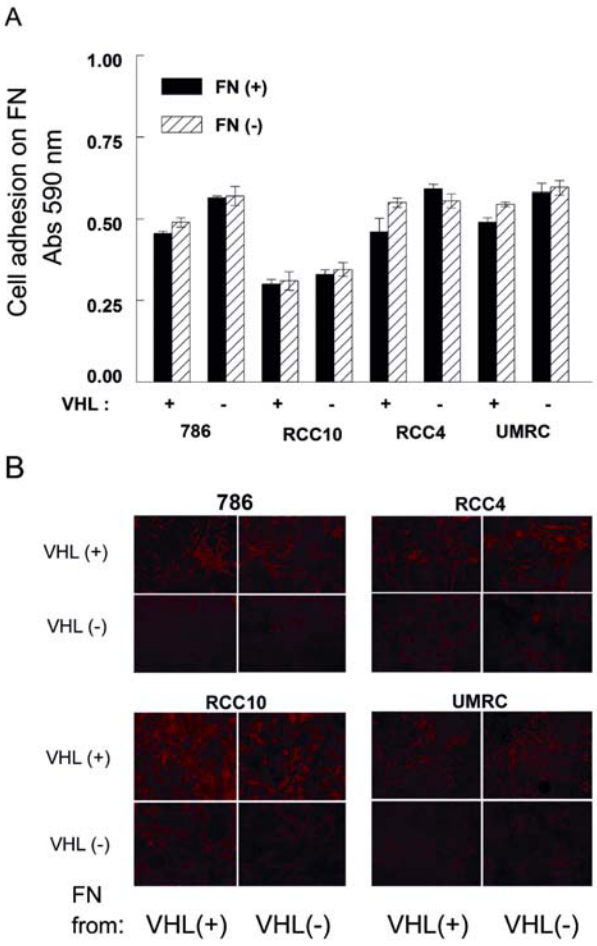

Feijoo-Cuaresma M Figure 4

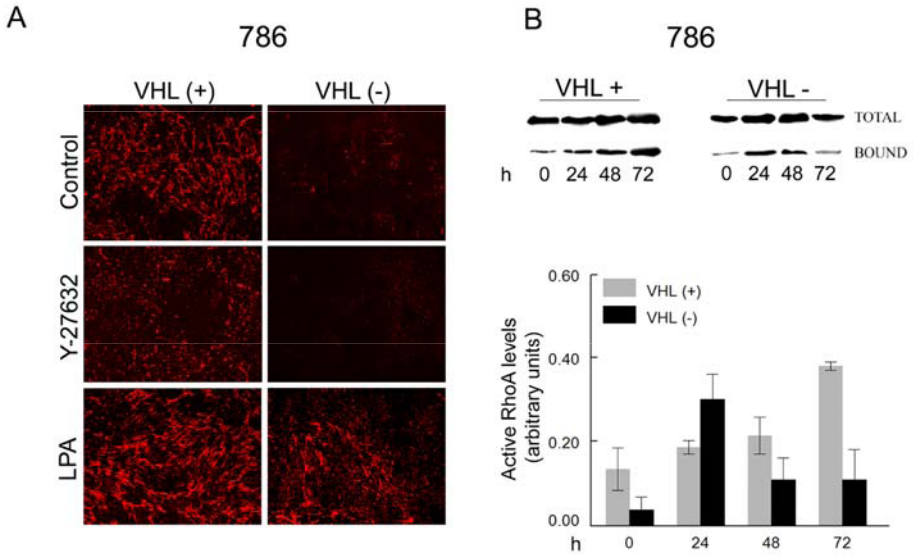

Feijoo-Cuaresma M Figure 5

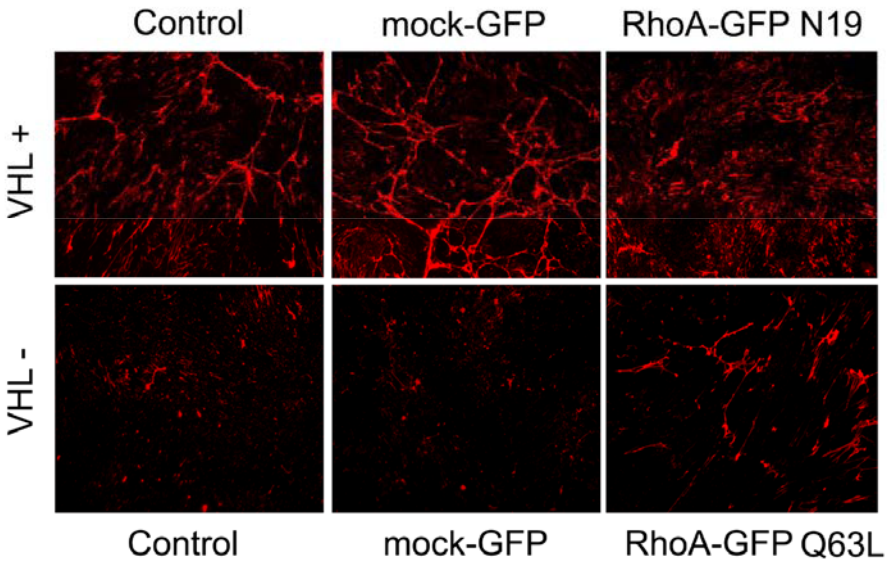

Feijoo-Cuaresma M Figure 6

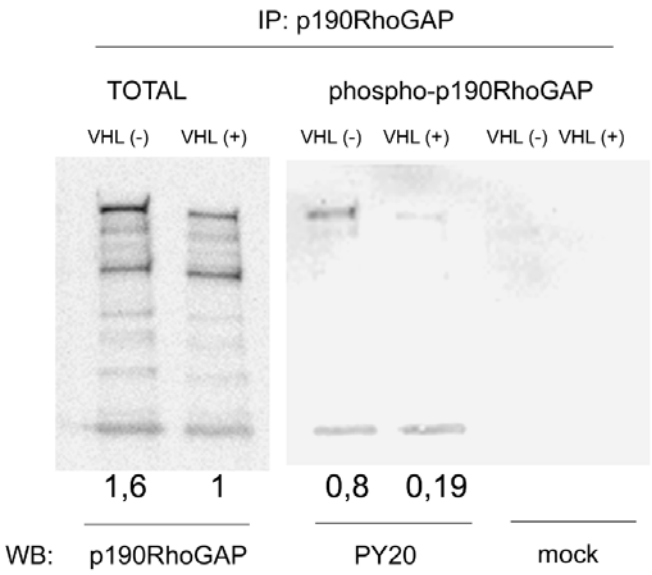

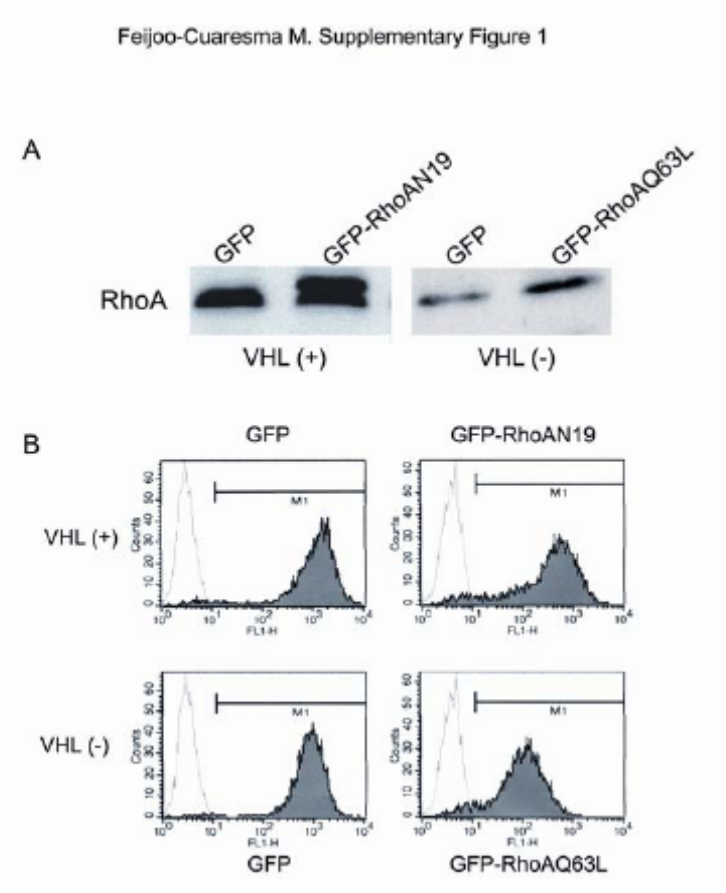

Feijoo-Cuaresma M. Supplementary Figure 2

786-O VHL (-)

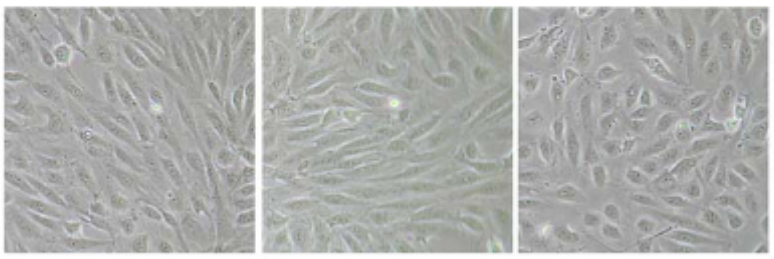

Anexo IV

A synthetic peptide from the heparin-binding domain III (repeats III4–5) of fibronectin promotes stress-fibre and focal-adhesion formation in melanoma cells

José V. MOYANO*, Alfredo MAQUEDA*, Juan P. ALBAR† and Angeles GARCIA-PARDO*[1]

*Departamento de Inmunología, Centro de Investigaciones Biológicas, Consejo Superior de Investigaciones Científicas (CSIC), Velázquez 144, 28006 Madrid, Spain, and †Departamento de Inmunología y Oncología, Centro Nacional de Biotecnología, CSIC, Cantoblanco, 28049 Madrid, Spain

Cell adhesion to fibronectin results in formation of actin stress fibres and focal adhesions. In fibroblasts, this response requires two co-operative signals provided by interactions of the RGD sequence with $\alpha5\beta1$ integrin and the heparin-binding domain II (Hep II) domain with syndecan-4. Within Hep II, this activity was mapped to repeat III13 and to the peptide FN-C/H-V(WQPPRARITGY, repeat III14). We previously described that the synthetic heparin-binding peptide/III5 (HBP/III5) (WTPPRAQITGYRLTVGLTRR, repeat III5) binds heparin and mediates cell adhesion via chondroitin sulphate proteoglycans. We have now studied whether HBP/III5 co-operates with $\alpha5\beta1$ and drives a full cytoskeletal response in melanoma cells. SKMEL-178 cells attached and spread on the RGD-containing FNIII7–FNIII10 (FNIII7–10) fragment, but did not form stress fibres or focal adhesions. Co-immobilization of HBP/III5 with FNIII7–10 or adding soluble HBP/III5 to cells prespread on FNIII7–10, effectively induced these structures. Cell transfection with dominant-negative N19RhoA, a member of the small GTPase family, abolished the HBP/III5 effect. Both chondroitinase and heparitinase diminished focal adhesions, indicating that both types of proteoglycans bound HBP/III5 in melanoma cells. We have mapped the active sequence of HBP/III5 to YRLTVGLTRR, which is a novel sequence in fibronectin with focal-adhesion-promoting activity. The last two arginine (R) residues of this sequence are required for activity, since their replacement by alanine completely abrogated the HBP/III5 cytoskeletal effect. Moreover, this sequence is also active in the context of large fibronectin fragments. Our results establish that the Hep III region provides co-operative signals to $\alpha5\beta1$ for the progression of the cytoskeletal response and that these include activation of RhoA.

Key words: cell-surface proteoglycans, cytoskeletal reorganization, fibronectin heparin-binding domain III (Hep III) domain, heparin-binding peptide, RhoA.

INTRODUCTION

Cell adhesion to fibronectin (FN), a major component of the extracellular matrix, leads to cell spreading and formation of stress fibres and focal adhesions [1,2]. Because this cytoskeleton reorganization is crucial for cell migration and delivery of intracellular signalling, it is important to determine the molecular interactions that regulate the initial post-adhesion events. Previous studies using proteolytic fragments of FN have established that the initial attachment and spreading is mediated by the interaction of the RGD (Arg-Gly-Asp)-containing cell-binding domain (repeats III9–10) with $\alpha5\beta1$ integrin, but that further progression of the cytoskeletal response requires additional signals. These may be provided by the interaction of fragments containing the heparin-binding domain II (Hep II) domain (repeats III12–14) with cell-surface proteoglycans (PG), mainly syndecan-4 [3–5]. Further characterization of these interactions revealed that the synthetic peptide FN-C/H-V, corresponding to the sequence WQPPRARI in FN repeat III14 [6], was a potent inducer of stress fibres and focal adhesions in fibroblasts [7,8] and that endothelial cells [9] attached via RGD/$\alpha5\beta1$. Another report, however, found this sequence inactive when present in a recombinant fragment containing FN repeat III14, and the main focal-adhesion-promoting activity in that study was located to repeat III13 [10], a ligand for syndecan-4 [11]. These apparent discrepancies suggest different signalling requirements dependent on the cell type and/or that the FN-C/H-V peptide may adopt a conformation which is similar to the ligand in repeat III13.

We previously reported that the WTPPRAQITGYRLTV-GLTRR sequence in FN III5 repeat within the Hep III domain, binds heparin and mediates T cell adhesion via chondroitin surface proteoglycans (CSPG) when presented as the synthetic heparin-binding peptide/III5 (HBP/III5) [12]. Because this sequence is similar to FN-C/H-V, we tested in the present study whether HBP/III5 could also provide the additional signalling required for induction of stress fibres and focal adhesions. Using melanoma cells, which, unlike T-cells, form these cytoskeletal structures, we show that HBP/III5 efficiently promotes stress fibres and focal adhesions, and that both CSPG and heparan sulphate proteoglycan (HSPG) are involved in this response. Furthermore, signalling via HBP/III5 involves activation of the small GTPase RhoA.

EXPERIMENTAL

Fibronectin fragments and synthetic peptides

The FNIII7–FNIII10 (FNIII7–10) recombinant fragment (repeats III7–III10 in FN, contains the RGD sequence) was

Abbreviations used: CSIC, Consejo Superior de Investigaciones Científicas; CS(PG), chondroitin sulphate (proteoglycan); DMEM, Dulbeccco's Modified Eagle's medium; FN, fibronectin; FNIII7–10, FNIII7–FNIII10; GFP, green fluorescent protein; HBP, heparin-binding peptide; Hep II, heparin-binding domain II; HS(PG), heparan sulphate (proteoglycan); KLH, keyhole-limpet haemocyanin; mAb, monoclonal antibody; TRITC, tetramethylrhodamine β-isothiocyanate.

[1] To whom correspondence should be addressed (e-mail agarciapardo@cib.csic.es).

Table 1 Synthetic peptides used in the present study

Amino acid sequences are shown in the one-letter code. Mutated arginine (R)→alanine (A) residues are depicted in **bold**.

Peptide name	Peptide sequence
HBP/III5	WTPPRAQITGYRLTVGLTRR
HBP/III5.rv	RRTLGVTLRYGTIQARPPTW
HBP/III5-R1	WTPP**A**AQITGYRLTVGLTRR
HBP/III5-R2	WTPPRAQITGY**A**LTVGLTRR
HBP/III5-R3R4	WTPPRAQITGYRLTVGLT**AA**
HBP/III5-R1R2R3R4	WTPP**A**AQITGY**A**LTVGLT**AA**
N11	WTPPRAQITGY
C10	YRLTVGLTRR
C10-R2	Y**A**LTVGLTRR
C10-R3R4	YRLTVGLT**AA**
C10-R2R3R4	Y**A**LTVGLT**AA**
FN-C/H-V	WQPPRARITGY

prepared by transforming *Escherichia coli* DH5α with FNIII7–10 cDNA in the pET vector, kindly donated by Dr Harold Erickson (Department of Cell Biology, Duke University Medical Center, Durham, NC, U.S.A.), and purified as described in [13]. The H0 recombinant fragment (FN repeats III12–III15, Hep II domain, lacks the IIICS region) was prepared as reported in [14]. The 80 kDa fragment (repeats III4-$_{1/2}$III11) was purified from tryptic digestions of plasma FN as previously described [15,16]. The synthetic peptides prepared and used in the present study are listed in Table 1. All peptides were synthesized on an automated multiple peptide synthesizer (AMS 422; ABIMED Analysen-Technik GmbH, Langenfeld, Germany) and conjugated to keyhole-limpet haemocyanin (KLH from *Megathura crenulata*; Calbiochem–Novabiochem Co., La Jolla, CA, U.S.A.) exactly as described in [12].

Antibodies, enzymes and other reagents

Monoclonal antibodies (mAbs) specific for vinculin and talin were purchased from Sigma (St. Louis, MO, U.S.A.); anti-paxillin mAb was from ICN Biomedicals Inc. (Costa Mesa, CA, U.S.A.); mAbs P1D6 and P4C2, reactive with α5 and α4 integrins respectively, were previously described [17]; anti-(αVβ3 integrin) mAb (LM609) and polyclonal antibody anti-NG2 were purchased from Chemicon International Inc. (Temecula, CA, U.S.A.); anti-syndecan-4 mAb was from Santa Cruz Biotechnologies (Santa Cruz, CA, U.S.A.). Chondroitinase ABC, heparin, heparan sulphate and chondroitin sulphate were purchased from Sigma; heparitinase was from Seikagaku America (Falmouth, MA, U.S.A.).

Cells and immunofluorescence assays

The human cell lines SKMEL-178 (melanoma) and Jurkat (T lymphocytes) were obtained from Dr Francisco Real (Hospital del Mar, Barcelona, Spain) and Dr Margarita López-Trascasa (Hospital La Paz, Madrid, Spain) respectively. Cells were maintained in Dulbecco's Modified Eagle's medium (DMEM; SKMEL-178) or RPMI (Jurkat), 10% fetal-bovine serum (Gibco, Paisley, Renfrewshire, Scotland, U.K.) and 40 μg/ml gentamycin (Gibco). Prior to immunofluorescence assays, cells were serum-starved for 3 h, detached from culture flasks with 1 mM EDTA/PBS, pH 7.5, washed, and resuspended in attachment medium (DMEM/1% BSA/10 mM Hepes). Immunofluorescence assays were carried out on glass coverslips previously coated for 2 h at 37 °C with 0.41 μg (0.71 μM) or 0.06 μg (0.1 μM) of FNIII7–10 in 40 μl of PBS, with or without 11 μl (at 135 μg/ml) of appropriate peptides. After washing and blocking with 1% BSA/PBS, serum-starved 2×10^4 SKMEL-178 cells in attachment medium were added to each well and incubated for 1 h at 37 °C. In some experiments cells were incubated with chondroitinase (1 unit/ml) or heparitinase (2 munit/ml) or both for 45 min at room temperature prior to their addition to substrate-coated wells. Attached cells were fixed with 3.5% formaldehyde/PBS, permeabilized with cold 0.5% Triton X-100/PBS and blocked with 1% BSA/PBS for 30 min. F-actin was stained with tetramethylrhodamine β-isothiocyanate (TRITC)–phalloidin, and focal-adhesion components were detected with specific mAbs (1 h, 37 °C) followed by rabbit FITC-labelled anti-mouse IgG Ab (Dako A/S, Glostrup, Denmark). For inhibition with chondroitin sulfate, heparan sulphate and heparin, the 80 kDa fragment, FNIII7–10 or the mixture FNIII7–10 + HBP/III5 were incubated in solution with 100 μg/ml of either of these reagents for 1 h at 37 °C prior to their immobilization on glass coverslips, and the assay was continued as explained above in the presence of these reagents. Samples were visualized under an epifluorescence Axioplan microscope (Zeiss, Oberkochen, Germany) and photographed with a CCD camera (Photometrics Inc., Tucson, AZ, U.S.A.). At least 100 cells were scored in each assay.

Cell-adhesion assays

Flat-bottomed eight-well strips with an *N*-oxysuccinimide amine binding surface (Costar, Cambridge, MA) were coated for 1–2 h with increasing concentrations of FNIII7–10 fragment diluted in 0.1 M sodium borate, pH 8.5. SKMEL-178 cells (20×10^3) with or without previous incubation with P1D6, LM609 or P4C2 mAbs or with enzymes [45 min at room temperature (23 °C)] were added to the wells and adhesion was allowed to occur for 1 h at 37 °C. Attached cells were fixed with 1.25% formaldehyde and stained with 0.1% Toluidine Blue in PBS. A_{620} was determined on a Multiskan Bichromatic plate reader (Labsystems, Helsinki, Finland), and quantification of cell attachment was done using calibration curves as described in [12,16]. The absorbance was found to be practically a linear function of the number of cells attached (1 A unit = 80×10^3 cells).

Cell transfection

Green fluorescent protein (GFP) fused to RhoA cDNAs encoding for V14RhoA (active mutant) or N19RhoA (dominant- negative) cloned into the pEGFP-C1 vector (Clontech, Palo Alto, CA, U.S.A.) in *E. coli* DH5α, were a gift from Dr Francisco Sánchez-Madrid (Hospital de la Princesa, Madrid, Spain). Plasmidic DNA from *E. coli* was isolated by performing minipreps. Subconfluent cells in fresh complete medium were transiently transfected with these cDNAs or with the empty vector using FuGENE™ 6 (Roche Biochemicals, Mannheim, Germany), following the manufacturer's instructions. After 24 h, transfected cells were used in immunofluorescence assays.

Statistical analyses

Significance of the difference between means was determined by the Student's t test for non-paired samples using the GraphPad Instat program (GraphPad Software, San Diego, CA, U.S.A.). Two-tailed statistical significances were determined. A P value of $\leqslant 0.05$ was considered significant.

RESULTS AND DISCUSSION

The WTPPRAQITGYRLTVGLTRR sequence (HBP/III5) promotes stress fibres and focal adhesions in melanoma cells

Initial characterization of SKMEL-178 cell adhesion to the FNIII7–10 fragment revealed that these cells attached to FNIII7–10 in a dose-dependent manner and that adhesion was completely blocked by the anti-α5 integrin mAb P1D6 but not by LM603 (anti-$\alpha V\beta 3$) or P4C2 (anti-α4) mAbs (Figure 1), indicating that $\alpha 5\beta 1$ was the receptor for FNIII7–10 in SKMEL-178 cells. To characterize the cytoskeletal response following attachment to this fragment, SKMEL-178 cells were added to glass coverslips coated with FNIII7–10 at 0.1 μM or 0.71 μM respectively. As shown in Figure 2(A) (left panels), melanoma cells attached to both concentrations of FNIII7–10, but the resulting morphological patterns were very different: at 0.1 μM, more than 80 % of cells showed limited spreading with extension of lamellipodia and absence of stress fibres and focal adhesions (Figures 2A and 2C); at the higher concentration of 0.71 μM, most cells displayed an elongated morphology, and approx. 70 % of them formed stress fibres (Figure 2A) and weak focal adhesions containing vinculin, little paxillin and no talin (Figure 2B).

To determine whether the HBP/III5 synthetic peptide (see Table 1) could provide a co-operative signal to $\alpha 5\beta 1$-integrin-mediated cytoskeletal reorganization, similar experiments were performed on glass coverslips coated with a mixture of FNIII7–10 and HBP/III5 peptide (135 μg/ml) coupled to KLH. Co-immobilization of HBP/III5 with FNIII7–10 dramatically induced cell spreading and formation of stress fibres on 86 % of cells plated on 0.1 μM FNIII7–10 (Figures 2A and 2C). HBP/III5 also clearly enhanced spreading and the number of stress fibres at the higher concentration of 0.71 μM FNIII7–10 (Figure 2A).

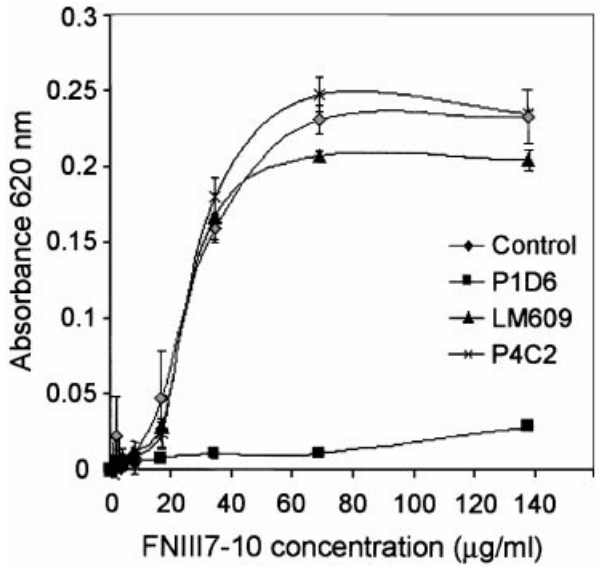

Figure 1 Melanoma-cell adhesion to the FNIII7–10 fragment is mediated by $\alpha 5\beta 1$ integrin

Cells (20×10^3), with or without (control) previous incubation with mAbs P1D6, LM609 or P4C2 (2 μg each), were added to wells coated with the indicated concentrations of FNIII7–10. After 1 h at 37 °C, attached cells were fixed, stained with 0.1 % Toluidine Blue and quantified by measuring the A_{620} as described in the Experimental section. Average values from three different experiments are shown.

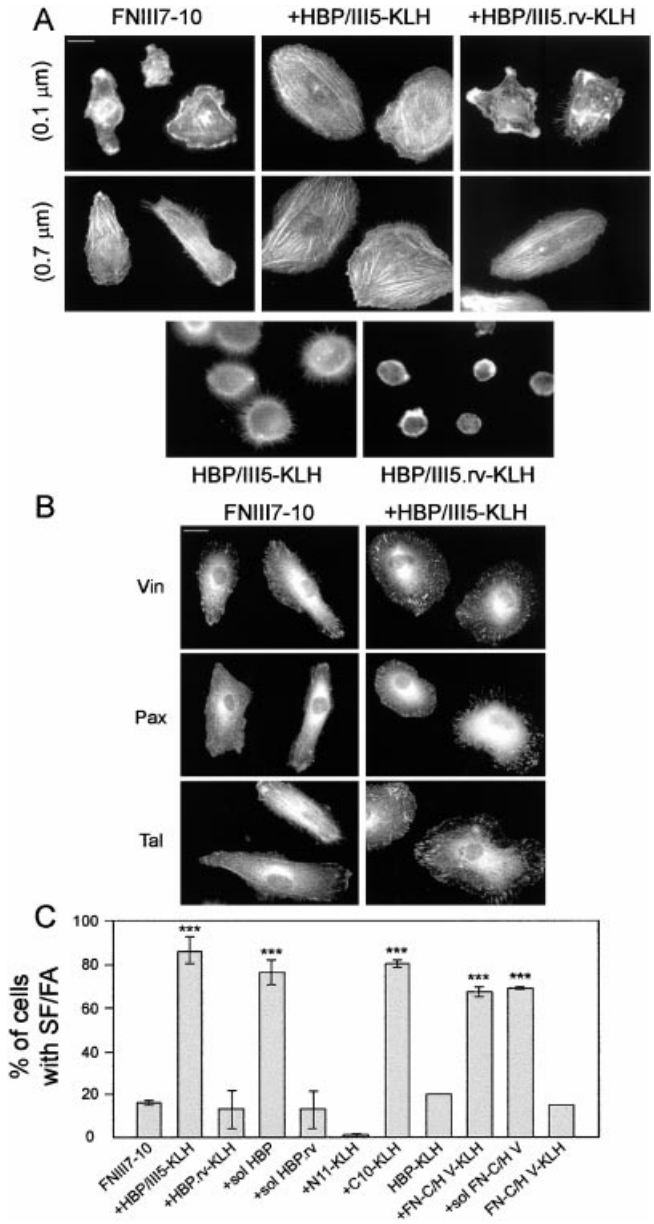

Figure 2 HBP/III5 peptide promotes stress fibres and focal adhesions

(**A**) SKMEL-178 cells (2×10^4) were added to glass coverslips previously coated with FNIII7–10 (0.1 or 0.7 μM respectively) alone or mixed with 135 μg/ml of HBP/III5 or HBP/III5.rv peptides coupled with KLH. After 1 h at 37 °C, actin filaments were visualized with TRITC/phalloidin. Cells were also added to coverslips coated with HBP/III5–KLH or HBP/III5.rv–KLH alone. The bar represents 10 μm. (**B**) Focal adhesions on cells plated on 0.7 μM FNIII7–10 + HBP–KLH were detected by staining with specific monoclonal antibodies to vinculin, paxillin and talin. The bar represents 10 μm. (**C**) Quantification of the effect of co-immobilization of peptides (135 μg/ml) with FNIII7–10 (0.1 μM) or addition of soluble (sol) peptides to cells prespread on FNIII7–10 for 1 h. The effect of immobilized peptides alone is also indicated. See Table 1 for the sequence of each peptide. SF, stress fibres; FA, focal adhesions. Values represent the average for at least three different experiments. ***$P \leqslant 0.001$.

Additionally, HBP/III5 induced formation of focal adhesions on cells plated on both concentrations of FNIII7–10 (shown in Figure 2B for 0.71 μM). These structures were more developed than those observed on 0.71 μM FNIII7–10 alone, since they now contained paxillin and talin besides vinculin (Figure 2B).

The primary structure of HBP/III5 was important for the activity, since reversing the entire sequence (HBP/III5.rv, Table 1) rendered the peptide inactive (Figures 2A and 2C). Cell adhesion to HBP/III5–KLH alone produced very limited spreading and no stress fibres or focal adhesions (Figures 2A and 2C). Cells attached to the control HBP/III5.rv (or to KLH; results not shown) remained round, with no appreciable spreading (Figure 2A).

The HBP/III5 peptide was also equally active (80% of cells with stress fibres) when co-immobilized with FNIII7–10 as a free peptide rather than coupled to KLH (results not shown). Moreover, soluble HBP/III5 (135 μg/ml) efficiently induced stress fibres and focal adhesions on cells pre-spread on FNIII7–10 for 60 min, whereas the control peptide HBP/III5.rv had no effect (Figure 2C). However, cells attached to HBP/III5–KLH did not form stress fibres or focal adhesions upon addition of FNIII7–10 (0.1 μM) in soluble form, indicating that immobilization of this fragment was required for the observed cytoskeleton reorganization (results not shown).

For comparison, we also tested the effect of the previously described FN-C/H-V peptide [6–8] (Table 1) in our melanoma cell system. As shown in Figure 2(C), immobilized FN-C/H-V-KLH peptide or soluble FN-C/H-V (135 μg/ml) significantly induced stress fibres and focal adhesions, but was 20% less efficient than HBP/III5. Furthermore, FN-C/H-V was inactive when co-immobilized with FNIII7–10 as a free peptide, in contrast with HBP/III5 (results not shown). While these differences suggest that HBP/III5 may be a better ligand for melanoma cell surface PG (see below), it should also be considered that HBP/III5 is a 20-residue peptide, while FN-C/H-V contains only 11 residues, and this may affect binding of the free peptide to the glass surface.

In a previous study the major activity of FN-C/H-V was mapped to the sequence PRARI [7], which is homologous to PRAQI, present in HBP/III5 (see Table 1). To determine whether PRAQI was the active sequence in HBP/III5 or there was a different site responsible for the cytoskeletal effect of this peptide, we prepared two smaller peptides, N11 and C10, corresponding to the N- and C-terminal halves respectively of HBP/III5 (see Table 1). As shown in Figure 2(C), C10 fully retained the ability to induce stress fibres and focal adhesions, while N11, containing PRAQI, did not. These results are in agreement with our previous findings showing that the C10 peptide retained partial heparin-binding activity, while the N11 peptide did not bind to heparin [12]. The lack of activity of the PRAQI sequence (HBP/III5) compared with the previously described sequence PRARI (FN-C/H-V) suggests that that the presence of two basic residues may be important for receptor recognition. To determine the role of the arginine residues in the activity of HBP/III5, we replaced each arginine with an alanine residue in both the HBP/III5 and C10 peptides (Table 1) and tested the effect of the mutated peptides on cell adhesion and cytoskeleton reorganization. As shown in Figure 3(A), mutation of the first arginine residue in HBP/III5 (HBP/III5-R1) did not affect the adhesion-mediating properties of this peptide, in agreement with the lack of cytoskeletal activity of the N11 sequence (Figure 2C). Mutation of the second arginine residue (HBP/III5-R2) or the equivalent arginine residue in C10 (C10-R2) decreased their ability to mediate adhesion by 25% (Figure 3A), suggesting a minor involvement of this residue in the activity of the peptides. In contrast, when the last two arginine residues were replaced by alanine (HBP/III5-R3R4 and C10-R3R4; Table 1), the resulting peptides no longer mediated cell adhesion (Figure 3A). Likewise, peptides HBP/III5-R1, HBP/III5-R2 and C10-R2 promoted stress fibres and focal adhesions as effectively as the parent

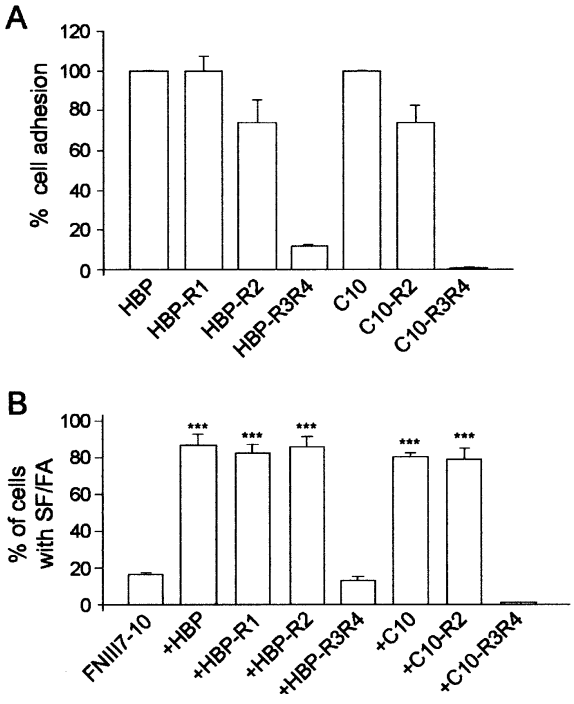

Figure 3 Effect of point mutations on the biological activity of HBP/III5 and C-10 peptides

(**A**) Melanoma-cell adhesion to the parental peptide HBP/III5 and various mutated peptides (see Table 1). Cells (20×10^3) were added to wells coated with the indicated peptides at 2.5 μg/cm^2. After 1 h, attached cells were fixed, stained with 0.1% Toluidine Blue, and quantified by measuring the A_{620} as explained above. Values represent the average for two independent experiments. (**B**) Parental or mutated peptides (135 μg/ml) were co-immobilized with FNIII7–10 (0.1 μM) and the number of cells showing stress fibres (SFs) and focal adhesions (FAs) was quantified using an epifluorescence microscope. Values are the average for three independent experiments. $^{***}P \leqslant 0.001$.

peptides (Figure 3B). However, mutation of the two C-terminal arginine residues (HBP/III5-R3R4 and C10-R3R4 peptides) completely inhibited their ability to promote stress fibres and focal adhesions (Figure 3B). As expected, mutation of all four arginine residues in HBP/III5 or the three arginine residues in C10 abolished the activity of both peptides (results not shown). These findings clearly demonstrate that the stress-fibre/focal-adhesion-promoting function of the HBP/III5 peptide resides in the C-terminal sequence YRLTVGLTRR and that the last two arginine residues are required for its activity.

CS and HS proteoglycans are melanoma-cell receptors for the HBP/III5 sequence

We previously showed that the cellular receptor for the HBP/III5 sequence in Jurkat T cells is a CSPG [12]. To determine the nature of the receptor involved in the cytoskeleton effect observed in melanoma cells, SKMEL-178 cells were incubated with chondroitinase ABC or heparitinase prior to their addition to FNIII7–10 or FNIII7–10 + HBP/III5. As shown in Table 2, these enzymes had no effect on the morphological pattern observed on cell adhesion to FNIII7–10. However, on mixed substrata, both chondroitinase and heparitinase diminished the proportions of cells with stress fibres and focal adhesions to 49 and 51% respectively (Table 2). Interestingly, the effect of the individual enzymes was additive, since treatment with both enzymes simultaneously completely reverted the focal-adhesion-

Table 2 Effect of enzymes on stress-fibre/focal-adhesion formation

Cells were treated with either or both enzymes and added to coverslips coated with FNIII7–10 or FNIII7–10 + HBP/III5. Values represent the mean for three different experiments.

	Proportion of cells with stress fibres or focal adhesions (%)	
Treatment	FNIII7–10	FNIII7–10 + HBP/III5
None	17.3 ± 2.2	75.2 ± 6.9
Chondroitinase ABC	20.9 ± 7.1	49.3 ± 2.8
Heparitinase	28.4 ± 4.7	50.9 ± 4.4
Chondroitinase ABC + heparitinase	21.5 ± 3.4	23.2 ± 2.5

Table 3 Effect of enzymes on cell adhesion

Cells treated with individual or combined enzymes were added to wells coated with the different peptides or the recombinant fragment H0 (Hep II domain). Values represent the average for three different experiments. Abbreviation: ND, not determined.

		Cell adhesion (%)				
	Cells ...	Jurkat			SKMEL-178	
Treatment	Substrate ...	HBP/III5	C10	H0	HBP/III5	C10
None		100	100	100	100	100
Chondroitinase ABC		0	0	90.5 ± 3.31	70.0 ± 7.1	54.0 ± 8.4
Heparitinase		96.0 ± 2.1	ND	5.5 ± 6.36	65.0 ± 3.5	54.5 ± 10.7
Chondroitin ABC + heparitinase		ND	ND	ND	17.5 ± 3.5	18.5 ± 8.5

promoting activity of HBP/III5 (Table 2). To confirm that the partial inhibition obtained with either enzyme alone was not due to poor enzymic activity, in parallel experiments we tested the effect of chondroitinase and heparitinase on the adhesion of Jurkat cells to HBP/III5, C10 and the H0 fragment. We have previously shown that Jurkat cell adhesion to HBP/III5 is completely dependent on CSPG but not HSPG and, by contrast, adhesion to the H0 fragment is mediated by HSPG [12]. In agreement with these previous results, Table 3 shows that chondroitinase ABC, at the same concentration used for the SKMEL-178 assays, completely inhibited Jurkat-cell adhesion to the HBP/III5 and C10 peptides, indicating that the enzyme was fully active. Similarly, preincubation of Jurkat cells with heparitinase completely blocked their adhesion to the H0 fragment, again confirming the activity of this enzyme (Table 3). These results suggested that, in contrast with our previous findings on Jurkat cells, recognition of the HBP/III5 sequence by melanoma cells involves both CSPG and HSPG. To confirm this, we performed adhesion assays to HBP/III5 and C10 peptides after preincubation of SKMEL-178 cells with either or both enzymes. As shown in Table 3, either chondroitinase or heparitinase when used alone, partially inhibited cell adhesion to both peptides, whereas the combination of both enzymes produced almost complete inhibition, in agreement with the results observed on cytoskeleton reorganization. Identical results were obtained for inhibition of adhesion to the HBP/III5-R1, HBP/III5-R2 and C-10-R2 peptides (results not shown). Altogether these data indicate that the sequence HBP/III5 interacts with both CSPG and HSPG at the melanoma-cell surface or, alternatively, with a unique PG that carries both CS and HS glycosaminoglycan chains, and that both chains appear to contribute to peptide

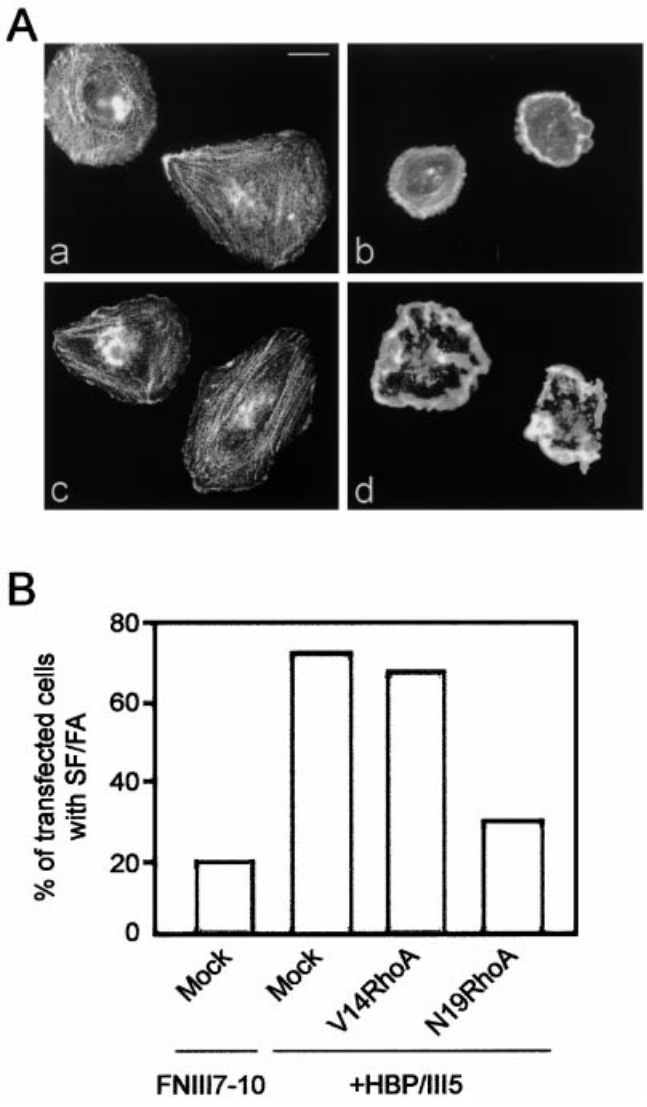

Figure 4 RhoA is involved in the cytoskeletal effect of HBP/III5 peptide

(**A**) SKMEL-178 cells were transiently transected with GFP–V14RhoA (panel a), GFP–N19RhoA (panel b), or GFP-empty vector (panels c and d) and added to coverslips coated with mixtures of FNIII7–10 (0.1 μM) + HBP/III5 (135 μg/ml) (panels a–c) or FNIII7–10 alone (panel d). Actin was visualized with TRITC/phalloidin. Only transfected cells, identified by fluorescence, are shown. The bar represents 10 μm. (**B**) Quantification of the effect of transfecting cells with V14RhoA or N19RhoA on formation of stress fibres (SF) and focal adhesions (FA). 'Mock' denotes transfection with the empty vector. The coating substrate (FNIII7–10 or FNIII7–10 + HBP/III5) is also indicated.

recognition. It is likely that the type of PG that recognizes HBP/III5 is cell-dependent, as already shown for the FN-C/H-V peptide, which interacts with HSPG in fibroblasts, but with both HS and CS PG in monocytic cells [18].

RhoA is involved in the cytoskeleton organization induced by HBP/III5-PG interaction

Although induction of stress fibres and focal adhesions in several cell types generally involves activation of the small GTPase RhoA [19,20], it was important to determine whether the novel signalling pathway provided by interaction of HBP/III5 with melanoma-cell-surface PG involved RhoA. We therefore tran-

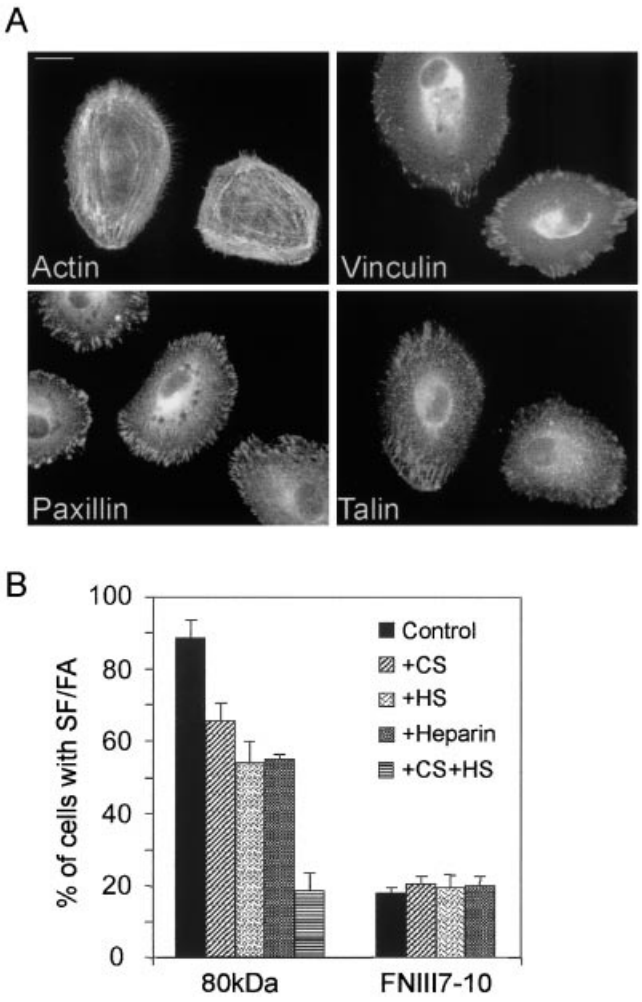

Figure 5 The HBP/III5 sequence is active in the context of a tryptic FN fragment

(**A**) SKMEL-178 cells (2×10^4) were added to glass coverslips previously coated with 0.1 μM 80 kDa fragment. After 1 h at 37 °C, actin filaments were visualized with TRITC/phalloidin and focal adhesions with specific mAbs to vinculin, paxillin and talin. The bar represents 10 μm. (**B**) The 80 kDa or FNIII7–10 fragments (0.1 μM) were incubated with 100 μg/ml of CS, HS, heparin or the mixture CS + HS for 1 h and used to coat glass coverslips. Cells were added and after 1 h, stress fibres (SF) and focal adhesions (FA) were quantified as described above. Values represent the mean for three different experiments.

siently transfected SKMEL-178 cells with the constitutively active V14RhoA or the dominant-negative N19RhoA forms, and studied their cytoskeleton reorganization upon attachment to FNIII7–10 + HBP/III5 or FNIII7–10 alone. On mixed substrata, the presence of the active GFP–V14RhoA did not significantly affect the cytoskeletal structures induced by HBP/III5, and 68 % of transfected cells displayed stress fibres (Figures 4A and 4B) and focal adhesions (results not shown), suggesting that maximal activation of RhoA was already achieved by the HBP/III5–PG interaction. By contrast, transfection with the dominant-negative GFP–N19RhoA resulted in reduced spreading and complete absence of stress fibres on 71 % of transfected cells (Figures 4A and 4B), a pattern that resembled that shown by mock-transfected cells on FNIII7–10 (Figure 4A). In agreement with this, transfection with GFP–V14RhoA induced spreading and stress-fibre formation on cells attached to FNIII7–10 alone (not shown). Transfection with the empty vector did not alter the stress-fibre pattern observed on cells attached to FNIII7–10 + HBP/III5 (Figure 4A). These results indicate that an active RhoA is required for induction of stress fibres and focal adhesions by HBP/III5 and that constitutively active RhoA can substitute for the effect of HBP/III5.

The YRLTVGLTRR sequence is active in the context of an 80 kDa FN tryptic fragment

Our results therefore establish that PG interaction with the YRLTVGLTRR sequence contained in the HBP/III5 and C10 peptides provides a novel co-operative signal to $\alpha5\beta1$-mediated cytoskeleton reorganization. The role of this sequence in the context of the entire FN molecule may be difficult to evaluate because of the presence of the Hep II domain, which is known to effectively induce stress fibres and focal adhesions on fibroblasts attached via $\alpha5\beta1$ [3]. We therefore studied whether the YRLTVGLTRR sequence was active in the context of large FN fragments devoid of the Hep II domain and which are usually present in many normal and pathological situations [21]. To this purpose, we analysed the melanoma cytoskeleton response upon adhesion to an 80 kDa tryptic fragment corresponding to FN repeats III4-$_{1/2}$III11 and thus containing the YRLTVGLTRR sequence (located in repeat III5) as well as the entire FNIII7–10 fragment [16]. As shown in Figure 5(A), adhesion of SKMEL-178 cells to the 80 kDa fragment (0.1 μM) resulted in cell spreading and formation of stress fibres and focal adhesions, which contained vinculin, paxillin and talin. This cytoskeletal response resembled that obtained when HBP/III5 was co-immobilized (or added in solution) with FNIII7–10 (see Figure 2A) and was very different from the response induced by FNIII7–10 alone (Figure 2A). These results suggested that the YRLTVGLTRR sequence (the only sequence in repeats III4–6 reported to bind heparin and PG [12]) was active when present in large FN fragments such as the 80 kDa and promoted stress-fibre and focal-adhesion formation. Indeed, we have previously shown that the 80 kDa fragment can be purified by heparin–Sepharose affinity chromatography, thus confirming that the heparin/PG-binding site is exposed in the fragment [15]. To prove further that the cytoskeleton organization induced by the 80 kDa fragment was mediated by interaction with cell-surface PG, this fragment was incubated in solution with CS, HS, heparin, or the mixture CS + HS, prior to its use as adhesion substrate. Treatment with these reagents partially inhibited cell spreading, stress fibres and focal adhesions, whereas pre-incubation with the mixture CS + HS completely abolished these structures (Figure 5B), resulting in a pattern very similar to that induced by the FNIII7–10 fragment (see Figure 2A). As expected, preincubation of FNIII7–10 with HS, CS or heparin did not affect the melanoma cytoskeletal response to this fragment (Figure 5B). These results confirmed that the HBP/III5 sequence was functional in the context of a large 80 kDa FN fragment and that disruption of its interaction with cell surface PG clearly impaired the cytoskeletal response induced by the 80 kDa fragment. Our results also establish that the requirements for this response may be different depending on the cell type. In this regard, fibroblasts have been shown to spread upon attachment to 85 or 105 kDa FN fragments, very similar to the 80 kDa used in the present study, but did not form the stress fibres or focal adhesions [3,7] that we observe on melanoma cells.

Co-operative interactions between integrins and PG have been extensively studied in fibroblasts attached to FN, where it is clear that $\alpha5\beta1$ and syndecan-4 co-operate in the progression of the cytoskeletal response [3–5]. These studies have shown that syndecan-4 signalling depends on RhoA activation [5], in agree-

ment with our present findings on HBP/III5 signalling. It is also clear that syndecan-4 is present in focal adhesions [22] and that the FN-C/H-V peptide causes syndecan-4 to relocate to these complexes [4]. The SKMEL-178 cells used in the present study did not express syndecan-4 (results not shown) and therefore another HSPG must recognize HBP/III5 (and peptide FN-C/H-V). Previous studies have shown that the main CSPG in melanoma cells is NG2 [23], which co-operates with $\alpha4\beta1$ integrin to promote spreading and focal adhesions, but is not found in these complexes [24]. In agreement with this, SKMEL-178 cells expressed NG2, but we were unable to detect it in focal adhesions (results not shown).

Our present results constitute a novel example of collaboration between integrins and PG that leads to a full cytoskeletal response upon attachment to FN. As mentioned above, previous studies on melanoma cells have focused on the co-operation between $\alpha4\beta1$ integrin and CSPG [24,25]. We now show, in the present study, that CSPG (and HSPG) can also signal in a co-operative manner with $\alpha5\beta1$ integrin in melanoma cells. We have identified the sequence in HBP/III5 that triggers this signalling as YRLTVGLTRR, which corresponds to the C-terminal portion of this peptide. It is noteworthy that the N-terminal sequence of HBP/III5 (WTPPRAQITGY), which is homologous with the previously described FN-C/H-V peptide (WQPPRARITGY), was clearly inactive in our system and YRLTVGLTRR is therefore a novel sequence in FN with the ability to induce stress fibres and focal adhesions. As we show, on the basis of point-mutation experiments, the last two arginine residues of this sequence are required for the biological effect. This may explain why the FN-C/H-V peptide was also active in the present study, since it contains two arginine residues (PRARI) which are absent in the N-terminus of HBP/III5 (PRAQI). Our results also suggest that the two arginine residues must be in the proper conformation, since altering the primary sequence of HBP/III5 (as in HBP/III5.rv peptide) abolished the cytoskeletal effect. The novel YRLTVGLTRR sequence described here is located in repeat III5 within the Hep III domain. Thus our results establish that at least two regions in FN (the previously described Hep II domain and the Hep III domain reported here) can modulate the cytoskeletal response initiated by $\alpha5\beta1$ integrin engagement and induce intracellular signalling. We show that the YRLTVGLTRR sequence is active in the context of large FN fragments and possibly also in the context of the entire FN molecule. The contribution of either or both heparin-binding domains to the regulation of cytoskeleton organization will probably depend on the presence of appropriate receptors in a given cell type and environment.

We thank Mercedes Hernández del Cerro for excellent technical assistance. This work was supported by grant SAF2000-0124 from the Comisión Interministerial de Ciencia y Tecnología (CICYT). J.V.M. was supported by a fellowship from GlaxoSmithKline.

REFERENCES

1 Sastry, S. K. and Burridge, K. (2000) Focal adhesions: a nexus for intracellular signalling and cytoskeletal dynamics. Exp. Cell Res. **262**, 25–36
2 Geiger, B., Bershadsky, A., Pankov, R. and Yamada, K. M. (2001) Transmembrane extracellular matrix–cytoskeleton crosstalk. Nat. Rev. Mol. Cell Biol. **2**, 793–805
3 Woods, A., Couchman, J. R., Johansson, S. and Hook, M. (1986) Adhesion and cytoskeletal organization of fibroblasts in response to fibronectin fragments. EMBO J. **5**, 665–670
4 Woods, A., Longley, R. L., Tumova, S. and Couchman, J. R. (2000) Syndecan-4 binding to the high affinity heparin-binding domain of fibronectin drives focal adhesion formation in fibroblasts. Arch. Biochem. Biophys. **374**, 66–72
5 Saoncella, S., Echtermeyer, F., Denhez, F., Nowlem, J. K., Mosher, D. F., Robinson, S. D., Hynes, R. O. and Goetinck, P. F. (1999) Syndecan-4 signals cooperatively with integrins in a Rho-dependent manner in the assembly of focal adhesions and actin stress fibres. Proc. Natl. Acad. Sci. U.S.A. **96**, 2805–2810
6 Mooradian, D. L., McCarthy, J. B., Skubitz, A. P., Cameron, D. J. and Furcht, L. T. (1993) Characterization of FN-C/H-V, a novel synthetic peptide from fibronectin that promotes rabbit corneal epithelial cell adhesion, spreading, and motility. Invest. Ophthalmol. Vis. Sci. **34**, 153–164
7 Woods, A., McCarthy, J. B., Furcht, L. T. and Couchman, J. R. (1993) A synthetic peptide from the COOH-terminal heparin-binding domain of fibronectin promotes focal adhesion formation. Mol. Biol. Cell **4**, 605–613
8 Huhtala, P., Humphries, M. J., McCarthy, J. B., Tremble, P. M., Werb, Z. and Damsky, C. H. (1995) Cooperative signalling by $\alpha5\beta1$ and $\alpha4\beta1$ integrins regulates metalloproteinase gene expression in fibroblasts adhering to fibronectin. J. Cell Biol. **129**, 867–879
9 Huebsch, J. C., McCarthy, J. B., Diglio, C. A. and Mooradian, D. L. (1995) Endothelial cell interactions with synthetic peptides from the carboxy-terminal heparin-binding domains. Circ. Res. **77**, 43–53
10 Bloom, L., Ingham, K. C. and Hynes, R. (1999) Fibronectin regulates assembly of actin filaments and focal contacts in cultured cells via the heparin-binding site in repeat III13. Mol. Biol. Cell **10**, 1521–1536
11 Huang, W., Chiquet-Ehrismann, R., Moyano, J. V., Garcia-Pardo, A. and Orend, G. (2001) Interference of tenascin-C with syndecan-4 binding to fibronectin blocks cell adhesion and stimulates tumor cell proliferation. Cancer Res. **61**, 8586–8594
12 Moyano, J. V., Carnemolla, B., Albar, J. P., Leprini, A., Gaggero, B., Zardi, L. and Garcia-Pardo, A. (1999) Cooperative role for activated $\alpha4\beta1$ integrin and chondroitin sulfate proteoglycans in cell adhesion to the heparin III domain of fibronectin. Identification of a novel heparin and cell binding sequence in repeat III5. J. Biol. Chem. **274**, 135–142
13 Aukhil, I., Joshi, P., Yan, Y. and Erickson, H. P. (1993) Cell- and heparin-binding domains of the hexabrachion arm identified by tenascin expression proteins. J. Biol. Chem. **268**, 2542–2553
14 Mould, A. P., Askari, J. A., Craig, S. E., Garrat, A. N., Clements, J. and Humphries, M. J. (1994) Integrin $\alpha4\beta1$-mediated melanoma cell adhesion and migration on vascular cell adhesion molecule-1 (VCAM-1) and the alternatively spliced IIICS region of fibronectin. J. Biol. Chem. **269**, 27224–27230
15 Garcia-Pardo, A., Ferreira, O. C., Valinsky, J. and Bianco, C. (1989) Fibronectin receptors of mononuclear phagocytes: binding characteristics and biochemical isolation. Exp. Cell Res. **181**, 420–431
16 Sánchez-Aparicio, P., Domínguez-Jiménez, C. and Garcia-Pardo, A. (1994) Activation of the $\alpha4\beta1$ integrin through the $\beta1$ subunit induces recognition of the RGDS sequence in fibronectin. J. Cell Biol. **126**, 271–279
17 Wayner, E. A., Garcia-Pardo, A., Humphries, M. E., McDonald, J. A. and Carter, W. G. (1989) Identification and characterization of the T lymphocyte adhesion receptor for an alternative cell attachment domain (CS-1) in plasma fibronectin. J. Cell Biol. **109**, 1321–1330
18 Kato, K., Mohri, H., Tamura, T. and Okubo, T. (1997) A synthetic peptide, FN-C/H-V, from the C-terminal heparin-binding domain of fibronectin pomotes adhesion of PMA stimulated U937 cells. Biochem. Biophys. Res. Commun. **239**, 205–211
19 Bishop, A. and Hall, A. (2000) Rho GTPases and their effector proteins. Biochem. J. **348**, 241–255
20 Ridley, A. (2001) Rho family proteins: coordinating cell responses. Trends Cell Biol. **11**, 471–477
21 Basbaum, C. B. and Werb, Z. (1996) Focalized proteolysis: spatial and temporal regulation of extracellular matrix degradation at the cell surface. Curr. Opin. Cell Biol. **8**, 731–738
22 Woods, A. and Couchman, J. R. (1994) Syndecan-4 heparan sulfate proteoglycan is a selectively enriched and widespread focal adhesion component. Mol. Biol. Cell **5**, 183–192
23 Bumol, T. F. and Reisfeld, R. A. (1982) Unique glycoprotein–proteoglycan complex defined by monoclonal antibody on human melanoma cells. Proc. Natl. Acad. Sci. U.S.A. **79**, 1245–1249
24 Iida, J., Meijne, A. M. L., Spiro, R. C., Roos, E., Furcht, L. T. and McCarthy, J. B. (1995) Spreading and focal contact formation of human melanoma cells in response to stimulation of both melanoma-associated proteoglycan (NG2) and $\alpha4\beta1$ integrin. Cancer Res. **55**, 2177–2185
25 Eisenmann, K. M., McCarthy, J. B., Simpson, M. A., Keely, P. J., Guan, J.-L., Tachibana, K., Lim, L., Manser, E., Furcht, L. T. and Iida, J. (1999) Melanoma chondroitin sulphate proteoglycan regulates cell spreading through Cdc42, Ack-1 and $p130^{cas}$. Nat. Cell Biol. **1**, 507–513

Received 28 August 2002/12 December 2002; accepted 8 January 2003
Published as BJ Immediate Publication 8 January 2003, DOI 10.1042/BJ20021344

Anexo V

Molecular Biology of the Cell
Vol. 14, 3699–3715, September 2003

$\alpha 4\beta 1$ Integrin/Ligand Interaction Inhibits $\alpha 5\beta 1$-induced Stress Fibers and Focal Adhesions via Down-Regulation of RhoA and Induces Melanoma Cell Migration[V]

José V. Moyano, Alfredo Maqueda, Benito Casanova and Angeles Garcia-Pardo*

Departamento de Inmunología, Centro de Investigaciones Biológicas, Consejo Superior de Investigaciones Cientificas, 28006 Madrid, Spain

Submitted October 18, 2002; Revised April 21, 2003; Accepted April 22, 2003
Monitoring Editor: Mark Ginsberg

We have studied the function of the Hep III fibronectin domain in the cytoskeletal response initiated by alpha5beta1 integrin-mediated adhesion. Melanoma cells formed stress fibers and focal adhesions on the RGD-containing FNIII7–10 fragment. Coimmobilization of FNIII4–5, a fragment spanning Hep III and containing the alpha4beta1 ligand H2 with FNIII7–10, or addition of soluble FNIII4–5 to cells preattached to FNIII7–10, inhibited stress fibers and induced cytoplasmic protrusions. This effect involved alpha4beta1 since: 1) mutations in H2 reverted the inhibition; 2) other alpha4beta1 ligands (CS-1, VCAM-1), an anti-alpha4 mAb, or alpha4 expression in HeLa cells inhibited stress fibers. This activity was apparently cryptic in fibronectin or large fibronectin fragments, but exposed upon proteolytic degradation. Indeed purified peptic fragments containing H2, inhibited stress fibers when mixed with FNIII7–10 or fibronectin. RhoA activation with LPA or transfection with V14RhoA reverted the inhibitory effect and induced stress fibers on FNIII7–10+FNIII4–5. Furthermore, addition of alpha4beta1 ligands to FNIII7–10, down-regulated RhoA and activated p190RhoGAP, which localized to cytoplasmic protrusions. alpha4beta1/ligand interaction induced cell migration, monitored by video microscopy and wound healing assays. These data indicate that alpha4beta1 provides an antagonistic signal to alpha5beta1 by interfering with the RhoA activation pathway and this leads to melanoma cell migration.

INTRODUCTION

Cellular interactions with the extracellular matrix (ECM) regulate cytoskeleton reorganization, cell migration, proliferation, survival and differentiation (Adams and Watt, 1993; Howe *et al*., 1998). Cell adhesion to the ECM is mainly mediated by the integrin family of receptors and results in actin filament polymerization and assembly into stress fibers, and formation of focal adhesions (Sastry and Burridge, 2000; Geiger *et al*., 2001). These multi-molecular complexes are active signaling centers which may assemble or disperse as cells attach and migrate, and therefore their precise regulation is crucial for normal cell behavior.

Article published online ahead of print. Mol. Biol. Cell 10.1091/mbc.E02–10–0667. Article and publication date are available at www.molbiolcell.org/cgi/doi/10.1091/mbc.E02–10–0667.

[V] Online version of the article contains video material. Online version is available at www.molbiolcell.org.

* Corresponding author. e-mail address: agarciapardo@cib.csic.es.

The cytoskeletal response following adhesion to fibronectin (Fn), a major component of the ECM, has been studied mainly in fibroblasts (reviewed in Sastry and Burridge, 2000; Geiger *et al*., 2001). These reports have clearly shown that attachment to Fn fragments containing the central cell binding domain (RGD and PHSRN sequences) via $\alpha 5\beta 1$ integrin, induces cell spreading but is not sufficient for formation of stress fibers and focal adhesions (Woods *et al*., 1986). This requires an additional signal provided by fragments containing the Hep II domain, a second cell-binding domain in Fn located in the carboxy-terminal region (Woods *et al*., 1986). The main cellular receptor that interacts with Hep II is syndecan-4 (Woods *et al*., 2000) and antibodies to syndecan-4 also provide a cooperative signal to $\alpha 5\beta 1$ integrin/RGD interaction that leads to formation of focal adhesions (Saoncella *et al*., 1999). Using recombinant Fn fragments, Yoneda *et al*. (1995) and Bloom *et al*. (1999) further demonstrated that the Hep II domain ability to drive focal adhesion formation resides within the Fn III13 repeat, a region that we recently showed to bind syndecan-4 (Huang *et al*., 2001). These intracellular effects are regulated by the Rho family of

small GTPases (Bishop and Hall, 2000; Schmitz *et al*., 2000; Ridley, 2001), which control the assembly of stress fibers and focal adhesions (RhoA), and the formation of lamellipodia (Rac) or filopodia (Cdc42). Control of actin filament assembly and disassembly is important for cell movement and this is also regulated by the coordinate contribution of RhoA, Rac and Cdc42 (Nobes and Hall, 1999).

We previously identified a third cell-binding region in Fn corresponding to the Hep III domain (repeats III4-III5, Moyano *et al*., 1997, 1999). This domain contains the active sequences KLDAPT or H2 site, which is a ligand for activated $\alpha4\beta1$ and $\alpha4\beta7$ integrins, and HBP/III5 which binds chondroitin-sulfate proteoglycans (CSPG). In this report we aimed to determine the biological role of the Hep III domain in the cytoskeletal response that follows adhesion to Fn and in particular, whether Hep III could provide a cooperative signal to the $\alpha5\beta1$/RGD interaction leading to cytoskeleton reorganization. Since cell adhesion to Hep III involves binding to $\alpha4\beta1$ integrin and CSPG, we chose melanoma cells for these studies, which unlike most fibroblasts, express both $\alpha4\beta1$ and $\alpha5\beta1$ integrins as well as CSPG. Using recombinant Fn fragments spanning the central cell binding domain (FNIII7–10) or the Hep III domain (FNIII4–5), as well as other $\alpha4\beta1$ ligands, we demonstrate that concomitant ligation of $\alpha5\beta1$ and $\alpha4\beta1$ integrins results in antagonistic rather than cooperative signals that prevent formation of stress fibers and focal adhesions. We show that the inhibitory signal provided by $\alpha4\beta1$ engagement is due to sustained down-regulation of RhoA via p190RhoGAP activation, and this leads to stimulation of melanoma cell migration.

MATERIALS AND METHODS

Antibodies and Reagents

mAb anti-vinculin (clone hVIN-1) was purchased from Sigma (St. Louis, MO); anti-RhoA, from Santa Cruz Biotechnologies (La Jolla, CA); anti-p190RhoGAP, from Upstate Biotech (Lake Placid, NY); PY20 anti-phosphotyrosine was from BIOMOL Research Laboratories Inc. (Plymouth Meeting, PA); anti-$\alpha v\beta3$ integrin (LM609) and anti-Fn central cell binding domain (MAB1933), from Chemicon International, Inc., (Temecula, CA). P1D6 and P4C2, anti-$\alpha5$ and $\alpha4$ subunits respectively, have been previously described (Wayner *et al*., 1989); IST-4, reactive with Fn repeat III5 (Carnemolla *et al*., 1996) was obtained from Dr. Luciano Zardi (Istituto Nazionale per la Ricerca sul Cancro, Genova, Italy); anti-CS-1 mAb P1F11 was previously described (Garcia-Pardo *et al*., 1992). Collagen type I, vitronectin, lysophosphatidic acid (LPA) and TRITC-labeled phalloidin were from Sigma. TPCK-Trypsin and pepsin were purchased from Merck (Darmstadt, Germany). FITC-Annexin-V was from Bender MedSystems (Vienna, Austria).

Fibronectin Fragments and VCAM-1

The 80 kDa Fn fragment (repeats III4-$_{1/2}$III11) was purified from tryptic digests of human plasma Fn (1:200 wt/wt, 90 min, 37°C) and further cleaved with pepsin (1:100 wt/wt, 1 h, 37°C) as reported (Sánchez-Aparicio *et al*., 1994). Peptic fragments of 20/30 kDa, corresponding to the III4–5 region, were purified by FPLC using a Mono Q column (Amersham Biosciences Europe GmbH, Barcelona, Spain) as described (Sánchez-Aparicio *et al*., 1994). These two fragments were separated from each other by SDS-PAGE and their N-terminal amino acid sequence determined using a 494 Protein Sequencer (Applied Biosystems, Foster City, CA).

The FNIII4–5 recombinant fragment, spanning the Hep III Fn domain (repeats III4–5), was prepared as previously described (Moyano *et al*., 1999). The FNIII7–10 fragment (repeats III7–10 including the RGD sequence) was kindly donated by Dr. Harold Erickson (Duke University Medical Center, Durham, NC) and purified as reported (Aukhil *et al*., 1993). The recombinant H89 fragment comprising the Hep II domain (repeats III12–14), 89 residues of the V/IIICS region including the CS-1 but not the CS-5 site, and repeat III15, was obtained from Dr. Martin Humphries (University of Manchester, UK) and prepared as described (Mould *et al*., 1994). Recombinant fragments FNIII13, (repeat III13) and FNIII7–15, containing repeats III7–15 and the entire IIICS/V region including CS-1 and CS-5, were obtained from Dr. Richard Hynes (Massachusetts Institute of Technology, Cambridge, MA) and purified as reported (Bloom *et al*., 1999), except that HiTrap™ Chelating HP columns (Amersham Biosciences) were used for the purification of FNIII7–15. Recombinant VCAM-1 was kindly provided by Dr. Roy Lobb (Biogen Inc., Cambridge, MA).

Generation of FNIII4–5 Mutants

FNIII4–5 mutants were prepared by PCR using as template the FNIII4–5 cDNA cloned in the pQE-3/5 vector, a gift from Dr. Luciano Zardi. Primers used for each mutation were as follows: H2-E mutation: forward, 5′-GACTGCCAACAGACAACCAAACTGGAAGCTCCCACTAC-3′; reverse, 5′-GTTAGTGGGAGCTTCCAGTTG-3′. H2-DL mutation: forward, 5′-CAAAGATCTTGCTCCCACTAAC-3′; reverse, 5′-GAGCAAGATCTTTGGTTGTCTG-3′. HBP/III5-R1 mutation: forward, 5′-TACTGTCCTGGTGAGATGGACTCCACCTGCGGCCCAGATA-3′; reverse, 5′-TCTGGGCCGCAGGTGGAGT-3′. HBP/III5-R2 mutation: forward, 5′-ACAGGATACGCACTGACCGTG-3′; reverse, 5′-GCCTCTTCGGGTAAGGCC CACGGTCAGGCGTATCCTGT-3′. HBP/III5-R3R4 mutation: forward, 5′-ACCGCAGCAGGCCAGCCCAG-3′; reverse primer, 5′-GCCTGCTGCGGTAAGGCCCAC-3′. For the double mutation HBP/III5-R1R2 we used HBP/III5-R2 as template and the primers used to generate HBP/III5-R1. The DNA sequence of all mutants cloned into the pGEM-T Easy Vector (Promega Corp., Madison, WI) was verified in an automated ABI-Prism 377 sequencer (Applied Biosystems-Prism-Perkin Elmer-Cetus, Foster City, CA), subcloned at the *Mfe* I and *Hin*d III sites in the pQE3 vector and transfected into DH5α *E. coli*. Mutated fragments were induced and purified as described for the parental FNIII4–5 fragment (Moyano *et al*., 1999).

Other Recombinant Proteins and Constructs

$\alpha4$ subunit cDNA (obtained from Dr. Martin Hemler, Dana-Farber Cancer Institute, Boston, MA) was subcloned into the pCI-neo vector (Promega) at the original restriction sites *Xba*I/*Sal*I and used to transform *E. coli* JM109. Plasmidic DNA was obtained by performing minipreps of positive colonies with the Plasmix kit (Talent Technologies, Torino, Italy).

Recombinant C3 transferase (C3) in the pGEX-2T vector (a gift from Dr. Alan Hall, University College, London, UK) was expressed in *E. coli* DH5α and purified as described (Dillon and Feig, 1995), except that bacteria were lysed in 50 mM Tris pH7.5, 100 mM NaCl, 5 mM $MgCl_2$, 1 mM DTT with 1 mM PMSF, 2.5 μg/ml leupeptin, and 10 μg/ml aprotinin (C3 buffer). Supernatants containing glutathione-S-transferase (GST)-C3 were incubated overnight at 4°C with glutathione-agarose beads, centrifuged, and cleaved with 5 U/ml thrombin (Sigma). Thrombin was removed by incubating with 10 μl of p-aminobenzamidine-agarose bead suspension for 30 min at 4°C. Beads were removed by centrifugation and C3 was dialyzed into C3 buffer without the inhibitors. Purity was checked by SDS-PAGE.

Green fluorescent protein (GFP) fused to RhoA cDNAs encoding for V14RhoA (active mutant) or N19RhoA (dominant negative) cloned into the pEGFP-C1 vector (Clontech, Palo Alto, CA) in *E. coli* DH5α, were a gift from Dr. Francisco Sanchez-Madrid. Plasmidic DNA from *E. coli* was isolated by performing minipreps.

Cells and Cell Cultures

The human melanoma cell lines SKMEL-178 and A375 were obtained from Dr. Francisco Real (Hospital del Mar, Barcelona, Spain). The human epithelial cell line HeLa was obtained from Dr. Angel Corbí (Centro de Investigaciones Biológicas, Madrid, Spain). All cells were maintained in DME medium, 10% FBS (Life Technologies, Paisley, Scotland, UK), 40 μg/ml gentamicin. Before all assays (except when indicated) cells were serum-starved for 3 h, detached from culture flasks with 1 mM EDTA, PBS pH 7.5, washed with PBS, and resuspended in attachment medium (DME, 1% BSA, 10 mM HEPES).

Immunofluorescence Assays

Glass coverslips were coated with Fn, fragments, VCAM-1 or antibodies diluted in 40 μl PBS for 2 h at 37°C and placed inside 24-well plates. Wells were washed and blocked with 1% BSA/PBS for 30 min. Serum-starved 2×10^4 cells in attachment medium were added to each well and incubated for 1 h at 37°C. Attached cells were fixed with 3.5% formaldehyde/PBS, permeabilized with cold 0.5% Triton X-100/PBS for 3 min and blocked with 1% BSA/PBS for 30 min. F-actin was stained with 25 μg/ml TRITC-phalloidin in PBS, 1% BSA, 10 mM NaN_3 for 15 min. Vinculin was detected with specific mAbs. Samples were visualized on an epifluorescence Axioplan microscope (Zeiss, Germany) and photographed with a CCD camera (Photometrics Inc., Tucson, AZ). Viability of cells in these assays was confirmed by DAPI staining and flow cytometry using propidium iodide and FITC-Annexin-V.

Cell Transfection

Subconfluent cells in fresh complete medium were transiently transfected using FuGENE™ 6 (Roche Biochemicals, Mannheim, Germany) following the manufacturer's instructions. Briefly, 2 μg of cDNA were mixed with 3 μl of FuGENE 6, diluted to a final volume of 100 μl with DME, incubated for 30 min at room temperature, and added to the cells. After 24 h transfected cells were used in immunofluorescence assays as described. Transfection efficiency was ~60% for SKMEL-178 cells and 20% for HeLa cells, assesed by flow cytometry.

Wound Healing Assays and Video-Microscopy

Confluent cells on 12-well plates were wounded by scraping a yellow-tip across the cell monolayer. After washing with DME, complete medium containing either 2.1 μM FNIII7–10 alone or mixed with 4.9 μM FNIII4–5, FNIII4–5-DL, or H89 or with 1.48 μM VCAM-1 was added to the wells. Wound closing was checked at different times during 24 h. Photographs were taken on an inverted phase-contrast microscope equipped with a CCD camera (Nikon Diaphot/DXM-1200, Tokyo, Japan). For video microscopy, 2×10^4 cells were added to glass coverslips previously coated with the various substrata and placed inside a 24-well plate. Individual wells were analyzed on a microscope equipped with a thermally-controlled plate set at 37°C. Photograms were taken every 30 s >3 h, using a CCD camera with the Act-1 acquisition software (Nikon). Digital videos were composed using the VideoMach software. Quantitation of wound and cell spread areas was performed using the IP Lab Spectrum program (Signal Analytics Co., Vienna, VA). Single cell tracking measurement was performed using the MetaMorph program (Universal Imaging Co., Downingtown, PA).

Regulation and Analysis of RhoA Activity

For C3 inactivation of RhoA, subconfluent cells were incubated overnight in DME, 0.5% FBS, 50 μg/ml C3 in 6-well plates. For LPA activation, cells with or without previous treatment with C3, were detached from plates with 1 mM EDTA/PBS, washed and incubated with 1 μM LPA in attachment medium for 60 min at room temperature on a rotary shaker. Fresh C3 was added again during this incubation to cells previously treated with this inhibitor.

The Rho binding domain of Rhotekin C21 fused to GST and cloned into the pGEX-3 × vector (Pharmacia) was a gift of Dr. John Collard (The Netherlands Cancer Institute, Amsterdam, The Netherlands). Protein was expressed in *E. coli* DH5α and purified as described (Sander *et al*., 1999). For pull-down assays, serum-starved cells were added to 6-well plates (7×10^5/well) previously coated with recombinant fragments. A total of 8×10^6 cells was used for each condition. At different times attached cells were lysed in 500 μl of cold 50 mM Tris pH7.5, 150 mM NaCl, 1% NP-40, 0.5% deoxycholate, 0.1% SDS, 1 mM $NaVO_4$, 1 mM NaF, 1 mM PMSF, 10 μg/ml aprotinin, and 2.5 μg/ml leupeptin (RIPA buffer) and lysates clarified by centrifugation. 15 μl of the supernatant were used to measure total RhoA and the remaining volume was mixed with 50 μl of C21-GST and 60 μl of glutathione-agarose beads for 60 min at 4°C. Beads were washed and bound protein was eluted by boiling in Laemmli buffer. Samples were separated on 15% SDS-PAGE and transferred to nitrocellulose membranes (BIO-RAD, Hercules, CA). Total and bound RhoA were detected with an anti-RhoA mAb, followed by HRP-conjugated antimouse Igs antibody (Dako), and visualized with the ECL SuperSignal West Pico kit (Pierce, Rockford, IL). Protein bands were quantified on a densitometer (Molecular Dynamics, Sunnyvale, CA) using the Quantity-One™ program (BIO-RAD).

Analysis of p190RhoGAP Phosphorylation

Cells were incubated in 6-well plates and lysed in RIPA buffer. 15 μl of the supernatant were used for analysis of total protein and the remaining 485 μl were incubated with protein G-agarose beads (Pierce) coated with 4 μg of anti-p190RhoGAP mAb or mock beads without antibody, at 4°C overnight. Beads were washed with RIPA buffer, and bound proteins extracted by boiling in Laemmli buffer and separated on 7.5% SDS-PAGE followed by western blotting. Phoshorylated proteins were detected using PY20 mAb followed by an HRP-labeled secondary antibody, and total p190RhoGAP with a specific mAb. Protein bands were visualized and quantitated as explained above.

Statistiscal Analyses

Significance of the difference between means was determined by the Student's *t* test for nonpaired samples using the GraphPad Instat program (GraphPad Software, San Diego, CA). A P-value of ≤ 0.05 was considered significant.

Online Supplemental Material

SKMEL-178 cells were added to glass coverslips coated with FNIII7–10 (video 1), FNIII7–10+FNIII4–5 (video 2), FNIII7–10+FNIII4–5-DL (video 3), FNIII7–10+H89 (video 4), or FNIII7–10+VCAM-1 (video 5). Images were recorded every 30 s for 3 h and videos were compiled with the VideoMach software. In videos 1 and 3, cells displayed slow membrane activity and spreading, but remained stationary. However, in the presence of FNIII4–5, H89 or VCAM-1 (videos 2, 4, 5) cells showed fast membrane activity, no spreading, and substantial random motility. See also Figure 9.

RESULTS

Melanoma Cells Form Stress Fibers and Focal Adhesions Upon Attachment to the FNIII7–10 Fragment

The SKMEL-178 and A375 melanoma cell lines used in this study expressed several integrins including the two main Fn receptors $\alpha5\beta1$ and $\alpha4\beta1$, and $\alpha V\beta3$, as determined by flow cytometry (our unpublished results). To study the cytoskel-

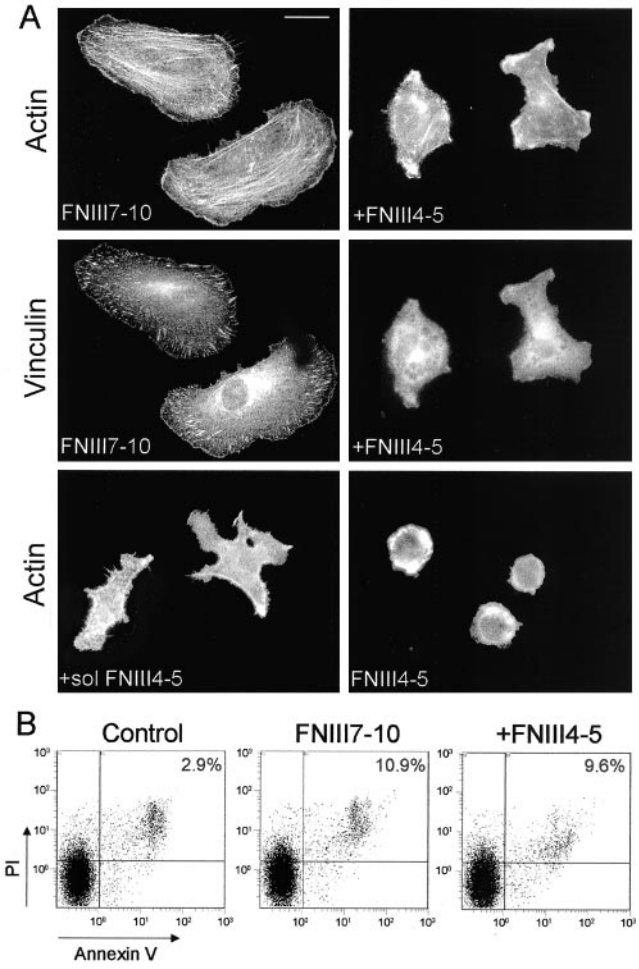

Figure 1. (A) Cystoskeletal organization following adhesion of melanoma cells to the FNIII7–10 fragment (2.1 μM) alone or mixed with 4.9 μM FNIII4–5 (+FNIII4–5). 2×10^4 SKMEL-178 cells were added to coverslips previously coated with the indicated fragments for 1 h at 37°C. In a different experiment, soluble FNIII4–5 (4.9 μM; +sol FNIII4–5) was added to cells previously attached to FNIII7–10 for 10 min and incubation continued for 1 h. After fixing and permeabilization, actin was visualized with TRITC-phalloidin and vinculin with specific antibodies. The morphological pattern of the few cells attached to FNIII4–5 alone is also shown. (B) Cells plated on FNIII7–10 or FNIII7–10+FNIII4–5 for 1 h were detached, incubated with propidium iodide (PI; 50 μg/ml) and 6 μl FITC- Annexin-V for 10 min in the dark, and analyzed by flow citometry. Values represent the % of apoptotic cells before (control) and after the two different conditions of the assay. Bar, 10 μm.

eton reorganization upon melanoma cell adhesion to the central cell-binding domain of Fn, serum-starved subconfluent SKMEL-178 cells were placed on glass coverslips previously coated with the FNIII7–10 fragment (2.1 μM, 40 μg/ml). Nearly 80% of cells plated on FNIII7–10 had a characteristic elongated morphology and formed fine stress fibers and some focal adhesions visualized by vinculin staining (Fig. 1A). $\alpha 5\beta 1$ integrin (but not $\alpha V\beta 3$ or $\alpha 4\beta 1$) localized to focal adhesions (our unpublished results), in agreement with its role as receptor for the FNIII7–10 fragment (Moyano *et al*., 2003). This cytoskeletal pattern was observed for the range of FNIII7–10 concentrations tested (0.71 μM - 2.88 μM), and did not change significantly by expanding the time of the assay up to six h.

Cell Interaction with the FNIII4–5 Fragment Disrupts the Cytoskeleton Reorganisation Induced by Attachment to FNIII7–10

To determine whether the Hep III domain of Fn could amplify the cytoskeletal response induced by $\alpha 5\beta 1$-mediated adhesion, as previously shown for the Hep II/syndecan-4 interaction, glass coverslips were simultaneously coated with FNIII7–10 and FNIII4–5 fragments at 2.1 and 4.9 (135 μg/ml) μM respectively. This molar ratio was found to be optimal after initial dose response experiments using several concentrations of FNIII4–5. As shown in Figure 1A, addition of FNIII4–5 produced a dramatic morphological change compared with cells plated on FNIII7–10 alone, with ~75% of cells lacking stress fibers and extending protrusions where actin patches accumulated. Additionally, vinculin had a difussed pattern on these cells (Figure 1A). This altered cytoskeletal pattern was not due to a diminished FNIII7–10 coating concentration caused by the presence of FNIII4–5 on the same surface, as confirmed by ELISA using specific mAbs reactive with either fragment (our unpublished results). Neither it was due to induction of apoptosis by the FNIII4–5 fragment since cell viability was almost identical for cells plated on FNIII7–10 or the mixed substrate (Figure 1B). Cells incubated in suspension with soluble FNIII4–5 (4.9 μM) for 40 min, did not form stress fibers or focal adhesions when added to FNIII7–10-coated coverslips (our unpublished results). Furthermore, addition of soluble FNIII4–5 fragment to cells preattached to FNIII7–10 also inhibited stress fiber formation by 68% (Figure 1A). This effect was clearly evident if FNIII4–5 was added at early times of up to 10 min after cells had been plated on FNIII7–10; at later times, there was a progressive loss of the ability of the soluble fragment to alter the cytoskeleton organization induced by FNIII7–10 (not shown). Very few cells (15%) attached to FNIII4–5 when coated alone and they remained round after 1 h (Figure 1A).

$\alpha 4\beta 1$ Integrin Interaction with the H2 Site in FNIII4–5 is Responsible for the Inhibition of Stress Fibers on Cells Attached to FNIII7–10

FNIII4–5 contains two cell-binding sites namely H2 and HBP/III5, which bind $\alpha 4\beta 1$ integrin or CSPG respectively (Moyano *et al*., 1997, 1999). To determine which of these sites was responsible for the observed inhibition of stress fibers, we performed directed mutations on both active sequences (Figure 2A) and tested their effect on cytoskeletal organization. SKMEL-178 cells were added to glass coverslips coated with either FNIII7–10 alone or mixed with FNIII4–5 mutants (all at 135 μg/ml). Figure 2B shows that the FNIII4–5-DL mutation efficiently reverted (78% of cells with stress fibers) the inhibitory effect produced by parental FNIII4–5. In contrast, the FNIII4–5-E mutant behaved as FNIII4–5 (not shown). Fragments carrying mutations on either or both of the first two R residues in HBP/III5 behave as parental FNIII4–5, with 80% of cells lacking stress fibers and extending protrusions (Figure 2B and not shown for the R1R2 mutant). Substitution of the last two R residues of HBP/III5

A

Site directed mutations performed on the FNIII4-5 fragment

H2 site		HBP/III5 site	
FNIII4-5:	KLDAPT	FNIII4-5:	WTPPRAQITGYRLTVGLTRR
FNIII4-5-E	KLEAPT	FNIII4-5-R1:	WTPP**A**AQITGYRLTVGLTRR
FNIII4-5-DL:	K**D**LAPT	FNIII4-5-R2:	WTPPRAQITGY**A**LTVGLTRR
		FNIII4-5-R1R2:	WTPPR**A**QITGY**A**LTVGLTRR
		FNIII4-5-R3R4:	WTPPRAQITGYRLTVGL**TAA**

B

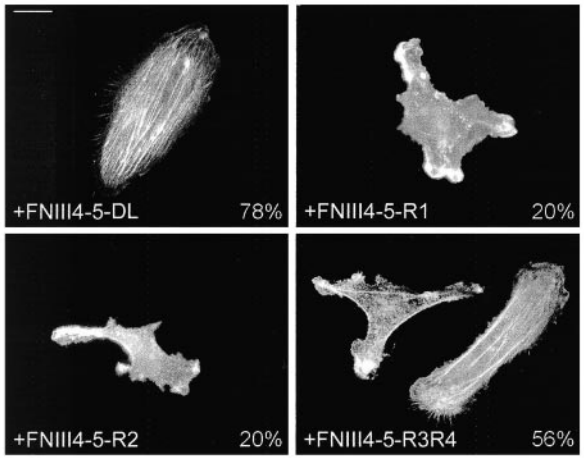

Figure 2. (A) Specific mutations (bold type) performed on the H2 and HBP/III5 sequences of the FNIII4–5 fragment. (B) A mutation on the $\alpha4\beta1$ integrin binding site in FNIII4–5 reverts the inhibitory effect of this fragment. Cells were incubated on glass coverslips previously coated with FNIII7–10 (2.1 μM) combined with either of the indicated FNIII4–5 mutants (all at 4.9 μM) for 1 h, 37°C. Cells were fixed, permeabilized, and stained for actin. Each experiment was performed at least three times. Values represent the % of cells with stress fibers. Bar, 10 μm.

by A residues (FNIII4–5-R3R4 mutant, Figure 2A) had a partial effect and ~56% of cells formed stress fibers (Figure 2B). These results showed that although some positively charged residues in HBP/III5 may play a certain role, altering the $\alpha4\beta1$ binding site in FNIII4–5 abolished its ability to inhibit the $\alpha5\beta1$/FNIII7–10-induced cytoskeletal response, thus implicating $\alpha4\beta1$ integrin in this signaling.

To determine whether $\alpha4\beta1$ inhibitory signals were specific for $\alpha5\beta1$ or could also affect other integrins, we coimmobilized FNIII4–5 with 2.1 μM collagen or vitronectin which are ligands for $\alpha2\beta1$ and $\alpha V\beta3$ integrins respectively. As shown in Figure 3, melanoma cells spread and formed stress fibers and focal adhesions on collagen (74.2% of cells) and vitronectin (85.1% of cells) when coated alone. Concomitant ligation of $\alpha4\beta1$ by FNIII4–5 inhibited the cytoskeleton organization induced via $\alpha2\beta1$ (10% of cells formed stress fibers) but did not affect the response mediated by $\alpha V\beta3$ ligation. This indicates that $\alpha4\beta1$ cross-talk signaling is not exclusive for $\alpha5\beta1$ but is specific for certain integrins.

Other $\alpha4\beta1$ Integrin Ligands and an Anti-$\alpha4$ mAb also Inhibit the FNIII7–10-Induced Stress Fiber Formation

To further establish that the observed cytoskeletal alterations were due to $\alpha4\beta1$ engagement, we tested the effect of other ligands of this integrin such as the H89 Fn fragment which contains the CS-1 site (Mould *et al*., 1994), and the endothelial protein VCAM-1 (Elices *et al*., 1990). Coimmobilization of FNIII7–10 with either 4.9 μM H89 or 1.48 μM VCAM-1 resulted in a morphological pattern resembling that induced by FNIII4–5, with cells extending lamellipodia where actin accumulated (69.3% of cells on H89; 68% of cells on VCAM-1) (Figure 4A). Lower concentrations of H89 or VCAM-1 (tested up to 0.7 μM, not shown) also inhibited stress fibers, probably due to their higher affinity for $\alpha4\beta1$ compared with FNIII4–5. In contrast, addition of 4.9 μM FNIII13, a recombinant Fn fragment which does not bind $\alpha4\beta1$, had no effect (Figure 4A). We also tested whether the anti-$\alpha4$ subunit P4C2 mAb would mimic the effect of $\alpha4\beta1$ ligands. As shown in Figure 4B, 74% of cells plated on mixtures of FNIII7–10 and P4C2 lacked stress fibers and formed cytoplasmic protrusions. The same concentration of a control mAb (LM609, anti-$\alpha V\beta3$) had no effect on the original cytoskeleton pattern (87% of cells with stress fibers) (Figure 4B). Moreover, cell incubation with soluble P4C2 for 40 min before their addition to FNIII7–10-coated coverslips also prevented formation of stress fibers on 72.1% of cells (Figure 4B), further confirming that P4C2 was mimicking the effect of $\alpha4\beta1$ ligands. Incubation with soluble LM609 had no effect (Figure 4B). Neither antibody induced a particular morphological pattern when coated alone (Figure 4B).

Inhibition of Stress Fibers on FNIII7–10+FNIII4–5 Is also Observed on A375 Melanoma Cells and $\alpha4$ Integrin Subunit-Transfected HeLa Cells

To determine whether the cytoskeletal effect of FNIII4–5/$\alpha4\beta1$ interaction was also observed on other cells, we carried out similar experiments using A375 melanoma cells, which as mentioned above express $\alpha4\beta1$ and $\alpha5\beta1$ integrins, and HeLa cells, which do not express $\alpha4\beta1$ and were transiently transfected with the $\alpha4$ subunit. Approximately 73% of A375 cells plated on FNIII7–10 spread and formed mainly peripheral stress fibers (Figure 5A). These fibers were completely lost upon adhesion to mixed substrata of FNIII7–10+FNIII4–5 and 78.7% of cells became smaller and extended protrusions (Figure 5A). As observed for SKMEL-178 cells, addition of the FNIII4–5-DL mutant to FNIII7–10 produced no effect (Figure 5A). Likewise, parental HeLa cells (72.3%) attached and formed stress fibers on FNIII7–10 and this pattern was not altered when cells were plated on mixtures of FNIII7–10+FNIII4–5 or FNIII7–10+FNIII4–5-DL (69.1% of cells; Figure 5B). A similar morphological pattern was obtained when $\alpha4$ subunit-transfected HeLa cells were added to FNIII7–10 alone (72% of cells; Figure 5B). However, when added to mixtures of FNIII7–10+FNIII4–5, 69.1% of $\alpha4$-HeLa cells did not spread and did not form stress fibers as previously observed for melanoma cells. As observed for parental cells, 71% of $\alpha4$-HeLa cells formed stress fibers on mixed substrata of FNIII7–10+FNIII4–5-DL

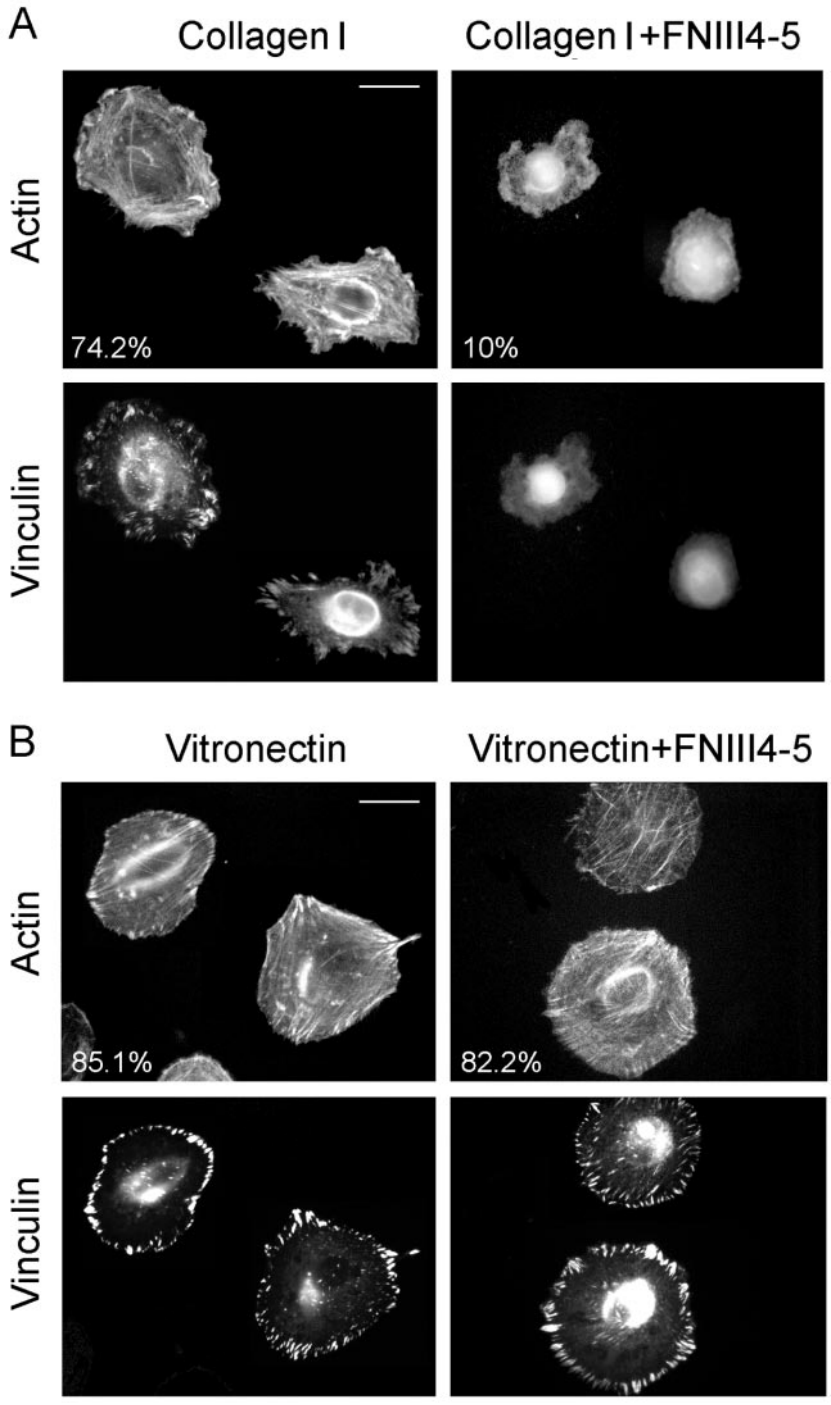

Figure 3. Interaction of FNIII4–5 with $\alpha 4\beta 1$ inhibits the cytoskeletal response induced via $\alpha 2\beta 1$ but not via $\alpha V\beta 3$. 2×10^4 SKMEL-178 cells were added to glass coverslips coated with 2.1 μM collagen (A) or vitronectin (B) alone or mixed with 4.9 μM FNIII4–5 fragment. After 1 h, actin was visualized with TRITC-phalloidin and vinculin with specific antibodies. Experiments were done at least three times. Values represent the % of cells with stress fibers on each condition. Bar, 10 μm.

(Figure 5B). Moreover, coinmobilization of the H89 fragment or VCAM-1 with FNIII7–10 also altered the morphological pattern of $\alpha 4$-HeLa cells resulting in inhibition of stress fibers in 68.8% of transfected cells (Figure 5B). Therefore, the presence of an engaged $\alpha 4\beta 1$ integrin clearly disturbs formation of stress fibers after $\alpha 5\beta 1$-mediated adhesion in several cell types.

Functional Role of the α4β1 Ligands H2 and CS-1 in a Physiological Context

To establish the role of the III4–5 region in the context of intact Fn, we first analyzed the cytoskeletal response of melanoma cells upon attachment to Fn. Figure 6A shows that 80.2% of these cells formed prominent actin stress fibers

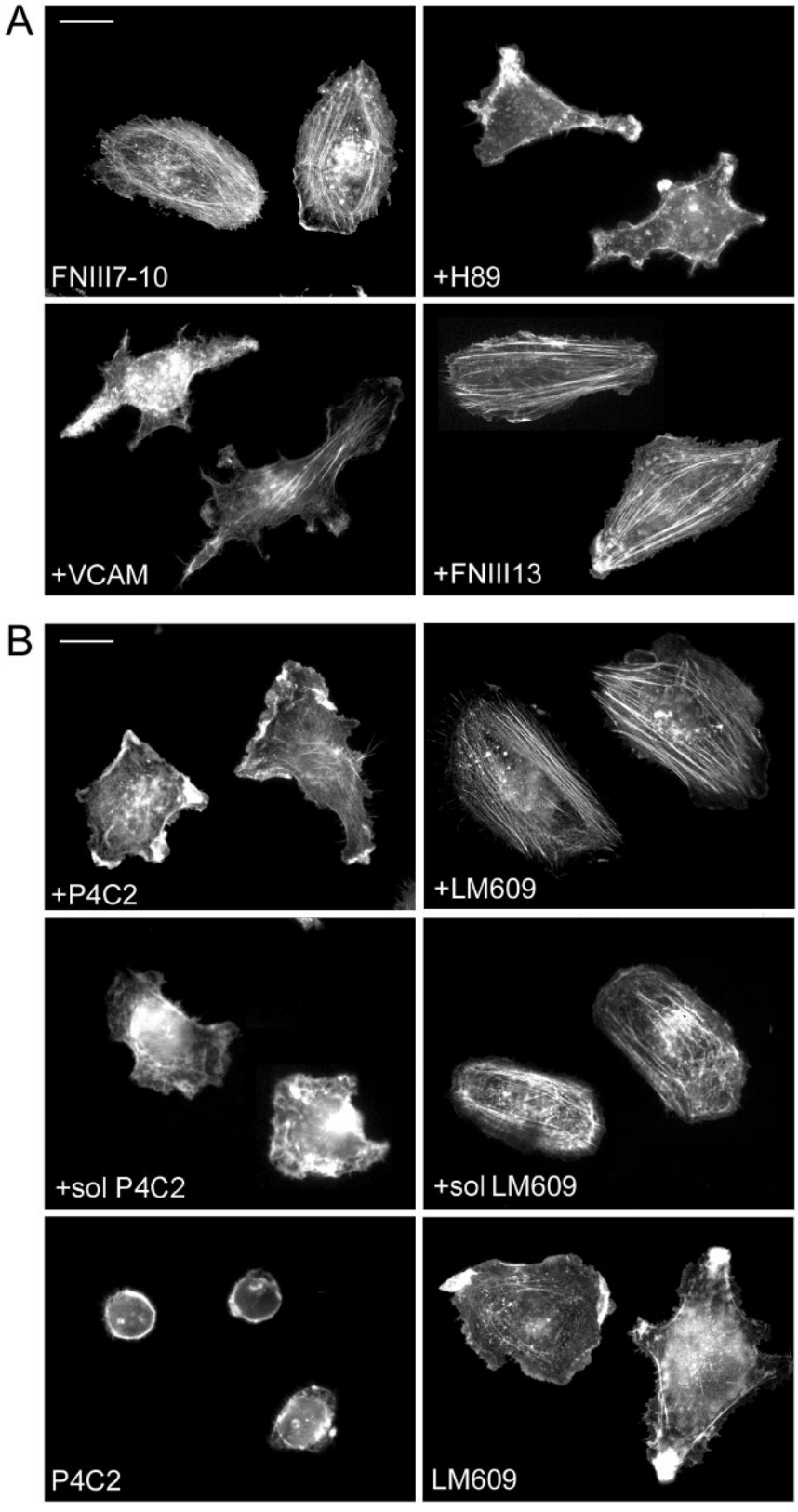

Figure 4. Inhibition of stress fibers by other $\alpha4\beta1$ integrin ligands and anti-$\alpha4$ mAbs. (A) Cells were incubated on glass coverslips previously coated with 2.1 μM FNIII7–10 alone or mixed with either 4.9 μM H89 fragment, 1.48 μM VCAM-1, or 4.9 μM FNIII13. After 1 h, cells were fixed, permeabilized, and stained for actin. (B) Cells were added to FNIII7–10 coimmobilized with 1 μg/ml P4C2 (anti-$\alpha4$; +P4C2) or LM609 (anti-$\alpha V\beta3$; +LM609) mAbs. In a different experiment, cells were incubated in suspension for 40 min with soluble P4C2 (+sol P4C2) or LM609 (+sol LM609) (5 μg/ml each) and added to glass coverslips coated with 2.1 μM FNIII7–10. Finally, cells were also added to coverslips coated with mAbs alone (lower panels). Actin was visualized in all cases with TRITC-phalloidin. Each experiment was done three times. Bar, 10 μm.

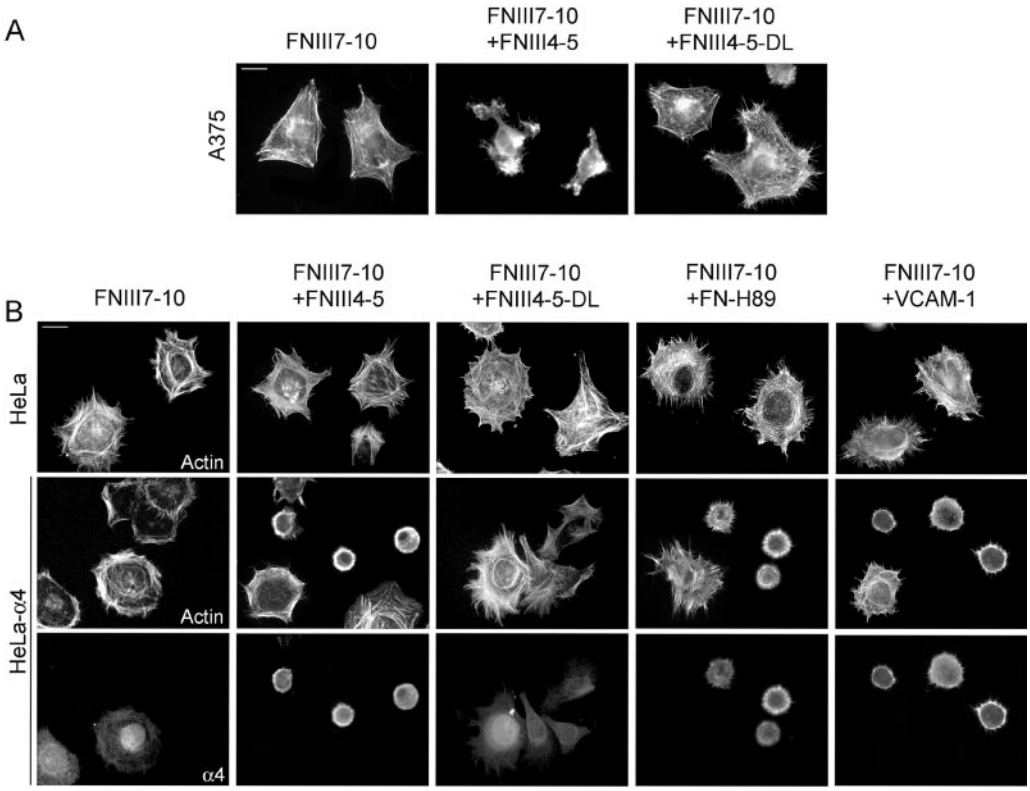

Figure 5. Effect of FNIII4–5, H89 and VCAM-1 in other cells. (A) The FNIII4–5 fragment inhibits stress fiber formation on A375 melanoma cells. 2×10^4 A375 cells were added to glass coverslips coated with FNIII7–10 alone or mixed with FNIII4–5 or the mutant FNIII4–5-DL. Cells were permeabilized after 1 h and stained with TRITC-phalloidin. (B) Expression of α4 subunit inhibits spreading and stress fibers on HeLa cells plated on mixed substrata of FNIII7–10 plus FNIII4–5, H89 or VCAM-1. Parental HeLa cells or transfected with α4 integrin subunit (HeLa-α4) were added to coverslips coated with FNIII7–10 alone, or mixed with $\alpha4\beta1$ integrin ligands. After 1 h, attached cells were stained with TRITC-phalloidin (top and center panels) or P4C2 mAb + FITC-labeled secondary antibodies (lower panels). Two different experiments were performed with identical results. Bar, 10 μm.

terminating in focal adhesions which contained vinculin (Figure 6A), paxillin and talin (not shown). This suggested two independent possibilities: 1) that the inhibitory activity of the III4–5 (and possibly CS-1) region was cryptic in Fn; 2) that the molar ratio for $\alpha5\beta1/\alpha4\beta1$ binding sites required to achieve the observed morphological change was not optimal in plasma Fn. To address these possibilities, we first studied the actin organization upon cell attachment to proteolytic digests of Fn and whether fragments similar to FNIII4–5 were produced by the degradation process. Trypsin digestion of Fn rendered several fragments including a major 80 kDa product (Figure 6B) which we previously showed to have the N-terminal sequence SDTVPS (beginning of repeat III4) and contain the RGD sequence (Sánchez-Aparicio *et al*., 1994). The molar ratio of $\alpha4\beta1/\alpha5\beta1$ binding sites (H2/RGD) in the 80 kDa fragment was therefore 1:1. Melanoma cells attached to an 80 kDa-enriched fraction (devoid of CS-1 containing fragments; Figure 6B) displayed a similar morphological pattern to that observed on Fn, with >80% of cells forming stress fibers and focal adhesions (Figure 6A). However, cells attached to a peptic digest of 80 kDa (a mixture of H2- and RGD-containing fragments) (Figure 6B) acquired a rounded morphology and lacked stress fibers and focal adhesions (Figure 6A). Western blot analysis of 80 kDa proteolytic products using mAb IST-4, which specifically recognizes Fn III5 repeat (Carnemolla *et al*., 1996), revealed two positive fragments of 20 and 30 kDa respectively with similar molecular size as the recombinant FNIII4–5 fragment used in this study (Figure 6B). Further characterization of the 20/30 kDa fraction after purification by FPLC and analytical separation by SDS-PAGE, rendered the N-terminal sequences ESKPLT (corresponding to the end of repeat III4, residue 985 in Fn) for the 20 kDa, and SDTVPS (also the beginning of the 80 kDa parental fragment at residue 904) for the 30 kDa fragment.

To determine whether the 20/30 kDa proteolytic fragments could reproduce the cytoskeletal effects of FNIII4–5, we coimmobilized the purified 20/30 kDa fraction (95 μg/ml, Figure 6B) with FNIII7–10 and studied the cytoskeleton organization after 1 h. As shown in Figure 6C, the 20/30 kDa mixture efficiently inhibited (63.5% of cells) the stress fibers and focal adhesions induced by FNIII7–10. mAb IST-4 did not abolish the 20/30 kDa (or the FNIII4–5) effect (not shown) indicating that the epitope recognized by this mAb was outside the H2 sequence. We next studied whether the 20/30 kDa fragments affected the cytoskeleton organization induced by adhesion to Fn. As shown in Figure 6C, coimmobilization of either 20/30 kDa (95 μg/ml) or FNIII4–5 (4.9

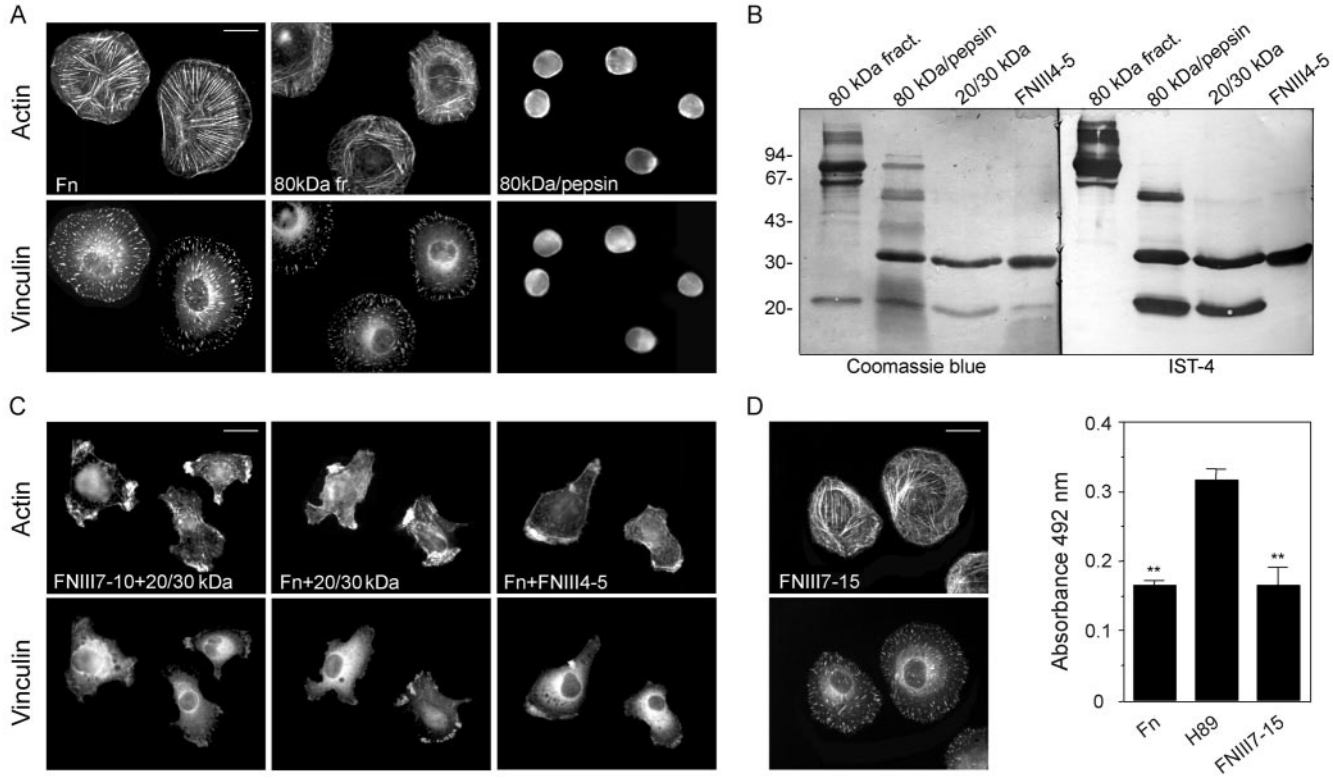

Figure 6. Functional role of $\alpha4\beta1$ ligands in the context of Fn or large Fn fragments. (A) 2×10^4 SKMEL-178 cells were added to glass coverslips coated with Fn (0.13 μM), an 80 kDa-enriched tryptic fraction of Fn (30 μg/ml; panel B) or a peptic digest of the 80 kDa fragment (70 μg/ml; panel B). After 1h, actin and vinculin were visualized as explained. (B) Analysis of the 80 kDa tryptic fraction and peptic digests of 80 kDa by 12.5% SDS-PAGE and western blotting with mAb IST-4, specific for repeat III5. Purified 20/30 kDa peptic fragments and their comparison with FNIII4–5 are also shown. (C) Cells were added to coverslips coated with mixtures of purified 20/30 kDa fragments and FNIII7–10 or Fn. The effect of coimmobilizing Fn with FNIII4–5 (4.9 μM) was also studied. (D) Cytoskeletal organization of melanoma cells attached to the FNIII7–15 recombinant fragment (2.1 μM). The expression of the CS-1 epitope in FNIII7–15, H89 and Fn was determined by ELISA using the P1F11 mAb. **p $\leq$0.01. Bar, 10 μm

μM) with Fn (0.13 μM) altered the morphological pattern observed on Fn and 74.6% of cells extended protrusions and lacked stress fibers and focal adhesions. At higher concentrations of Fn (0.3 μM) there was a progressive reversion of the inhibitory effect (not shown).

We also performed similar studies using the recombinant fragment FNIII7–15 which, like the 80 kDa fragment, contained binding sites for $\alpha5\beta1$ (RGD) and $\alpha4\beta1$ (CS-1) integrins at a 1:1 M ratio. FNIII7–15 also contains CS-5 but its affinity for $\alpha4\beta1$ is very low compared with CS-1 (Mould *et al.*, 1991), thus its effect within the fragment is probably very minor. 66.8% of melanoma cells plated on FNIII7–15 spread and formed stress fibers and focal adhesions (Figure 6D), resembling the pattern obtained on the 80 kDa fragment. To further determine whether the CS-1 site was exposed on FNIII7–15 (or in Fn), we performed ELISA assays using the anti-CS-1 mAb P1F11 and equimolar concentrations of Fn, H89 and FNIII7–15. As shown in Figure 6D, CS-1 was significantly more exposed on the H89 than on the FNIII7–15 fragment, whose reactivity was similar to that of intact Fn. Altogether these results suggested that in the context of Fn or large Fn fragments, the $\alpha4\beta1$ ligands H2 and CS-1 appear to be at least partially cryptic and proteolytic cleavage uncovers their biological activity.

Exogenous Activation of RhoA by LPA or Transfection with V14 RhoA Reverts the Stress Fiber-Inhibitory effect Caused by $\alpha4\beta1$ Integrin Ligation

It is well established that formation of actin stress fibers in several cell types involves activation of RhoA (Bishop and Hall, 2000; Ridley, 2001). To determine whether $\alpha4\beta1$ engagement was interfering with the function of RhoA in melanoma cells, we first carried out exogenous activation using the RhoA-specific activator LPA (Ridley and Hall, 1992). As shown in Figure 7A, activation of RhoA resulted in enhanced spreading and stress fiber formation for cells attached to FNIII7–10 as expected. Interestingly, treatment with LPA had a dramatic effect on cells attached to FNIII7–10+FNIII4–5, as cells spread and formed stress fibers similar to those observed on FNIII7–10. Quantitation of these results (Figure 7B) revealed that activation of RhoA by LPA reverted the phenotype observed on untreated cells (26% of cells with stress fibers and 69% with cytoplasmic protru-

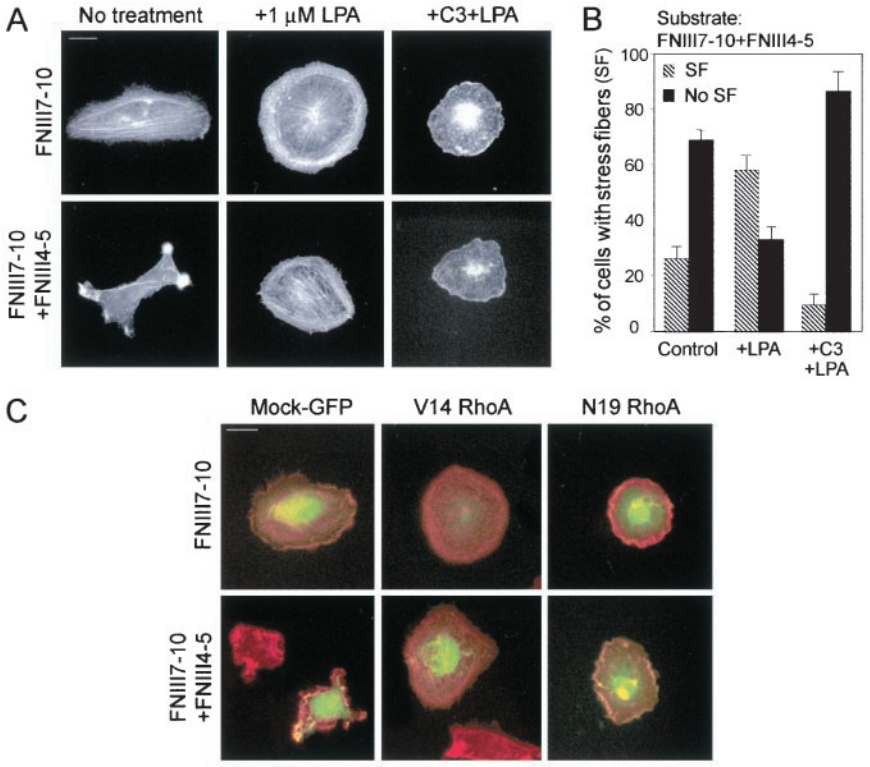

Figure 7. Active RhoA reverts the effect of FNIII4–5. (A) Cells, with or without previous incubation with 50 μg/ml C3 were treated with 1 μM LPA for 1 h and added to coverlips previously coated with FNIII7–10 alone or mixed with FNIII4–5. After 1 h, actin was visualized with TRITC-phalloidin. (B) Quantitation of the different morphologies was performed by counting a minimum of 100 cells/condition by two independent observers. Values represent the mean of three different experiments. SF, stress fibers. Bar, 10 μm. C) SKMEL-178 cells were transiently transfected with GFP-V14RhoA (active mutant), N19RhoA (dominant negative), or empty vector (mock), and added to coverslips coated with FNIII7–10 alone or mixed with FNIII4–5. Fluorescence images of GFP (green) and actin filaments (red) in the same cell are shown. Bar, 10 μm.

sions) resulting in 69% of cells with stress fibers and 33% without fibers. Preincubation of cells with the RhoA inhibitor C3, abolished the effect of LPA on both substrata (Figure 7A, B).

These results indicated that exogenous activation of RhoA overcomes the effect induced by $\alpha4\beta1$ ligation. To further confirm the involvement of RhoA in this process, we transiently transfected SKMEL-178 cells with the constitutively active GFP-V14Rho form and studied their cytoskeletal response after attachment to FNIII7–10 or FNIII7–10+FNIII4–5 fragments. As shown in Figure 7C, 74% of GFP-V14Rho-transfected cells showed enhanced spreading and actin stress fibers on FNIII7–10 similar to the pattern obtained after activation with LPA. Likewise, 72% of GFP-V14Rho-transfected cells spread and formed stress fibers on the mixed substrate FNIII7–10+FNIII4–5, clearly indicating that constitutive activation of RhoA was sufficient to overcome the cytoskeletal effects induced by $\alpha4\beta1$ integrin engagement (Figure 7C). As expected, transfection with the dominant negative mutant GFP-N19Rho resulted in reduced spreading and lack of stress fibers on both substrata. Transfection with the empty vector (mock-GFP) had no effect (Figure 7C). Altogether these results indicate that the stress fiber inhibitory activity induced by the $\alpha4\beta1$ ligand FNIII4–5 appears to involve the RhoA activation pathway.

$\alpha4\beta1$ Integrin Ligation Prevents RhoA Activation Due to Increased p190RhoGAP Phosphorylation

To determine whether RhoA was inactivated as a result of $\alpha4\beta1$/ligand interaction, we performed affinity binding assays using the C21-GST fusion protein which only binds GTP-Rho (Sander *et al*., 1999; Ren *et al*., 1999). Lysates from SKMEL-178 cells that had been serum starved for 3 h and plated on FNIII7–10 alone or mixed with either FNIII4–5, H89, P4C2 mAb or P1D6 mAb for 50 min, were analyzed for the presence of active RhoA. As shown in Figures 8A and 8C, there was a basal RhoA activity (time 0), which increased after the 50 min of adhesion to FNIII7–10. In contrast, active RhoA levels at this time, for cells attached to mixtures of FNIII7–10 and $\alpha4\beta1$ integrin ligands or P4C2 were similar to basal levels (Figure 8AC) and significantly lower than those induced by FNIII7–10 (Figure 8C). Coimmobilization of FNIII7–10 with the anti-$\alpha5$ subunit mAb P1D6 did not reduce the active RhoA levels induced by FNIII7–10 (Figure 8AC), thus confirming the specificity of the $\alpha4\beta1$-mediated effect. Adhesion to H89 alone did not modify the basal activity of RhoA (Figure 8AC) in agreement with the lack of cells forming stress fibers on this substrate (not shown).

Down-regulation of RhoA has been attributed to activation/phosphorylation of p190RhoGAP by c-Src (Arthur *et al*., 2000). To establish whether the observed lack of activation of RhoA in the presence of $\alpha4\beta1$ ligands followed this pathway, we measured the levels of p190RhoGAP tyrosine phosphorylation upon adhesion to FNIII7–10 or to the above mentioned mixed substrata. As shown in Figures 8B and 8C, these levels were significantly elevated in the presence of FNIII7–10 mixed with $\alpha4\beta1$ ligands or P4C2 but not when FNIII7–10 was used alone or mixed with P1D6. Adhesion to the H89 fragment

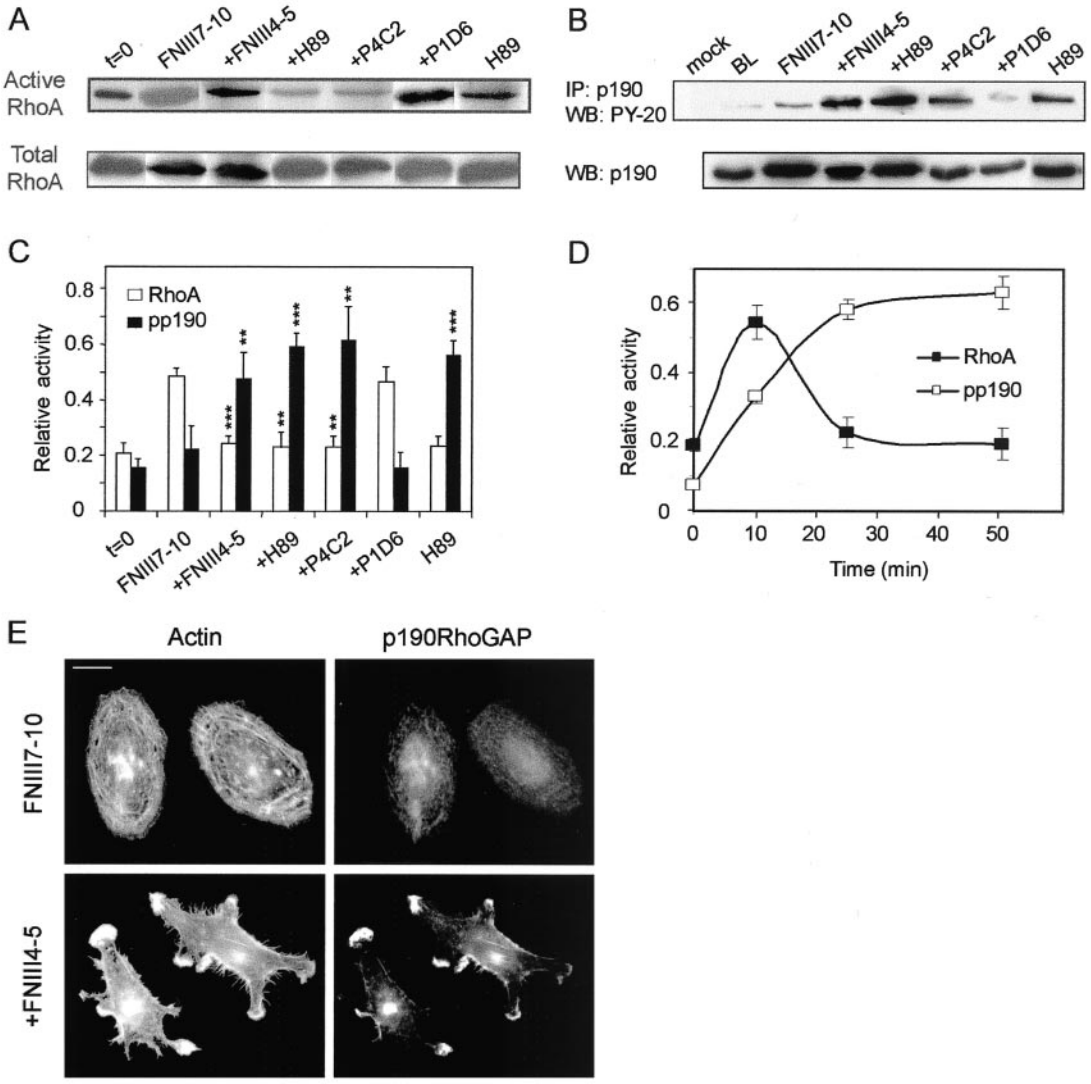

Figure 8. Regulation of RhoA and p190RhoGAP by $\alpha 4\beta 1$ interaction with its ligands. (A) Cells (7×10^5/well) were added to FNIII7–10 alone or mixed with the indicated fragments or mAbs. Cells were also added to H89-coated wells. After 50 min, attached cells were lysed, lysates incubated with C21-GST and bound and total RhoA analyzed by western blotting using an anti-RhoA mAb. A representative experiment out of four performed is shown. (B) p190RhoGAP was immunoprecipitated from cell lysates after 50 min of adhesion to FNIII7–10 or the indicated mixed substrata with a specific mAb, and phosphorylation measured in western blots using PY20 mAb. Mock, protein G-agarose beads without antibody; BL, basal levels at time 0. Total p190RhoGAP was also analyzed by Western blotting (WB: p190). A representative experiment out of three performed is shown. (C) Quantitation (arbitrary units) of the relative amount of active RhoA and p190RhoGAP on cells attached to the various substrata. Average values from three independent experiments are shown. pp190, phosphorylated p190RhoGAP. **$p \leq 0.01$; ***$p \leq 0.001$. (D) Time course of RhoA and p190RhoGAP regulation upon cell attachment to mixtures of FNIII7–10 and FNIII4–5. Values represent the mean of two experiments. (E) Localization of p190RhoGAP on cells attached to FNIII7–10 or FNIII7–10+FNIII4–5. Cells were fixed after 1 h and stained with anti-p190RhoGAP. Notice the colocalization of p190RhoGAP and actin at the protrusions. Bar, 10 μm.

alone also induced p190RhoGAP phosphorylation (Figure 8BC), in agreement with the low RhoA active levels observed on this substrate (Figure 8AC).

To determine whether there was a time course correlation between the observed RhoA inactivation and p190RhoGAP phosphorylation, we performed kinetic analysis on cells attached to mixtures of FNIII7–10 and FNIII4–5. As shown in Figure 8D, there was an early enhanced RhoA activity after 10 min followed by a decrease to basal levels over the 50 min of the assay. In parallel to this inactivation, there was a progressive increase of p190RhoGAP phosphorylation (Figure 8D). These results suggested that $\alpha 4\beta 1$ ligation prevents RhoA activation and stress fiber formation by inducing p190RhoGAP phosphorylation. In support of an important role for p190RhoGAP in $\alpha 4\beta 1$ signaling, p190RhoGAP colocalized with actin in the cytoplasmic protrusions of cells plated on FNIII7–10+FNIII4–5, while it remained diffused on cells attached to FNII7–10 (Figure 8E).

Interaction of α4β1 with FNIII4–5 or with Other Ligands Stimulates Melanoma Cell Migration

To determine whether the observed $\alpha4\beta1$-mediated signaling resulted in cell migration, we first monitored SKMEL-178 cell movement on FNIII7–10, FNIII7–10+FNIII4–5, or FNIII7–10+FNIII4–5-DL substrata using a CCD camera and the VideoMach software. Video 1 (see supplemental material) shows that cells seeded on FNIII7–10 (2.1 μM) attached, spread and displayed certain membrane activity but remained at their original position without any detectable migration overthe 150 min monitored. In contrast, when $\alpha4\beta1$ was simultaneously engaged to FNIII4–5 (4.9 μM), cells became very motile, extended protrusions and displayed significant random migration (Video 2). Cells plated on the control substrate FNIII7–10+FNIII4–5-DL behave very similar to those plated on FNIII7–10 (Video 3). These results are also shown in Figure 9A, which displays four representative photograms taken at different times during the assay. As can be observed with the help of black and white arrows (Figure 9A) and by single cell tracking measurements (Figure 9B), melanoma cells did not move from their initial position (black arrows) when plated on FNIII7–10 or FNIII7–10+FNIII4–5-DL. Cells however clearly migrated on FNIII7–10+FNIII4–5 to new positions, indicated by white arrows (Figure 9AB).

To determine whether the H89 fragment or VCAM-1 also stimulated cell migration when coimmobilized with FNIII7–10, we monitored cells added to these substrata overthe same period of time. As shown in Figures 9C and 9D and videos 4 and 5 (see supplemental material), cells became very motile in the presence of either H89 (4.9 μM) or VCAM-1 (0.75 μM) and extended cytoplasmic protrusions. Cell movement on FNIII7–10+H89 was more limited than in the presence of VCAM-1 or FNIII4–5 but it was clearly evident when compared with cells plated on FNIII7–10 alone or mixed with FNIII4–5-DL (see corresponding videos). The concentration of VCAM-1 had to be adjusted in these experiments to obtain maximal movement, in agreement with the reported short range of VCAM-1 concentrations that support cell migration (Mould *et al*., 1994). These results were further confirmed by cell surface area measurements, which showed a significant decrease overtime for cells plated on mixed substrata of FNIII7–10 and FNIII4–5, H89 or VCAM-1 (Figure 9E). These areas however showed a moderate increase with a maximum at 60 min, for cells plated on FNIII7–10 alone or mixed with FNIII4–5-DL (Figure 9E).

We also performed wound-healing assays using the various $\alpha4\beta1$ ligands. Nearly confluent SKMEL-178 cells were monitored for their ability to fill a small wound in the presence of FNIII7–10, FNIII7–10+FNIII4–5, or FNIII7–10+FNIII4–5-DL. The response to wounding in all cases was slow and after 3–6 h no appreciable migration could be detected. However, after 24 h there were clear differences in cell migration depending on the ligand used. In the presence on FNIII7–10 or FNIII7–10+FNIII4–5-DL, cells moved very similarly to control cells in the absence of Fn fragments and 33–40% of the area of the wound remained open when compared with the wound at time 0 (Figure 10A, 10C). In contrast cells cultured in the presence of FNIII7–10+FNIII4–5 clearly migrated from both edges and filled nearly 93% of the wound surface after 24 h (Figure 10A, 10C). This was not due to increased cell proliferation in the presence of FNIII4–5 fragment since quantitation of cells by trypan blue at the end of the assay revealed almost identical numbers on all three substrata: 438×10^3/ml (FNIII7–10), 440×10^3/ml (FNIII7–10+FNIII4–5) and 443×10^3/ml (FNIII7–10+FNIII4–5-DL), and no significant growth with respect to the number of starting cells (440×10^3/ml).

A similar wound-healing response was obtained in the presence of FNIII7–10 plus H89 fragment or VCAM-1. As shown in Figures 10B and 10C, 95 and 92% of the wound respectively had closed after 24 h in the presence of H89 or VCAM-1. As in the case of FNIII4–5, these ligands did not induce increased cell proliferation compared with FNIII7–10 alone (not shown). The results from video microscopy and wound healing assays therefore showed that $\alpha4\beta1$ signaling upon interaction with its ligands leads to melanoma cell migration.

DISCUSSION

In this report we have studied the role of the Hep III domain of Fn on cytoskeleton organization, in an effort to clarify the physiological function of this region. We show that melanoma cells, unlike previous findings on fibroblasts (Woods *et al*., 1986; Bloom *et al*., 1999), formed stress fibers and focal adhesions upon attachment to the FNIII7–10 fragment via $\alpha5\beta1$ integrin, although the response was not as developed as on Fn. Addition of FNIII4–5 (a fragment representing the Hep III domain), either immobilized or in soluble form, to FNIII7–10 inhibited these cytoskeletal structures and induced formation of cytoplasmic protrusions. Thus, although FNIII4–5 was only weakly adhesive (this study and Moyano *et al*., 1999) it effectively induced intracellular signals to cells attached via $\alpha5\beta1$. A similar behavior was previously described for a FNIII13 fragment which was also poorly adhesive but induced stress fibers and focal adhesions on fibroblasts attached via $\alpha5\beta1$ (Bloom *et al*., 1999). In our present study, we provide conclusive evidence for a primary role of $\alpha4\beta1$ integrin in the cytoskeleton response induced by FNIII4–5. First, point mutation experiments clearly showed that disruption of the native H2 sequence KLDAPT ($\alpha4$ ligand) rendered the FNIII4–5 fragment inactive. The D/E mutation had no effect, in agreement with the fact that the KLEAPT peptide inhibited cell adhesion to FNIII4–5 while the KDLAPT peptide did not (Moyano *et al*., 1997). Similarly, a D/E substitution in the GRGDS peptide was inactive, while the peptide GRDGS did not inhibit cell adhesion (Mould *et al*., 1991). Second, other $\alpha4\beta1$ ligands such as the H89 fragment, containing the CS-1 site or VCAM-1 as well as an anti-$\alpha4$ mAb, produced the same cytoskeletal response when mixed with FNIII7–10 as FNIII4–5, while the nonintegrin binding fragment FNIII13 had no effect. Third, transfection of HeLa cells with $\alpha4$ subunit clearly impaired their ability to form stress fibers in the presence, but not in the absence, of FNIII4–5.

Our results differ from a previous study (Huhtala *et al*., 1995) in which rabbit synovial fibroblasts, which unlike most fibroblasts express $\alpha4\beta1$ integrin, formed weak focal adhesions when attached to mixtures of a 120 kDa Fn fragment ($\alpha5\beta1$ ligand) and the CS-1 synthetic peptide ($\alpha4\beta1$ ligand). This apparent discrepancy may be explained by the different cell type used in both studies and/or by the use of a peptide

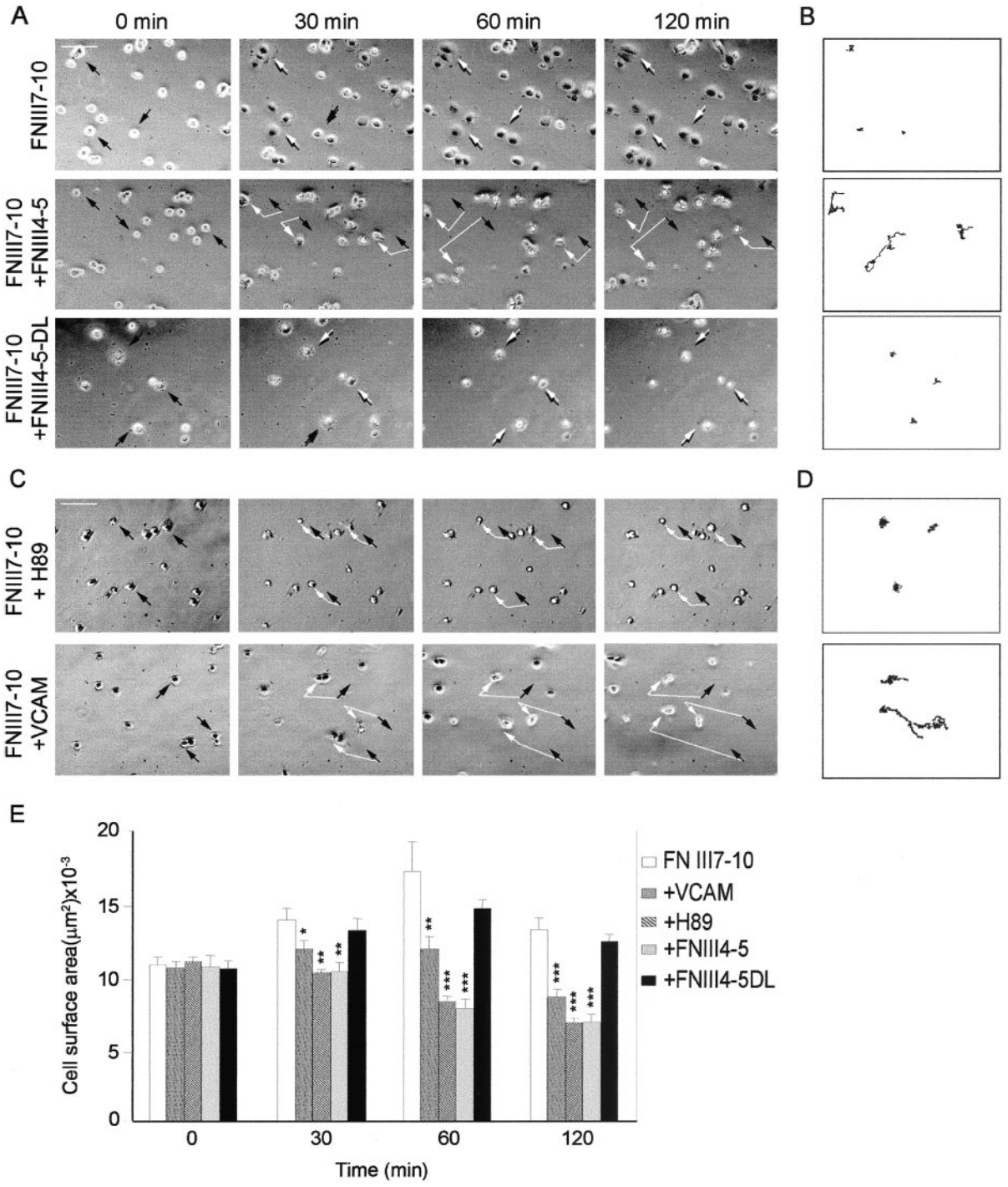

Figure 9. Time-lapse analysis of melanoma cell movement. SKMEL-178 cells were added to coverslips coated with FNIII7–10 alone or mixed with either FNIII4–5 or FNIII4–5-DL (A) or with H89 or VCAM-1 (C), placed on a thermally-controlled plate and photographed every 30 s for 3 h. Four representative times are shown. Black arrows indicate the initial position of selected cells and white lines the movement and final position of those cells after 24 h. Single cell tracking analyses for all substrata are also shown (B, D). See online material for the corresponding videos. Bar, 100 μm. (E) Cell surface areas were quantified using the IP Lab Spectrum program. At least six different determinations were done for each panel. A representative experiment out of three perfomed is shown. *p $\leq$0.05; **p $\leq$0.01; ***p $\leq$0.001.

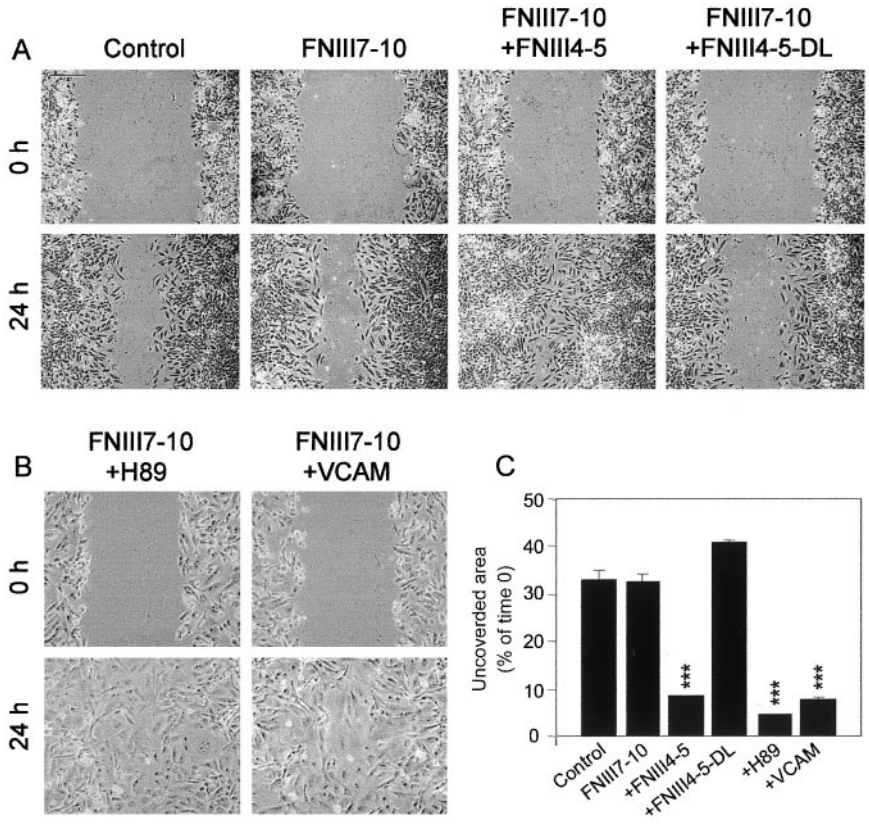

Figure 10. Stimulation of melanoma cell migration (wound-healing) by $\alpha4\beta1$/ligand interaction. Confluent SKMEL-178 cells in 12-well plates were wounded and incubated with complete medium (control) or medium containing 2.1 μM FNIII7–10 alone or mixed with 4.9 μM FNIII4–5 or FNIII4–5-DL (A), or with 4.9 μM H89 or 1.48 μM VCAM-1 (B). Wound closure was monitored >24 h and photographed. Bar, 200 μm. (C) The wound area (μm^2) that remained open for each condition after 24 h was calculated as in Figure 9. Values are expressed as % of the area of the original wound (time = 0) and represent the average of two different experiments with duplicate determinations. *** $p \leq 0.001$.

vs. a fragment (our study) as substrata, which certainly affects the concentration/density and conformation of the active sites, probably modifying the cellular response.

Several reports have documented the existence of cross-talk between integrins, which frequently leads to antagonistic signaling (Huhtala *et al*., 1995; Porter and Hogg, 1997; Retta *et al*., 1998). Our present results are the first to show that induction of stress fibers and focal adhesions upon $\alpha5\beta1$ engagement is inhibited by concomitant ligation of $\alpha4\beta1$, thus establishing that $\alpha4\beta1$ may be an important regulator of $\alpha5\beta1$-mediated cytoskeletal responses. Our results also show that $\alpha4\beta1$ cross-talk is not restricted to $\alpha5\beta1$ since it can also affect $\alpha2\beta1$ (but not $\alpha V\beta3$)-induced cytoskeletal response. The antagonistic roles of $\alpha4\beta1$ and $\alpha5\beta1$ integrins in melanoma cytoskeleton reorganization contrast with the well established cooperative effect of syndecan-4 and $\alpha5\beta1$ integrin that promotes formation of stress fibers and focal adhesions in fibroblasts (Woods *et al*., 2000; Saoncella *et al*., 1999; Bloom *et al*., 1999). Coordinate functions for $\alpha4\beta1$ integrin and the melanoma cell CSPG that lead to cell spreading and focal contact formation have also been clearly demonstrated (Iida *et al*., 1995). These previous findings support the conclusion that simultaneous engagement of an integrin and a proteoglycan results in a cooperative response. Since melanoma cells also express CSPG, our current results suggest that signaling via $\alpha4\beta1$ dominates oversignaling via CSPG. We believe that inhibition of $\alpha5\beta1$ function was not previously observed because most cytoskeleton organization studies have been done in fibroblasts, which generally do not express $\alpha4\beta1$ integrin, and thus only the cooperative effect of syndecan-4/Hep II interaction was functional.

Our results indicate that the activity of the H2 and CS-1 sites appears to be cryptic in the context of native Fn, since melanoma cells formed stress fibers and focal adhesions when attached to Fn. This conclusion is supported by the fact that large Fn fragments such as 80 kDa and FNIII7–15, which contain equimolar ratios of $\alpha5\beta1$ and $\alpha4\beta1$ binding sites, also induced stress fibers. Moreover, our results also show that the inhibitory activity mediated by $\alpha4\beta1$ was clearly exposed upon proteolytic degradation of Fn, an important physiological process essential during development, cell migration and invasion, wound healing, and in pathological situations (Basbaum and Werb, 1996; Davis *et al*., 2000), that we reproduced here using trypsin and pepsin digestions as a model system. Indeed, cells attached to peptic digests of the 80 kDa fragment lacked stress fibers and we were able to purify fragments of 20/30 kDa from these digests which contained the H2 sequence and produced similar cytoskeletal effects as the recombinant FNIII4–5 used throughout our study. Therefore, our present results clearly establish that fragments containing $\alpha4\beta1$ integrin ligands are released upon proteolytic degradation of Fn and may modify the cytoskeletal reponse in physiological situations. The fact that the 20/30 kDa fragments also affect the morphological pattern induced by adhesion to Fn, further extends the physiological role of proteolytic fragments. Although we have focused this study on the functional role of the H2 sequence in repeat III5 and thus have purified fragments containing this region, a similar situation is likely to occur

for CS-1-containing fragments, which we previously showed to be readily produced upon trypsin digestion of Fn (Garcia-Pardo *et al*., 1986). These fragments would be equivalent to the recombinant H89 fragment used here, which produced inhibition of stress fibers and focal adhesions. Interestingly, we found that the CS-1 epitope was partially buried in Fn and in FNIII7–15, in agreement with a previous study showing that CS-1 was cryptic in Fn and exposed upon proteolytic degradation, mainly by acidic proteases such as cathepsins and pepsin (Ugarova *et al*., 1996).

We have aimed to identify some of the biochemical signals triggered by α4β1 integrin engagement, which account for the inhibition of stress fibers and focal adhesions in melanoma cells. Previous reports on fibroblasts have shown that during the early phase of attachment to Fn (via α5β1 integrin), RhoA is rapidly and transiently inhibited and this is followed by an activation phase which peaks at 60–90 min and induces formation of stress fibers and focal adhesions (Ren *et al*., 1999). The initial suppression of RhoA requires FAK (Ren *et al*., 2000) and is apparently due to c-Src phosphorylation and activation of p190RhoGAP leading to the formation of membrane protrusions, which allow fibroblast spreading and migration (Arthur *et al*., 2000; Arthur and Burridge, 2001).

In the present study we show that activation of RhoA or transfection with constitutively active V14Rho, restored formation of stress fibers in cells attached to FNIII7–10+FNIII4–5 fragments. Furthermore, our results establish a different modulation of RhoA by α5β1 and α4β1 integrins in melanoma cells. Thus, ligation of α5β1 resulted in sustained activation of RhoA while concomitant engagement of α4β1, down-regulated RhoA after an early activation phase. Interestingly, this correlated with an increased p190RhoGAP phosphorylation, indicating that α4β1 ligation prevents activation of RhoA by activating p190RhoGAP. At difference with the previously described pathway for the early RhoA inactivation in fibroblasts (Ren *et al*., 1999), α4β1 mediated signaling apparently lacks the stimulus that results in RhoA activation at a later time, and RhoA activity remains low. The involvement of p190RhoGAP in α4β1 signaling is further supported by its localization at cytoplasmic protrusions on FNIII7–10+FNIII4–5 but not on FNIII7–10. This is in agreement with a role for p190RhoGAP in protrusion formation as previously shown for the melanoma cell line LOX following α6β1 engagement (Nakahara *et al*., 1998) and for dominant negative p190-fibroblasts (Arthur and Burridge, 2001).

Although a role for α4β1 in cell motility has already been established (Holzmann *et al*., 1998), we describe here a novel mechanism by which cross-talk between α5β1 and α4β1 integrins results in cell migration. We also report for the first time that the Hep III domain of Fn induces melanoma cell migration as effectively as the "classical" CS-1 and VCAM-1 α4β1 ligands. This involves down-regulation of RhoA whose levels appear to be critical for melanoma cell motility, as previously found for fibroblasts and some leukocytes (Nobes and Hall, 1999; Schmitz *et al*., 2000; Alblas *et al*., 2001; Worthylake *et al*., 2001).

The finding that Fn contains positive and negative regulators of RhoA may be particularly important for melanoma cells in which the presence of an unligated or engaged α4β1 integrin may determine whether the cytokeletal response leads to firm adhesion or to cell migration. α4β1/VCAM interaction has already been shown to regulate the metastatic capacity of melanoma cells (Holzmann *et al*., 1998). Moreover, high expression of α4β1 was shown to inhibit invasiveness of murine B16 cell lines and induction of homotypic aggregation, which resulted in retention of the cells at the primary injection site (Quian *et al*., 1994). The regulation of α4β1 expression and function may therefore be critical for the progression of melanoma tumors. A previous report has shown that the adaptor protein paxillin binds to the α4 subunit cytoplasmic domain and this results in inhibition of stress fibers and focal adhesions and enhanced cell migration (Liu *et al*., 1999). Since this is similar to the pattern observed in the present report, it is possible that paxillin and the α4 subunit also associate in melanoma cells leading to the migratory phenotype characteristic of this cell type. While this possibility remains to be clarified, our present results provide new data on the role of α4β1 integrin in regulating melanoma cell cytoskeleton organization and migration. They also establish novel functions for α4β1 integrin ligands in the Hep III domain and the IIICS region that although latent in the native Fn molecule, become exposed during physiological processes.

ACKNOWLEDGMENTS

We thank all mentioned investigators for providing reagents used in this study; Dr. Miguel Abal (Institut Curie, Paris, France) for the single cell tracking analysis; Fernando Martin and Mariana Gómez for help with videomicroscopy; Teresa Diaz-López for expert advice in molecular cloning; and Mercedes Hernández del Cerro for excellent technical assistance. This work was supported by grants SAF2000-0124 from the Comisión Interministerial deCiencia y Tecnología and 08.1/0028/1999.1 from the Comunidad Autónoma deMadrid. J.V.M. was supported by a fellowship from GlaxoSmithKline; B.C. was supported by a fellowship from Comunidad Autónoma deMadrid.

REFERENCES

Adams, J.C., and Watt, F.M. (1993). Regulation of development and differentiation by the extracellular matrix. Development *117*, 1183–1198.

Alblas, J., Ulfman, L., Hordijk, P., and Koenderman, L. (2001). Activation of RhoA and ROCK are essential for detachment of migrating leukocytes. Mol. Biol. Cell *12*, 2137–2145.

Arthur, W.T., Petch, L.A., and Burridge, K. (2000). Integrin engagement suppresses RhoA activity via a c-Src-dependent mechanism. Curr. Biol. *10*, 719–722.

Arthur, W.T., and Burridge, K. (2001). RhoA inactivation by p190RhoAGAP regulates cell spreading and migration by promoting membrane protrusion and polarity. Mol. Biol. Cell *12*, 2711–2720.

Aukhil, I., Joshi, P., Yan, Y., and Erickson, H.P. (1993). Cell- and heparin-binding domains of the hexabrachion arm identified by tenascin expression proteins. J. Biol. Chem. *268*, 2542–2553.

Basbaum, C.B., and Werb, Z. (1996). Focalized proteolysis: spatial and temporal regulation of extracellular matrix degradation at the cell surface. Curr. Opin. Cell Biol. *8*, 731–738.

Bishop, A., and Hall, A. (2000). Rho GTPases and their effector proteins. Biochem. J. *348*, 241–255.

Bloom, L., Ingham, K.C., and Hynes, R.O. (1999). Fibronectin regulates assembly of actin filaments and focal contacts in cultured cells

via the heparin-binding site in repeat III13. Mol. Biol. Cell *10*, 1521–1536.

Carnemolla, B., Leprini, A., Querzé, G., Urbini, S., and Zardi, L. (1996). Novel self-association fibronectin sites. Biochem. Cell Biol. *74*, 745–748.

Davis, G.E., Bayless, K.J., Davis, M.J., and Meininger, G.A. (2000). Regulation of tissue injury responses by the exposure of matricryptic sites within extracellular matrix molecules. Am. J. Pathol. *156*, 1489–1498.

Dillon, S.T., and Feig, L.A. (1995). Purification and assay of recombinant C3 transferase. Methods Enzymol. *256*, 174–184.

Elices, M.J., Osborn, L., Takada, Y., Crouse, C., Luhowskyj, S., Hemler, M.E., and Lobb, R.R. (1990). VCAM-1 on activated endothelium interacts with the leukocyte integrin VLA-4 at a site distinct from the VLA-4/fibronectin binding site. Cell *60*, 577–584.

Garcia-Pardo, A., Rostagno, A., and Frangione, B. (1986). Primary structure of human plasma fibronectin. Characterization of a 38 kDa domain containing the C-terminal heparin-binding site and a region of molecular heterogeneity. Biochem. J. *241*, 923–928.

Garcia-Pardo, A., Sánchez-Aparicio, P., and Wayner, E.A. (1992). Two novel monoclonal antibodies to fibronectin that recognize the Hep II and CS-1 regions respectively. Their differential effect on lymphocyte adhesion. Biochem. Biophys. Res. Commun. *186*, 135–142.

Geiger, B., Bershadsky, A., Pankov, R., and Yamada, K.M. (2001). Transmembrane extracellular matrix-cytoskeleton crosstalk. Nat. Rev. Mol. Cell. Biol. *2*, 793–805.

Holzmann, B., Gosslar, U., and Bittner, M. (1998). α4 integrins and tumor metastasis. Curr. Top. Microbiol. Immunol. *231*, 125–141.

Howe, A., Aplin, A.E., Alahari, S.K., and Juliano, R.L. (1998). Integrin signaling and cell growth control. Curr. Opin. Cell Biol. *10*, 220–231.

Huang, W., Chiquet-Ehrismann, R., Moyano, J.V., Garcia-Pardo, A., and Orend, G. (2001). Interference of tenascin-C with syndecan-4 binding to fibronectin blocks cell adhesion and stimulates tumor cell proliferation. Cancer Res. *61*, 8586–8594.

Huhtala, P., Humphries, M.J., McCarthy, J.B., Tremble, P., Werb, Z., and Damsky, C.H. (1995). Cooperative signaling by α5β1 and α4β1 integrins regulates metalloproteinase gene expression in fibroblasts adhering to fibronectin. J. Cell Biol. *129*, 867–879.

Iida, J., Meijne, A.M.L., Spiro, R.C., Roos, E., Furcht, L.T., and McCarthy, J.B. (1995). Spreading and focal contact formation of human melanoma cells in response to the stimulation of both melanoma-associated proteoglycan (NG2) and α4β1 integrin. Cancer Res. *55*, 2177–2185.

Liu, S., Thomas, S.M., Woodside, D.G., Rose, D.M., Klosses, W.B., Pfaff, M., and Ginsberg, M.H. (1999). Binding of paxillin to α4 integrins modifies integrin-dependent biological responses. Nature *402*, 676–681.

Mould, A.P., Komoriya, A., Yamada, K.M., and Humphries, M.J. (1991). The CS5 peptide is a second site in the IIICS region of fibronectin recognized by the integrin α4β1. Inhibition of α4β1 function by RGD peptide homologues. J. Biol. Chem. *266*, 3579–3585.

Mould, A.P., Askari, J.E., Craig, S.E., Garrat, A.N., Clements, J., and Humphries, M.J. (1994). Integrin α4β1-mediated melanoma cell adhesion and migration on vascular cell adhesion molecule-1 (VCAM-1) and the alternatively spliced IIICS region of fibronectin. J. Biol. Chem. *269*, 27224–27230.

Moyano, J.V., Carnemolla, B., Domínguez-Jiménez, C., García-Gila, M., Albar, J.P., Sánchez-Aparicio, P., Leprini, A., Querzé, G., Zardi, L., and Garcia-Pardo, A. (1997). Fibronectin type III5 repeat contains a novel cell adhesion sequence, KLDAPT, which binds activated α4β1 and α4β7 integrins. J. Biol. Chem. *272*, 24832–24836.

Moyano, J.V., Carnemolla, B., Albar, J.P., Leprini, A., Gaggero, B., Zardi, L., and Garcia-Pardo, A. (1999). Cooperative role for activated α4β1 integrin and chondroitin sulfate proteoglycans in cell adhesion to the heparin III domain of fibronectin. Identification of a novel heparin and cell binding sequence in repeat III5. J. Biol. Chem. *274*, 135–142.

Moyano, J.V., Maqueda, A., Albar, J.P., and Garcia-Pardo, A. (2003). A synthetic peptide from the heparin-binding domain III of fibronectin promotes stress-fibre and focal adhesion formation in melanoma cells. Biochem. J. *371*, 565–571.

Nakahara, H., Mueller, S.C., Nomizu, M., Yamada, Y., Yeh, Y., and Chen, W-T. (1998). Activation of β1 integrin signaling stimulates tyrosine phosphorylation of p190RhoGAP and membrane-protrusive activities at invadopodia. J. Biol. Chem. *273*, 9–12.

Nobes, C.D., and Hall, A. (1999). Rho GTPases control cell polarity, protrusion, and adhesion during cell movement. J. Cell Biol. *144*, 1235–1244.

Porter, J.C., and Hogg, N. (1997). Integrin cross talk: activation of lymphocyte function-associated antigen-1 on human T cells alters α4β1 and α5β1-mediated function. J. Cell Biol. *138*, 1437–1447.

Quian, F., Vaux, D.L., and Weissman, I.L. (1994). Expression of the integrin α4β1 on melanoma cells can inhibit the invasive stage of metastasis formation. Cell *77*, 335–347.

Ren, X-D., Kiosses, W.B., and Schwartz, M.A. (1999). Regulation of the small GTP-binding protein RhoA by cell adhesion and the cytoskeleton. EMBO J. *18*, 578–585.

Ren, X-D., Kiosses, W.B., Sieg, D.J., Otey, C.A., Schlaepfer, D.D., and Schwartz, M.A. (2000). Focal adhesion kinase suppresses Rho activity to promote focal adhesion turnover. J. Cell Sci. *113*, 3673–3678.

Retta, S.F., Balzac, F., Ferraris, P., Belkin, A.M., Fassler, R., Humphries, M.J., De Leo, G., Silengo, L., and Tarone, G. (1998). β1-integrin cytoplasmic subdomains involved in dominant negative function. Mol. Biol. Cell *9*, 715–731.

Ridley, A.J., and Hall, A. (1992). The small GTP-binding protein Rho regulates the assembly of focal adhesions and actin stress fibers in response to growth factors. Cell *70*, 389–399.

Ridley, A.J. (2001). Rho family proteins: coordinating cell responses. Trends Cell Biol. *11*, 471–477.

Sánchez-Aparicio, P., Domínguez-Jiménez, C., and *Garcia-Pardo, A.* (1994). Activation of the α4β1 integrin through the β1 subunit induces recognition of the RGDS sequence in fibronectin. J. Cell Biol. *126*, 271–279.

Sander, E. E., ten Klooster, J. P., van Delft, S., van der Kammen, R. A., and Collard. J. G. (1999). Rac downregulates Rho activity: reciprocal balance between both GTPases determines cellular morphology and migratory behavior. J. Cell Biol. *147*, 1009–1021.

Saoncella, S., Echtermeyer, F., Denhez, F., Nowlem, J.K., Mosher, D.F., Robinson, S.D., Hynes, R.O., and Goetinck, P.F. (1999). Syndecan-4 signals cooperatively with integrins in a Rho-dependent manner in the assembly of focal adhesions and actin stress fibers. Proc. Natl. Acad. Sci. USA *96*, 2805–2810.

Sastry, S.K., and Burridge, K. (2000). Focal adhesions: a nexus for intracellular signaling and cytoskeletal dynamics. Exp. Cell Res. *262*, 25–36.

Schmitz, A.A.P., Govek, E-E., Böttner, B., and Van Aelst, L. (2000). Rho GTPases: signaling, migration and invasion. Exp. Cell Res. *261*, 1–12.

Ugarova, T.P., Ljubimov, A.V., Deng, L., and Plow, E.F. (1996). Proteolysis regulates exposure of the IIICS-1 adhesive sequence in plasma fibronectin. Biochemistry *35*, 10913–10921.

Wayner, E.A., Garcia-Pardo, A., Humphries, M.J., McDonald, J., and Carter, W.G. (1989). Identification and characterization of the T lymphocyte adhesion receptor for an alternative cell attachment domain (CS-1) in plasma fibronectin. J. Cell Biol. *109*, 1321–1330.

Woods, A., Couchman, J.R., Johansson, S., and Hook, M. (1986). Adhesion and cytoskeletal organization of fibroblasts in response to fibronectin fragments. EMBO J. *5*, 665–670.

Woods, A., Longley, R.L., Tumova, S., and Couchman, J.R. (2000). Syndecan-4 binding to the high affinity heparin-binding domain of fibronectin drives focal adhesion formation in fibroblasts. Arch. Biochem. Biophys. *374*, 66–72.

Worthylake, R.A., Lemoine, S., Watson, J.M., and Burridge, K. (2001). RhoA is required for monocyte tail retraction during transendothelial migration. J. Cell Biol. *154*, 147–160.

Yoneda, J., Saiki, I., Igarashi, Y., Kobayashi, H., Fujii, H., Ishizaki, Y., Kimizuka, F., Kato, I., and Azuma, I. (1995). Role of the heparin-binding domain of chimeric peptides derived from fibronectin in cell spreading and motility. Exp. Cell Res. *217*, 169–179.